Visual Impact Assessment of BIPV in building retrofits using saliency models

THÈSE N^O 7236 (2016)

PAR

Ran XU

ÉCOLE POLYTECHNIQUE
FÉDÉRALE DE LAUSANNE

Suisse
2016

Abstract

Limited fossil energy resources and the potential danger of nuclear power plants led to growing popularity of solar energy. In Switzerland, Building Integrated Photovoltaic (BIPV) is expected to be responsible for up to quarter the energy production from renewable resources by the time of 2035. In order to protect the existing natural landscape, BIPV must be concentrated in urban spaces, which means that certain amount of existing building envelopes have to be turned into energy generators. There is a growing concern about BIPV retrofits because they may change the visual appearance of the existing city images to a large extend and/or in a negative way.

In order to manage the potential visual impact resulting from BIPV expansion in urban spaces, evaluation methods should be able to measure it appropriately. Existing evaluation methods show insufficiencies for this purpose: either they cannot guarantee objectivity and continuity of evaluation standards throughout assessments of different BIPV projects, because their qualitative criteria are vulnerable to subjective preferences; or they only use formal design parameters to evaluate the visual integration quality of BIPV and therefore lack neurobiological base. In order to tackle these insufficiencies, an objective evaluation method is proposed that is capable of measuring the BIPV visual impact in building retrofits in a quantified approach based on neuroscience knowledge. The assessment should be made in concept phase of the project, so as to identify the BIPV designs that have the least negative visual impact.

The proposed evaluation method integrates saliency model, which imitates the mechanism of human visual attention, into assessment procedures. First, the probability of a BIPV installation attracting human visual attention in the respective visual scene is calculated quantitatively with the saliency model. Then the modifications of saliency values in this very visual scene before and after the BIPV retrofit are assessed. In the end, the modifications of saliency values are transformed into BIPV visual impact and objectively expressed as single values. The analyses are based on renderings generated from RADIANCE and programming in MATLAB. This method is demonstrated with a small case study that simultaneously serves as proof-of-concept.

The proposed evaluation method is applied on a realistic case study: BIPV designs for a church roof. In total, 5 designs were developed with variations in BIPV installation location, roof coverage percentage, module size, PV material und design approach. The lowest visual impact value was induced by the BIPV design with the most careful and considerate integration approach, the design with the boldest integration approach obtained the highest visual impact value. The evaluation method proved to be feasible to a large extend.

It is believed that the synergy between architecture and neuroscience can contribute to a growing

understanding of human responses to the built environment. Hopefully the findings from this thesis can help in minimizing the negative visual impact induced by BIPV expansion in urban spaces, and also aid architects in gaining new understandings for visual aspects in architecture design.

Kurzfassung

Begrenzte fossile Ressourcen und die potenzielle Gefahr von Kernkraftwerken haben zu einer wachsenden Beliebtheit der Solarenergie geführt. In der Schweiz wird von der GIPV erwartet, dass sie für ca. 25% der Stromproduktion aus erneuerbaren Ressourcen ab dem Jahre 2035 verantwortlich sein soll. Um die existierenden Landschaften zu schützen, müsste die meiste Gebäudeintegrierte Fotovoltaik (GIPV) in den Städteräumen eingesetzt werden. Das bedeutet, dass eine bestimmte Anzahl von der existierenden Gebäudehüllen in Energiegeneratoren umgewandelt werden müsste. Diese Situation hat sehr viele Besorgnisse erregt, weil die GIPV die bestehenden Ortsbilder in hohem Masse und/oder auf einer negativen Weise beeinflussen könnten.

Um die negativen visuellen Auswirkungen, die durch den GIPV Ausbau verursacht werden können unter Kontrolle zu halten, muss man erstmals die Auswirkungen zielgerecht messen können. Die bestehende Bewertungsmethoden haben Mängel in dem Sinne: sie können entweder die Kontinuität der Bewertungsstandards in verschiedenen GIPV Projekten schwer garantieren, da ihre qualitative Kriterien sehr von subjektiven Präferenzen abhängig sind oder sie verwenden bei der Bewertung der visuellen Auswirkungen lediglich formale Entwurfsparameter und fehlen an neurowissenschaftlichen Grundlagen. Deshalb wird hiermit eine objektive Bewertungsmethode vorgeschlagen, die die visuelle Wirkung der GIPV auf Gebäudehüllen in einer quantitativen Weise mit neurowissenschaflichen Grundlagen bemessen kann. Die Evaluierungen sollen in der Entwurfsphase stattfinden, so dass die GIPV Designs mit den niedrigsten visuellen Auswirkungen identifiziert werden können.

Die Bewertungsmethode integriert das Saliencymodell, welches den Mechanismus der menschlichen visuellen Aufmerksamkeit imitiert. Zuerst wird die Wahrscheinlichkeit, die eine GIPV Anlage in einer visuellen Szene die visuelle Aufmerksamkeit auf sich zieht, quantitativ mit dem Saliencymodell berechnet. Danach wird die Veränderung von Saliencywerte in der gleichen Szene vor und nach der GIPV Installation bewertet. Zuletzt werden die Saliencyveränderungen ins visuellen Wirkungsgrad umgewandelt und quantitativ ausgedrückt. Die Analysen basieren auf RADIANCE Renderings und MATLAB Programmierungen. Die Methodik wird mit einer kleinen Fallstudie demonstriert, die auch als Proof-of-concept dient.

Das vorgeschlagene Verfahren ist an einer realistischen Fallstudie angewendet worden: GIPV Entwürfe für ein Kirchendach. Insgesamt wurden 5 Entwürfe entwickelt mit Variationen in den GIPV Standorten, Dachabdeckungen, Modulgrössen, PV Materialien und Entwurfsansätzen. Der niedrigste visuelle Wirkungsgrad wurde von dem GIPV Entwurf hervorgerufen, der im Entwurfsansatz am konservativsten war. Der GIPV Entwurf mit dem radikalsten Ansatz hatte den höchsten visuellen Wirkungsgrad. Das vorgeschlagene Verfahren erwies sich bei der praktischen

Anwendung als weitgehend durchführbar.

Heutzutage ist man überzeugt, dass die Synergie zwischen Architektur und Neurowissenschaft zu einem wachsenden Verständnis der menschlichen Reaktion auf die bebaute Umwelt beitragen kann. Hoffentlich können die Entdeckungen in dieser Doktorarbeit nicht nur zur Minimierung der negativen visuellen Wirkungen von GIPV in den Städteräumen beisteuern, sondern zusätzlich auch den Architekten neue Erkenntnisse in visuellen Aspekten von Architekturdesign bringen.

Stichwörter: GIPV, visuelle Auswirkung, Saliencymodell, Saliencykarte, Gebäudesanierung

Acknowledgements

Content

List of figures

List of Tables

Nomenclature and abbreviations

In general:

PV: Photovoltaic

BIPV: Building integrated Photovoltaic

BISTS: Building integrated Solar Thermal Systems

Neuroscience:

Dimension: In Chapter 3, it refers to categories such as colour, orientation, spatial frequency, brightness, direction of movement etc. It is a set of features.

Feature: In Chapter 3, it refers to a particular value on the dimension set, such as red is the feature in the dimension colour.

Firing: The signal output of a neuron.

Neurons: Cells of nervous system that can process and transmit information through electrical and bio-chemical signals.

Receptive field: A particular region of a sensory space for a single cell.

Saliency: Conspicuity, the visual prominence

Saliency map: A topographical map that illustrates the visual prominence of a certain region relative to its surrounding in the visual scene

Saliency model: Certain algorithms set for calculation of saliency maps

Scanpath and   In the process of measuring where one was looking on the image, eyes would fixate on certain

Fixation points: points in the test image. The series of these fixation points is called scanpath.

Stimulus: Something that causes a physiological response, e.g. a light beam will evoke responses from neuron cells.

Abbreviations for saliency models:

IKN   Itti-Koch-Niebur saliency model, the classic saliency model.

GBVS   Graph Based Visual Saliency model, it is inspired by the Markov Chain.

SWD   Spatially Weighted Dissimilarity saliency model. The input image is divided into several patches, whose dissimilarities are compared with each other and weighted by their locations.

Universities and laboratories:

EPFL   École polytechnique fédérale de Lausanne

LESO-PB   Laboratoire d'Energie solaire et de Physique du Bâtiment

HSLU   Hochschule Luzern

CC EASE   Competence Centre Envelopes and Solar Energy

Chapter 1   Introduction

1.1 PV in the world and in Switzerland

Driven by the advances in technology, improvements in manufacturing and the raising awareness for sustainable future, Photovoltaics (PV) are becoming more and more popular all over the world. The International Energy Agency (IEA) showed several encouraging signs indicating that the PV sector is turning into a maturing industry. In addition to a steady growth in annual PV installations (Figure 1.1-1), year 2014 was also the first time that PV provided more than 1% of the global electricity supply [1].
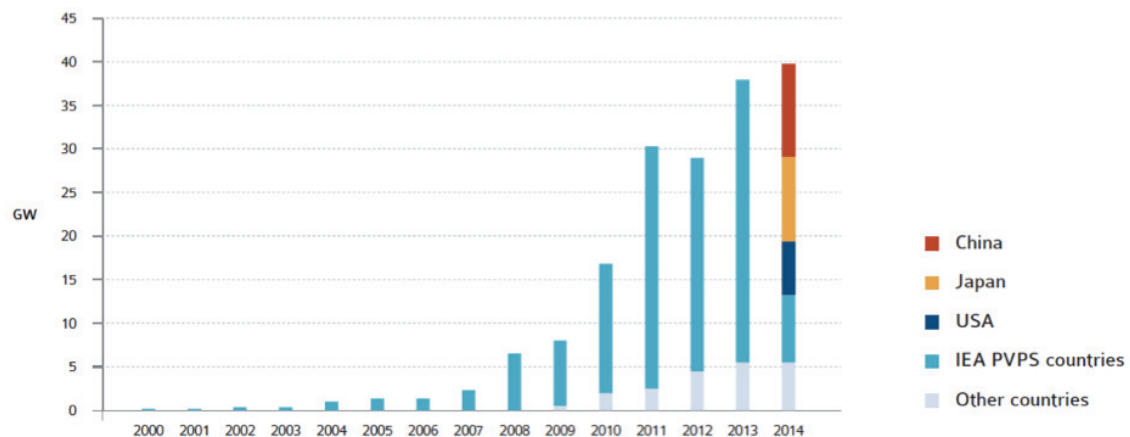
Figure 1.1-1: Global PV installations according to the year. Image source: [1], with permission for reuse from International Energy Agency Photovoltaic Power Systems Programme (IEA PVPS).

In 2009, the European Union published the Renewables Directives and listed the increased use of renewable energy as one of the effective measures to reduce greenhouse gas emissions [2]. Around the same time, Switzerland already expressed worries about the indispensable waste produced by domestic nuclear power stations and decided to depend mainly on renewable energy to provide electricity starting from year 2030 (Figure 1.1-2). BIPV (Building Integrated Photovoltaics) installations on building envelopes were expected to contribute 25% of the overall electricity production [3]. Shaken by the nuclear disaster in Fukushima in 2011, the Swiss Federal Council and Parliament reinforced their decision by gradually withdrawing Switzerland from the use of nuclear power plants. The power plants will not be replaced at the end of their life span. The Swiss Federal Office of Energy worked out plans called Energy Strategy 2050, which are strategies on how Switzerland should slowly grow independent of nuclear energy. Ambitious goals were set, such as

the increase of energy efficiency, stabilization of electrical consumption and the expansion of renewable energy [4]. Solar energy has become, among other renewable energies, a hopeful alternative to nuclear energy. Different measures were discussed under the assumptions of different scenarios, in which the exact electricity contribution by PV may vary, but all of them required enormous development of solar energy installations.
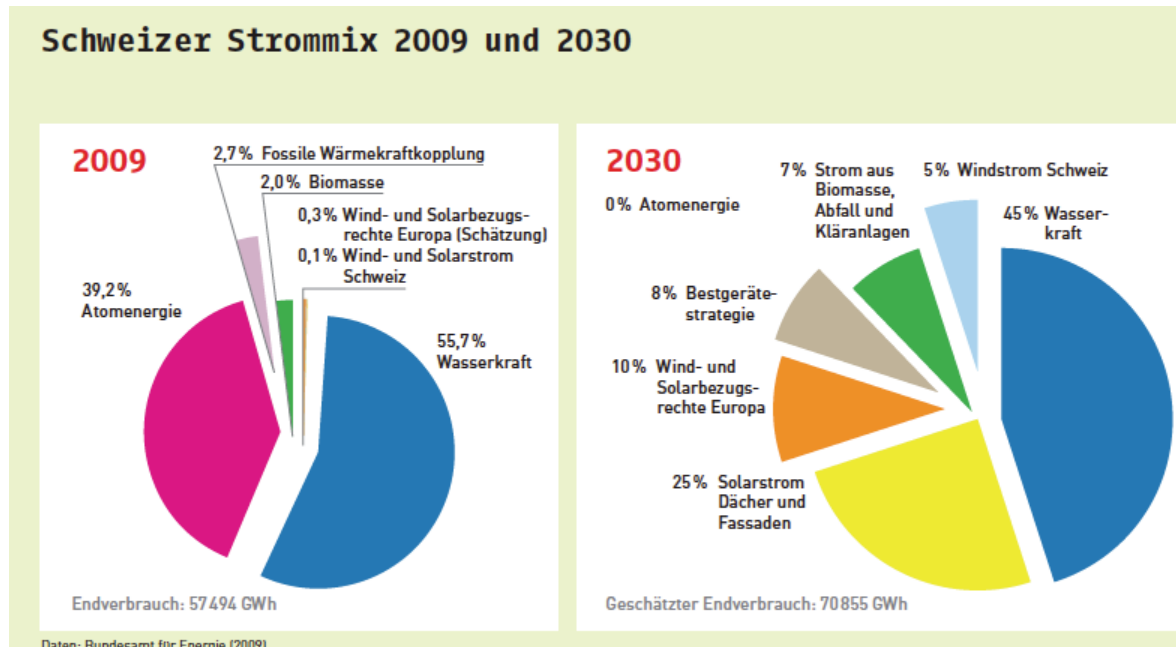
Figure 1.1-2: Swiss electricity-mix in 2009 and 2030. Image source: [3], with permission for reuse from CR Communications.

The expansion of PV was decided to take place slowly but fierce. The potential of Swiss renewable energies was estimated to be 0.9 - 25 TWh/a by the time of year 2050, depending on the exact settings of the hypothetical scenarios. PV would be responsible for approximately 50% of the renewable energy production [5], [6]. In the summary of the report „Energy perspective 2050" published by Swiss Federal Office of Energy, a special attachment was dedicated to the PV, discussing matters such as at which speed the expansion should take place, its cost and effects [7]. On the cantonal level, the Energy Strategy 2050 is supported by the MuKEn (Model prescriptions of cantons in energy sector) drafted by the Conference of Cantonal Energy Directors (Konferenz Kantonaler Energiedirektoren). The MuKEn is a prescription to promote building energy efficiency in order to achieve better and more sustainable built environment. For instance, the present MuKEn 2014 suggests that in the future all newly built buildings must produce certain amount of electricity by themselves; and the existing buildings, when replacing their existing fossil fuel heating systems, have to produce at least 10% of the required heating energy from renewable sources [8]. It will be proposed for integration into cantonal laws latest by the time of 2018, so as to make sure that it will take effect in 2020.

Encouraged by the Energy Strategy 2050 and the new Energy law [9], analyses have been made on the solar energy potential on building facades and roofs throughout Switzerland, also called the

"solar cadastre". The results will be used as a promotion tool for solar energy usage targeted at private customers on the one hand, but also as information for Swiss authorities when developing future planning strategies [10].

1.2 PV expansion and heritage protections

As mentioned before, according to the Energy Strategy 2050, the potential of electricity production from PV was estimated to be 11.12 TWh in 2050 in several hypothetical scenarios. Assuming the yearly sum of global horizontal solar irradiation in Switzerland is 1000kWh/m^2, and the average efficiency of PV modules is 12%, then at least 90 km^2 of BIPV need to be installed on building envelopes by 2050.

Switzerland is known for treasuring their natural and heritage goods. The notion of installing BIPV in relation with their visual impact to the surrounding environment was given much attention. Hence the Swiss Federal government established corresponding law articles to limit the impact. The most up-to-date Swiss urban planning law article 18 a (Raumplannungsgesetz, short: RPG) [11] states that "Solaranlagen [...] in Bau- und in Landwirtschaftszonen bedürfen auf Dächern genügend angepasste Solaranlagen keiner Baubewilligung nach Artikel 22 Absatz 1; [...] Solaranlagen auf Kultur- und Naturdenkmälern von kantonaler oder nationaler Bedeutung bedürfen stets einer Baubewilligung. Sie dürfen solche Denkmäler nicht wesentlich beeinträchtigen." (Translation: In building and landscape zones, solar installations on roofs that are considered appropriately installed do not need to file in installation applications according to article 22 (1); [...] Solar installations on cultural and natural heritages of cantonal or national importance always need to file in an installation application. They mustn't affect these heritages obviously). This law was published in order to avoid installing solar energy systems in natural landscapes, to prevent urban sprawl and to promote the use of existing urban space, but also to encourage careful integrations of PV onto building envelopes and limit the negative impact within a certain amount. It is also supported by local regulations, where the cantonal authorities explain in brochures how they expect appropriate BIPV installations to look like [12]-[15].

As it is discouraged by the RPG article 18a to locate solar power plants in open landscapes, therefore the amount of BIPV in order to fulfil the above mentioned electricity production requirement by the time of 2050 would ultimately lead to irreversible changes in Swiss urban spaces. This provoked awareness among people from heritage protection sectors. Interventions on heritage buildings are usually only permitted when no harms are caused to the building's material substances, appearances and its existing impact to the surrounding. Extra effort, interdisciplinary knowledge and patience are required to develop a feasible renovation concept for heritage buildings. Heritage departments are continuously seeking for a proper balance between preserving the limited cultural resource for the past and the limited energy resource for the future. In recent years, efforts were shown from their sides to be open for discussions and urge planning teams to integrate them in early phases of renovation designs [16] [17] [18], [19]. However, disputes and disagreements are still quite common between the heritage departments and applicants [20]-[27]. According to the position paper by the Swiss heritage organisation, solar installations will affect the image of landscape, city

and single buildings ("Sie (Solaranlagen) werden das Erscheinungsbild von Landschaften, Ortsbildern und Einzelbauten beeinflussen.") [28]. The visual impact is in the first place the most apparent and striking factor in the dilemma between the PV expansion and heritage protection.

In contrast to urban areas, before the installation of renewable energy plants on rural landscapes, it is common to make thorough studies of their potential visual impact. The landscape qualities, after the hypothetical installations, are evaluated based on the "naturalness" of the scenery. In some approaches, formal design features are the decisive criteria to investigate, such as forms, lines, colours of the scene etc. In other approaches, the biophysical features of the landscape are treated as stimuli that evoke aesthetically relevant psychological responses of the landscape viewers. The existing evaluation methods have their drawbacks, such as what are the most relevant features of a "natural" landscape remain unclear, and how the features are presented to the viewer are also not standardized. Nevertheless, it is the dynamics between landscape features and the human perceptions that are emphasized [29]. Visual impact assessments are carried out especially in dispute-prone projects such as setting wind turbines and solar installations in rural areas. Prior their installations, possible visual impacts to the existing landscape will be evaluated along with other technical studies [30]-[33].

1.3 Building labels and BIPV's visual impact

This section is a literature review on how the popular building labels, which are strong promotion tools for green architectures, deal with the visual impacts of BIPV.

Building labels are quality certifications for green buildings and evaluation systems that mainly focus on assessing the sustainability and design, including the integration of renewable energy systems. The recognition for the building quality is beneficial for marketing and advertising, therefore these labels are strong drives for enhancing building qualities. In contrast to building laws and regulations, building labels don't represent the minimum standards, but set the maximum goals to reach for, and examine the buildings by comparing their measured results with these goals. The three most popular building labels are DGNB, LEED and BREEAM [34]. DGNB (German society for sustainable building) was developed in Germany, LEED (Leadership in Energy and Environmental Design) originated from the United States and BREEAM (Building Research Establishment Environmental Assessment Methodology) was established in the United Kingdom. They evaluate the quality of green buildings mainly from the aspects of sustainability, environment friendliness and energy efficiency. BIPV are usually rated positively in these labels because they are efficient measures to reduce greenhouse gas emissions. Aside from focusing on the technical benefits of BIPV, the attention these building labels pay to the social functional quality of the green buildings are quite different (Table 1.3-1) [35]. It can be observed that the LEED and BREEAM do not integrate the criteria "aesthetic and art" of the green building into their assessments. DGNB is the only one that has high requirements in this aspect, assessing it based on the urban planning quality, architectural quality and functionality of the design. However, DGNB also struggles with defining an appropriate evaluation of the topic „aesthetic and art. So instead of listing fixed requirements in an evaluation sheet, they subcontract this evaluation mission to a professional jury

group [36]. In all three certification systems, no special considerations are given to the visual impact of BIPV installations.

Quality	Criteria	DGNB (New office building)	LEED (NC 3.0)	BREEAM (International)
Social functional quality	Thermal comfort	Medium requirement	High requirement	High requirement
	Indoor air quality	High requirement	High requirement	High requirement
	Acoustic quality	Medium requirement	Not mentioned	Not mentioned
	Visual comfort	High requirement	Medium requirement	Medium requirement
	Influence of the users	High requirement	High requirement	Low requirement
	Outdoor quality	Medium requirement	Not mentioned	Not mentioned
	Safety and risks in malfunctions	Medium requirement	Not mentioned	Not mentioned
	Accessibility and safety	High requirement	Not mentioned	Low requirement
	Public accessibility	Medium requirement	Not mentioned	Not mentioned
	Biking comfort	High requirement	High requirement	High requirement
	Concept of urban planning and aesthetic	High requirement	High requirement	High requirement
	Aesthetic and art	High requirement	Not mentioned	Not mentioned
	Quality of floor plans	High requirement	Not mentioned	Not mentioned

Legend

High requirement	(dark green)
Medium requirement	(light green)
Low requirement	(pale green)
Not mentioned	(white)

Table 1.3-1: Comparison of the three most popular building certifications in aspect of social functional quality. Translated and recreated with permission from the author of [35].

Table 1.3-2 summarises the MINERGIE and SNBS building labels in a similar way. The MINERGIE is the most important building label in Switzerland and was institutionalized in 1998 [37]. It evaluates the quality of a green building mainly based on its energy consumption per area and is therefore strictly technical [38]. One of the key measures to be qualified for MINERGIE certification is to have airtight and high quality building envelopes. However, this does not apply for heritage buildings, where an insulation upgrade is not always possible. The energy efficiency of the building can be improved, among others, by integrating renewable energies instead. For retrofitted buildings, the energy consumption must not exceed 60 kWh/m^{2}a considering the heating, warm water, air ventilation and air conditioning. The official MINERGIE website also points out that the building label does not involve criteria concerning heritage protection issues [39] and therefore recommends applicants to take reference from the position paper of Swiss heritage organization [28], and the "Energy and heritage buildings" recommendation brochure published mutually by the Swiss Commission for heritage protection and the Swiss Federal Office of Energy [18]. It also suggests an early participation of the corresponding heritage protection authorities in building retrofit projects.

The relatively new building label SNBS (Standard for sustainable buildings of Switzerland) tries to evaluate buildings holistically by focusing equally on their social, economic and environmental

impacts [40]. In the social category, the building is evaluated from the perspectives of architecture and context, design approach, social dynamic between the building and its surrounding, and user comfort (visual, acoustic and thermal). From Table 1.3-2 it can be read that the evaluation of the building's social aspect is quite considerate and holistic, thus making SNBS an evaluation system one of a kind. However, in the survey that investigated the public opinion concerning the necessity of SNBS, this advantage in comparison to MINERGIE was not emphasized. In fact, around 70% of the 53 professional interviewees expressed that there are already plenty of building labels available on the market and hence no special reason to choose this particular building label over others [41]. The visual impact of BIPV is integrated in the general architectural evaluations in SNBS and not mentioned specifically.

Quality	Criteria	MINERGIE	SNBS (Residential)
Social functional quality	Thermal comfort	■	■
	Indoor air quality	■	■
	Acoustic quality		■
	Visual comfort	■	■
	Influence of the users		■
	Outdoor quality		■
	Safety and risks in malfunctions		■
	Accessibility and safety		■
	Public accessibility		■
	Biking comfort		
	Concept of urban planning and aesthetic		■
	Aesthetic and art		■
	Quality of floor plans	■	■

Legend

Mentioned directly or indirectly	■
Not mentioned	

Table 1.3-2: Comparison of the MINERGIE and SNBS building labels, the two most important building labels in Switzerland.

So it can be concluded that even though the visual impact is an apparent and striking factor in the dilemma between PV expansion and heritage protection, popular building labels haven't dedicated special attention to this topic yet.

1.4 Review of BIPV and visual assessment

The lack of appropriate evaluation tools drove the development of complementary methods, which were made especially for evaluating BIPV's visual impact and related aspects. A literature review on these methods is presented in this section. The visual evaluations of both PV panels and solar thermal collectors in both urban spaces and landscapes were reviewed, since all of them could be

inspirational for evaluating the BIPV visual impacts in urban areas. Depending on the nature of the evaluation methods, they can be roughly divided into three categories, namely qualitative, hybrid and quantitative approaches.

1.4.1 Qualitative approaches

In qualitative approaches, there is no clear definition for the term "visual impact". It is sometimes convertible with the term "integration quality", while at times the latter can also be composed of technical/constructional and aesthetical aspects. The boundary between the relevant terms is rather fuzzy. The criteria of qualitative evaluation methods are mostly based on semantic parameters that describe the integration quality or the visual impact of the solar installations. Due to the vagueness of linguistic descriptors, standards are often flexible and depending on the person that is in charge of the evaluation. The advantage of qualitative evaluations is that their evaluation standards can quickly be adapted according to the particular project situation.

Originally a PV module wasn't conceived as a building element, but rather as an add-on technical appliance. Their dark, glossy and unconventional appearances made them stand out in almost everywhere. It was such a difficult building element to handle that usually only pioneering architects were willing to take the risk and apply them on their building facades. Some of these pioneering architects categorized the BIPV based on their "presence" in architectures. For instance, the participants in IEA Task 16 raised the awareness that both the technical and aesthetic characteristics of PV modules should be considered to achieve satisfactory results in designs [42]. In regard to BIPV's colour, texture, cell spacing and dimensions, their suitability for integration on sloped roofs, flat roofs, walls, windows and as shading elements could be given one of the three qualitative grades: high suitability, low suitability and not suitable.

Kaan and Reijenga proposed that the following "aesthetic" criteria are crucial for BIPV to be recognized as good integrations [43], [44]:

o   The PV is a logical part of the building's structure or composition
o   The PV system is architecturally pleasing within the context of the building
o   The colours and textures of PV match with the rest of the building
o   The dimensions of the PV fit well into the grid/visual pattern of the building, they are in harmony together
o   The PV system matches with the building context
o   Besides fulfilling basic functions, the structural and technical details are well engineered
o   The application of PV leads to innovative designs.

This being the criteria, the architectural approaches of BIPV integration can be divided into five types, listed in the following with an order that has an increased amount of architectural value [45]:

o   Applied invisibly to the architecture
o   Added to the architecture design
o   Integrated beautifully into the building without affecting its image

- o   Determining the architecture's image
- o   Leading to new architectural concepts.

With the growing number of installations, more and more professional architects became interested in BIPV. Due to their easiness in application, PV have been largely installed on existing building envelopes, modifications on which were a matter of delicacy according to Hermannsdörfer and Rüb [46]. Architects were urged to include BIPV in an architecture refurbishment project not only from the perspective of energy engineering and construction, but also from the perspective of architecture design. Using the building's original historical appearance as reference, the design approaches can be divided into three levels according to the strength of BIPV's intervention in the building context. The first one is maintaining the opposition between the old and new: the difference between the existing building and PV is left as it is, so as to emphasize the contrast between them. The second approach is to create a dialogue between the old and new: the BIPV respect e.g. the rhythms, grids and shapes of the existing building, while remaining unique in their own characteristics by material or colour properties. The last alternative is the blending in of the new into the old: the harmony between the BIPV and the existing building is the focus. The visual impact of BIPV decreases from approach one to three. Aesthetic characteristics are the key considerations. Similar concepts can be found in [47] [48].

Munari Probst and Roecker [49] introduced a checklist to evaluate the "integrability" of Building integrated Solar Thermal Systems (BISTS). The criteria can be retrieved from Table 1.4-1, with which the integration potential of the solar thermal installations is evaluated. Each criterion is graded manually by providing a "+" sign for good, "+/-" for medium and "−"for bad integration potential. This method is extended to BIPV evaluation with a slight adaption [50]. It is believed that a solar energy product with larger flexibilities has a better potential to be well integrated onto a building envelope.

Multifunctional element	+
Shape & size flexibility	+
Glazing: surface texture choice	+/-
Absorber: surface texture choice	-
Absorber colour choice	-
Jointing options	+
Availability of dummies	-
Complete construction system	+/-

Table 1.4-1: Evaluation table for BISTS issued from Munari Probst and Roecker method [49]. Permission for reuse from EPFL Press.

The integration quality (or "applicability") of solar installations to building envelopes can also be evaluated by their architectural aspects along with their energy performances [51]. The architectural quality of a solar installation is grouped into four main categories, namely "Application", "Building physics", "Integration and "Construction". "Application" mainly deals with the location of a solar installation and its adaptability, "Building physics" evaluates its multi-functional features as a building envelope element, "Integration" assesses its profile, colour and texture, and "Construction" examines in what kind of facade construction the solar installation can be integrated into. Each

category is divided into several sub-criteria. Most of the sub-criteria are qualitative and evaluated manually on a scale from 1 – 16, the higher the number, the better the result (see Table 1.4-2).

| | | | Applicability on New Buildings | | | | | | | Applicability on Existing buildings | | | | | | |
| | | | BIPV | | | | BISTS | | | BIPV | | | | BISTS | | |
			Modules	Solar Cell Glazing	Foil	Tiles	Unglazed Flat Plate Air Collectors	Unglazed Flat Plate Hydraulic Collectors	Vacuum tube hydraulic collectors	Modules	Solar Cell Glazing	Foil	Tiles	Unglazed Flat Plate Air Collectors	Unglazed Flat Plate Hydraulic Collectors	Vacuum tube hydraulic collectors
System	Application	Air Heating					16							16		
		Water Heating						4	1						4	1
		Electricity Production	5	13	1	2				5	12	1	2			
Architectural	Application	Replacement of a building component	3	12		2		4		3	12		2		3	
		On Façade	3	9			16	2	1	3	8			16	1	1
		On Roof	4	4	1	2		1	1	4	4	1	2			1
		On Building Component		1				2			1				2	
	Building Physics	Flexibility														
		Ease on application														
		Transparency														
		Thermal Insulation		2							2					
		Weather proofing	5	11		2		2		5	11		2		1	
		Noise Reduction	3	3			16	1		3	2			16	1	
		Shading	2	12				3	1	2	11				3	1
	Integration	Structural														
		Visible Collector Profile	5	5				1		5	5				1	
		Surface Colour Texture		1		1	16	1			1		1	16		
	Construction	Pre - Fabricated Units	5	8		2		1		5	8		2		1	
		Customised Design		5	1		16	3	1		4	1		16	2	1
		Curtain Wall	2	3						2	3					
		Double Envelope Structure		3			16	1			2			16	1	

| 1 | | 16 | | Low | | High |

Table 1.4-2: The integration quality of solar installations onto building envelopes based on their energy performances and architectural aspects. With permission for reuse from the authors of [51].

Zanetti et al [52] assessed solar installations based on five qualitative architectural standards, and coupled with recommendations of how to fix them if the standards weren't met sufficiently. The five standards are:

- „Coplanarity" - the solar installation should be on the same surface of the building envelope it is located on.
- "Respect of the lines" – the solar installation should respect the lines of the existing building.
- "Shape" - special consideration should be given to what kind of shape the solar installation should have (e.g. a random shape will draw attention to the installation itself).
- "Grouping" - the solar installation should be rather grouped than scattered.
- "Accuracy" - details in design and construction should be accounted for (such as hiding cables, plumbing etc.).

Lopez and Frontini applied these standards in [53], [54], with considerations to have an informed

knowledge before proceeding with the retrofit work of historical buildings, and to balance the building preservation with energy savings. Three colours are used to manually tag the difficulty of whether each standard or recommendation can be met (see Figure 1.4-1). Green means that the standard/recommendation can easily be met, yellow means that the standard/recommendation can be met easily if the solar installation was integrated early enough in the design process, and red means that the standard/recommendation can be met only with very careful planning.
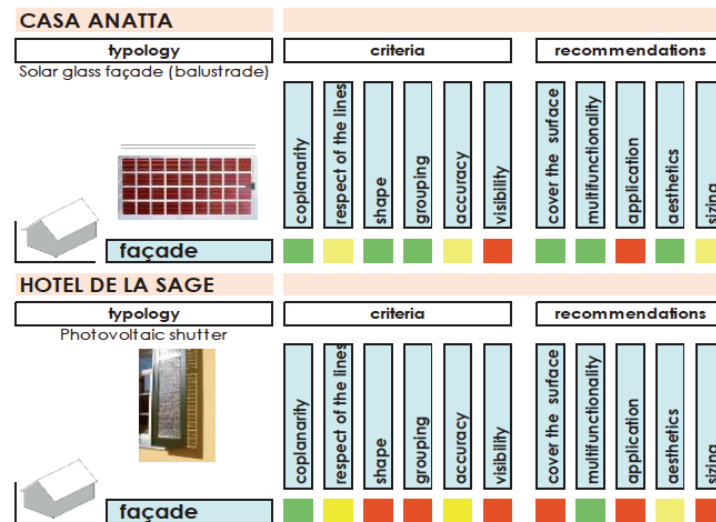
Figure 1.4-1. Evaluation of BIPV's integration quality on historical buildings by Lopez and Frontini. Reprinted from [53] with permission from Elsevier.

In order to let architects, planners and even manufacturers to be well informed of the advantages of BIPV, the architectural aspect of BIPV is evaluated on two levels: the module level and the system level [55]. For instance, the architectural aspect for BIPV and other building materials on commercial facades is assessed based on whether they have following features: "multi-functionality", "light reflection", "homogeneity of surface perception", "variability of colours", "variability of materials/textures', "variability of form/dimension/size", "opaqueness", "semitransparency", "visible joints", "substructures", "frameless" and "flexibility". Here several criteria are qualitative by nature. The grade for each criterion is either "o" for positive answer, or "x" for negative answer.

According to the "Rules and Regulations" (version of year 2012) developed by the Solar Decathlon Committee, the architectural integration quality of solar elements and technological systems is evaluated by qualitative criteria "how naturally the modules/systems are integrated in the house design concept and their coherence, and how they improve the perception of the house – which may consider aspects like form, colour, texture, materials, light and transparency to create stimulating spaces" [56]. The architectural "presence" of BIPV is categorized as following with increased visual impact:

o   Invisible application: modules are either invisible due to location or intentionally designed to be indistinguishable from the rest of the building
o   Added application: the modules have functions besides transforming electricity from solar energy, e.g. they are shading elements above windows

- o   Highlighted application: modules enhance the building image without being dominating
- o   Leading application: modules are dominating and decide the building image.

Multi Element II evaluation tool is another evaluation tool for BIPV [57]. They are evaluated according to their aesthetic (Gestaltung), flexibility, ecological performance & sustainability, production, economy & building physical and construction aspects. The aesthetical aspect, in contrast to others, is evaluated based on semantic and qualitative descriptions. For instance, the BIPV system is evaluated by whether it has a contemporary appearance or not by grading it on a scale from 1-5, the higher the value the better the result.

As more experiences were gained from practices, the trend slowly shifted from evaluating the integration quality of single modules to evaluating the overall integration quality of the active solar system in the larger urban context. LESO-QSV [58], [59] was developed on the basis of the aforementioned method by Munari Probst & Roecker, with the purpose to mutually encourage the preservation of the urban landscape and the promotion of solar installations. This tool was developed for local authorities in order to help them finding appropriate standards for solar installations depending on specific requirements. "Visibility" and "Sensibility" set the required level of architectural "Criticity" (see Figure 1.4-2). The "Visibility" shows how much the intended location for solar installation is visible from a public domain. The "Sensitivity" decides whether the respective architectural context is of delicate situation, such as an old city centre is much more delicate than an industrial area. Both "Visibility" and "Sensibility" are graded qualitatively as either of high, medium or low level by the relevant authorities. The architectural integration quality – the "Criticity" - of a solar installation is evaluated threefold, according to the "Geometry", "Materiality" and "Details" of the system (see Figure 1.4-3). "Geometry" measures the size/position of the solar installation. "Materiality" assesses the system's visible materials, surface textures and colours. "Details" analyses the shape/size and joints of the modules. The qualities of these three indicators are graded qualitatively on three levels: fully, partly or not coherent integrated. Fixed standard do not exist for the architectural integration quality in each "Criticity" level. In fact, the standards were kept flexible on purpose so as to be adaptable to different settings, e.g. local regulations, solar radiation, city "green" image etc. A three-leveled "Grid choice" (Choix de grille) parameter can be used to modify the strictness of the requirements according to individual demands.
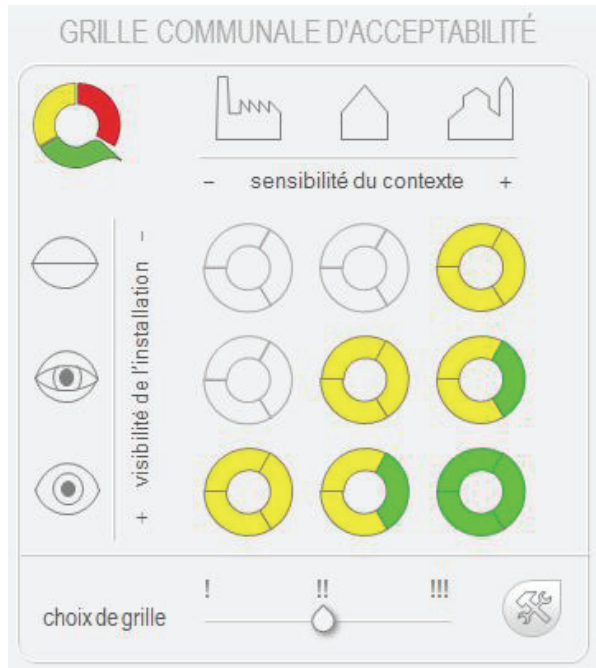
Figure 1.4-2: The "Visibility" and "Sensibility" defined within the LESO-QSV BISTS and BIPV evaluation method. With permission for reuse from the authors of [58].
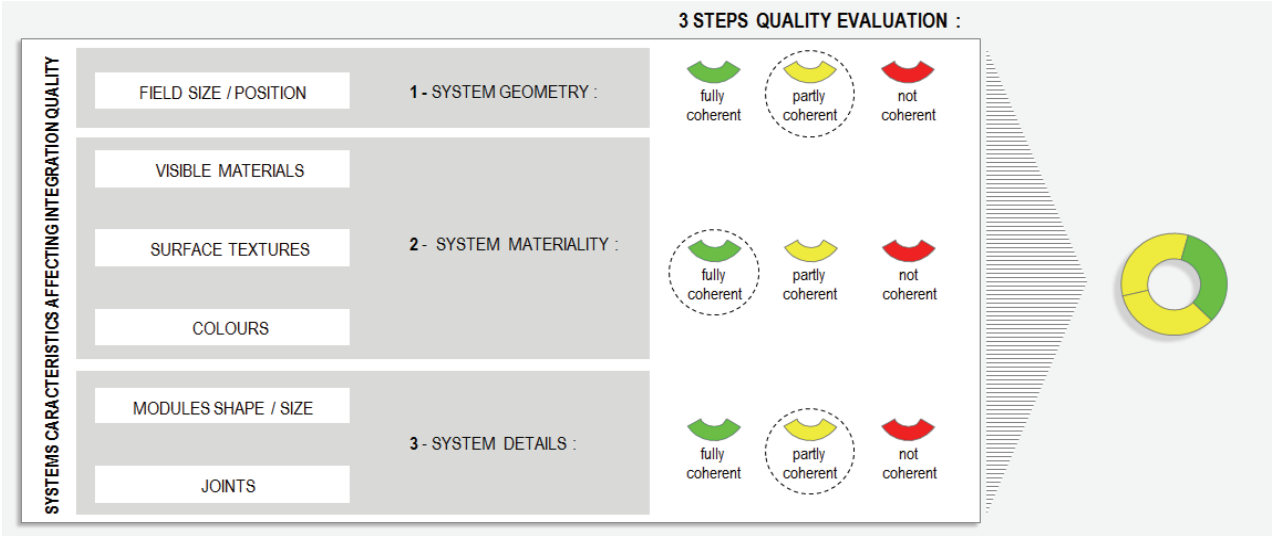
Figure 1.4-3: The "Criticity" of the solar installations suggested by the LESO-QSV BISTS and BIPV evaluation method. With permission for reuse from the authors of [58].

The Bipv.tool is a method that evaluates the overall integration quality of BIPV in 7 aspects listed in Table 1.4-3 with respective weights [60], [61]. Each aspect is again divided into several criteria, graded on a score from -1 to 5. The overall score varies on a scale from G to A+, with A+ representing the best BIPV integration quality. The morphological-figurative aspect is mainly about the architectural integration of the BIPV, for instance the criteria "recognize-ability" of the BIPV system can be divided in several qualitative levels by its relationship with the building: "obedient",

12

"integrated", "subordinate" and "dominant". The authors of the paper [62] consider that the PV integration should be designed on a higher level than only contemplating the building itself. An urban space must be seen as a complex of spaces, roads, city image, adjacent topography and morphology. Beside technical requirements, the PV impact on the "urban-landscape" and "building - aggregate" should also be examined. By looking at e.g. a minor historical centre as a holistic unit, conceptual requirements (without specific standards mentioned in the paper) were listed to evaluate the urban impact assessment of PV. For instance, the quality of PV integration in urban spaces should be examined from the perspectives of space openness, city pattern, perceptual quality (natural or artificial), heritage level, urban/architectural beauty, zone visibility, and the detailed layout and design of BIPV plant itself. If the PV integrations are expected to be enhancements of urban qualities, then the PV's urban visual impact should be minimized.

Class of PV integrability	Object of assessment	Weight
Procedural	Regulatory and legal system that addresses procedural conditions, limits and incentives	5%
Morphological - figurative	Quality of perceptual and formal characterization of the architectural language of the building envelope	30%
Technological-constructive	Constructive role in the technological apparatus, as a basis-functional component, or a fabric element	15%
Building performance	Level of satisfaction of the different buildings and technological requirements	15%
Bioclimatic-ecological	Reduction of energy consumption and environmental efficiency throughout the building lifecycle	15%
Energetic-plant	Principles of solar design, functional and electrical efficiency	15%
Landscape - contextual	Coherence and acceptability compared to a system of values worthy of significant contextual protection	5%
	Total	**100%**

Table 1.4-3: The Bipv.tool evaluation table. Recreated from [60], with permission from P. Bonomo.

1.4.2 Hybrid approaches

The hybrid approach, as qualitative ones, started also with empirical qualitative evaluations. The difference is that the empirical evaluations are translated into quantitative and objective standards that are continuous and constant even in light of different personal preferences or project characteristics. The advantage is that it enables a cross-comparison between different projects without being vulnerable to subjective factors.

Objective Aesthetic Impact of solar power plants (OAI_{SPP}) [63] [64] measures the contrasts between the solar power plants and the surrounding natural landscape. Panoramic photographs of the solar power plants and the surrounding landscapes were presented to 10 environmental sustainability experts. They graded the impact factors according to 4 aspects: visibility, colour contrasts, fractality and concurrence of the solar power plants in comparison to the surrounding landscape on a scale ranging from 0 (no impact) to 1 (full impact) based on their professional experiences. These impact

factors were then transformed into functions in relation with objective variables retrieved from the panoramic photograph:

- o Impact factor visibility I_v is related to different area percentage of solar power plants compared to the total background landscape
- o Impact factor colour I_{cl} is related to the mean colour contrast between the solar power plants and their surrounding landscape
- o Impact factor fractality I_f is related to how natural the solar power plants' silhouette is in comparison to the natural landscape. (E.g.: A straight line rarely exists in nature and therefore would be graded as very unnatural).
- o Impact factor concurrence I_{cc} is related to area and density comparison between different plants within the same solar power station

The final evaluation metric OAI_{SPP} is calculated by

$$OAI_{SPP} = \beta * (0.64 I_v + 0.19 I_{cl}) + 0.09 I_f + 0.08 I_{cc}$$

Empirical weights are given to each impact factor. Both the visibility and colour impact factors are corrected with an atmospheric coefficient β, which is an indicator issued from different weather situations (sunny, cloudy etc.). The visibility and colour have greater importance compared to fractality and concurrence. A survey involving 123 people was also made, asking to subjectively rank five case studies according to their visual impacts. The calculated OAI_{SPP} coincided approximately with the survey results. The method is, however, very much affected by the condition prevailing when the photography is made, for instance the season will have a strong impact on the perception of the solar power plants. A similar adapted version and application can be found in [65].

Pellegrino et al believe that harmonious appearance on BIPV module can be achieved if the Modulor proportion developed by Le Corbusier can be found in the design [66]. For instance in Figure 1.4-4, besides optimizing the colour, texture, size and shape of a glass-glass PV module, the cell spacing was designed following the Modulor proportion to obtain satisfactory integration quality.
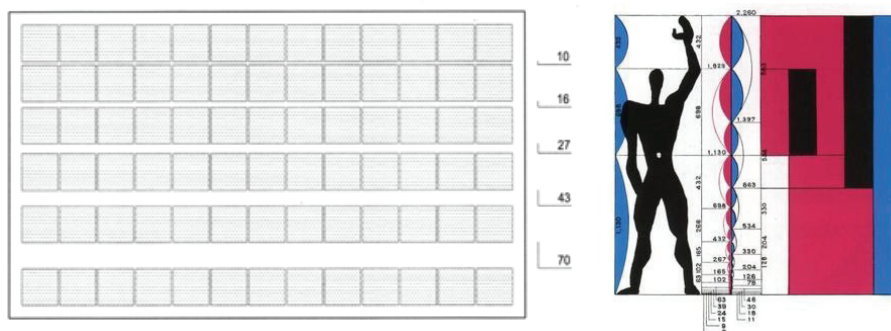
Figure 1.4-4: Left: On a PV module, the distances between the cell rows increases from top to bottom   Right: The Modulor – the anthropometric scale proportions by Le Courbusier (Source: [66], with permission for reuse from "PV in Europe- From PV Technology to Energy Solutions" conference).

1.4.3 Quantitative approaches

Quantitative approaches usually do not involve semantic descriptions and the evaluation results are presented in a numeric manner. In most of these approaches, the term "visual impact" is also interchangeable with the term "visibility". The analysis processes are fully logical and not affected by the preferences of individuals. They also enable cross-comparisons of the visual impact between separate case studies, for the evaluation processes and standards are identical.

The visual impact can be expressed by the visibility of the solar installation from the viewpoint of an observer determined in a geometric way. A simple geometric approach was used in [67] to provide a preliminary verification of the visibility (see Figure 1.4-5). From a graphical chart containing information about the building height, observer's height, tilting angle and observer distance, it is possible to affirm, for instance, that a solar panel with a 15° tilting angle located at the height of 7m, would not be visible by an observer who is less than 25 m away from the building facade.
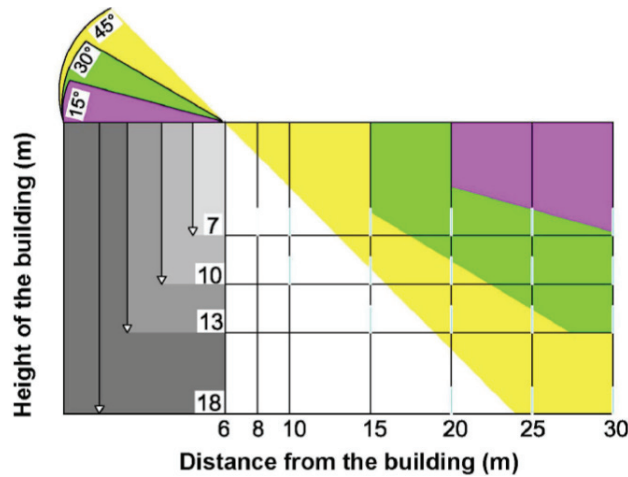
Figure 1.4-5: The chart with which the visibility of BIPV can be checked. Source [67], with permission for reuse from V. Dessi.

Another way to express the visual impact is to accumulate the visual exposure time of given PV power plants for all the possible viewers located in the surrounding [68]. It adds up the maximal possible hours for all viewers during which they are able to see the PV power plants. The viewers are categorized into stationary and mobile ones. The area that can be visually affected by the PV power plant is divided into many cells. For stationary observers in the cell j, the cumulative viewing hours for them to look at the PV in location i are calculated as

$$HoursS_j = V * DD_{ij} * n_j * h_{daylight}$$

where V is a visibility filter, which equals 1 if the PV power plants are visible from the cell j, and equals to 0 if not. DD_{ij} is a distance decay metric expressing the recognition acuity of humans eyes, which decays if the distance between i and j is larger. The n_j is the number of possible stationary observers in cell j. $h_{daylight}$ is the mean daylighting hours per day throughout the year (12h).

Mobile observers (pedestrians, car drivers etc.) are people who are moving on the road segment k, which is again divided into evenly distributed nodes. The accumulated viewing hours of the observers in segment k looking at the PV in location i are expressed by

$$HoursM_k = V * DD_{ik} * n_k * t$$

where t is the time the observers need to get from one node to the next one.

Both HoursS$_j$ and HoursM$_k$ are normalized so that their values are distributed in a range from 0 to 1. The higher these values are, the higher the PV power plants located in location i are causing visual impact to the location j or k. Then these values are applied to a colour map to enable a good overview of the visual impact distributions in concerned areas. Another similar approach can be found in [30].

The visual impact can also be presented by the probability of the observers seeing the solar installation. The Gaussian normal distribution is used to predict the visual impact of a BIPV installation [69]. Assuming that the human view angle θ is equal to 90° in both vertical and horizontal directions, and that 0° is the line perpendicular to the centre of the human eyes (see Figure 1.4-6), one has

$$\theta \epsilon \left[-\frac{\pi}{4}, \frac{\pi}{4} \right]$$

and because the integral of the observer's probabilities to see the BIPV along the angle θ is equal to 1, one gets

$$\int_{-\pi/4}^{\pi/4} f_\theta(\theta)d\theta = 1$$

$$\therefore f_\theta(\theta) = \frac{1}{\frac{\pi}{2}} = \frac{2}{\pi}$$

Assuming that L is the distance from the observer to the BIPV visual image and x and h are the horizontal and vertical coordinates on the visual image, (0,0) being located on the normal projection of human eyes centre to the BIPV visual image, using variable x instead of θ to express the above mentioned function, one gets

$$\because tg(\theta) = x/L$$

$$\therefore f_x(x) = f_\theta(\theta) \frac{d\theta}{dx} = \frac{2}{\pi} * \frac{L}{L^2 + x^2}$$

The combined probability of an observer seeing a BIPV installation located at height h$_i$ and x$_i$ can be calculated as

$$f(h_i|x_i) = f_x(x_i) * f_h(h_i) = 4 * \frac{L^2}{\pi^2} * \frac{1}{L^2 + x_i^2} * \frac{1}{L^2 + h_i^2}$$

The probability density curve along the h and x axis of the observer seeing the BIPV on a certain roof can be see in Figure 1.4-7. This method is inspired by [70].
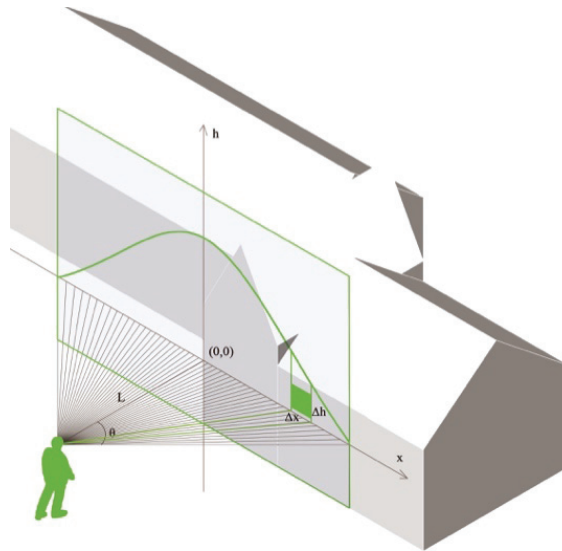
Figure 1.4-6: Using Gaussian normal distribution to calculate the probability of the observer seeing the BIPV in a visual image.
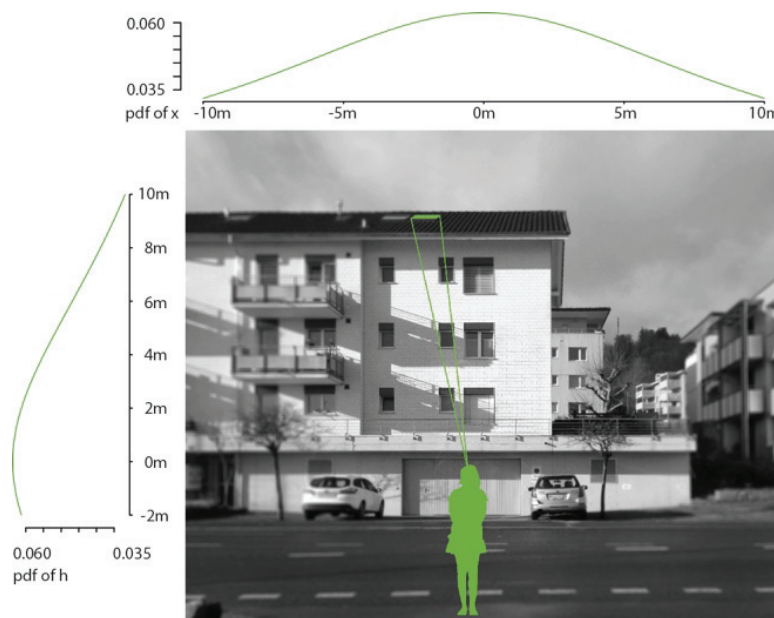
Figure 1.4-7: Probability density functions (pdf) of an observer to see a BIPV installation (green area on the roof) along the h and x-axis [69].

Minelli et al proposed another way to quantify the visual impact [71]. The static human view area is assumed to have the form of an ellipse. With the PV panels located somewhere on the landscape projected on the ellipse, the visual impact of PV panels is calculated by the fraction of PV's projected area on the ellipse compared to the ellipse area. The colour difference and material properties of the PV panels are not taken into considerations.

Other studies on visual impact assessment of solar installation with purely objective approaches were conducted by examining the reflections of sunlight from BIPV. Yang et al [72] integrated a 3D digital model of the target building and its surrounding, material properties of the building envelope and surfaces of the surrounding, as well as annual weather data in their evaluation method. It is possible to determine which surrounding area is enduring excessive reflections from the target building, as well as the frequency, quantity and origin of the sunlight. An application of this method on BIPV can be found in [73]. Other similar researches in landscapes [74] [75] and aviation area [76] [77] also exist.

1.5 New technologies and products to ease PV integration

Over the last decades, many technical and aesthetical solutions were developed for BIPV so as to provide more flexibility for their appearances and hence manipulate the visual impact. This section presents some new developments in BIPV components, colours and forms with the intention to provide a simple overview of the new possibilities that are brought to architecture design.

1.5.1 Component variations

Most contemporary PV modules are equipped with crystalline cells. Aside from trying to enhance their efficiency through modifying manufacturing processes, material composition and others, appearance varieties in PV modules can be achieved by using different backsheet materials, cell spacing, coating materials and construction details. Figure 1.5-1 - Figure 1.5-4 are four selected architectures that can present the development of architect's way of working with crystalline BIPV. The Spiller house in Figure 1.5-1 was designed by Frank Gehry in the 1980's, showing the avant-garde attitude of the architect by demonstrating PV modules loudly and sculpturally on the roof. The idea of subtly blending in of the PV modules into the architecture context was not the topic. The PV modules used in this building are clumsy in volume with opaque backsheets and bright heavy metal frames. The Sporthalle Burgweinting (Figure 1.5-2) was built 25 years later and it exhibits that the idea "subtleness" gained more weight in comparison to the Spiller house. The sculptural quality in the BIPV application is replaced by the rhythmic and calm array of PV cells on the facade. The spacing between the cells and the glass-glass construction enable an elegant integration. Functionally the PV cells work as shading device for the indoor space. Another version of structural lightness can be seen in Figure 1.5-3. BIPV modules with opaque backsheets are installed on the building facade with minimum visible construction components, thus showing

homogeneity in material and clarity in appearance. Then the conventional metal conductors with widths of 2-3mm that connected the solar cells are replaced with extremely slim wires. The Metal Wrap Through technology makes it possible to interconnect the solar cells more on the rear sides than on front-sides [78] and hence weakened the visual contrast between the metal wires and crystalline cells. Similar improvements in technologies make it possible to achieve more homogenous BIPV appearances and hence giving the architects the confidence to use them on the building facade in large numbers with the same attitude they do with other conventional building materials such as stone or metal. The Umweltarena Spreitenbach (Figure 1.5-4) is a representative example from this perspective.

Figure 1.5-1: Spiller House, Venice, USA by Frank Gehry (1980). Photo credit: Mary Ann Sullivan.

Figure 1.5-2: Sporthalle Burgweinting, Regensburg, Germany by Tobias Ruf (2005). Source: [79]

Figure 1.5-3: Headquarter of their own office by Berger und Frank architects (2012), Lucerne, Switzerland.

Figure 1.5-4: Umweltarena Spreitenbach, Spreitenbach, Switzerland by René Schmid Architekten (2012). With permission for reuse from Umwelt Arena AG.

PV with thin-film solar cells can also be semi-transparent using partial coating or de-coating procedures. Transparent substrates are divided into areas that are either coated or uncoated with thin

film solar cells. The areas are of such fine sizes so that the module appears to be quite homogenous from afar. Economically speaking, the appropriate light transmission for a-Si modules is around 10%, and up to 50% for CIS modules [80]. A solar module with much higher transparency is the newly developed transparent luminescent solar concentrator (TLSC). The TLSC mainly depends on ultraviolet and infrared lights that are not visible to the human eyes. The waves are then guided to the edges of the module where actual solar cells are located and transformed into electricity. Even though this discovery is still in laboratory phase and not suitable for mass-production yet [81], it has great potential to replace the window panels in building envelopes.

1.5.2 Colour variations

Colour variations are mainly achieved by modifying components other than the solar cells themselves. As is shown in Figure 1.5-5, one way to do that is to have digital prints on the front glazing, which covers the dark and glossy crystalline solar cells [82]. To avoid mismatch and hotspots in PV modules, identical efficiency must be maintained everywhere in the same module. Therefore, each colour on the same glazing must have its unique transparency. Revolutionary white BIPV can be achieved by integrating selective scattering filters into the modules. Since crystalline solar cells mainly respond to the infrared part of the light, filters are integrated on micro-structured surfaces so that the invisible infrared rays can reach the solar cells, while the visible part of light are filtered for reflection [83]. By modifications of the filters, other colours of BIPV can also be accomplished [84], an example is shown in Figure 1.5-6. The add-value in aesthetic is always acquired, of course, by giving up certain amount of PV efficiency.

Dye-sensitized solar cells, also known as Grätzel cells, can also be produced in different colours as is shown in Figure 1.5-7. The decorations of Swiss Convention Centre's west facade are designed by the artist Catherine Bolle, having mainly yellow and red colours. These cells are not only energy generators for the building, but also protect its indoor from excessive solar radiation [85].

Organic Solar Cells (OPV) mainly refer to solar cells that are based on organic polymers or small organic molecules [86]. By using inkjet printers to deposit the solar cells onto substrates [87], [88], it allows the production of solar cells in any desired shape. Therefore the design restraint is much lower than in any other solar technologies. Figure 1.5-8 is a solar cell designed in the form of a leaf [89]. Recent barriers of their development lie mainly in the low efficiency, and the material requirements are designed only for laboratories and are not suitable for printing large panels yet [90].

Figure 1.5-5: BIPV module with digital prints on the front glazing by CC EASE, HSLU. Photo credit: Stephen Wittkopf.

Figure 1.5-6: The coloured BIPV on a carport roof. Photo credit: Stephen Wittkopf.

Figure 1.5-7: The Grätzel cells on the west facade of Swiss Convention Centre in EPFL.
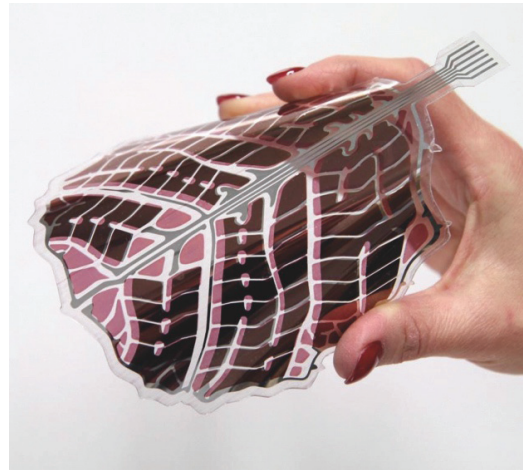
Figure 1.5-8: Printed OPV in imitation of a leaf. Photo credit: Antti Veijola, with permission to reuse from VTT Technical Research Centre of Finland.

1.5.3 Form

Traditionally people expect the PV modules to be stiff and inflexible. However, organic, inorganic and organic-inorganic solar cells deposited over flexible substrates [91] do not only make lightweight and economic solar modules possible, but also open more possibilities for integration in architectures with free forms. One common application of flexible PV can be found on ETFE membranes. The carport for Munich's municipal waste management department has their roof made of ETFE cushions with three layers [92]. The innermost layer serves as shading for the interior space

and the amorphous silicon solar cells are mounted in the middle layer (see Figure 1.5-9).

The Pure Tension pavilion designed by Synthesis Design + Architecture integrates stiff crystalline solar cells into their steel-framed structure with fluid lines (see Figure 1.5-10 and Figure 1.5-11). The roof is made of vinyl encapsulated polyester mesh membrane with crystalline solar cells attached to it. The layout of the cells follows the form of the pavilion construction and delivers it with a futuristic look [93].

Figure 1.5-9: ETFE cushions roof with integrated photovoltaic cells of Munich's municipal waste management department by Ackermann & Partner (2011). (Photo credit: Michael Fischbacher)

Figure 1.5-10: The Pure Tension pavilion. With permission for reuse from SDA|Synthesis Design.
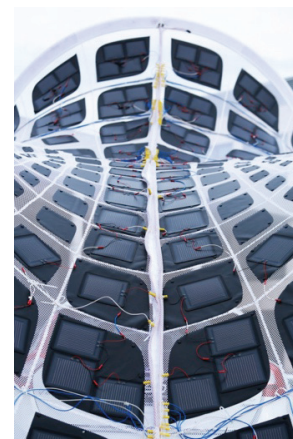
Figure 1.5-11: Closer look of the roof of the Pure Tension pavilion. With permission for reuse from SDA|Synthesis Design.

By showing the above examples, it is also apparent how technology developments affect design approaches over the time. Huge diversity of products offers new potential for architectural integration. With the PV expansion in urban spaces, the evaluation methods should be able to assess

the visual impact of BIPV made of any technology, so as to be able to minimize the negative impact.

1.6 Conclusion
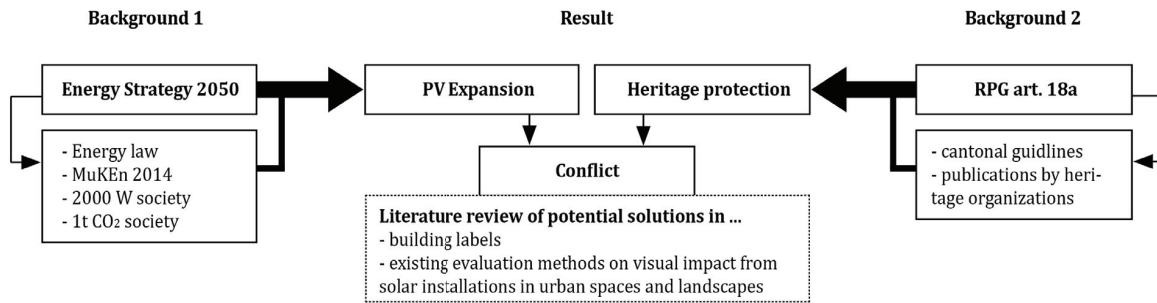
Figure 1.6-1. Conclusion of Chapter 1.

This chapter sums up the research background of the thesis. The relationships between each section are concluded in Figure 1.6-1. On the left side, the Energy Strategy 2050 led to the formation of Energy law and MuKEn 2014, and helped the existing society concepts such as the "2000 Watt society" and "1 ton CO_2 society" [94] to become even more acknowledged by the public. They are shaping the strong driving forces for creating an energy efficient and sustainable future in Switzerland, and of course are encouragements for architects to integrate BIPV in their designs. These backgrounds constitute to the inevitable expansion of PV on existing building envelopes in urban spaces.

Despite the rising popularity of BIPV, there is still a huge gap between PV and traditional building elements such as bricks, glasses and similar due to design experiences, materiality differences and implementation numbers. This mismatch has caused worrying attitudes of some parties (especially the heritage departments) concerning the negative effect that the BIPV will have on the existing city image (German: "Ortsbild"). The right side of Figure 1.6-1 shows efforts made so far to limit the negative effect. When it comes to preservation of city image, the visual impact is in the first place the most obvious factor. In order to minimize the potential negative visual impact from BIPV, tools are needed that can measure it, so as to be able to evaluate the trade-off between the past and future needs. Literature reviews were made on building labels, relevant cantonal guidelines and existing evaluation methods, so as to find out whether there are already tools available that can appropriately assess the BIPV visual impact. However, no suitable solutions were found and the reasons will be stated in Chapter 2.

Chapter 2   Problem statement

2.1 Research questions

From the literature review in Chapter 1, following drawbacks that make existing evaluation systems insufficient to assess the BIPV visual impact are identified as following:

Problem 1: Lack of measureable criteria

The goal of the RPG law article 18a is to limit the BIPV visual impact within a certain threshold. However, some outstanding characteristics can be outlined from it, namely that:

a. The criteria of "appropriately applied" (German: "genügend angepasst") solar installations on existing roofs are defined by article 32a of urban planning regulation [95].

b. Solar installations must not "obviously affect" (German: "wesentlich beeinträchtigen") the historical buildings.

The first confusion is that how an "appropriately applied" BIPV installation on an existing building facade should be like is not defined but left to cantonal authorities to decide. The second confusion is that the semantic terms "appropriately applied" and "obviously affect" are rather ambiguous in definition except for the case with roof-integrated BIPV installations. Literature reviews show that popular building labels generally avoid evaluating the architectural aspect of green buildings, probably because that would involve the use of such quantified and ambiguous terms. Not to mention how these standards should be set still remains questionable. If such cases can't be avoided, professional juries are asked for consultation. Existing qualitative evaluation methods assess the BIPV integration quality/visual impact with criteria expressed in linguistic descriptions.

The side effect in using semantic terms as criteria is that they are qualitative and can't be measured. Most of them are only valid when comparisons can be made. Expressions as "appropriately" and "obviously" are relative terms and wording is not always capable of accurately expressing human feelings in illustrating BIPV visual impact. In an experiment where 35 individuals were provided with semantic criteria such as "pleasantness", "complexity", "coherence", "openness", "affection", "originality", "naturalness", "liveliness", "degree of protection", and they were asked to evaluate the visual impact of 5 different solar power plants in different rural environments [63]. It was noticed that in some cases, no significant linguistic differences were found among individuals, even though most of them fully agree that one example case was visually more impacting than the other. This reflects the possibility that qualitative criteria, such as linguistic descriptions, cannot sufficiently

reflect human's feeling towards visual impact the way they are expected to. It is recommended accordingly to use both subjective and objective criterion mutually when assessing the visual impact of solar installations. The use of quantitative criteria can help to discover the bias in results generated from qualitative criteria.

So in order to manage the potential visual impact caused by BIPV installations on existing building envelopes, it is not enough only to determine which BIPV installation has more or less visual impact on the existing building envelopes with the use of qualitative criteria, but the knowing of the exact quantity (the "how much") of the potential visual impact is also essential. This can be achieved with the help of quantitative criteria.

Problem 2: Discontinuity of evaluation standards

Despite their advantages of rapidness and straightforwardness in the assessment procedure, another drawback of qualitative criteria on BIPV visual impact is that they are very vulnerable to subjective preferences. If the evaluations are made based on the opinions of different people, then no continuity of the standards can be expected.

Even within the same project, discrepancies can be found in the choice of words among stakeholders due to their different backgrounds and interests. This phenomenon has already been outlined by many studies [96]-[98]. The same assertion can be used for cases of BIPV in existing buildings. Engineers and building owners would consider a design that leads to a maximal solar energy yield and/or an optimal cost-efficient alternative. Architects are more likely to value the architectural harmony with the building context as well as the taste of the building owner. The local authorities cherish the bigger picture – the city image or the historical value of the building (see Figure 2.1-1). Lopez and Frontini [53] fine tuned the phenomenon stating that on one hand the engineers are not aware about the preservation issues, and on the other hand, officials who are responsible for preservation issues are not always aware of the possibilities that solar products can offer. If provided with the same subjective and qualitative criteria, different results would come out depending on the personal preferences of the jury. Worries about the lack of consistency of rating standards in different projects carried out by a small group of individuals were also expressed in landscape design that have comparable evaluation procedures [29], [99]-[101].
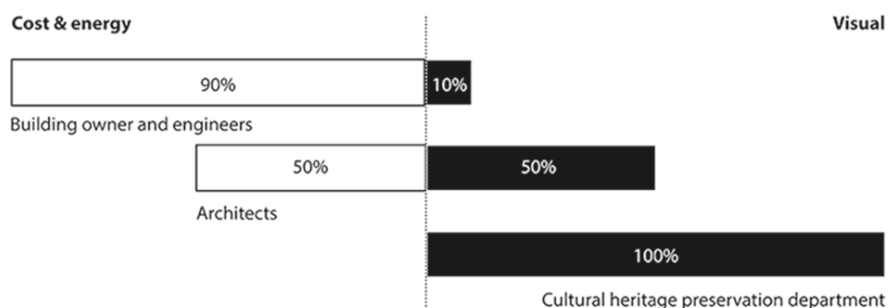
Figure 2.1-1: An abstract demonstration of the different stakeholders within the same BIPV project and their percentage of interests in cost & efficiency and visual impact.

Objective criteria on BIPV visual impact can eliminate personal preferences in assessment procedures and make sure that the evaluation standards are continuous in all projects. So the first research question is concerned about the quantification and objectivity of the criteria in the evaluation:

Research question 1: Is there a way to use measureable criteria to objectively evaluate the BIPV visual impact?

Problem 3: Missing neuroscientific relevance and result generality

The criterion "obviously affect" is a relative term. Whether a BIPV installation is considered to be "obviously affecting" the existing building envelope or its context can only be affirmed after it is compared to its environment. This comparison should also be made with the human sense of seeing and not by formal design criteria or geometric visibility, especially under the circumstance that more and more people have realized the importance of neuroscience to architecture designs [102]. However, existing quantitative and objective evaluations that assess the BIPV's integration quality/visual impact usually don't have much relationship to how human eyes perceive the outside world, e.g. the colour contrast in the human visual perception between the BIPV and the building facade hasn't been taken into account. They usually overlook the possibility that a BIPV installation may be very visible from a given point of view, but it has a camouflage cover applied on it so well that it is not easily detectable by human eyes. The cantonal guidelines have set some ground rules to make sure that the BIPV is "appropriately applied" to the existing building envelope and doesn't "obviously affect" the existing environment. The rules, however, are rather formal requirements. When integrating the neuroscientific working principle of human eyes into the evaluation method, the comparison between the BIPV with its surrounding isn't based on the subjective opinions of a small group of people, or formal geometric criteria, but rather on how humans perceive the contrast with their eyes in general. This way the generality of the results can be guaranteed. Hence the second research question is as following:

Research question 2: Can the BIPV visual impact be assessed using a neuroscientific inspired approach?

Problem 4: Difficult to combine with other technical metrics

Existing evaluation methods that evaluate the BIPV visual impact or related issues produce many different formats of results. This doctoral thesis hopes to find a way to use one single value to express the strength of BIPV visual impact on an existing building envelope. In BIPV projects, numeric results also enable easier combinations with other quantitative metrics such as energy yield, cost, payback time etc.

Research question 3: Is it possible to use a single value to express the strength of BIPV's visual impact?

The doctoral thesis is aiming at developing an objective and quantitative evaluation method for

visual impact of BIPV systems located on existing building envelopes, with an approach that has neuroscientific ground. The strengths of the BIPV visual impact are presented with single values that also enable easier combinations with other quantitative technical metrics, and offer more holistic evaluation procedures in the future. The final results of the proposed evaluation aren't subjective opinions of small group of individuals about how they perceive the visual impact, but averaged opinions of humans in general.

It is always possible to evaluate the potential BIPV visual impact on existing building envelopes by using questionnaires. Large numbers of people can be asked about what they think of the respective BIPV design. This method can reveal more straightforward opinions of the folk and guarantee the generality of the results, but it is also very expensive and time-consuming. By adapting the proposed method in practice has the advantages of saving time and lowering costs compared to conventional methods (such as passing out questionnaires).

2.2 Structure of the thesis

Figure 2.2-1 shows a rough structure of the thesis, with each chapter paired with a sentence about its key content. **Chapter 1** begins with a background introduction, presents the recent trends in BIPV and the necessity of developing an evaluation method that can objectively measure the BIPV visual impact on existing building envelopes in Swiss urban spaces. **Chapter 2** lists the drawbacks found in the existing evaluation methods and raised three research questions. **Chapter 3** introduces some simple principles of human vision, three representative saliency models, their accuracy metrics and application fields. The potential of the saliency models to assess the BIPV visual impact is discussed in the end. **Chapter 4** proposes a methodology to objectively and quantitatively evaluate the visual impact of BIPV on existing building envelopes using saliency models. The strengths of the BIPV visual impacts are expressed by single values. The application of the proposed method takes place on an actual project and is recorded in **Chapter 5**. **Chapter 6** discusses the open questions, the advantages and possible future applications of the proposed evaluation method. **Chapter 7** summarises the findings of this doctoral thesis.
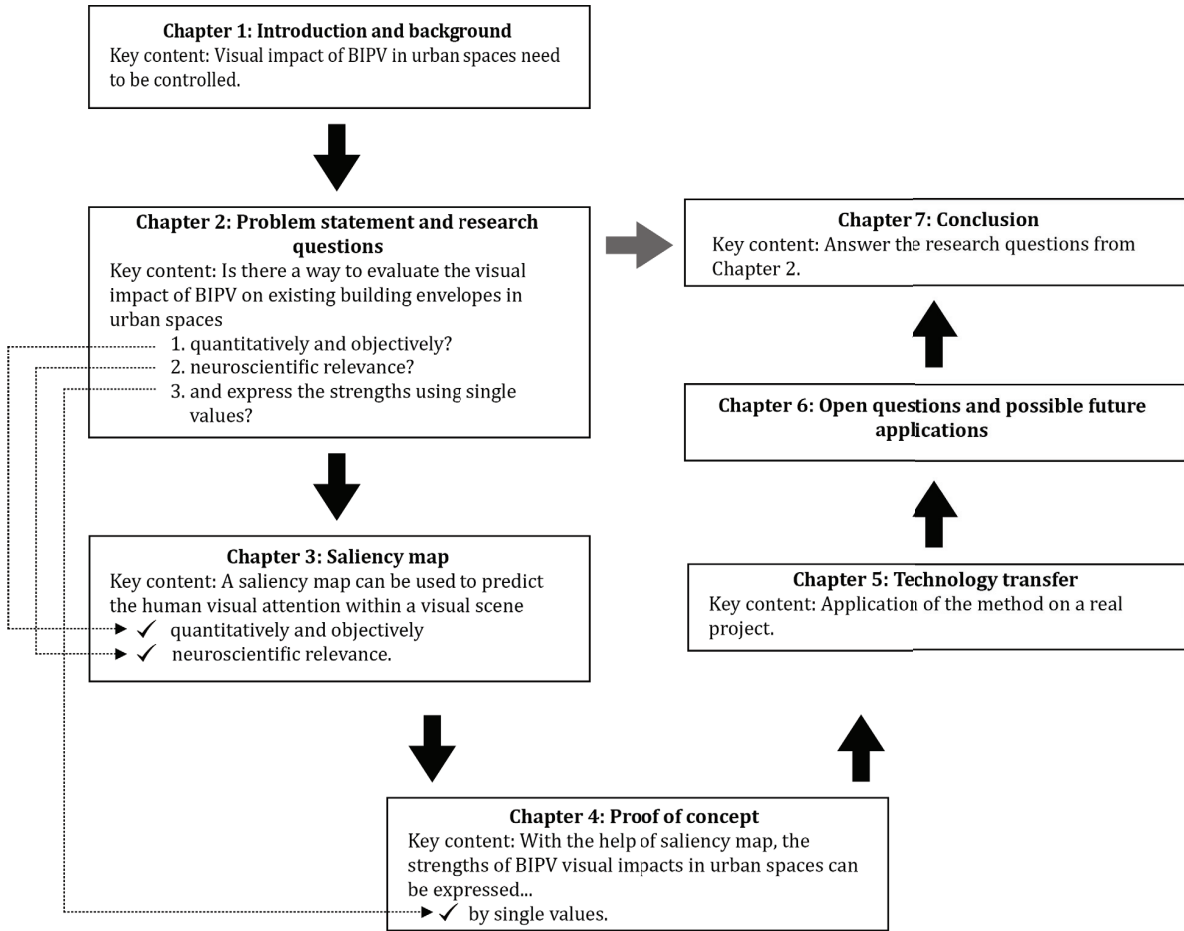
Figure 2.2-1: Thesis logic.

Chapter 3 Saliency map

The saliency map is a topographically arranged map that predicts the human visual attention towards a corresponding visual scene. It has the potential to make the evaluation method proposed in this doctoral thesis an appropriate tool to investigate the BIPV visual impact on existing building envelopes because it answers the research questions 1 and 2 stated in Chapter 2. A saliency map is produced with a saliency map model, which is a model that mainly imitates the contrast comparison mechanism of human visual attention. However, in order to comprehend saliency models, some basic introductions about human visions need to be made first. This chapter then reviews three representative saliency models, their accuracies and the usual application areas of saliency maps. In the end, the fitness of saliency maps to the purpose of this thesis is discussed.

3.1 Basic working principles of human vision

Vision plays one of the most important roles in the survival of the mankind. The human field of view is approximately 100° in the vertical direction and ca. 200° in the horizontal direction in order to get a coarse overall information of the surrounding at the first sight [103]. To avoid overload of visual information, the resolution is peaking only on the vision centre and drops sharply into the peripheral area. By detecting certain features, the focus of the vision will be guided to regions that are more salient relative to their surroundings, so as to gain more detailed information. People have spent centuries trying to understand how exactly human vision works, and the mechanism has greatly inspired the forming of saliency map models. Normally animals such as cats and monkeys were studied first so as to generalize the findings regarding their visual systems to that of human beings [104]. Take macaque as an example, if considering its outer layer (cerebral cortex) of its brain (cerebrum) as an unfolded map, the visually related areas occupy around 55% of the cerebral neocortex (the largest part of cerebral cortex) [105], [106]. The early stage of our visual processing includes neural responses in the retina, the lateral geniculate nucleus (LGN) and the primary visual cortex V1 [107], [108]. Understanding how these parts work will contribute to better understandings of the saliency models, as some mathematical operations (especially in the classic Itti-Koch-Niebur saliency model) are being inspired from the mechanism of human eyes. In the following sections, closer looks will be given to these particular parts of human visual system as well as their working principles.

3.1.1 Retina

The transport of visual information from outside world into our brains begins with the retina, which transduces light into electric and then bio-chemical signals. The rods and cones at the back of the retina are light receptors. The rods are active in dim lights and responsible for our night vision and insensitive to colours. Cones, on the other hand, work in bright light and are responsible for our colour and detail vision. Photo-pigments in the rods and cones are unstable pigments, which will change their molecule shapes and release energy when absorbing light photons. Humans are colour-blind at dim light conditions, because photo-pigments in rods only care about the photon's number instead of their wavelengths. So in certain saliency models, colour is not taken into consideration if the environment brightness is below a certain threshold. There are three types of cones, each containing different kinds of photo-pigments with different peak sensitivities to different spectrums. Different lights activate photo-pigments in different ways. These combinations of visual responses allow humans to identify different colours in the visual world (see Figure 3.1-1). A lot of saliency models start their processing with analysing the colour information of the input image.
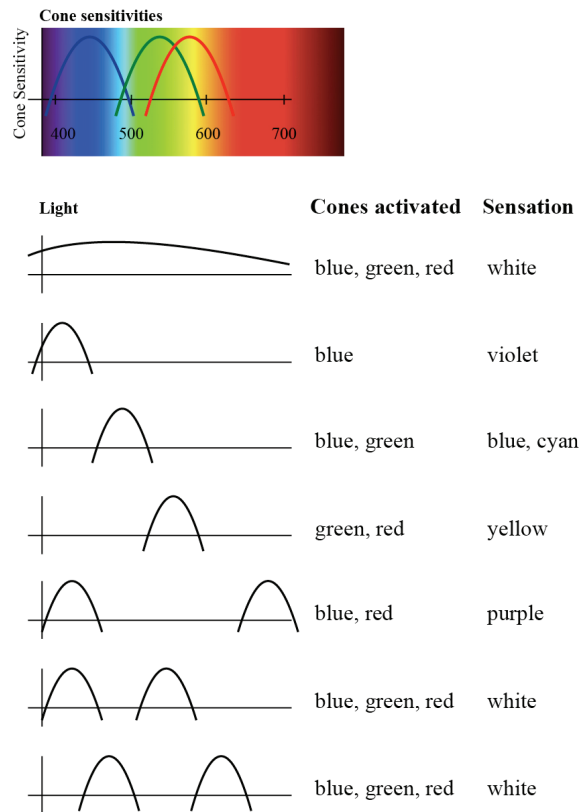
Figure 3.1-1: Cone sensitivities of colours. The graph shows the cone sensitivity along the spectrum in an arbitrary manner. Lights activate the three types of cones in different combinations, allowing humans to identify different colours (sensation). For instance, as the photo-pigments for blue and green in cones activated, colours such as blue or/to cyan can be perceived. Image with small adjustments from [109].

These "light receptors" then feed the ganglion cells in the front through the connecting nerve cells

(Figure 3.1-2). The centre of the retina, where the detail vision is maximal, is called fovea and has only cones. In this area, one cone is linked to only one single nerve cell and one single ganglion cell, thus resulting in high acuity of vision. In the periphery, several "light receptors" are linked to one intermediate nerve cell, several of which being again linked to one single ganglion cell, and thus resulting in a crude vision [109]. This explains why human vision is most acute in the centre of the view field, and become blurred in the peripheral area. This is also the reason why in saliency models, regions on the same input image are weighted differently.
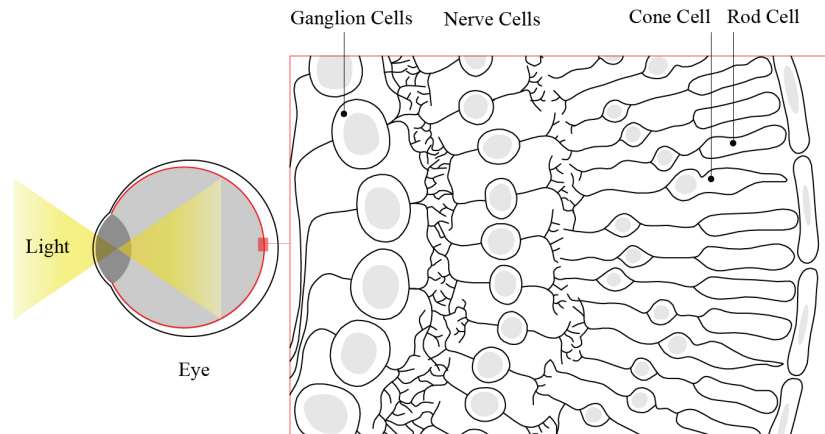
Figure 3.1-2: A schematic drawing of the retina construction.

3.1.2 Ganglion Cells

The visual information is passed on from the cones and rods to the ganglion cells. There are two types of ganglion cells, the ON-centre and OFF-centre ones. Experiments revealed that the receptive field of a ganglion cell consists of a circled centre surrounded by a large ring-shaped surrounding. The cell with an ON-centre has an OFF-surrounding, while the OFF-centre cell has an ON-surrounding. Their reactions to visual information can be observed by their firing[1] frequencies. When a stimulus (such as a light beam) is present, the ON-area responds to this by firing more frequently, while the OFF-area responds to this by suppressing the firing. The Kuffler experiment [110] explained this phenomenon in detail (Figure 3.1-3). Row 1 and 3 present the situation that when there is full light or no light on the receptive field, both ON-centre and OFF-centre ganglion cells send out slow and random signals. Row 2 presents the situation when a light spot hit the centre of the receptive field, the firings of the ON-centre ganglion cells get much more frequent; at the same time the OFF-centre ganglion cell's actions are suppressed. When the light spot moves to the surrounding receptive field, then the opposite happens: the OFF-centre ganglion cells become active (Figure 3.1-3 right, row 4), while there are no firings from ON-centre cells (Figure 3.1-3 left, row 4). This indicates that the human eyes respond to relative intensity instead of absolute intensity of the light [110]. This comparison does not only happen to brightness, but also between red-green and

---

[1] Sending out signals.

blue-yellow colour contrasts. Some operations in the saliency models are very rough imitations of how these cells function [111].
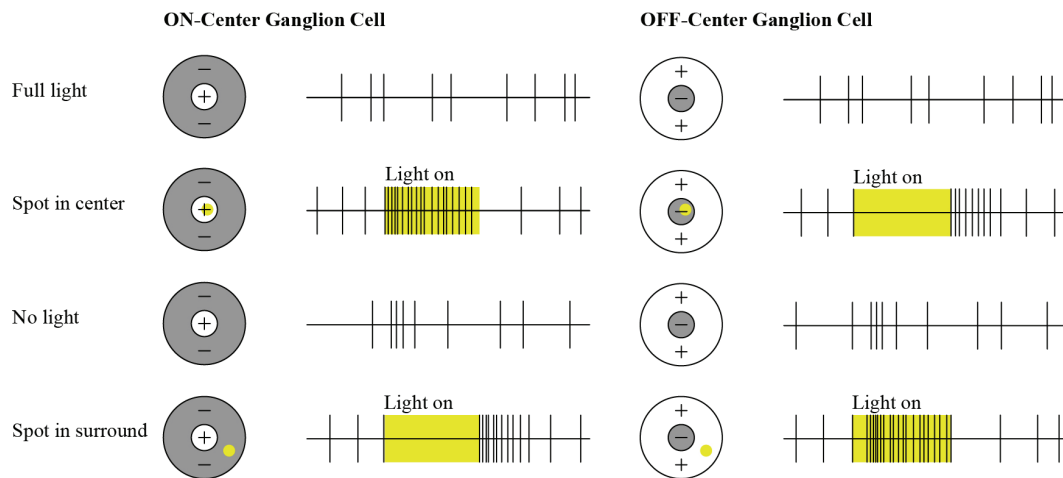
Figure 3.1-3: The Kuffler Experiment. The circle with a surrounding ring-shaped region represents the receptive areas of a ganglion cell. The area with a "+" sign represents the ON-field, the area with a "-"sign represents the OFF-field of the cell. The vertical lines on the diagrams show the frequency of the cell firings along the horizontal time axis.

3.1.3 Lateral geniculate nucleus and primary visual cortex

The information is transferred from the retina to the brain (see Figure 3.1-4). One of the many stops is in the lateral geniculate nucleus that does not only transmit the information from the eye to the brain, but also receives information from the brain. Single cells in the lateral geniculate bodies also respond similarly to light and colour in a centre-surround comparison way like ganglion cells in the retina do.
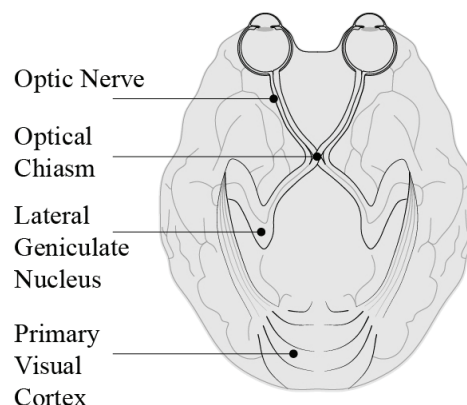
Figure 3.1-4: A schematic drawing of information pathway from human eyes to the brain.

The cerebral cortex is the outer layer of the brain made of neural tissue. The visual cortex, located in the back of our head, is the area of cerebral cortex responsible for the seeing. The primary visual cortex receives input from lateral geniculate nucleus, processes the visual information, and then sends its main output to the higher visual areas in the cortex. The neurons in the primary visual cortex can be classified into simple and complex cells; both of them are especially sensitive to oriented lines or slits, or in other words, the angle of the stimulus [105], [109], [112]. There are three kinds of simple cells in total, and two among them have long narrow slots tilted in a certain angle acting as their ON-fields or OFF-fields, with the opposite fields on outer sides (Figure 3.1-5). For the cell type a) in Figure 3.1-5, only if the light as a stimulus covers the ON region and has the same tilting angle, the cell will respond fully (Figure 3.1-6). If the stimulus touches the OFF region, then the cell response will be suppressed. For the cell type b) in Figure 3.1-5 only a dark line covering the OFF-field would evoke a full response.
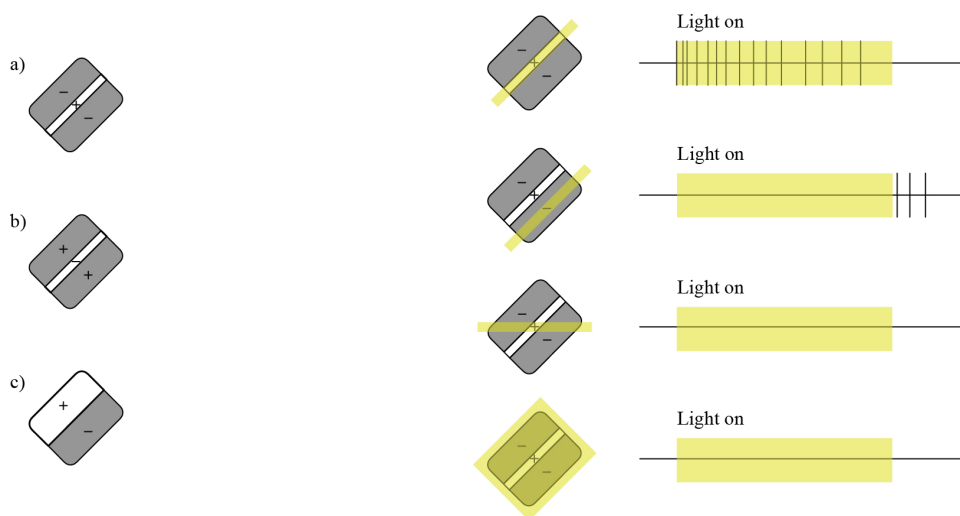
Figure 3.1-5: The three typical receptive field maps of the simple primary visual cortex cells. The "+" sign stands for ON-field and the "-" sign stands for OFF-field. Image with small adjustments from [109].

Figure 3.1-6: Examples of how the type a) simple cells from Figure 3.1-5 work under light as stimulus. Image with small adjustments from [109].

The last kind of primary visual cortex simple cells responds best to dark lines (Figure 3.1-5 c) or edges between dark & bright areas with certain tilting angles (orientation). A dark line covering the middle section or an edge of dark & bright regions falling on the boundary between both receptive fields would induce full response from the cell.

Complex cells are distinctive by the fact that simple cells only respond strongly to stationary edges/lines with certain orientations, while complex cells response to both moving and stationary edges/lines with certain orientations as long as they are on their receptive fields (Figure 3.1-7). When the orientation is false, then no firing will take place. If a person contemplates an object with a certain shape, then the contour of it will only activate a selected set of primary visual cortex cells. Both complex and simple cells response badly to dim lights.
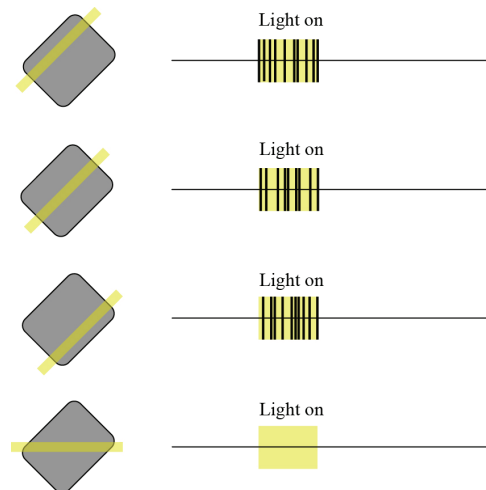
Figure 3.1-7. The complex cells in primary visual cortex. They react to long, narrow lights as long as they are placed in their receptive fields (grey area) and are in certain angles. False angles will evoke little or no response from the cells.

In a nutshell, the rods and cones in the retina transmit the visual information to the ganglion cells, lateral geniculate nucleus and other brain areas. By comparing the relative brightness, the orientation-sensitive cells in primary visual cortex will filter the edges between dark & bright areas and provide humans with information about shapes. The imitation of these features can often be found in saliency models in the form of Gabor filters.

3.2 Bottom up attention

The visual world contains enormous amount of information. In order to avoid information overload and to notice potential danger quickly, the human eyes have developed a selective attention system in order to select and prioritize visual information. There are two kinds of attention mechanisms: the bottom-up and the top-down [113]. The bottom-up attention makes a person recognize information with certain features within milliseconds instinctively and effortlessly [114] (e.g. recognizing a white object on a black background). The top-down attention happens, on the other hand, with the selection bias of one's own choices (e.g. knowledge, expectations, goals), such as finding a white object with a certain tilting angle among other white objects each with a different tilting angle. So the bottom-up attention is exogenous (caused by factors from outside of the organism or system) while the top-down attention is endogenous (caused by factors inside of the organism or system) [115]. Since in top-down attention, the visual selection bias varies for every situation and person, therefore it is not covered in this doctoral thesis due to its complexity and unpredictability.

In order to avoid information overload, first the human eyes have the highest resolution limited to the central fovea, instead of an equal resolution throughout the whole view field: the acuity declines sharply into a low-resolution periphery. Second, in order to select suitable objects for further

processing, the visual system has integrated attention mechanisms that rapidly preselects them based on certain attributes [116], [117]. These attributes can make a stimulus more noticeable from its surrounding, or in other words, make it "salient".

Wolfe and Horowitz listed the possible attributes that guide our visual attention [116]. Some of the attributes they mentioned are listed in Table 3.2-1 and categorized into five groups; the confidence level that they are attributes that guide human visual attention drops from left to right columns. Undoubted attributes, whose effects have been proven by many experiments and studies, include colour (example see Figure 3.2-1), motion, orientation (example see Figure 3.2-2-Figure 3.2-3) and size. Due to many reasons (for instance contradictory results), neuroscientists are still not clear whether the attributes listed in the most right column guide human visual attention at all. An example from this category can be seen in Figure 3.2-4, which shows the findings from investigating intersection as an attribute. Wolfe and Horowitz did not and could not make a complete list of all the attributes that guide the human visual attention, because further attributes will be added as more discoveries are gained in the future; these attributes are used as inspirations for many saliency models.

Undoubted attributes	Attributes with high confidence	Attributes with medium confidence	Attributes with low confidence	Attributes that probably do not guide visual attention
• Colour • Motion • Orientation • Size	• Shape • Line termination • Closure • Topological status • Curvature	• Glossiness • Number • Aspect Ratio	• Novelty • Letter identity • Alphanumeric category	• Intersection • Optic flow • Colour change • Faces • Your name

Table 3.2-1. Possible attributes that guide human visual attention, with the level of certainty dropping from left to right columns. This table shows some examples of the attributes mentioned in [116].
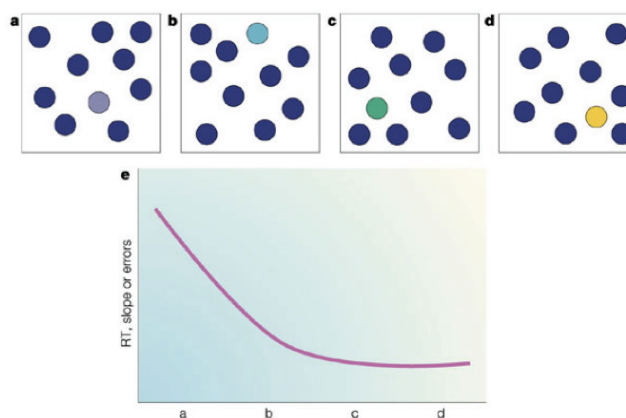
Figure 3.2-1: Finding a target among distractors using colour as an attribute. The response time depends largely on how much different the target is comparing to the distractors. From a) to d), the chromatic contrast becomes larger, therefore the response time shortens. Reprinted by permission from Macmillan Publishers Ltd: Nature Reviews Neuroscience [116], copyright 2004.
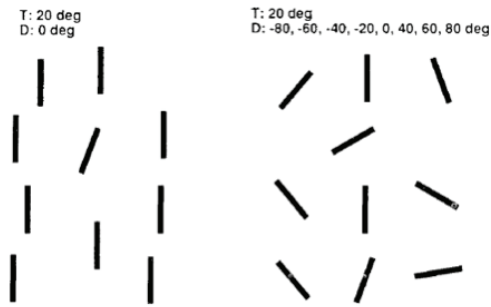
Figure 3.2-2: Example of investigating orientation or tilting angle as an attribute. In the left picture, the target is a line that is tilted 20°, and the distractors are all strictly vertical lines; in the right image, the distractors are more diverse. Results are given in Figure 3.2-3. Experiment and images from [118]. Copyright ©1992 by the American Psychological Association. Reproduced with permission.
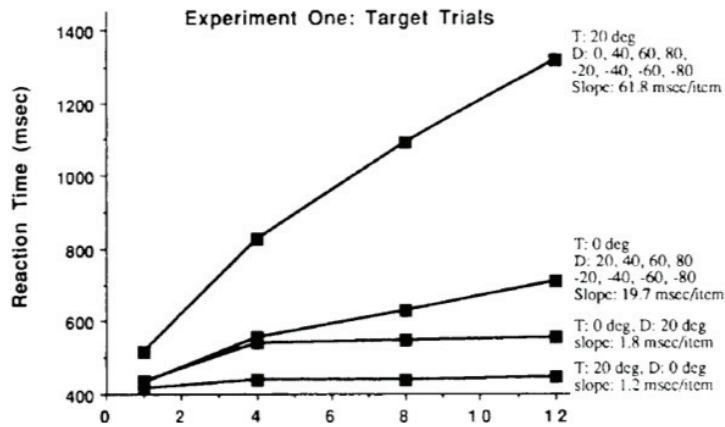
Figure 3.2-3: Example of investigating orientation as an attribute. The response time is strongly related to the difficulty of the task. If the target is surrounded by identical distractors (the two graph lines below), the response time is short; if the distractors become more diverse (two graph lines above), the response time is longer. Image source: [118]. Copyright ©1992 by the American Psychological Association. Reproduced with permission.
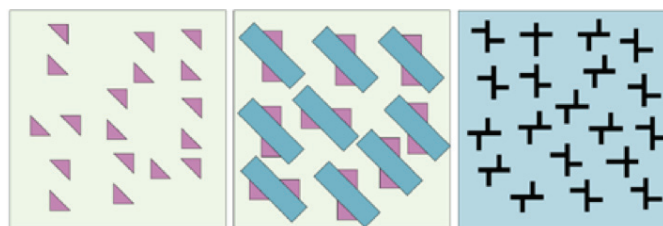
Figure 3.2-4: Finding a target among distractors using intersection as an attribute. In the left image: it is difficult to find a pair of triangles that are in horizontal angle. In the middle image: with the help of intersections between the blue rectangles and pink ones, it becomes easy because intersections can help in identifying the target. In the right image: The target, namely a "+" sign – can not be easily found using intersections as attributes. Reprinted by permission from Macmillan Publishers Ltd: Nature Reviews Neuroscience [116], copyright 2004.

In their very influential paper "A Feature-Integration Theory of Attention", Treisman and Gelade [119] suggested that the visual scene is coded in different dimensions, such as colour, orientation, size, motion, depth etc. and assumed that the visual processing comprises of two stages (see Figure 3.2-5). In the first pre-attentive vision stage, the features are recognized early and instinctively. In the second attentive vision stage, stimuli are processed serially again with focal attention and are put together for object recognition: the features are "glued" into objects by the focused attention. In simpler words, a person grasps crude information about the visual field at the first sight and then pays special attention to detailed information regarding certain regions (guided by e.g. colours, orientation etc.). After putting together the detailed information by quickly moving his eyes, objects can finally be recognized.

| Visual field | → | **Preattentive Processing** | → | **Focused Attention** | → | **Object recognition** |

Registration of
feature 1 of dimension 1
feature 2 of dimension 2
etc. early, automatically and parallely

Processing the stimulus locations
serially with focal attention in order
to recombine these features for each
object
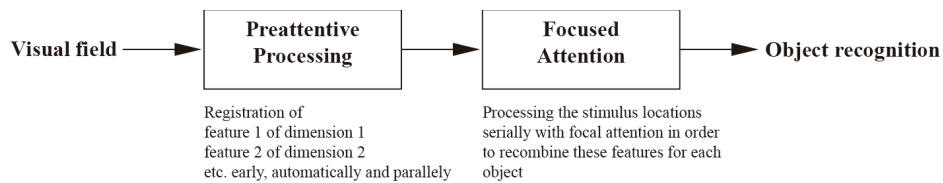
Figure 3.2-5: The two-stage visual processing of *Feature Integration Theory*.

Later, Wolfe and Horowitz [116] suggested that the dimensions should be considered as "control devices" instead of conventional "filters". If a person were asked to search for a red line, "filtering" for colour red would pass red objects and make everything else that is not red invisible for us; this is not the case in reality since the awareness for other colours still exists. A "control device" would, on the other hand, let the colour red pass for object recognition, but the human eyes are still aware of the rest of the image (see Figure 3.2-6).
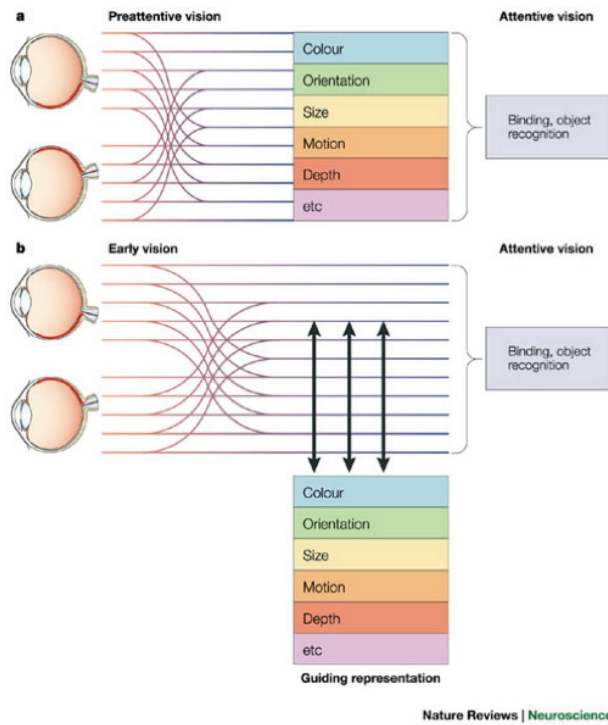
Figure 3.2-6: a) Traditional understanding of the two-stage attentive vision: the visual information is screened by "filters" of different dimensions, deciding which ones induce the object recognition. b) The suggestion made by Horowitz and Wolfe states that the dimensions must be referred as "control devices" deciding which features are important and which ones are not for the object recognition. Reprinted by permission from Macmillan Publishers Ltd: Nature Reviews Neuroscience [116], copyright 2004.

In 1985, Koch and Ullman introduced the concept of saliency map based on the decisive features mentioned in *Feature Integration Theory*. The saliency map is a topographical map that predicts the visual saliency of a corresponding visual scene. On a scale from 0 to1, the saliencies of the regions are indicated. A more salient spot in the map has higher saliency values, indicating that its respective region in the visual scene has a higher probability to be paid attention to by human eyes [120]. The implementation of the saliency map was published in 1998 by Itti, Koch and Niebur [121]. Thus giving a head start to the flourishing development of visual attention modelling. An example of saliency map is given in Figure 3.2-7.
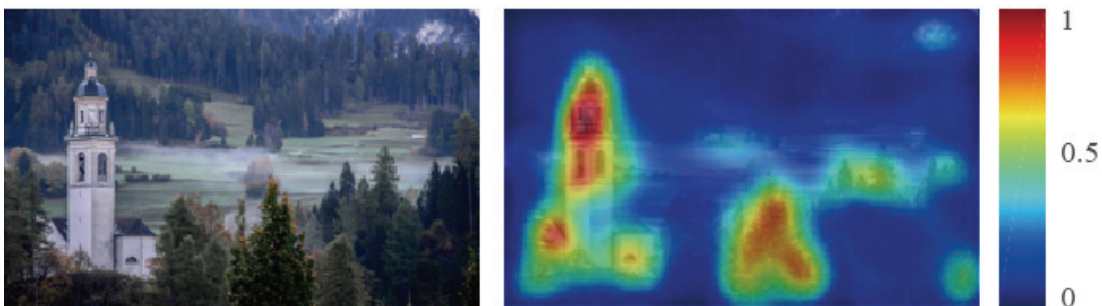
Figure 3.2-7: An input image (left) and its saliency map (right).

3.3 Saliency Models

In this chapter, three representative saliency models are introduced by explaining the crucial procedures. An input image is needed from which digital information is retrieved. The saliency model analyses the information by evaluating the contrasts between the pixels or patches with different approaches. At the end, a saliency map that combines all the evaluation results will be produced. The three saliency models are chosen based on certain selection procedures that will be explained in section 4.1.1.

3.3.1 Itti-Koch-Niebur Saliency Map Model (IKN)

First, three early visual features are extracted through linear filtering of an input image in this model. These features, namely colour, intensity and orientation, not only show a strong relationship with the *Feature Integration Theory* [119], but also with the neuroscientific working principle of human eyes. The approximate workflow of the IKN saliency model is illustrated in Figure 3.3-1.

1   **Input Image**   1

Linear Filtering

Intensity
$I=(r+g+b)/3$
- r, g, b are normalized by I
- if I<Imax/10, then I=r or g or b

Color

Red	Green	Blue	Yellow
R = r - (g+b)/2	G = g - (r+b)/2	B = b - (r+g)/2	Y = (r+g)/2 - |r-g|/2 - b

Orientation
$\theta=0°$ $\theta=45°$ $\theta=90°$ $\theta=135°$

2

----

3   Gaussian pyramid $\sigma=[0..8]$ Gaussian pyramid $\sigma=[0..8]$ Oriented Gabor Pyramids $\sigma=[0..8]$ 3

----

4   Center-Surround Operation $I(c,s)=|I(c) \ominus I(s)|$ Center-Surround Operation $RG(c,s)=|R(c)-G(c)) \ominus (G(s)-R(s))|$ Center-Surround Operation $BY(c,s)=B(c)-Y(c)) \ominus (B(s)-Y(s))|$ Center-Surround Operation $O(c,s,\theta)=|O(c,\theta) \ominus O(s,\theta)|$ 4

----

5   6 feature maps   12 feature maps   24 feature maps   5

----

6   Combination of 42 feature maps
- across-scale addition
- point by point addition
- N(.) normalization operator which is used to ignore homonegous area and promote peak values   6

----

7    $\overline{I}$ conspicuity map $\overline{C}$ conspicuity map $\overline{O}$ conspicuity map   7

----

8   Linear Combinations $S = (N(\overline{I}) + N(\overline{C}) + N(\overline{O}))/3$ 8

----

9   **Saliency map**   9

----

10   Winner Take All   Inhibition of Return   10

Attended location

Figure 3.3-1: Workflow overview of IKN according to [121]. The columns A, B, C and rows 1-10 will be used as map locations and referred to as '(location: xx)' in the following text.

As shown in Figure 3.3-1, the intensity information I (location: A2) is extracted by the way of the following equation:

$$I = (r + g + b)/3$$

whereas r, g and b being the red, green and blue channel of the input image. Based on the intensity information I, a Gaussian pyramid[2] (location: A3) is created; through centre-surround operations[3]

---

[2] The Gaussian pyramid is often used to extract information or structures of interest and to attenuate noise in images. A low pass Gaussian pyramid is used to smooth and reduce (sub-sampling) the original image by several times, usually each time by the factor of 1/2 along each coordinate. In this paper, the low pass Gaussian pyramid has 8 levels, meaning that the sizes of the reduced images are $1/2^0$ to $1/2^8$ of the original.

[3] Centre-surround operation is processed in order to roughly imitate the functions of centre-surround cells in our

(location: A4), six intensity feature maps are produced.

The colour information extraction from the input image starts by normalizing the colour channels r, g, and b with intensity value, so as to decouple hue from luminous intensity. Since the rods in the retina are responsible for the vision in the dark and insensitive to colours, only locations of colour channels with an intensity value larger than a given threshold are normalized. The threshold is set to 1/10 of the maximum intensity value in the image; r, g, b values for locations with intensity values lower than this threshold remain unchanged. Then four broadly tuned colour channels are generated (location: B2), namely:

$$R = r - \frac{g + b}{2} \; for \; red,$$

$$G = g - \frac{r + b}{2} \; for \; green,$$

$$B = b - \frac{r + g}{2} \; for \; blue,$$

$$and \; Y = \frac{r + g}{2} - \frac{|r - g|}{2} - b \; for \; yellow,$$

with negative values set to zero. For each of these 4 broadly tuned colour channel, Gaussian pyramids are created (location: B3).

The human visual system is sensitive to the contrasts between red-green and blue-yellow colour pairs. These contrast information are provided through centre-surround operations (location: B4):

$$RG(c,s) = \left| (R(c) - G(c)) \ominus (G(s) - R(s)) \right| \; for \; green \; and \; red \; color \; pair,$$
$$and \; BY(c,s) = \left| (B(c) - Y(c)) \ominus (Y(s) - B(s)) \right| for \; blue \; and \; yellow \; color \; pair,$$

where centre scale $c \in \{2,3,4\}$ and surround scale $s=c+\delta$, $\delta \in \{3,4\}$, thus resulting in 12 colour feature maps. The $\ominus$ sign stands for across-scale difference between two maps, which are calculated by the way of interpolation to the finer scale and point-by-point subtraction.

The Orientation features focus on edges with orientation angles of 0°, 45°, 90°and 135° (location: C2). 24 Orientation feature maps are generated by the oriented Gabor filters[4] (location: C3), 6 for each orientation angle.

---

visual system [111]. It is calculated by the differences between the finer and coarser scales of images, where finer scales having pixels at the scale of c={2,3,4} and the coarser scales being s=c+δ, with δ={3,4}. Then the differences between the finer and coarser maps are calculated by interpolation to the finer scale and point-by-point subtraction.

[4] Oriented Gabor Pyramids: involve 2D Gaussian kernels and sinusoidal plane waves [122], [123]. By giving frequency and orientation as parameters, they can be used for edge detection in an image. The sensitivity of the orientation simple cells within their receptive field in human visual cortex can be roughly imitated with operation.

At the end, with the 12 feature maps for colour information, 6 feature maps for intensity and 24 feature maps for orientation, 42 feature maps are generated in total (location: row 5).

The next step is to combine the features maps within the categories of colour, intensity and orientation respectively. Conspicuity maps C_C, C_I and C_O are produced accordingly. In order to avoid the conspicuity maps to be overly homogenous, a normalization operator N(.) is used to foster the peak values within the feature maps and suppress the homogenous areas (location: row 6 and 7). These three maps are then linearly combined into a single final saliency map (location: row 8):

$$S = \frac{C_C + C_I + C_O}{3}$$

Itti, Koch and Niebur affirm that the values of saliency map can be considered as excitatory inputs that can activate certain visual neurons when reaching a certain threshold. In case the first neurons (winners) are being activated, all the others will be inhibited simultaneously and the focus of attention will be directed to the target of the "winner" neurons: this is called the "Winner Take All" mechanism. An "Inhibition of Return" mechanism prevents the same "winner" neurons being excited repeatedly and the attention being directed to the same location. Instead, the fovea of attention will then attend to the next salient places after being done with the current one.

The IKN saliency model's first implementation was described in [121], and later improved by [124]. An adaption was also made by J. Harel [125].

3.3.2 Graph-Based Visual Saliency (GBVS)

Harel et al [126] suggested to divide the processes of the leading visual saliency models into three main stages, namely:

Stage 1: Feature extraction: Retrieving information from the input image.

Stage 2: Activation. Using information extracted in the Stage 1, certain maps can be produced for the activation of the next step.

Stage 3: Normalization/Combination. The activation maps can be combined into a single final map. During the combination process, certain normalization procedures must be applied so as to avoid getting a homogeneous final map.

Using the IKN saliency model as an example, stage 1 consists in extracting colour, intensity and orientation features from the input image. Stage 2 is centre-surround operations, and stage 3 the normalization and combination of the feature maps and conspicuity maps into a final saliency map. In this saliency model, a different approach is proposed for step 2 and 3, which were inspired by the

Markov chains[5] and Directed Graph[6].

For the Step 2: Activation. It is assumed that for this step the feature maps already exist. The goal is to find out locations that are unusual compared to their surroundings. The dissimilarity between locations (i,j) and (p,q) is expressed as:

$$d((i,j)||(p,q)) = |log M(i,j) - \log M(p,q)|$$

where M(i,j) and M(p,q) are proxies of locations (i,j) and (p,q) respectively. The purpose is to calculate the difference between these proxy values; depending on the situation, is was found out that sometimes the simpler version |M(i,j) − M(p,q)| would work as well. Then a Directed Graph is created, each of its vertices being connected with all the other vertices. The next step is to assign weighting coefficients to the arcs, which can then be calculated as:

$$w_1((i,j),(p,q)) \triangleq d((i,j)||(p,q)) \times F(i-p, j-q), \text{ where}$$

$$F(a,b) \triangleq \exp(-\frac{a^2+b^2}{2\sigma^2}).$$

σ is a free parameter and its value is set to approximately 1/10 − 1/5 of the maps width. The weight is dependent on both the values on locations (i, j) & (p,q) and their physical distance between each other. The vertices are treated like discrete states in a Markov chain, the weights w being the transition probabilities from one state to the other; the outgoing edges of a single vertex are normalized in such way so as to guarantee that its sum equals 1 [129]. Higher values are accumulated at vertices that have higher differences compared to their surroundings. Lower values are accumulated at vertices in homogenous areas that have lower differences with their surrounding.

If M(i,j) and M(p,q) had similar values, then $\left| log \frac{M(i,j)}{M(p,q)} \right|$ would be close to 0, or if located close to

each other then $\exp(-\frac{(i-p)^2+(j-q)^2}{2\sigma^2})$ would also be close to 0.

---

[5] A Markov chain studies a time-discrete stochastic (random) process at discrete time points 0, 1, 2…and is characterized by a serial of states and the transition probabilities between the states. The process Z_n and $n \in \mathbb{N}$ is considered to be having the Markov property, if the probability for the state Z_{n+1} $(n \geq 1)$ is only determined by the state Z_n of the process at time n, and not by any other past events [127].

[6] A Directed Graph (also: Digraph) D consists of a (non-empty and finite) set V made of vertices, and a finite set A made of arcs (ordered pairs of vertices). Therefore a Digraph is often expressed as D=(V;A) [128]. The figure below is an example Digraph. The vertices are x, y, z, u, v and w. The arcs are (u,v), (u,w), (w,u), (z,u), (x,z) and (y,z) with directions and weights. The lines with arrows are called edges. Take the arc (u,v) as an example, the vertex u is its tail, and the vertex v is its head. Its weight is 0.7.

An example of Digraph
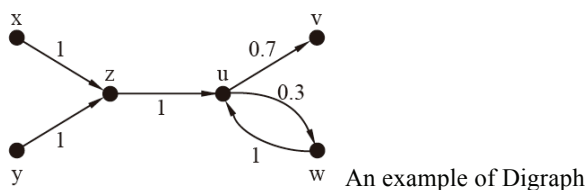
Harel et al believed that this approach has a neuroscientific ground because the human visual neurons work also in a connected and organized network. The synaptic firings (signals through which a neuron passes information to another neuron) could be seen as the edges that connect the vertices.

Step 3: Normalization/Combination is carried out in a similar way as step 2. Its goal is to guarantee the conspicuity of a few key locations. This is necessary because if normalization of the individual activation maps did not take place before the combination, the final combination map would be very homogeneous and therefore uninformative. For each node (i,j) and (p,q) on the activation map A from step 2 that needs to be normalized, a Directed Graph G is created. The weight of the edge in G that goes from node (i,j) to node (p,q) can be expressed from the values in the activation map A and the relative distance between the two nodes:

$$w_2((i,j),(p,q)) \triangleq A(p,q) \times F(i-p, j-q)$$

The edges need to be normalized so that all outgoing edges values sum up to one. In the end, vertices with higher differences compared to their surroundings will have higher values as well.

To summarize, the main advantages of the GBVS saliency model are the following:

1. Due to the nature of the algorithms, vertices in the centre have higher values accumulated than vertices on the border of the image; this is favourable since the human eyes are centre-biased.

2. The fact that every vertex is connected to all the other vertices in the Directed Graph is a significant advantage compared to the centre-surround operation in e.g. IKN saliency model, where only the relationships between locations with their limited immediate surroundings are investigated.

This saliency model was published in the journal paper [126].

3.3.3 Visual Saliency Detection by Spatially Weighted Dissimilarity (SWD)

In contrast to the IKN and GBVS saliency models, [130] no special features are initially designated in this methodology: it is believed that these information are included automatically in the image data. The first step is to divide the image I with dimensions of (H x W) into patches of size (k * k) pixel sizes. The total number of the patches is therefore equal to L=(H/k) * (W/k). The three colour space components for each pixel of the patch p_i (where i=1, 2, ..., L) are presented by a column vector f_i with $3k^2$ values. For the whole image, the matrix A comprises all the vectors, so that $A = [f_1, f_2, ..., f_i, ..., f_L]$. A schematic drawing of step 1 is illustrated below on Figure 3.3-2.
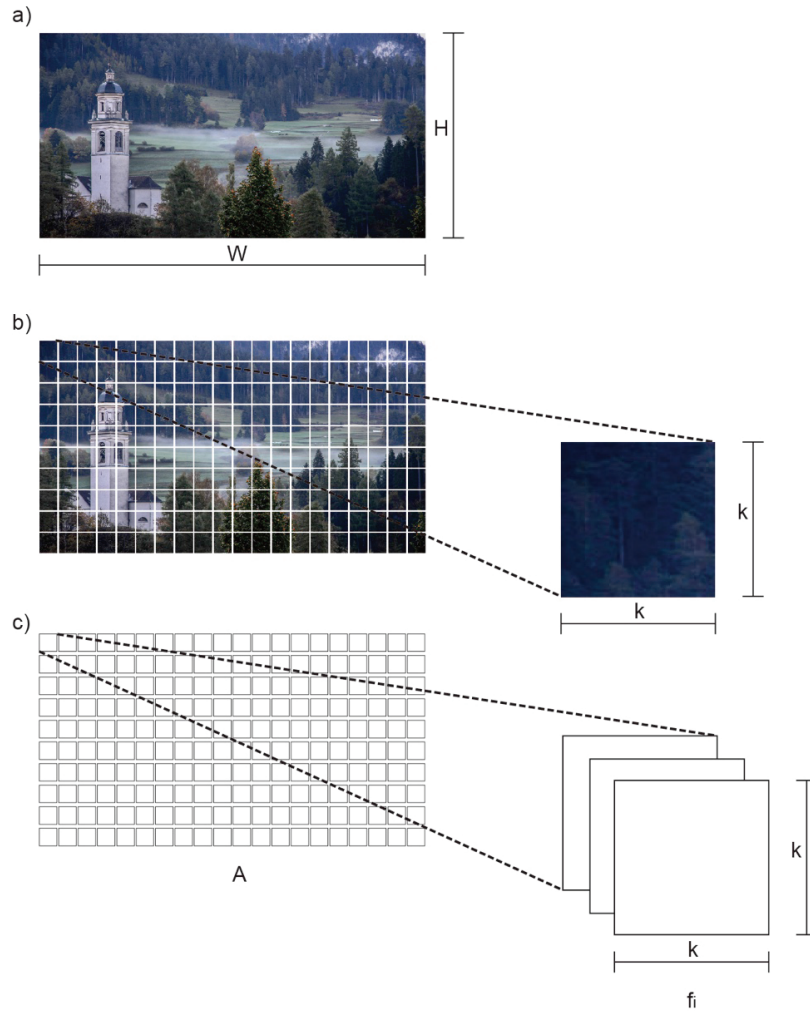
Figure 3.3-2: The step 1 of SWD saliency model. a) The original image and its size; b) the original image is divided into several patches; c) each patch is represented by the column f_i with $3k^2$ values.

The second step is to reduce the dimensionality of A, in order to foster an overall data trend by extracting the most important data and abolishing the less important ones. In each vector f_i, the average along the vector is subtracted; a co-similarity matrix is produced by $G = (A^T A)/L^2$. The size of G is L^2. Normally the largest matrix eigenvalues and their eigenvectors can best represent in an optimal way the distribution of the data. In the case of matrix G, the largest eigenvalues and their eigenvectors $U = [X_1, X_2, \ldots, X_i]^T$ are chosen. The size of U is (d * L). By the end of this step, each patch p_i is no longer presented by the vector f_i, but by the eigenvector $X_i = [x_{1i}, x_{2i}, \ldots, x_{di}]^T$ that represents the general trend of the patch's data distribution.

The third step consists of evaluating the dissimilarities between the patches based on their proxies, in addition to their respective distance with each other and to the image centre. The saliency of the patch p_i in comparison to p_j is calculated as following:

$$Saliency(i) = w_2(i) \times \sum_{j=1}^{L} \{w_1(i,j) \times Dissimilarity(i,j)\}$$

where

$$Dissimilarity(i,j) = \sum_{s=1}^{d} |x_{si} - x_{sj}|$$

$$w_1(i,j) = \frac{1}{1 + Dist(p_i, p_j)}$$

$$w_2(i) = 1 - DistToCenter(p_i)/D$$

$$D = \max_j \{DistToCenter(p_j)\}$$

where x_{si} is the i-th value in eigenvector X_i and x_{sj} the respective value in X_j. It can be seen that the dissimilarity between patches p_i and p_j is represented by the difference between their proxy values. Weight w_1 is the impact from the spatial distance between the two patches; the farer they are from each other, the less they have impact on each other's saliency values. Weight w_2 is introduced based on the fact that human eyes tend to be directed to the image centre, therefore the closer the patch is to the centre, the larger is its contribution to the saliency value. The D is a normalization factor. Figure 3.3-3 shows that after comparing the results of this saliency model with human eye fixations, better results can be achieved by including the dimensionality reduction operation (second step) of the saliency model. The ideal size for the patches is k=14.
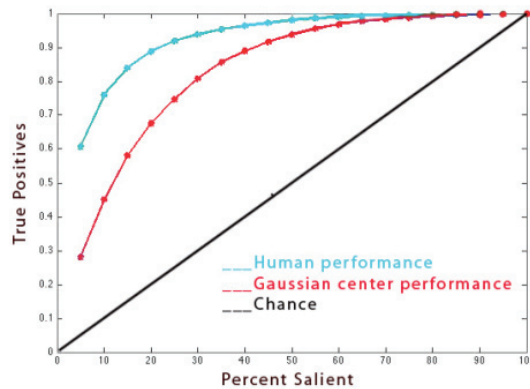
Figure 3.3-3. Patch sizes and AUC score. Image with slight adaption from: [130], ©2011 IEEE.

3.4 Accuracy evaluations for saliency models

In general, in order to measure the accuracies of the saliency models, input images are fed to saliency models; the same images are also given to humans and their eye fixations on these images are being tracked. Then the saliency maps are compared with the eye tracking results. The more similar the saliency map is to the human eye fixations, the higher the accuracy. It is important to note that a map containing discrete human eye fixations can be transformed into a continuous saliency map if needed.

There are several methods to evaluate the similarities between a saliency map and the human eye fixations. According to Riche et al [131], the current similarity metrics can be categorized according to their application areas:

i. The common metrics, which are existing scientific metrics that were not developed specially for saliency model evaluations
ii. The hybrid metrics, which are existing metrics that were adapted to become suitable for the saliency model evaluations
iii. The specific metrics, those were specifically developed for saliency model evaluations.

Borji et al [132] suggested to use the Linear Correlation Coefficient (CC), the Normalized Scanpath Salience (NSS) and the Area Under Curve (AUC-Borji) as accuracy metrics in their saliency map benchmarking system. Judd et al [133] proposed to use the Area Under Curve (AUC-Judd), the Similarity Score, and the Earth Mover's Distance (EMD). Table 3.4-1 shows these metric categories. Each of them will be explained in the following content.

Category	Metric
Common	AUC-Judd
	CC
	Similarity Score
Hybrid	EMD
Specific	NSS
	AUC-Borji

Table 3.4-1: Categorizations of selected metrics that measure the accuracies of saliency maps according to [131].

AUC (Area Under Curve)

This metric was inspired by the ROC (Receiver Operating Characteristic) from signal detection theory and measures the similarity between two sets of data. Two continuous saliency maps are given: the first one is the ground truth saliency map (GSM) and is obtained from a discrete human scanpath (information containing the eye fixations in a serial order). The other one is the prediction saliency map (PSM), which is generated from a saliency model. A threshold is used to assess the

relative fraction of salient pixels on the GSM and the PSM. By comparing the saliency values with the given threshold, both maps are transferred into binary maps respectively. On the binary maps, each one pixel is classified as either salient or non-salient given whether its value is larger or lower than the threshold. In a similar way to trials in the signal detection experiments, four criteria are used: true positives (TP), false positives (FP), false negatives (FN) and true negatives (TN) are applied (see Figure 3.4-1 a). The TP is the number of salient pixels that are among top n percent and are found in both GSM and PSM, the TN is the number of salient pixels among top n percent that can not be found in either maps. The FP is the number of salient pixels among top n percent that can only be found in the PSM and the FN is the ones that can only be found in the GSM. The TP rate is calculated according to the following function:

$$TP\ rate = \frac{TP}{TP + FN}.$$

A value of one indicates that there is no FN, and therefore that the two saliency maps GSM and PSM matches perfectly with each other.
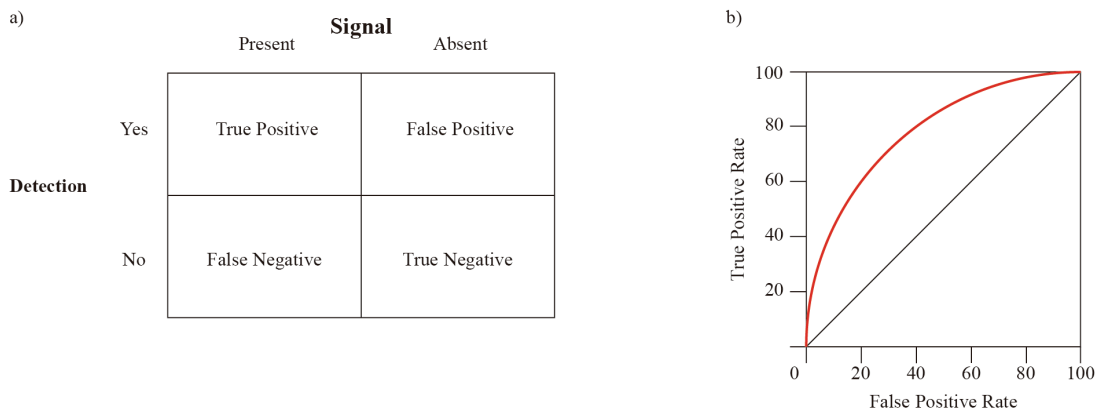
Figure 3.4-1: Diagram a) shows the example of experiments in Signal Detection Theory. The signal can be either present or absent, an observer has to express whether he has detected the signal or not by pressing yes or no button. This experiment was designed to observe how humans detect signals under foggy situations, for instance in a noisy environment that disturbs the reception of signals. Note that the sum of TP rate and FN rate equals 1, and the same goes for FP and TN. Diagram b) shows a classical ROC curve. Red line shows the relationship between TP and FP rate. The black diagonal line is the chance line, where the observer detects the signal completely by chance (50% TP and 50% FP).

The AUC-Judd suggested by Judd et al [134] compares two saliency maps in a similar way. By producing a binary classifier from a saliency map, the pixels that are categorized as among top n percent in the map are counted as TP if they overlap with the human fixation points. Unlike traditional ROC curve, here the curves are used to express the relationship between the TP rate and the top n percent salient pixels (Figure 3.4-2).
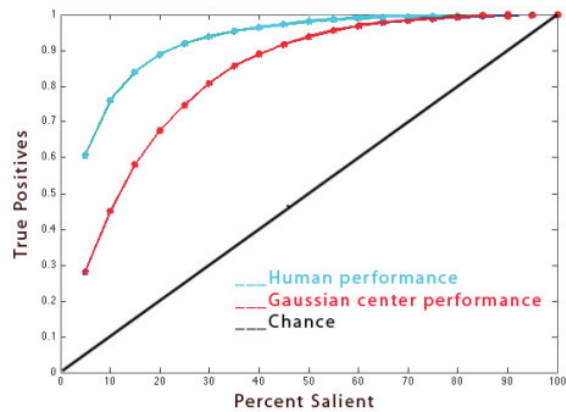
Figure 3.4-2: The AUC-Judd diagram. The correlation between the TP and the n percent salient is computed in this diagram. The black diagonal line is the boundary that indicates a result that happened by random guessing (50% TP and 50% FN). This graph shows that in predicting where other humans may look in the picture, a saliency map transformed from actual human eye fixations has a higher TP rate than a saliency map with only a Gaussian blob in the centre. Source: [134], ©2009 IEEE.

The shuffled AUC metric suggested by Borji et al in [132] is similar to the traditional ROC curve (Figure 3.4-1b). The same binary classifiers are generated from saliency maps like the AUC-Judd. The difference is that while there is a positive set of values for the human fixation points of this particular image, a negative set of values exists as well, which is composed of all eye fixations of other viewers on all the other images except the positive set. This is done in order to eliminate the centre-bias effect (human tend to look into the centre of the image) and provide with more weight on the off-centre fixations. In the end, the relationship between the TP rate and FP rate has been demonstrated: the area under the curve shows how well the saliency map performs. On a scale from 0 to 1, the higher the value, the more consistent the saliency map is with the eye fixation points.

Linear Correlation Coefficient (CC)

The CC metric is also called the Pearson correlation coefficient [131], [135] and can be used to compare the correspondence between two variables. Given two saliency maps H and P, one has:

$$CC = \frac{cov(H,P)}{\sigma_H \sigma_P}$$

where the cov(H,P) stands for the covariance between maps H and P, and the $\sigma_H \sigma_P$ for the standard deviation of the maps H and P respectively. The CC varies between -1 and 1; with -1 or 1 indicates that there is a perfect correlation between two maps, only the direction of correlation changes with the negative value in comparison to the positive one. The closer the CC value is to 0, the lower is the correlation between the two maps.

Similarity Score

This score measures the similarity between two distributions. Each distribution is scaled so that each of their total sum is 1. The similarity is measured by the sum of the minimum values of two respective bins in the two distributions. Two maps P and Q are transformed into two histograms with n bins, their similarity can be calculated as following:

$$S = P \cap Q = \sum_{i=1}^{n} \min(P_i, Q_i)$$

$$where \sum_{i=1}^{n} P_i = \sum_{i=1}^{n} Q_i = 1.$$

On a scale from 0 to 1, S=0 indicates that there is no similarity between the two maps, and 1 means that they are identical. This method was inspired by Swain and Ballard's histogram matching method [136].

Earth Mover's Distance (EMD)

The Earth Mover's Distance measures the minimum required effort to transform one histogram into the other. Given two saliency maps P and Q, they are transformed into histograms, and the EMD is given by:

$$\widehat{EMD}(P, Q) = (\min_{\{f_{ij}\}} \sum_{i,j} f_{ij}\, d_{ij}) + |\sum_{i} w_{pi} - \sum_{j} w_{qi}| \propto \max_{i,j} d_{ij}$$

$$s.t. \sum_{j} f_{ij} \leq w_{pi}, \sum_{i} f_{ij} \leq w_{qi}, \sum_{i,j} f_{ij} = \min\left(\sum_{i} w_{pi}, \sum_{j} w_{qi}\right), f_{ij} \geq 0$$

where $\{f_{ij}\}$ denotes the flow. f_{ij} is the amount that should be transformed from location i to j. d_{ij} is the ground distance between bin[7] i and bin j in the distribution; w_{pi} and w_{qi} represent the weight of these locations respectively. The ground distance between this supplier/demander to all other demander/supplier is set to be $\propto$ times the maximum ground distance. The larger the EMD is, the more effort it takes to make two maps similar, therefore the larger is the difference. Judd et al [133] used the EMD fast implementation method without ground distance threshold suggested by Pele and Werman [137] .

Normalized Scanpath Salience (NSS)

This metric was proposed by Peters et al [138] to assess the correspondence between a saliency map

---

[7] A column of a histogram.

with a set of eye fixations. Based on the original saliency map, a standardized saliency map (SM) is created which has a zero mean (μ_{SM}) and a unity standard deviation (σ_{SM}). Then, on each spot of the actual eye fixation point x, the saliency value on the SM, the SM(x) is provided to calculate the NSS value of point x:

$$NSS(x) = \frac{SM(x) - \mu_{SM}}{\sigma_{SM}}$$

The final NSS score is calculated from the average of NSS(x) for all locations:

$$NSS = \frac{1}{N} * \sum_{x=1}^{N} NSS(\ x),$$

where N is the total number of eye fixations.

This metric was built assuming that if human attention was fixed on certain spots, then the saliency value of this point must be high, meaning that its value should be very far away from the mean. Therefore if a NSS value is larger than zero, it means that the difference between the standardized saliency value and the average is high, suggesting a large correspondence between fixation locations and salient values; a value of zero means that the standardized saliency value in this location is equal to the average (in other words, not standing out at all). A demonstration example is shown in Figure 3.4-3.
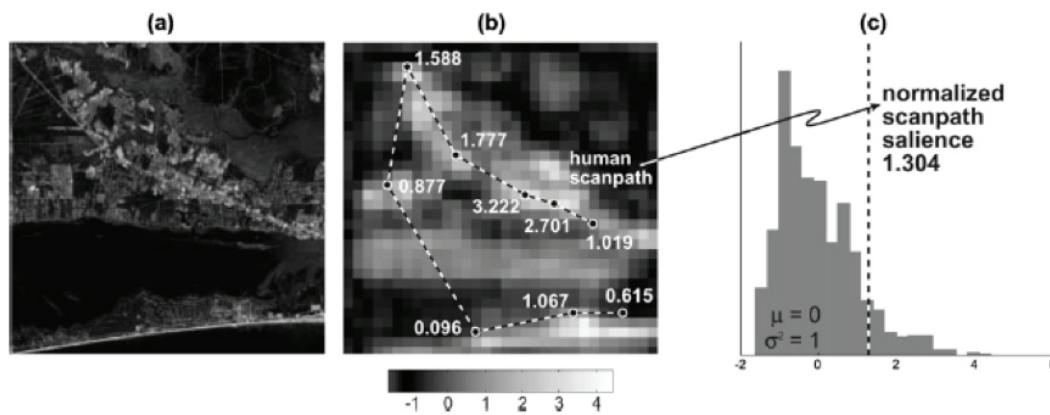
Figure 3.4-3: Application of NSS metric according to Peters et al. (a) The original image. (b) The standardized saliency map SM, with dotted line indicating the scanpath of the human eye, and the black dots the human eye fixations. The numbers are NSS(x) values. (c) The value distribution of SM in a bar graph. The final NSS result is 1.304. Reprinted from [138], copyright (2005), with permission from Elsevier.

To conclude, numerous saliency models are developed each year and it is important to have a sound idea of their accuracies and how they are measured during applications. Each accuracy metric adapts a different approach but one thing they all have in common is that the saliency maps and the human eye fixations are both transformed into data sets so as to be able to compare them with each other.

The drawback of the accuracy metrics is that they all use eye fixation points as ground truth to determine the accuracy of the saliency maps. However, eye fixations vary according to each different person and viewing time and yet there are no experimental standards for these assessments (e.g. number of viewers or viewing time). The performance of the same saliency map will be evaluated differently based on which evaluation metric is used. It is important for this reason to grasp the essence of these accuracy metrics before looking into the accuracy results.

3.5 Usual applications of saliency map

Saliency maps find their main application in the areas such as computer vision & graphics, robotics and others [117] (as illustrated by Table 3.5-1). Its application in design sectors is quite rare. The latter will be further explained in the following section.

Area	Application
Computer vision and graphics	Rendering
	3D modelling
	Image resizing and smart scaling
	Image segmentation
	Image matching
Robotics	Object finding and landmark detection
Others	Workload manager
	Detect signage for visually impaired people
	Visual perception inducement for patients with retinal prosthesis
	Face detection
	Improving photograph compositions
	Billboard advertisement evaluation
	Abstract painting research
	Decision making in design projects

Table 3.5-1: Application areas of saliency maps.

3.5.1 Computer vision and graphics

The application of saliency maps can be found in industries that have close relationships with direct visual perception of human eyes. Take rendering and 3D modelling for instance: being two of the computationally most expensive stages in animation industry, researches have been carried out on how to save time and manpower with the help of, among others, the saliency map. It can be adapted to predict the visual sensitivity of different image regions. In that way, it allows more computer calculation time spent on locations with high visual sensitivity and low tolerance for errors, and less

time on regions with low visual sensitivity and high tolerance for errors.

In rendering, Yee et al [139] introduced a method using certain guidance to accelerate the calculation of global illumination in animation. The guidance is a prediction map that is combined from spatiotemporal sensitivity and visual attention information. Spatiotemporal sensitivity shows when and where human eyes allow more errors (such as to fast moving objects), and a IKN saliency map predicts where the visual attention goes to [121]. Attempts to solve similar problems were made by Cater el al [140] and Debattista et al [141].

An example of saliency map adaption in 3D modelling can be observed in the work of C. H. Lee et al [142], where they proposed a "mesh saliency" as parameters so as to outline which regions in the 3D digital model need enhancing in the model details. By using an algorithm inspired by the centre-surround operations of the IKN saliency algorithms, the perceptual importance and interest on the model are calculated. For example, unified and homogenous areas are usually places that draw less visual attention than areas that have unusual or unexpected bumps/pits. Simplifications will be applied to model regions with less visual importance in order to minimize the model file size and to reduce labour (see Figure 3.5-1).

(a)   (b)
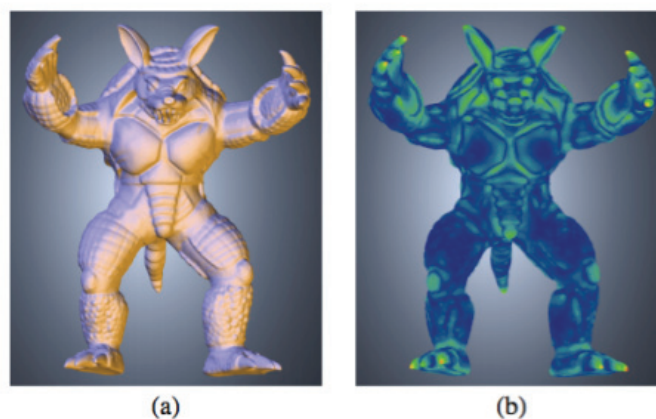
Figure 3.5-1: (a) The digital 3D model. (b) The mesh saliency. The warmer the colour, the more visual attention this region draws and therefore asks for finer modelling detail. [142] ©2005 Association for Computing Michinery, Inc. Reprinted by permission. http://doi.acm.org/10.1145/1186822.1073244

In image resizing, saliency maps can also play an important role. Image or videos[8] should be able to be displayed on different sizes and screen proportions (smart phones, tablets, computer screens etc.). Simple linear one-dimensional scaling methods were abandoned because they are usually very uncomfortable for the human eye due to distortions (see Figure 3.5-2). Smart scaling, on the other hand, can both make sure that the rescaled images are comfortable to look at and the main informations of the images are not lost (e.g. the ball in a rescaled football match video). An optimal procedure is taken so that the main focus region of the image is less resized and allows less important image regions to be more distorted. Wang et al [139], [143] applied each pixel in the

---

[8] "Video" will also referred to as "image" in the following text because videos can be seen as image series.

image with a saliency score, which is made from three items: i) a significance map, ii) a face detector, and iii) a motion detector. The significant map is a product from a gradient map (which is retained by applying the grayscale intensity value of each point to the $L^2 - Norm$) and the IKN saliency map. However, IKN saliency map has a drawback, which is that regions that are not in the vicinity of the edges are not given a high saliency values, so that the salient regions are not uniform; thus leading the object of interest being given lower importance than they are supposed to [140], [144].

Figure 3.5-2: Left column: The original images. Centre column: Images resized without smart scaling. Right: The images after smart scaling. [142], [143] ©2008 Association for Computing Machinery, Inc. Reprinted with permission. http://doi.acm.org/10.1145/1409060.1409071

In image compressing procedures, the resizing of the image quality also does not need to be uniform across the scene. Due to the non-uniform distribution of photoreceptors on the human retina, human eyes can either focus on a small region in the scene with high resolution, or pay attention to the overall scene with low resolution. This means that an image can be compressed in a way that high quality is preserved in the region where most important visual information is contained, and lower quality where the visual information is less important. Guo and Zhang [142], [145] proposed using saliency map as a guide to detect where the image regions with high saliency are; the image is then compressed but regions with high saliency are preserved with higher image quality (see Figure 3.5-3).

Figure 3.5-3: Left: the original image. Right: the image after compression. The foreground and background of the image are more compressed than the medium part. Image source: [145], © 2010 IEEE.

In image library management, in order to let human being able to quickly scan through large image data files, the images need to be compressed down to a certain size; this shrinking process is called image thumb-nailing. If a large image is shrunk down directly, then there won't be enough information for the library users to retrieve because everything is too small. The crucial information of the original image must be preserved; otherwise the thumbnail image would be illegible. Suh et al [146] integrated the IKN saliency model and a face detector to decide which region of the image contains the most significant visual information. The goal is to find the smallest possible rectangle image cropping that contains just enough information from the original image. This extracted rectangle is then resized to thumbnail (see Figure 3.5-4).
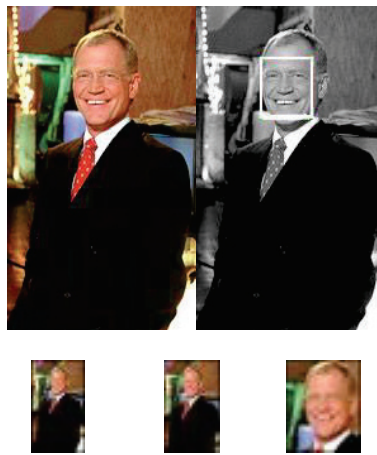
Figure 3.5-4: Top left: the original image. Top right: the application of a face detector. Bottom: Thumbnails generated with different methods. Bottom left: No cropping. Bottom centre: Saliency map based cropping. Bottom right: face detection based cropping. [146] © 2003 Association for Computing Machinery, Inc. Reprinted by permission. http://doi.acm.org/10.1145/964696.964707

Another application of saliency maps in image segmentation is to extract segments of image pixels that share similar properties, with the ultimate goal of e.g. identifying objects and making the images easier to analyse. Han et al [147] used the IKN saliency model as a base, and upgraded it by integrating algorithms that put more weight on the centre of the image similar to human habit; an edge detection that contains all the boundary pixels of one attention object and a homogeneity measure that indicates the colour-texture distribution over one attention object (see Figure 3.5-5). Other image segmentation researches with the help of saliency maps are also available [148] [149].

Figure 3.5-5: Some examples on extracting the target objects. Source: [147], ©2006 IEEE.

Based on image segmentation, image matching is used in situations such as recognizing and tracking certain objects in unsupervised surveillance videos if the target objects match certain given parameters (see Figure 3.5-6) [150] [151]. The algorithm can also be used in comparison of satellite or aerial images, where particular objects need to be found (e.g. change in terrain, a certain type of sick tree, newly built building etc.). C. Davies et al [152] discussed the possibility of using a saliency map to discover changes between existing maps and the newly made aerial photos, which is still a manually-dependent and tedious work nowadays. Since it is computationally expensive to compare pictures on a pixel-to-pixel basis to see whether they are identical, therefore they are only compared at critical regions that are pre-filtered out by the saliency maps.

Figure 3.5-6. A demonstration of person tracking. Green points mark the regions that match with the target, while cyan points mark regions that don't. Yellow rectangle means that more than 30% of the region matches with the target, otherwise the object is framed with a blue rectangle. Source: [151] with permission of Springer.

3.5.2 Robotics

In robotics research, if the robot is required to be in strong corporation with humans - a social robot (e.g. home assistance for the elderly) - it will be more efficient if it perceives the world in a similar fashion as humans. Equipped with an attention system based on visual perception principle similar to the human eyes, it will help the robot to better understand the human needs. Breazeal and Scassellati [153] developed their attention system for a social robot based on Wolfe's human attention and visual search theory [154], which is a combination of colour feature maps, motion feature maps and face pop-out feature maps. On top of that, a habituation function guarantees that the centre of the visual scene is weighted more than other image areas. By normalizing and combining the three maps, they generate an activation map that guides the eye movement of the robot.

Social robots are also required to deal with unfamiliar situations where they have to acquire the knowledge about the unknown environment on their own by searching through the World Wide Web. One example is by giving semantic descriptions of a certain object, the Curious George [155] had to look for relevant images on the Internet and get to know the relevant object features. With the information about the objects given, the robot identified which one in the given realistic environment matches with the information provided. Among many other algorithms, saliency map was used to search for suspicious objects that were possible for matching in the unfamiliar environment. The map was generated based on the spectral residual saliency measurement principle [156]. Other researches about localization of robots' vision also exist [157] [158].

F. Orabona et al [159] modeled a robot which can perform visual search and recognition tasks with the help of an object-based visual attention saliency map. The difference between their saliency map and the feature based saliency map (e.g. IKN saliency map) is that instead of focusing on image regions, their focus are on objects – hence "object-based" saliency map. It is a linear combination of two sub maps: the first sub map examines the uniformity of different colours in the surrounding environment and the second sub map provides the goal colour (which is the average colour from part of the object the robot is looking for). By various comparisons the robot checks whether the uniform colour in the surrounding environment matches with the colour of the object-in-search. The authors of the paper presented an example where the humanoid robot searched for a particular toy plane in the visual scene (Figure 3.5-7).
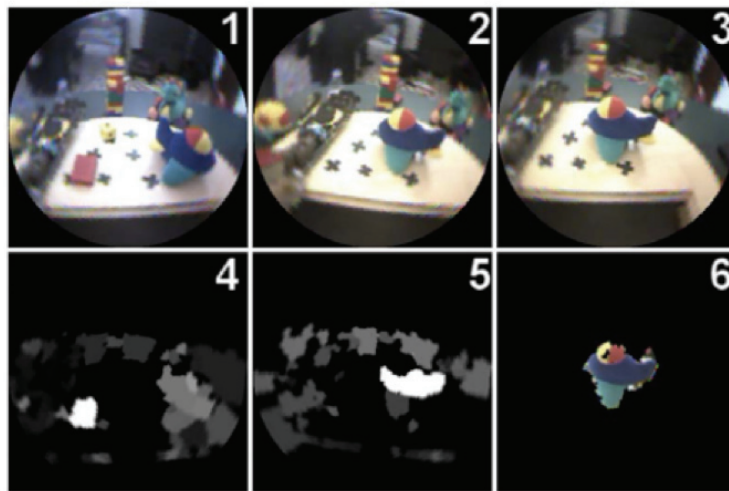
Figure 3.5-7. With a bottom up saliency map (no. 4), the robot recognized that the red colour was the most salient region in the image (no. 1). With a top down saliency map (no. 5), the robot was directed to find the blue colour that matched with the toy plane in the visual scene (no. 2). Picture no. 6 shows that the robot had recognized the toy plane as target in the visual scene (no. 3) and separated it from its background. Image source: [159], © 2005 IEEE.

Other object-searching applications can be found in robot localization. Since it is very unlikely to store all the information regarding the surrounding, robots mainly localize themselves by detecting and referring to visual landmarks (e.g. trees, rocks and buildings etc.) with known positions. The main research is about how to develop systems that can detect natural landmarks in 3D spaces, facilitated by biologically inspired visual features [160] [161], [162].

3.5.3 Other applications

Other miscellaneous applications of saliency maps can be found in a workload manager. It is a device that helps to screen out unnecessary information source so that the driver can concentrate on driving. Due to audio from several in-vehicle appliances (radio, navigation system, mobile phones

etc.) and the languishing eyesight of the aging population, drivers may not be able to handle the overload of information properly. A workload manager can for instance automatically divert an incoming phone call to an answering machine when a driver is turning at an intersection [163]. Won et al [164] developed a visual based traffic sign detection model that can be integrated into a workload manager in the future. In their paper, the IKN saliency algorithm is integrated in the traffic sign detection model.

Saliency map algorithm can also be helpful to visually impaired people. Wang et al [165], [166] developed a method to detect signage (signs indicating where stairs, elevators, etc. are located) for visual-impaired people in indoor environments. With a camera scanning through the scene, only the regions whose saliency values exceed certain threshold would be analysed. Here, also the IKN saliency model is used. The system then compares the pattern detected from scanning with the existing patterns in the system, and checks if there is a match. In case of a successful matching, the user would then be informed.

Similarly it can help patients with impaired retina, which is a coat inside the human eyes that has a light-sensitive layer of tissue. In case of a retina dysfunction, a retinal prosthesis can provide electrical stimulation to the retina cell to induce visual perception. One current method is to first have an exterior camera taking images from the environment, the image data are transferred to the implanted retinal stimulator. However, there is only a limited amount of electrodes to activate the retina cell; if the whole image was compressed to fit the human field of view, the resolution would be very low. It is more sound if only the 15°–20° field angles of camera image is transferred to the eye with the limited electrodes. The problem is that the user would be unaware of the important information outside the 15°–20° camera view. Parikh et al [167] proposed to use biologically based saliency map to identify the most informative areas (obstacles, landmark etc.) in the camera image and inform the user accordingly.

Salah et al [168] proposed an application of face recognition with their saliency map, where they only processed visual information in the crucial area such as eyes, nose, mouth, etc. and left out the redundant areas.

Saliency map can also help amateur photographers in improving the composition of a photograph. Greco and Cascia [169] included the GBVS saliency algorithm [126] for that purpose along with three other filters. One filter detects the edges of the object so as to keep the object of interest complete, one filter is used to increase the difference between the object of interest and its background, and the third one smooths up the hard edges in the saliency map. The most interesting region selected by the saliency map and the filters is preserved as much as possible, and the rest is cropped out.

Wilson et al [170] conducted a field study of billboard advertising to explore how salient an advertisement must be in order to be remembered by people. This investigation was conducted, among other methodologies, with IKN saliency map. They also found it to be a useful implication for designers because in that way they do not have to solely depend on their instinct during designs, but also have objective references as a complementary tool during the creation processes. The use of visual saliency simulation is considered to be beneficial under circumstances when a survey is costly,

or takes place in environments where the application of eye trackers is impractical. Other experimentations with advertisements also exist [171] [172].

Koide et al [173] investigated the behaviour of people contemplating abstract paintings. By comparing the eye scan paths of artists and common people against visual saliency maps, they found out the gazing points of artists were different from those of common people. The visual attentions of common people were more similar to the calculated saliency maps than that of professional artists. This could be due to the reason that common people contemplated the painting driven by basic stimulus, while artists tend to use their professional knowledge to direct their gazes in appreciation of the paintings.

3.6 Fitness of saliency map for the research purpose

As mentioned in Chapter 2, this thesis is aiming at developing an appropriate method to measure the BIPV visual impact on retrofitted building envelopes from a quantified, objective and neuroscientific based approach. This section discusses the benefits saliency models can bring to the proposed evaluation method.

By containing BIPV and the respective building envelopes in an input image, the saliency model can be used to predict whether the respective BIPV are salient or not for the human's visual attention. Thus providing preliminary information for analysing the BIPV visual impact. The analysis procedures are entirely based on digital data and hence a fully quantified process. The objectivity and the continuity of evaluation standards can be guaranteed in the assessments because no subjective judgments are involved.

Saliency models imitate the mechanism of human visual attention mainly by reproducing its contrast comparison mechanism. Accuracies of the models can be concluded from comparisons of saliency maps with human eye fixations. By integrating saliency models into the evaluation method, these two factors can guarantee the generality of the results and neuroscientific base of the BIPV's visual analysis.

To conclude, the integration of saliency model into the evaluation method can provide visual saliency analysis of the BIPV in facade retrofits in a quantitative, objective and neuroscientific based approach. Thus first two of the three research questions from Chapter 2 are answered and the fitness of saliency models for the purpose of this doctoral thesis is checked. The next chapter aims to tackle the question of how to transform the visual saliency information of BIPV on retrofitted building envelope into visual impact, and using one single value to indicate its strength.

Chapter 4   BIPV visual impact assessment (Proof of concept)

In this chapter, the methodology to evaluate the BIPV's visual impact on retrofitted building envelopes with the help of saliency models is explained in detail. The method is supposed to be used before the actual BIPV installation takes place so as to have reasonable predictions of the potential visual impact.

An application example, which is a villa located in Hergiswil (Switzerland), will also be presented in order to explicitly illustrate the whole approach. The owner of the villa wished to install BIPV on the building facade. Since this architecture is listed in the canton heritage list, where it is required that its facade should be treated with care during any renovations, this building fits well into the purpose of the research. Figure 4.1-0 shows the main façade of the villa, on which BIPV installations are to be installed.

The application of the proposed evaluation method is carried out under the assumption that technical requirements, such as energy yield, cost, life cycle assessment and similar, are already met before investigating the BIPV visual impact.

Figure 4.1-0: The main facade of the villa. This is also the view of the villa that has the highest probability to be seen by the passing pedestrians.

4.1 Preparation of the simulation environment

4.1.1 Selection of saliency models

Hundreds of saliency models have already been developed based on different approaches and yet more are to come each year. This section aims at finding appropriate saliency models for the purpose of the thesis based on two preliminary requirements: acceptable accuracy and accessible & robust code.

Reasonable accuracy

The accuracy results of the saliency models can be found on the MIT saliency benchmark website [174] and are reasonable enough for the applications planned. The models were tested using the MIT300 and CAT2000 image datasets. The MIT 300 evaluation involves eye-tracking data of 39 viewers on 300 natural images[9] and acts as benchmarks. The CAT 2000 evaluation has the eye tracking data of 24 viewers on 2000 images of both natural and synthetic kind that acts as benchmarks. Both the MIT 300 and CAT 2000 accuracy results were retrieved from the MIT saliency benchmark website on 8th March 2016.

Accessible and robust scripts

The code should be accessible Matlab code, easily applicable and robust. The execution of the code should not require cumbersome debugging work or installations of additional software or plugins.

11 saliency models on top of the list from the MIT saliency benchmark website were reviewed (Table 4.1-1) and 5 among them fulfil the two preliminary requirements.

---

[9] Natural images refer to photos that are not abstract and contain scenes that people can see in their daily lives. Synthetic images are abstract images made by photo-editing software or similar sources; the target on synthetic images differs from all the other items by colour, intensity, orientation or other attributes.

No.	Saliency model	Code	Problem	Decision
1	Deep Gaze [175]	Not found	No available code	Discarded
2	SALICON [176]	Python		Discarded
3	Boolean Based Saliency (BMS) [177]	MATLAB	Special compiler required	Discarded
4	Judd Model [134]	MATLAB	Extensive debugging required	Discarded
5	CovSal [178]	MATLAB	Inaccessible website link	Discarded
6	Graph-Based Visual Saliency (GBVS) [126]	MATLAB		
7	Spatially Weighted Dissimilarity (SWD) [130]	MATLAB		
8	RARE 2012 – Improved [179]	MATLAB		
9	Fast and Efficient Saliency (FES) [180]	MATLAB		
10	IKN (Harel) [125]	MATLAB		
11	IKN (Dirk Walther) [124]	MATLAB	Less accurate than IKN (Harel) according to several accuracy metrics	Discarded

Table 4.1-1: Selection of saliency models from MIT saliency benchmark based on code format and availability.

Four of the remaining five saliency models do not show much difference in overall accuracy results. Some are ranked higher in certain metrics but lower in others. The IKN (Harel) model is an exception, but still included because it is an interpretation of the classic IKN saliency model [121]. Considering the time investment/payback ratio, it makes more sense to eliminate two more saliency models. Therefore, a second filtering process was made based on the influence impacts of the saliency models, which were indicated by the citation numbers of their publications. As the Table 4.1-2 shows, the GBVS saliency model was cited around 1700 times by 20th May 2016, and the SWD model 96 times. RARE2012 and FES were cited 52 and 26 times respectively. Thus making the IKN (Harel), GBVS and SWD the more representative saliency models among the remaining five and hence selected for application in this thesis. A test image is used as an example for demonstration of their saliency maps (see Figure 4.1-1 and Figure 4.1-2).

Saliency model	Citation number (Retrieved from scholar.google.com on 20 May 2016)
Classic Itti-Koch-Niebur saliency model [125]	7183
Graph-Based Visual Saliency (GBVS) [126]	1767
Spatially Weighted Dissimilarity (SWD) [130]	96
RARE 2012 - Improved [179]	52
Fast and Efficient Saliency (FES) [180]	26

Table 4.1-2: Selection of the remaining five saliency models based on citation numbers.

Figure 4.1-1: An example input image to test the remaining three saliency models.

GBVS   IKN   SWD
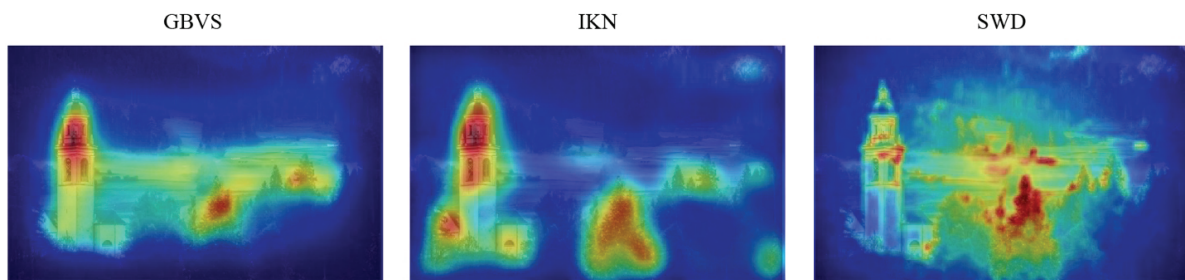
Figure 4.1-2: The resulting saliency maps of Figure 4.1-1 generated with the three selected saliency models.

The accuracies of these three saliency models are concluded in the Table 4.1-3 and Table 4.1-4. On the MIT benchmark, both the GBVS and SWD were quite accurate and above the "one human baseline"[10], possibly because both of them set more weight onto the image centre in their saliency model. Even though the overall accuracy of the classic IKN saliency model is low, according to Borji et al [132], it achieves outstanding results in predicting salient locations on synthetic patterns (examples of which can be seen in Figure 4.1-3). This is due to the fact that this model is very connected to the *Feature Integration Theory* principle, meaning that it was designed to recognize simple features such as colour, intensity, orientation differences, etc. Since the MIT300 image database only includes natural images (examples of which can be seen in Figure 4.1-4), and the CAT 2000 image database includes both synthetic and natural images, the *Feature Integration Theory* was not sufficient and making the IKN saliency model yield less satisfactory results.

---

[10] This baseline is created by evaluating how well the fixation map of one observer (whose eye fixation points are transformed into a continuous saliency map) predicts the fixations of the other N-1 observers. This was computed for every observer in turn, and averaged over all N observers.

Model Name	AUC-Judd	Similarity Score	EMD	AUC-Borji	CC	NSS
Baseline: infinite humans[11]	0.91	1	0	0.87	1	3.18
GBVS	0.81	0.48	3.51	0.80	0.48	1.24
SWD	0.81	0.46	3.89	0.80	0.49	1.27
IKN (Harel)	0.75	0.44	4.26	0.74	0.37	0.97

Table 4.1-3: MIT300 experimentation results

Model Name	AUC-Judd	Similarity Score	EMD	AUC-Borji	CC	NSS
Baseline: infinite humans[11]	0.90	1	0	0.84	1	2.85
GBVS	0.80	0.51	2.99	0.79	0.50	1.23
IKN (Harel)	0.77	0.48	3.44	0.76	0.42	1.06

Table 4.1-4 : CAT2000 experimentation results
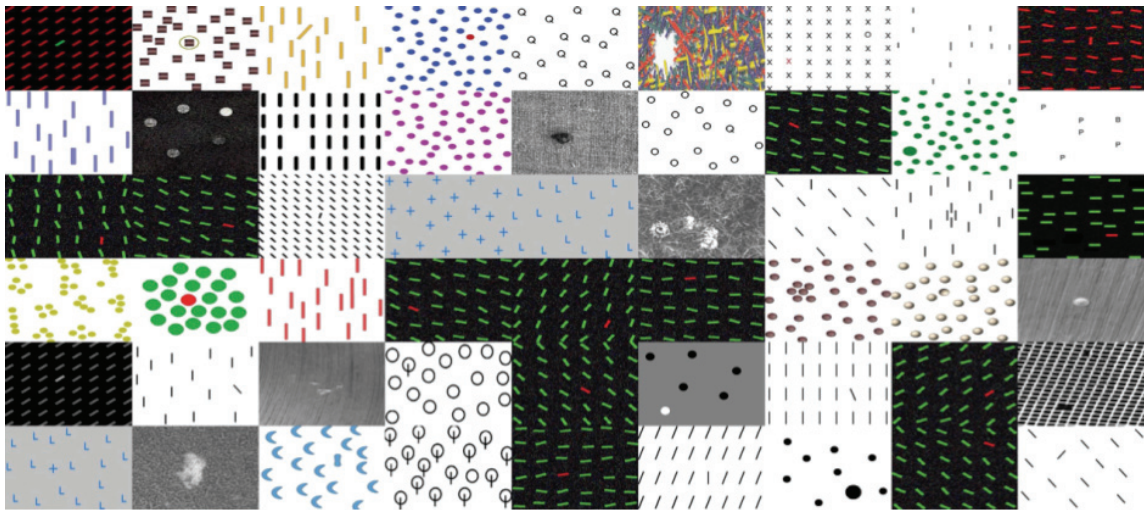
Figure 4.1-3: Synthetic images used in [132] © 2013 IEEE. In this kind of images, the target differs from all the other items on the image by colour, intensity, orientation or other attributes.

Figure 4.1-4．Examples of natural images from the MIT300 dataset [133].

---

[11] Judd et al measured the human performance from a finite number of observers and approximated the limit with infinite viewers by extrapolation [133].

To conclude, the final selected saliency models to use in this doctoral thesis are the GBVS, IKN (Harel) and SWD. Their Matlab codes are robust, don't require extensive debugging works and are available for download on the respective websites. The IKN (Harel), despite being less accurate than the other two, is a classic saliency model that is very influential and still used in many applications. The GBVS has a high research impact due to the novelty in its approach. The citation number of the SWD paper is very low compared to the other two, but the MIT benchmark results show that its performance is of high accuracy. The three saliency models are effective for different scenarios. GBVS and SWD have strong centre bias integrated and perform in an optimal way for natural images, while the IKN (Harel) model is more applicable in predicting salient locations in synthetic images.

4.1.2 Generating the input images

To make reasonable predictions about the visual saliency of BIPV systems on retrofitted building facades, the saliency models need credible input images to produce plausible saliency maps. The input images need to reflect the visual perception in a valid manner. This is why it is not ideal to use images where the BIPV system is photo-montaged on the building, or produced by artistic architectural renderings when the sky and materials are manipulated to "appear" realistic. The procedure to generate input images in this thesis is shown in Figure 4.1-5. Beside the 3D digital model containing information about the BIPV and the building, physically realistic descriptions about the materials used in the model and the sky condition are fed into a lighting simulation software RADIANCE [181]. The generation processes of the resulting HDR renderings follow the physical behaviour of light as closely as possible in an effort to make the final appearance of the BIPV design as realistic as possible. The dynamic range of a *HDR* image is also more consistent with the real-world scenes and has high level of detail that is close to the range of human vision. In order to make it being able to be displayed on common computer screens, the RADIANCE operation *pfilt* is used to set the exposure of the image to the correct average value. However, HDR images are not accepted saliency models (the reasons will be stated in Chapter 6), the operation *ra_tiff* is used to transform the image from HDR format to TIFF format.

```
        model          sky        material
     information   information   information
                   │         │         │
                   ▼         ▼         ▼
view angles ────▶ ┌─────────────────────────┐
                  │ RADIANCE command rpict  │
                  └─────────────────────────┘
                              │
                              ▼
                   renderings in HDR format
                              │
                              ▼
                  ┌─────────────────────────┐
                  │ RADIANCE command pfilt  │
                  └─────────────────────────┘
                              │
                              ▼
                 anti-aliased and scaled render-
                       ings in HDR format
                              │
                              ▼
                  ┌─────────────────────────┐
                  │ RADIANCE command ra_tiff│
                  └─────────────────────────┘
                              │
                              ▼
                  renderings in TIFF format
```
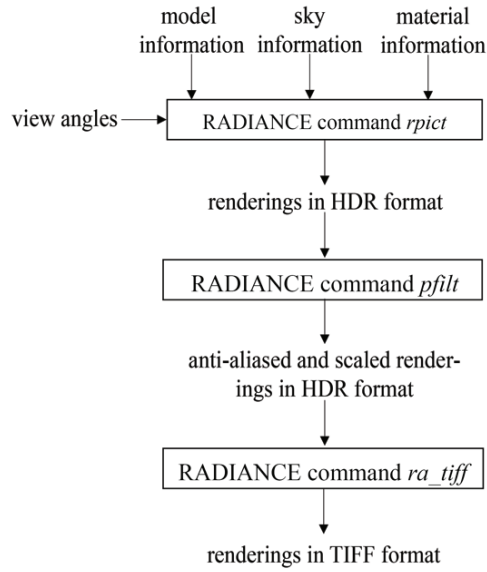
Figure 4.1-5: Generation of an input image for saliency models.

4.1.1 Measurement of the BSDF materials

BSDF (bidirectional scattering distribution functions) are in effect a set of hemispherical luminous coefficients defined by paired incident and outgoing angles [182]. It can be used to describe the complicated material properties of PV by measuring the angular distribution of light scattering on their surfaces. With the Scanning Goniophotometer located in the laboratory of CC EASE, HSLU, BSDF characteristics of PV can be measured. Figure 4.1-6 illustrates an isometric view of the Goniophotometer. A collimated light beam would be projected from the optical bench onto the sample fixated on the post. The angles of the light beam can be described using the θ and ϕ: θ is the angle between the light beam and the face normal of the sample, and the ϕ is the angle between the light beam and the sample's upside direction (Figure 4.1-7). A detector then rotates spherically around the sample, collects lights reflected off from the sample and transmitted through the sample, thus gaining the reflection and transmission descriptions. The BSDF data is interpolated into a tensor format with 16000 incident and 16000 outgoing directions. Applying an adaptive data reduction technique, the tensor size is then reduced by approximately 99% [183]. The mechanical accuracy and precision, the quality of the measured data and its numerical processing of this Goniophotometer can be found in [184]. Later, the measurement results are put into a *XML* file, and integrated in the material descriptions for RADIANCE renderings [185].
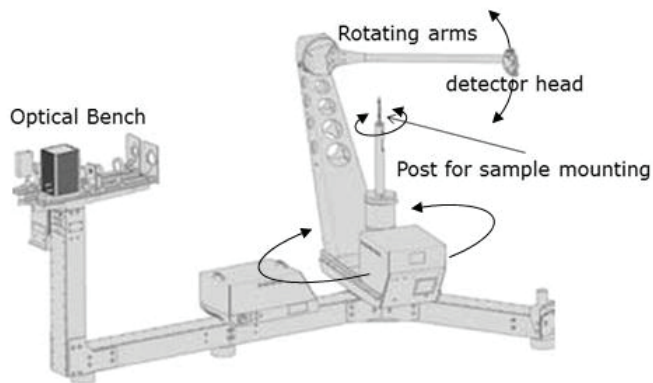
Figure 4.1-6: Pictogram of the Scanning Goniophotometer of CC EASE, HSLU. Permission to reuse from authors of [185].
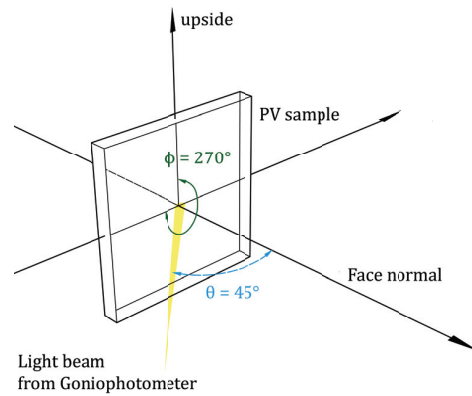
Figure 4.1-7: The theta and phi angles of the light beam.

4.2 Methodology

The methodology in this section shows how to transform the visual saliency information to visual impacts of BIPV on retrofitted building envelopes, and using single values to express their strength. The general idea is by giving a visual scene that contains the retrofitted building envelope, one needs to find out by how much the visual attention has been modified in this very scene before and after the BIPV are installed. A methodology is developed that can generate single values to express the visual impact strength by weighted "extraction" of the representative informations from saliency maps.

The methodology comprises pre-processing, processing and post-processing stages:

i)   The first stage involves creating the 3D digital model of the building, and 2D renderings of the existing building with and without the BIPV from the same perspective.

ii)   The second stage is to produce saliency maps for the 2D renderings.

iii)   The last stage is to compare the saliency maps of renderings before and after the BIPV installation and evaluate the difference. Table 4.2-1 shows the approximate workflow of the methodology.

Stage	Step	Step focus	Description	Deliverable
1 **Pre-Processing**	1)	Existing building	Capture a photo of the building's original state	2D photo 'as is'
	2)		3D model and 2D rendering of the existing building in its original state. Viewpoint must be the same as 2D photo 'as is'.	2D rendering 'as is'
	3)	BIPV	3D model rendering of the existing building with BIPV. Viewpoint must be the same as 2D photo 'as is'.	2D rendering 'new'
2 **Processing**	4)	Saliency	Generate saliency maps from both 2D renderings 'as is' and 'new'	saliency map 'as is' and saliency map 'new'
3 **Post-processing**	5)	Comparison	Analysis of the difference between the saliency map 'as is' and saliency map 'new'.	'delta' map, binary map 'result' and value S

Table 4.2-1. Summary of work steps and deliverables of the proposed methodology.

Stage 1 – Pre-processing: Creating 2D renderings of the existing building with and without BIPV

The photo 'as is' of the existing building in its original state is taken at a viewpoint where the building is mostly likely to be seen by the passing viewers. A 3D digital model that includes most essential information of the building, such as its proportion, facade openings, colours and materials is created. Using this model with material and sky descriptions, the software RADIANCE produces the 2D rendering 'as is' that imitates the original photo 'as is' (as described in section 4.1.2). With the same viewpoint, BIPV are applied to the 3D model and the 2D 'new' rendering is also generated. Both renderings are generated under the overcast sky conditions (CIE sky definition [186]): it won't result in hard shadows, glaring sun reflections and exaggerated brightness in rendering images opposite to a clear sky condition (for comparison, see Figure 4.2-1). Parameters for a clear sky vary strictly according to location and time, omitting these parameters enables cross-comparisons for BIPV visual impact across different projects because they are all measured under identical sky conditions independently of the time and location.
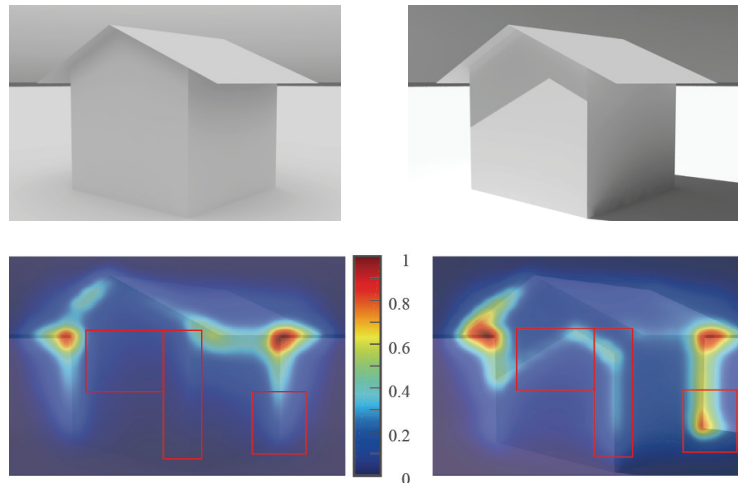
Figure 4.2-1. Saliency maps from the renderings of the same object with and without hard shadows. Top left is a rendering of a simple hut in an overcast sky condition, while the top right is rendered under a clear sky. Respective saliency maps are below the renderings. The border of the shadow area is also very high in saliency values in the clear sky condition. The red squares mark the main differences between two maps.

Stage 2 – Processing: Generating saliency maps for the 2D renderings

The two 'as is' and 'new' renderings in TIFF format are imported into the MATLAB. With the given scripts, saliency maps 'as is' and 'new' are generated. Figure 4.2-2 shows the saliency maps generated using the GBVS saliency model. All the values on the saliency maps are automatically normalized to the range of 0 to 1 and then mapped with corresponding colour range to show the value distributions. Saliency maps have the same pixel number as the renderings.
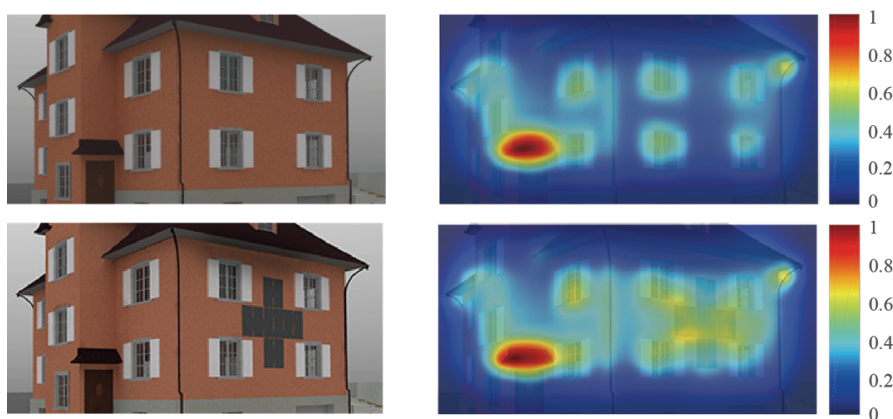
Figure 4.2-2. Left above: The rendering 'as is' presenting the existing building in its original state. Left below: The rendering 'new' presenting the existing building after the BIPV installation. The saliency map 'as is' (right above) and 'new' (right below) generated for renderings 'as is' and 'new' with the GBVS saliency model.

Stage 3 – Post-processing: Analysing the differences between saliency maps 'as is' and 'new'

Given the identical view perspective, the difference between the saliency maps 'as is' and 'new' represents the variation of the visual attention in the renderings with and without the BIPV installation (see Figure 4.2-3); it is calculated using the absolute difference between the saliency map 'as is' and 'new':

$$'Delta'\ map = |Saliency\ map_{as\ is} - Saliency\ map_{new}|$$

Figure 4.2-3. The 'delta' map produced from GBVS saliency model.

Inspired by the AUC metrics [133] [132] [131], all the pixels are sorted as either among the top 10% salient pixels or among the bottom 90% in the 'delta' map. The result is shown on a binary map 'result' (Figure 4.2-4). Pixels whose values are ranked among the top 10% are marked in white and 90% rest in black. The strength of the difference between the saliency map 'as is' and a saliency map 'new' is expressed by:

$$S = 100 * ST_{t=10\%} * Max_{DeltaMap}$$

The $ST_{t=10\%}$ is the threshold value between the top 10% salient pixels and the bottom 90% pixels, meaning that 10% of the pixels on the 'delta' map have higher values than the $ST_{t=10\%}$, and that 90% of the pixels on the 'delta' map have lower values than $ST_{t=10\%}$. S is the product between the $ST_{t=10\%}$ value and the maximum value on the 'delta' map; they are multiplied by 100 for better expression. On a scale from 0 to 100, a low S value means either the vast majority of pixels have rather small values in 'delta' map, or/and that the maximum value in the 'delta' map is low, representing that the overall variation in visual attention in the visual image before and after the BIPV installation is small. A larger S value means either that most of the pixels are distributed within a value range with a larger upper bound, or that a particular region is having especially high values in the 'delta' map, therefore the overall change in visual attention is large. So a smaller S value means that the building is most similar to its original state even after the BIPV installation. Therefore the BIPV visual impact is low and hence this design can be considered as beneficial for the heritage building regarding the protection of its original appearance.

Figure 4.2-4. Binary maps 'result' based on Figure 4.2-3.

Figure 4.2-5 is a graph of the relationship between the accumulated sum of pixel number according to different value ranges deducted from 'delta' map of Figure 4.2-3. An overview of the workflow is shown in Figure 4.2-6. In this thesis, the saliency models are used unmodified with default settings. An example MATLAB script of the post-processing stage can be seen in Appendix 1.
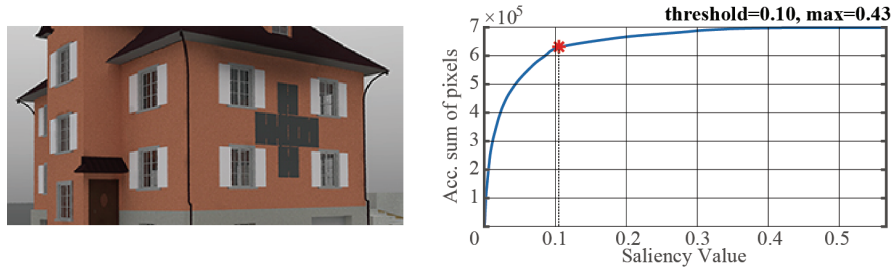

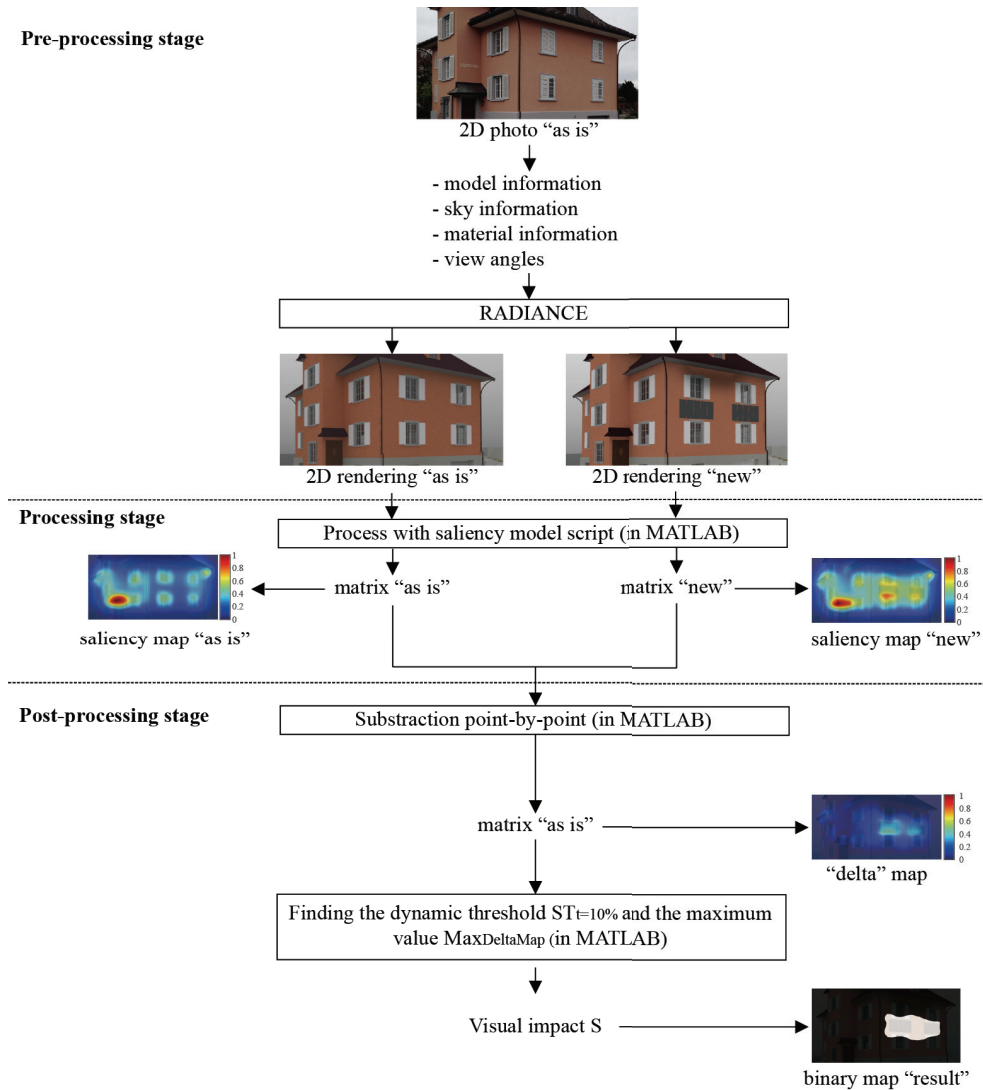Figure 4.2-5. The accumulated sum of pixel number within different value ranges from 'delta' map.

Figure 4.2-6. Overview of the workflow.

4.3 Discussion

Several factors play a role in the visual impact evaluation process of different BIPV system designs for building refurbishment based on saliency models. The most significant factors are briefly discussed in this section.

4.3.1 Threshold setting for salient and non-salient pixels in 'delta' map

The main difference between the proposed methodology in this thesis and its older version published in [187] is how to analyse the visual attention change before and after the BIPV installation. The key lies in what threshold to use to filter out the noise in the 'delta' map and to decide which pixels on it must be considered as salient and which mustn't. The older version used an absolute value as threshold: all the pixels in the 'delta' map with values larger than 0.1 were considered as salient and marked white in the corresponding binary saliency map 'result'. The strength of the BIPV visual impact was expressed by the percentage of the white area in comparison with the total area of binary map 'result'. Its drawback is that it fails to conclude in what value range the vast majority of pixels from 'delta' map lie, and in what range the outlier values lie. 'Delta' maps can have values distributed in different ranges depending on which saliency model was used. When using an absolute threshold, the binary saliency map 'result' could only mark the pixels that have values larger than 0.1 in 'delta' map, but could not show the overall distribution of the values. Also, all pixels above the fixed threshold were treated with the same weight.

Using the old, absolute threshold can be very disadvantageous in predicting BIPV visual impact in the following two example scenarios:

Scenario 1: 'Delta' map A has overall higher values than and 'delta' map B, but the latter has a few very high peak values. Using an absolute threshold, the peak values in 'delta' map B would be overlooked and the resulting visual impact underrated.

Scenario 2: Both 'delta' maps A and B have the same number of pixels with values higher than the absolute threshold. However, the overall value of 'delta' map A is higher than the overall value of 'delta' map B. This difference wouldn't be visible using the old method because all pixels marked as ''salient' were weighted equally.

The drawbacks detected in the above mentioned scenarios can be avoided using the new method proposed in this doctoral thesis, because both the overall value distribution and the maximum value in 'delta' map are taken into account, and combined into the final S value that sufficiently demonstrates the BIPV visual impact.

4.3.2 Characteristics of different saliency models

This section aims to show the uniqueness of the three saliency models GBVS, IKN (Harel) and SWD and why it is important not to choose just one of them but to use them simultaneously. Hereby four different designs of BIPV on the villa facade are used to illustrate the strength and weakness of each saliency model. As seen in the left column of Figure 4.3-1, the first design shows 10 PV panels being divided in two groups and placed horizontally under the windows of second floor. In the second design, the 10 PV panels are lined up in a horizontal group and also located under the same windows. The third design places the PV panels in a cross-formed layout and put them into the middle of the four windows. In the last design, the 10 PV panels are arranged in a vertical group between the left and right windows. In all designs, black glazing is used for BIPV.

From Figure 4.3-1, it shows that all three saliency models can outline the presence of BIPV installations in the renderings 'new' and predict their saliency. In case of the GBVS, it is possible to "see" the BIPV system by identifying its edges: horizontally oriented edges seem to have more impact than the vertical ones. The IKN (Harel) model outlines the existence of BIPV more strongly, as if it depends more on colour difference rather than the edge orientations, so that the whole BIPV installation is very salient as a whole area, possibly due to the high intensity of the colour itself. The SWD model puts far more weight into the image centre and edges compared to the other two models, e.g. that the edges of BIPV installation can be recognized, but are not marked as salient as the window frames that have more details.

Another observation is that the GBVS saliency model puts a little more weight on the edges than the colours. The entrance area of the façade remains the most salient area on the image possibly due to its irregular oriented shape in addition to higher colour contrast in comparison to the rest of the image. The IKN (Harel) model weighs colour more than the edges, so that distinct borders between bright and dark are marked with higher saliency values, e.g. between the left or the right façade edge and the sky background. While the GBVS and IKN (Harel) saliency models both use blobs to mark the regions they consider as "salient", the SWD gives far more importance to the details and identify targets in a more meticulous way, e.g. the hose in the image centre gains much attention in SWD, while the other two saliency models merge it with other salient regions. Also the edges of other parts of the images are highlighted as separated edges rather than as whole areas.

Figure 4.3-2 shows that all 'delta' maps can outline the differences on the existing building façade before and after the BIPV installation. The GBVS and IKN (Harel) models can mark the differences in a much more apparently way than the SWD. It is also noticeable in the 'delta' maps that some pixels outside the BIPV area also have a change in values. This is due to the fact that the saliency models use comparison between features in an image to calculate the conspicuity. If certain parts in the input image are having changes in the feature (e.g. colour), then the overall saliency value distribution will also change. It is unrealistic to only have a feature changed in a particular region in the 2D rendering, and expect only a stationary change in the respective saliency maps.
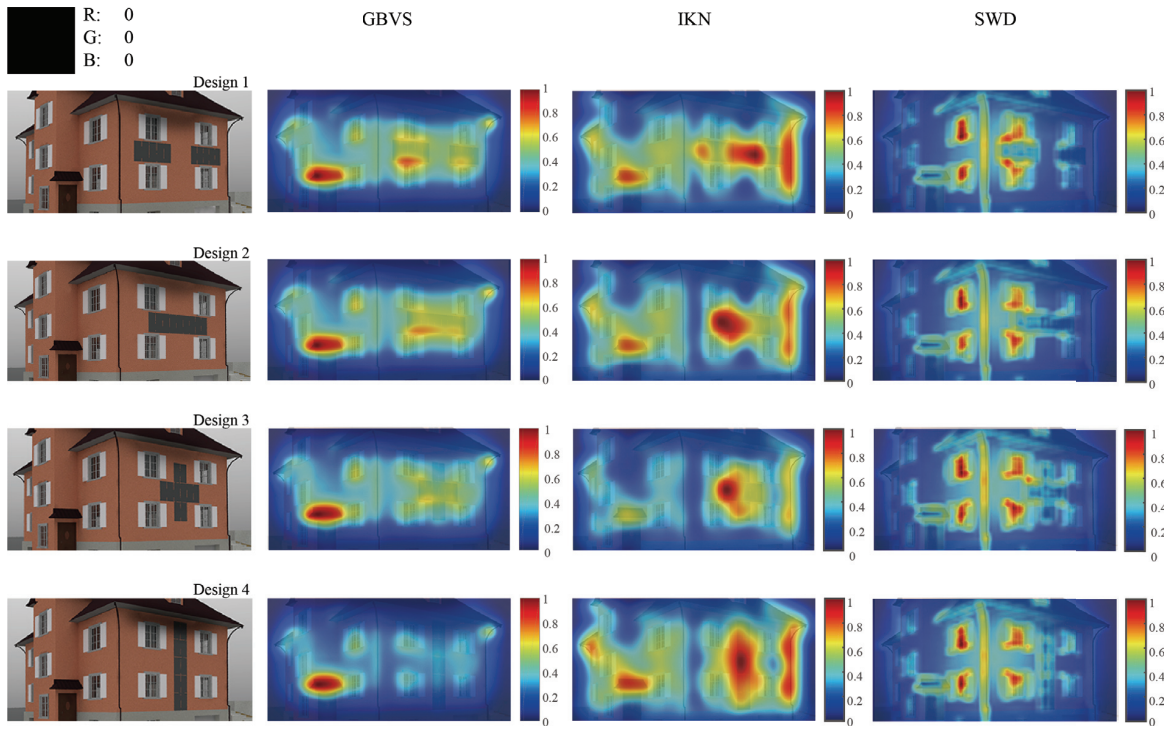
Figure 4.3-1. Saliency maps 'new' produced with saliency models GBVS, IKN (HAREL) and SWD.
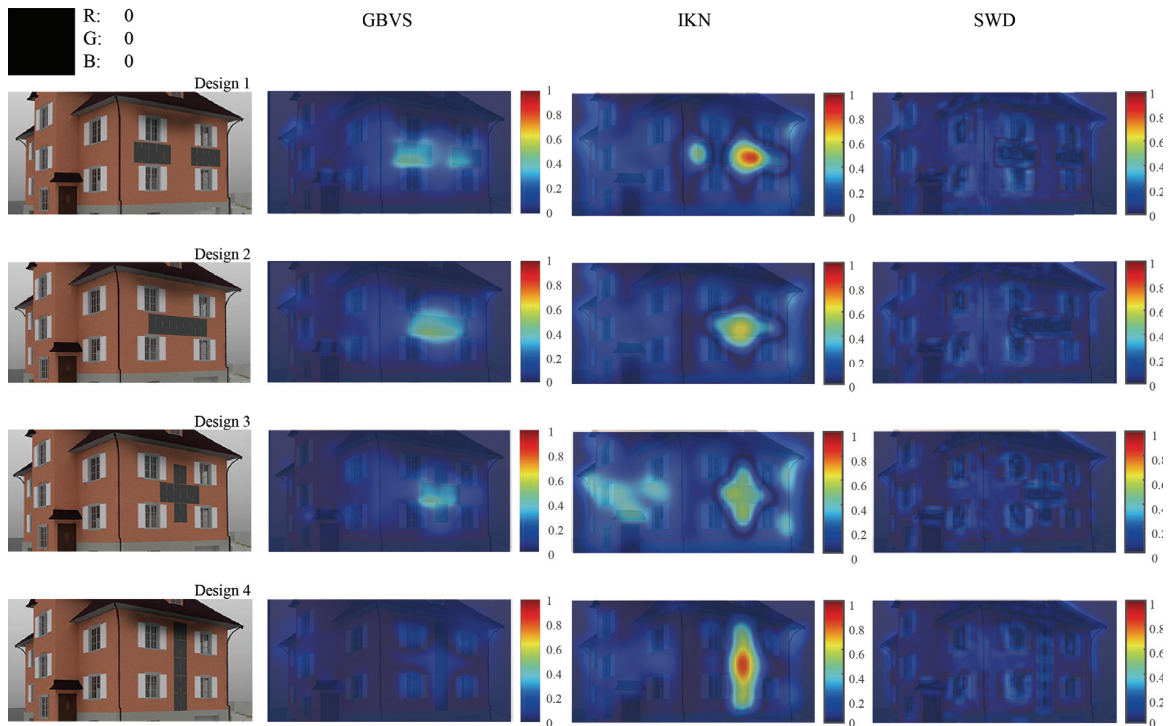
Figure 4.3-2. Comparison of 'delta' maps generated from GBVS, IKN (Harel) and SWD saliency models.

Figure 4.3-3 illustrates binary maps 'result' that are pointing out in white all the pixels that are

among the top 10% most salient pixels white and leaving the rest in black. While the GBVS and IKN (Harel) model can mark out the BIPV installation region among the top 10% salient pixels, the SWD is only able to mark the BIPV partially right. The SWD model predicts that the visual attention towards window frames also varies after the BIPV installation. It can be seen in Figure 4.3-4 that for the same design, 'delta' maps generated from different saliency models have salient pixels distributed in different value ranges. 'Delta' maps of IKN (Harel) model generally show the value distribution in a wider range, followed by the GBVS version, and the SWD version has the narrowest range of value distribution. At the end, both GBVS and SWD models consider the Design 1 as causing the largest modification in visual attention respective to the existing facade and therefore the most visually impacting design. Design 4 is inducing the least visual impact. IKN (Harel) considers the BIPV Design 3 to be the most visually impacting to the existing facade, and Design2 to be the least. A better overview of the result can be seen in Figure 4.3-5.

Figure 4.3-3. The binary maps 'result' based on results from GBVS, IKN (Harel) and SWD saliency models.

Figure 4.3-4. The accumulated sum of pixel number within different value ranges according to 'delta' map generated from GBVS, IKN (Harel) and SWD saliency models.

Figure 4.3-5: Visual impacts of different BIPV designs generated with different saliency models.

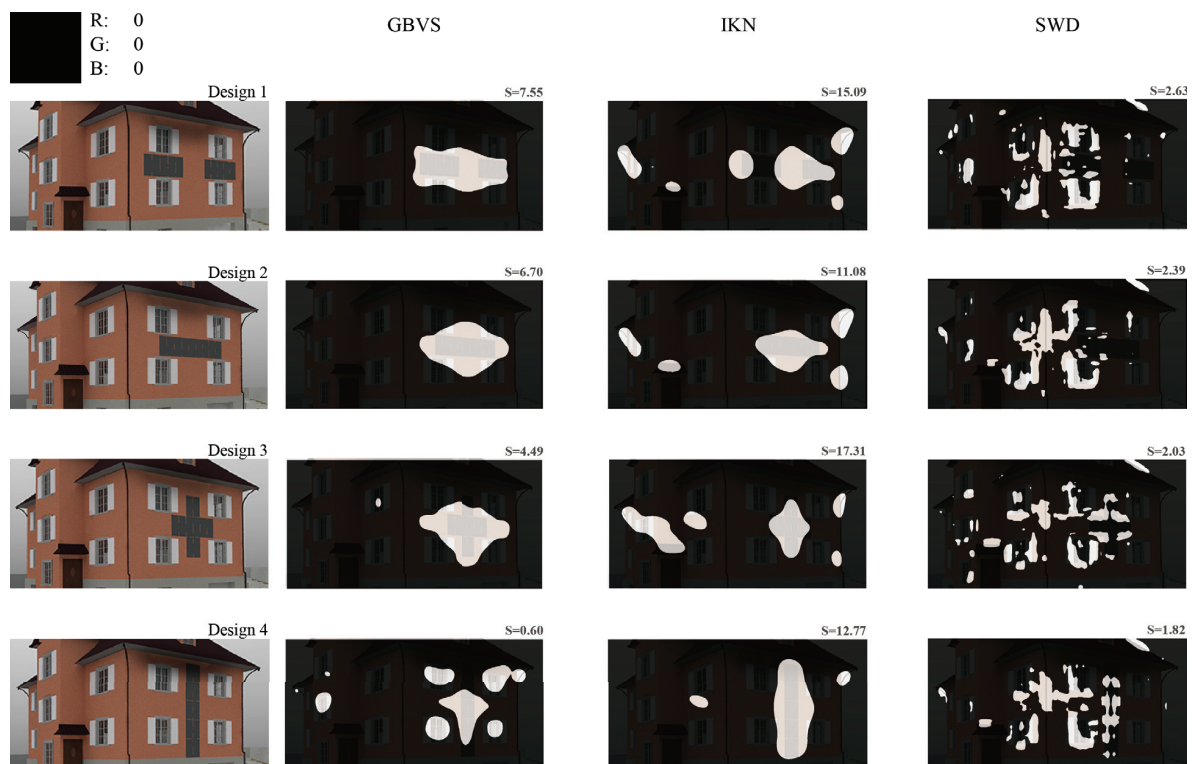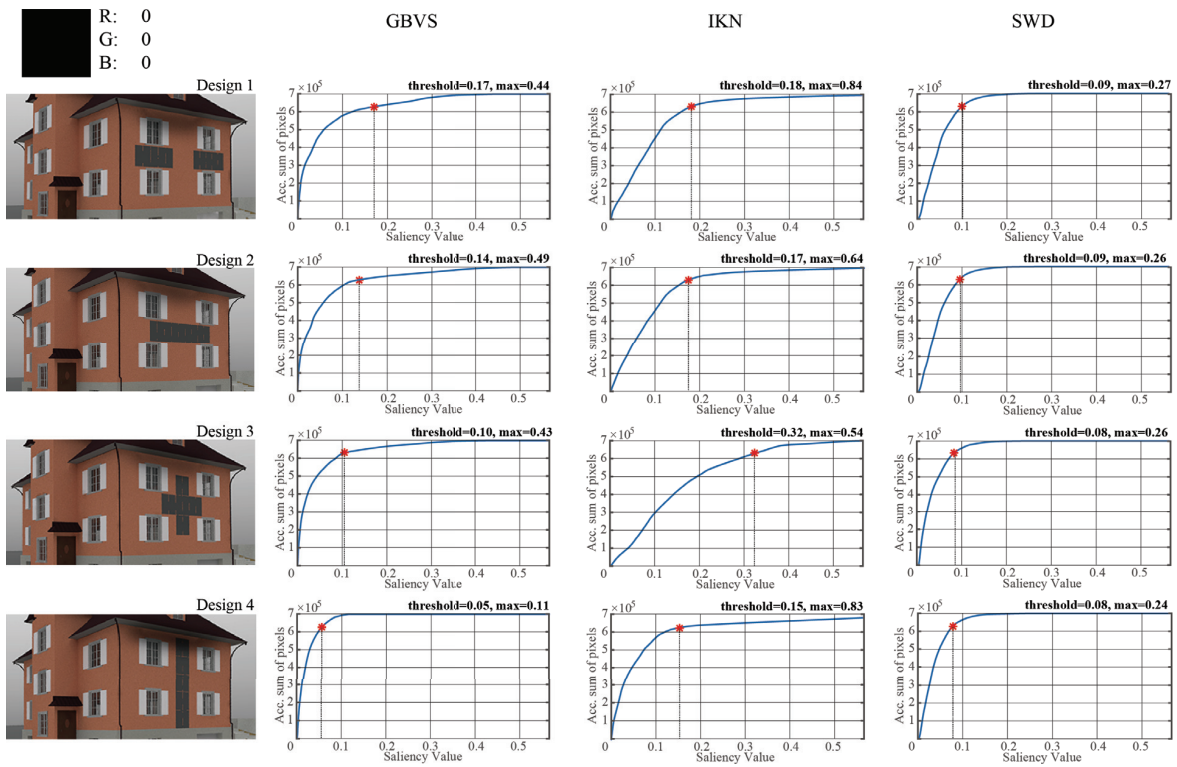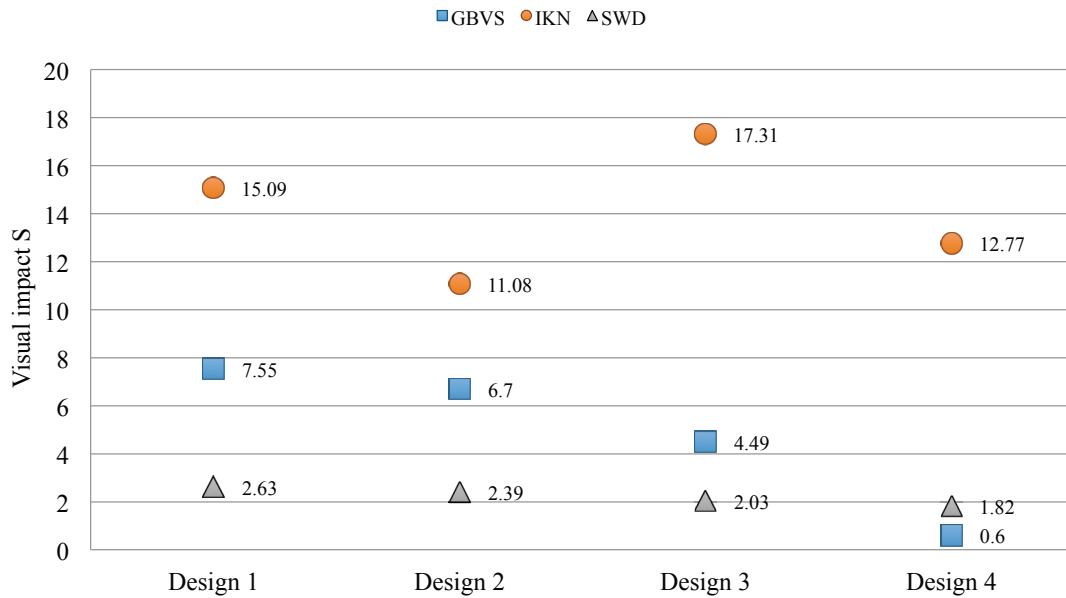| Saliency model	Advantages	Disadvantages
GBVS	• The image centre is more weighted than other regions. • The fact that every vertex is connected to all the other vertices in the Directed Graph allows the contrasts in the input image to be analysed holistically.	• Details can not be outlined
IKN (Harel)	• The relationship between design parameters colour, intensity and orientation can be shown and is easy to understand.	• All image regions are weighted equally. • Details can not be outlined. • The pixel contrasts in the input image is analysed regionally.
SWD	• The image centre is more weighted than other regions. • Details can be outlined.	• An image with many details will generate saliency map with redundant regions outlined with high saliency values, thus providing an inefficient visual analysis.

Table 4.3-1: The advantages and disadvantages of GBVS, IKN (Harel) and SWD saliency models from architecture design point of view.

The Table 4.3-1 summarizes the advantages and disadvantages of the three saliency models from architecture design point of view. It is impossible to choose one single saliency model because each of the three saliency models responds differently to BIPV designs. Each one uses its own unique approach to predict visual saliency of the visual scene. As introduced in section 3.3 – the saliency models, the IKN (Harel) does not have centre bias integrated. The GBVS and SWD saliency models apply larger weights to pixels that are more closely located to the image centres, therefore these pixels are more likely to get higher saliency values. From Figure 4.3-1 it can be observed that the most salient regions of GBVS and SWD saliency maps are mostly found adjacent image centres, while the same can not be inspected from the IKN (Harel) saliency maps. The IKN (Harel) saliency model involves Gaussian pyramid and centre-surround operations, resulting in colour blobs in saliency maps. The similar phenomenon can also be observed in the GBVS saliency maps, probably because similar variance (σ) value is used for Gaussian smoothing of the saliency map. The salient regions in SWD saliency maps are more separated and distributed than the maps from other two models, possibly because relatively small variance (σ) value is used for Gaussian blur. The different value ranges in saliency maps are due to distinctive normalization procedures of each saliency models.

To conclude, each saliency model has its own approach in imitating the contrast comparison mechanism of human visual attention, but also resulting in its unique advantages and disadvantages. The IKN (Harel) can offer an insight of visual saliency of the visual scene based on *Feature Integration Theory*, eliminating the centre-bias of human eyes and revealing how colour, intensity and orientation simultaneously affect the BIPV visual impact. The fact that every vertex is connected to all the other vertices in the Directed Graph of GBVS saliency model allows the input image to be analysed holistically, and automatically involving the centre-bias feature due to the nature of the models principle. The SWD can outline the saliency distribution in a more detailed way

because small default variance (σ) value is used in calculations. When applying them simultaneously, the resulting saliency maps can compensate each other and offer special insights into the visual aspects of BIPV design.

4.3.3 Image resolution

In order to verify how image resolution affects the outcome of saliency maps, 3D digital models of huts in three different complexity levels were made – simple, medium and complex (Figure 4.3-6). Then 2D renderings of these huts from the same perspective were made in different resolutions. The highest resolution of the renderings is 1600 x 1600 pixels. The qualities were reduced gradually to 400 x 400 pixels in 200 pixels per step. Extra renderings of resolution 180 x 180 pixels were also included because this is the smallest image size acceptable by the GBVS and IKN (Harel) saliency models.

The detailed results can be seen in Appendix 2. For the GBVS model, images with resolutions above and including 800 x 800 pixels don't have significant impact on the saliency maps. The qualities of saliency maps from renderings of size 800 x 800 pixels are still acceptable. When the input image drops below 800 x 800 pixels, the features in the resulting saliency maps are marked rather roughly in the form of interconnected colour bubbles. The IKN (Harel) saliency model performs quite unsteadily in relevance to the input image quality. While the distributions of the saliency values seem to be quite consistent across all IKN (Harel) saliency maps, the high values are disseminated rather oddly. The blurring in colour-mapping also grows in saliency maps as the images quality continues to fall further below 800 x 800 pixels. For the SWD saliency model, whose advantage is its detail identification ability, the higher the image quality, the more exquisite the resulting saliency maps. However, it doesn't necessarily mean that the higher the input image resolution, the better the quality of the resulting SWD saliency map. Since renderings with higher resolution also include abundant of details so that the majority areas of the saliency maps would be marked as salient regions and therefore risking the saliency map to become invalid for further analysis. So in conclusion, as long as the input image has resolutions above 800 x 800 pixels, satisfactory saliency maps can be generated with all three saliency models applied in this thesis.
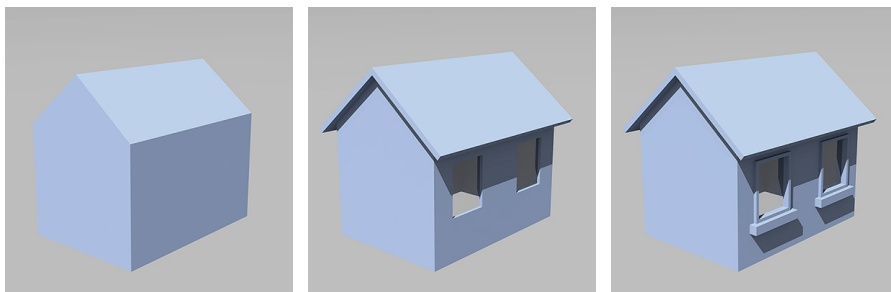

Figure 4.3-6: 3D digital models of huts from the same perspective. The complexity of the models gradually rises from left to right.

4.3.4 Public feedback

In the frame of the 12th workshop "Photovoltaik-Modultechnik" organized by TÜV Rheinland, the author of this doctoral thesis gave an invited talk concerning the topic using saliency models to evaluate the BIPV visual impact on retrofitted building envelopes [188]. After the presentation, questionnaires were passed out to find out the opinions of the audiences (Table 4.3-2). In total, 50 sheets were handed out and 38 of them were returned. Among the audiences, 87% of them were engineers active in PV sector, such as physicists, electricity engineers and similar. The rest of the audiences were either not specific about their profession, or they were people in relevant areas such as patent manager or sales person. Such combination made them a suitable crowd to investigate the sense of the proposed evaluation method. Concerning the question asking how many of them have encountered the issue about aesthetical acceptance of BIPV on building envelopes in their work, around 40% claimed that they rarely or never dealt with this topic. The majority of them, around 60%, were often or sometimes confronted with this matter.

Questionnaire "Visual assessment for solar architecture"

1. What is your profession?_____

2. How often in practice have you encountered the discussion with the topic "Photovoltaics and their aesthetic acceptance"?

☐ often ☐ sometimes ☐ seldom ☐ never

3. Do you generally consider the present qualitative assessment standards of the topic "Photovoltaics and their aesthetic acceptance" as

☐ very well comprehensive ☐ depends on the situation ☐ difficult to understand

4. Do you consider the saliency map as a helpful tool to visualize the visual aspect of BIPV more comprehensively?

☐ Yes ☐ I am not sure yet ☐ No

Table 4.3-2: Questionnaire handed out to audiences in 12th workshop "Photovoltaik-Modultechnik" , organized by TÜV Rheinland (Contents are already translated from German to English).

The absolute majority of the audiences (84%) consider the qualitative evaluation standards of "BIPV and aesthetical evaluation standards" mentioned in RPG law 18a to be difficult to understand, or its clarity depends on which project is concerned (Figure 4.3-7). Only 5% among them found this law article to be very well comprehensive. The remaining 11% of audiences either didn't understand the question, or left the answer field to this question blank. In response to the question whether the proposed method with the help of saliency models can be a useful tool to illustrate the visual aspect

of BIPV, around 24% of the audiences held positive attitudes (Figure 4.3-8). Most of the audiences were not sure how to answer the question, probably because the old method with absolute value as threshold was used in the presentation (see also section 4.3.1), therefore making the analysis results less persuasive. Only 18% of the audiences held negative attitude towards the proposed method.

Do you see the qualitative evaluation standards of the topic "BIPV and aesthetical acceptance" as...

Very well comprehensive 5%

No answer 11%

Difficult to understand 26%

Depends on the situation 58%
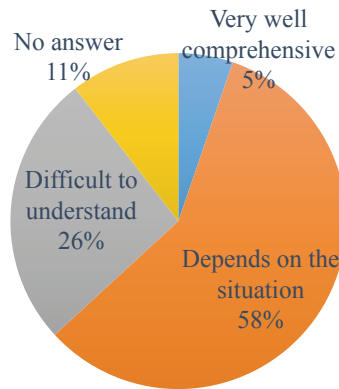
Figure 4.3-7. Questionnaire result on question 3.

Do you consider the saliency map as a helpful tool to visualize the visual aspect of BIPV more comprehensivly?

No 18%

Yes 24%

I am not sure yet 58%
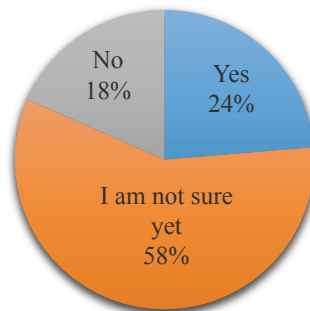
Figure 4.3-8. Questionnaire result on question 4.

4.4 Conclusion

This chapter introduces the methodology and explains how saliency models can be used to transform the BIPV visual saliency information to visual impact information on retrofitted building envelopes. The strength of the visual impact is represented by one single value. Thus answering all three research questions from Chapter 2. The proposed method should be used before the BIPV

installation takes place on existing building envelope so as to have a proper estimation of the potential visual impact.

First, 2D renderings of an existing building facade before and after the BIPV installation are generated. These renderings act as snapshots of the human visual perception concerning the target building before and after the BIPV installation. They are used as input images to be fed into saliency models that therefore should be rendered with credible parameters in RADIANCE software. Then saliency models are used to produce visual analysis information for the renderings with saliency maps. The weighted change in visual attention between renderings with and without BIPV equals the visual impact of BIPV on the existing building envelope. The less change in visual attention before and after the BIPV installation, the less the BIPV is visually affecting the existing building. A final S value shows the strength of the BIPV visual impact to the existing building.

A comparison is made between the old and new version of the proposed method. They differ from each other because the old version uses absolute threshold to distinguish which values in the 'delta' maps are salient and which aren't. The new version uses a dynamic and weighted threshold to tell the salient pixels apart from the non-salient ones. Advantages of the new version are explained.

Three different saliency models with default parameter settings are applied in the methodology, each of them having its unique strengths. The GBVS and IKN (Harel) saliency models can outline the BIPV system with a high accuracy, and should be used as main tools. These two models predict the salient regions with colour blobs, while the SWD saliency model can analyse the renderings with a lot of attention to details. The SWD can therefore be used as a complementary tool in cases where a lot of texture variations or details are involved. It is important to use the three of them simultaneously.

How the resolutions of input images affect the resulting saliency maps were also tested and the conclusion is that as long as the input images are above 800x800 pixels in sizes, then the resulting saliency maps would be qualified for further steps of the methodology.

Questionnaires were handed out to professional audiences in order to find out their opinions on the proposed method. The results are positive.

Chapter 5   Practical Implementation

The management team of the church St. Michael approached CC EASE, HSLU in 2012, with the wish to apply BIPV on their building envelope. This consideration was based on the fact that other necessary measures to increase the building energy efficiency had been completed. They hoped to take the energy efficiency to the next level on the one hand, and on the other hand to be a role model for the community by demonstrating their green and pioneering attitude outwards. The integration of BIPV should be architecturally of good quality. This project is still on-going and involves the management team of the church, the CC EASE of HSLU and the heritage protection department of Lucerne city. The planning has been a long and cautious procedure of BIPV design that requires consideration of the interests from different stakeholders already from early stages.

Several different BIPV design proposals were developed, visualized and analysed for St. Michael. Two general approaches were either demonstrating the functional and aesthetical added value of BIPV deliberately, or integrating the BIPV as invisible as possible. Both standard economic PV modules as well as custom made ones were considered in the designs. Strong suggestions came from the heritage protection department of Lucerne, for whom the visual impacts of the BIPV and heritage values are of great importance. Beside subjective opinions from different stakeholders, the proposed method from Chapter 4 was used to objectively predict the potential visual impacts of different BIPV designs on the existing appearance of the church. This chapter is a record of this on-going project with strong bias on the application and feasibility test of proposed evaluation methodology.

5.1 Churches and their suitability for BIPV installation

5.1.1 From theoretical point of view

Since the oil crisis, many Christian peace and environment initiatives have been using the slogans "care for creation" and "climate justice" to declare that humans are responsible in taking care of the God's creation – the natural environment. The opinion that human kind is obliged in protecting the earth and saving energy is also shared among main Christian organizations. In 1980, the German Bishops' Conference (Deutsche Bischofskonferenz) published an announcement under the name "Future of creation – future of humans", declaring and explaining what kind of attitude a person

needs to hold towards energy, resource and environment crisis [189]. Back then exact solutions to the problems were not mentioned, the announcement was rather a call for the necessity to sustain God's creation. The focus of the announcement was the spirituality of the behaviour towards the world ("Spiritualität unseres Verhaltens zur Welt"). In 2011, the same organization reported about some success cases in Germany, such as that German churches, having over 500 facilities, were the biggest group among organizations to apply environmental management schemes according to EU standards [190]. In Switzerland, this trend can be reflected, among many others, in the action "CreationTime" (Schöpfungszeit) organized by the ecumenical organization oeku Kirche und Umwelt [191]. The organization oeku Kirche und Umwelt is the consulting department of Swiss Bishops Conference (SBK) and Federation of Swiss Protestant Churches (FSPC) in matters concerning ecology. The action is held annually in order to promote the engagement of taking care of God's creature from Swiss Christians. The organization also requests the parish authorities to integrate the topic "CreationTime" into their liturgies. In 2014, the central committee of the World Council of Churches (WCC) called the members of churches, related ministries and networks to "make positive changes in energy consumption, efficiency, conservation, and the use of energy from renewable sources; and build on the experience of environmentally conscious churches in the WCC" [192]. In 2015, Pope Franziskus announced that the 1st September is to be celebrated as the "World Day of Prayer for the Care of Creation" [193]. Nowadays, the topic environment protection and clean energy is considered a serious matter in the ecumenical area the same way it is anywhere else in the world.

On the social level, churches play very central roles in the Western society. They are usually located in the centre of a community, are places for liturgical activities and people often go there for spiritual support. As light towers for believers, they also create a strong link between people within the same area and enhance the community spirit. They carry heavy moral weights within and are reflections of the values and standards the Christians hold. In order to show that the values and standards advocated by the churches are also valid and feasible in today's practice, they need to show that they are aware of the latest global happenings. A pose showing open, communicative and responsible attitude towards contemporary society is especially important when acting as role models for the young people. Installation of BIPV on church envelopes will show this supporting attitude of the church towards energy turn (Energiewende) and that they are striving for a sustainable environment in capital letters. By welcoming the renewable energy sources, it implies that the churches are active actors in the aspect of "caring for the creation"[194], [195]. As the churches usually carry heavy emotional weight from the perspective of local inhabitants, thus making installing BIPV installation a very sensible and risky matter: as much as a good BIPV installation can be praised for adapting clean energy and their pioneering role to care for creation, a bad integration can also have negative social impacts in the same strength.

5.1.2 From practical point of view

Most churches have the altar located in the east because this orientation has biblical meanings. First, it symbolizes the second coming of Christ in kingly glory[12], and it's also the same direction that Jewish high priests faced in the Jerusalem Temple on the Day of Atonement. The entrance is usually set opposite the altar, on the other narrow end of the rectangle church nave. People enter a church by the entrance, see the altar and usually reach it after passing a long narrow space formed by the high pillars. It is believed that this purposeful arrangement is a visual and sensual rendering of the biblical concept that the "time is linear, processive and moving towards a conclusion" [196]. Such cognition of time naturally results in that the entrance and the altar are located on the two shorter sides of the rectangle church nave respectively. The sloped roof parts covering this narrow long nave eventually face to the north and south respectively. In order to be able to hold a large crowd during liturgical events, a church usually covers large spaces and hence needs large sloped roofs. With its remarkable height decided by its social status, the roofs are also rarely shaded. This kind of area, orientation, slope and height are all very ideal for installing BIPV.

5.1.3 The difficulties

The first concrete measures people normally take in order to "care for creation" is to increase the energy efficiency of the church buildings. The FSPC published a brochure, stating that the goal of the overall energy consumption should be following the standard of "2000-Watt-Gesellschaft" (2000 Watt Society) [197]. The action "Brot für alle" (bread for everyone) pledged that the Swiss domestic Greenhouse Gas Emmission (GHG) should be reduced by 40% until 2020 [198]. oeku Kirche und Umwelt suggested that measures such as improving envelope insulations, using advanced heating measures and enhance energy efficiency are of primary importance. Up to 30% of heating energy consumption could be saved simply by improving operational arrangements [199]. The integration of solar technology is, compared to above mentioned measures, rather of secondary importance. Even though solar technology will take the energy efficiency of the building to the next level, however, most churches are listed as heritage buildings of national or regional importance [200], [201]. Due to their physical and aesthetical sensibility, a solar installation could possibly impact the existing external appearance and cause damages to the historical fabric of the church. With these reasons, EnergieSchweiz – an organization below the Swiss Federal Office of Energy, strongly suggests careful planning, consideration of alternative energy resources and the application for installation permissions [202]. Considering the Swiss urban planning law RPG art. 18a [11], it is apparent that the benefits to society in terms of sustainable environment must be weighed against the harm caused to the heritage asset. The intervention of the domestic heritage departments and similar authorities must be included in the early stage of design.

---

[12] "For as lightning that comes from the east is visible even in the west, so will be the coming of the Son of Man."(Matthew 24:27).

5.2 Case study: St. Michael in Lucerne

The church St. Michael is located in Lucerne and is the subject of the case study. The management team hopes to integrate BIPV on its building envelope. Several designs were already proposed before but not granted building permissions because the heritage protection department of Lucerne city regarded the architectural considerations to be insufficient. To respect the copyright of the architect, it is important to find out what was his main concept in the architecture design, his style and therefore being succinct about the main characteristics of the architecture that need to be preserved.

The architect Hanns A. Brütsch designed several churches in the 1960s, and all of them can be categorized to Brutalism architecture. Architectures of this kind usually distinguish themselves by using exposed raw concrete constructions, massive volumes and possessing solemn and fortress-like qualities. Those are also the characteristics that marked the works of Brütsch during this era. Two example works of the architect are shown in Figure 5.2-1 -Figure 5.2-2.
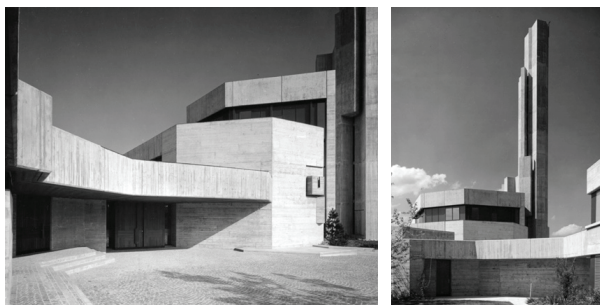
Figure 5.2-1: Church St. Johannes (Buchs, Switzerland), built in 1967. With permission for reuse from [203]

Figure 5.2-2: Private Hospital St. Franziskus (Menzingen, Switzerland), built in 1967. With permission for reuse from [203]

The church complex St. Michael in Lucerne was built in year 1967 after the architect won the 1st prize in the competition. The architecture is located on a very small hillock surrounded by residential buildings. When people slowly approach the main entrance along a slope and enter the church courtyard, they will be impressed by the grading volume and sloped roofs of the church, which make it appear very much cliff-alike (Figure 5.2-3). The use of raw concrete texture on the facade endows the church with a monumental appeal. In the original state, the silhouette and

materiality of the church were distinctively visible and the visual perception of the church was undisturbed. The massiveness and heaviness were the most striking characteristics of the main church building. The sculptural feature of the building volume was emphasized by the crude cut of the roof and spare use of facade openings. Steep and wide stairs lead to the contemplative courtyard of the building complex (Figure 5.2-4), which is formed by the church, a pastor office, a residential building and an activity centre. Annex buildings share the same monumental charisma as the church by being abstinent in window and door settings (Figure 5.2-5-Figure 5.2-6). Figure 5.2-7 is a photo of the design model built by the architect, from where the sculptural properties of the church are visible. Figure 5.2-8 is a pictogram that shows the functional arrangement of the building complex.

The setting of natural daylight in the altar area is an important architectural language used by the architect. He was active in the years where the historic high altars were no longer popular, instead it was expected that the priests celebrated the Mass facing the crowd (Latin: "versus populum"). Therefore the architect located the altar close to and on the same level as the audience, but emphasized it by introducing skylight to this area (Figure 5.2-9).

Figure 5.2-3: Approaching the church. On the way to the main entrance to the courtyard. With permission for reuse from [203]

Figure 5.2-4: Before entering the courtyard, one has to climb up the wide and steep stairs. With permission for reuse from [203]

Figure 5.2-5. View in the courtyard towards the church. With permission for reuse from [203]

Figure 5.2-6. View in the courtyard towards the activity centre and residential building. With permission for reuse from [203]
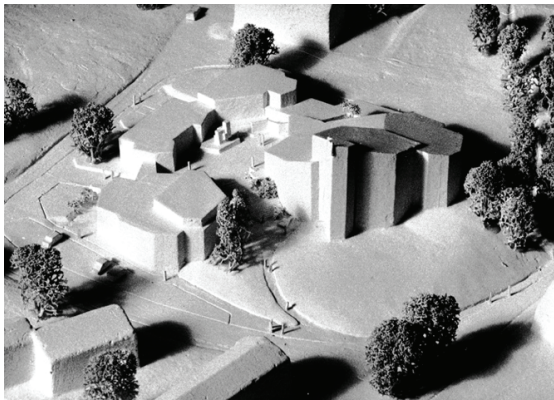
Figure 5.2-7: The building model built by the architect. With permission for reuse from [203]
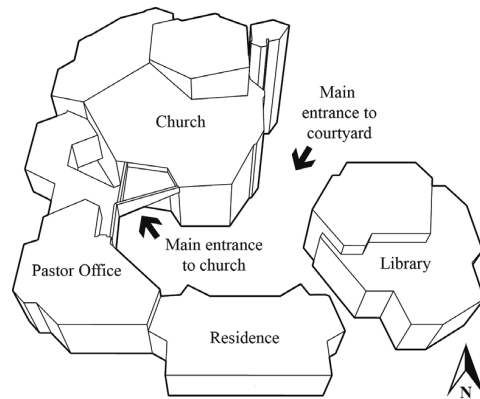
Figure 5.2-8: Functional layout plan of the church complex.

Figure 5.2-9: The indoor view of the church in 1960s, with accentuation to the altar area. With permission for reuse from [203]

Figure 5.2-10: The indoor view of the church, with accentuation to the altar area today.

Today some changes can be observed in the building complex, which are mainly caused by the growing vegetation over the years. The Figure 5.2-11 shows the main entrance to the courtyard today in comparison to Figure 5.2-3, where the building is hidden behind giant pine trees and weakened the perception of the voluminous figure of the church. Inside the courtyard, some trivial vegetation along with a gigantic birch tree was affecting the impression of architecture's plasticity in a negative way in 2012 (Figure 5.2-12), causing that its monumentality and solemn beauty can't be sensed adequately. This situation has visibly been improved after the birch was cut down (Figure 5.2-13). Differences can also be observed on the windows of the light tower. At its original state, the window frames, the glasses and the rest of the room were melting into a monotonous unification. Today the unification is disturbed by the bright coloured window frames and irritates the feeling of the monotonous unification. The view towards the activity centre inside the courtyard can be seen in Figure 5.2-14. The clarity of the volume is only hardly recognizable due to the vine growing on the concrete facade and excessive trees in the background. Compared to the initial state in Figure 5.2-6, more livelihoods are applied to this part of the building complex. The atmosphere of serenity that

was to be perceived when standing on the wide steep stairs, which was originally intended by the architect, clearly diminished (Figure 5.2-15). Changes indoor are rather trivial compared to the outside (Figure 5.2-10).

Figure 5.2-11. The entrance to the main courtyard in April 2016.

Figure 5.2-12. The main church building. Photo taken in 2012.

Figure 5.2-13. The main church building. Photo taken in 2016.

Figure 5.2-14. View towards the activity centre. Photo taken in 2016.

Figure 5.2-15. The wide stairs of the main entrance to the courtyard in 2016.

5.2.1 Roof of the main church

The most likely location for BIPV installation would be on the sloped roof of the church. The existing roof is covered in Eternit plates. Being used over decades, these tiles aren't in a suitable condition today because their textures are weather-beaten, porous and partially broken (Figure 5.2-16 - Figure 5.2-17). A renovation of the roof is essential.

Figure 5.2-16: The roof quality of the church from afar. It can be seen from the greenish colour that mosses fully occupy the roof tiles today.

Figure 5.2-17: A closer look of the weather beaten roof tiles. (Photo credit: Christian Röske)

From an architectural point of view, the materiality of the concrete, the sculptural mass and the exquisite setting of facade openings are the most crucial aspects in the St. Michael that need to be preserved during any retrofitting procedure. These are the qualities that will eventually decide the perception of the overall architecture. The main goal of the project is to renovate the existing damaged church roof, further it is desired to preserve the original architectural appeal in the frame of cultural heritage preservation and integration of renewable energy by BIPV installation. The very fine balance between solar energy harvesting, appropriate visual demonstration and moderate amount of visual impact needs to be found.

5.3 BIPV designs

A rough solar radiation analysis was done with the software ECOTECT in order to identify suitable locations for BIPV. The 3D model contained approximate geometric information of the building complex. Surrounding vegetation was not integrated in the model because the management team of the church expressed that they have the freedom to remove them when necessary, as was the case with the birch tree in the courtyard that was blocking the perception of the church (Figure

5.2-12-Figure 5.2-13). Figure 5.3-1 shows that in general, all building roofs are unshaded. The sloped roof is oriented to the southeast direction and has a tilting angle of approximately 25 degrees. Moreover, the main goal of BIPV installation is to be demonstrative of the supportive attitude towards greener future, the sloped roof of the church is the most visible location by visitors and hence most suitable. The areas near the light tower of the church harvest less solar energy annually because the light tower itself is blocking sunlight from east and west in early mornings and late afternoons. The terrace above the pastor's office is also an appropriate location in respect of visual demonstration and solar radiation.
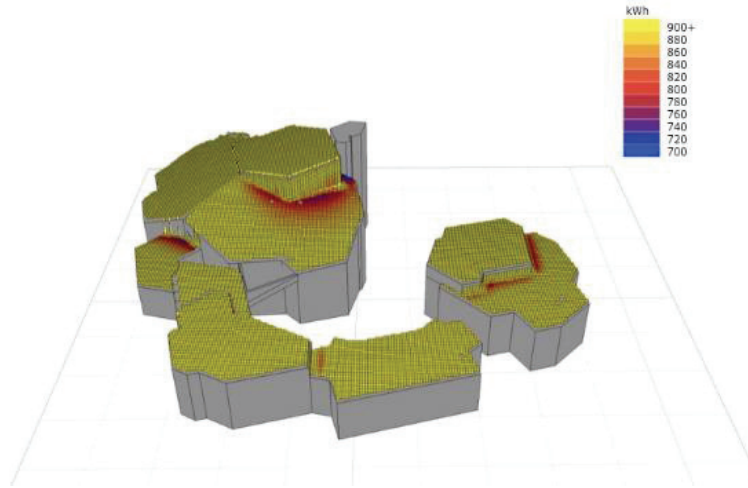

Figure 5.3-1: Annual solar radiation (without trees).

There are 5 designs in total. 4 of them place the BIPV on the sloped church roof, and the remaining one proposes to install the BIPV above the pastor's office. The first 3 designs take quite conceptual and bold approaches, while the other two are more practical and cautious. The installed area and power of the BIPV in different designs can be seen in Table 5.3-1.The high preference of the sloped church roof as location for BIPV is due to the general concept that the church roof inevitably needs a renovation due to its functional decay. The existing damaged Eternit plates will be eventually replaced by new ones, so the existing visual appearance will be changed anyway. In light of this circumstance, the roof might as well be covered with BIPV that imitate the tiled characteristic of the existing pattern and its architectural appeal maintained in this way.

Design name	Total BIPV area (m^2)	Total installed power (kWp)
PVUp	82.5	13.0
PVPolygon	40.0	5.1
PVTerrace	79.2	12.5
PVBig	336.9	58.3
PVSmall	414.3	53.8

Table 5.3-1: The installed area and power of the BIPV in different designs.

5.3.1 Design1 - PVUp

This design intends to apply the BIPV on the upper side of the sloped roof adjacent of the light tower. Standard BIPV modules are split into two rectangle groups and follow the edges of the light tower. This location provides just enough visibility to the visitors in achieving demonstrative effect, but is visually not dominating from most viewpoints due to its height. The arrangement in two groups avoids confrontations with the irregular silhouette at the bottom of the roof. In addition, the edges of the roof are bordered with rainwater drainage with many turns, it would make the placing of standard BIPV modules even more complicated. No dummy modules are intended. This design also requires less time and effort in installation and less technical equipment, e.g. cable connections. With the huge advantage in cost, the drawback of this design is that the outlines of the two PV groups are not exactly following the profile of the church and hence architecturally not very ideal. Generally speaking, this design is a very simplified solution without much architectural delicacy. By lowering the BIPV's visibility through placing them as high as possible on the roof, the quality of the church is preserved. The location of BIPV is shown in Figure 5.3-2.
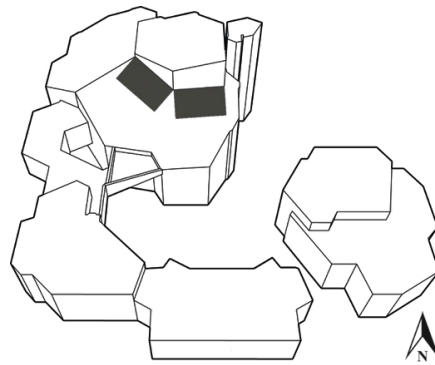

Figure 5.3-2. The location of BIPV in design PVUp

5.3.2 Design 2 - PVPolygon

Custom-made hexagon PV panels are applied at the bottom of the sloped church roof (Figure 5.3-3). The angle of the BIPV profile can approximately follow the profile edges of the sloped roof. Blanks between the hexagon PV panels and roof borders are filled with modified dummy modules. This location ensures more visibility compared to the design PVUp because of lower height, therefore it is possible that the glazing colour of the PV could have a huge impact on the overall perception. Custom made PV modules and the integration of dummy parts would result in higher costs. This design approach is to set a contrast between the existing building and the BIPV. The goal is not to hide the PV, but rather to separate the old and new by their own silhouettes. However, the separation is less radical in comparison to the design PVUp. Consistency between the old and new is mainly achieved by the dark front glazing colour of the BIPV, and the dummy parts fill up the unmatched places between the silhouette of the existing roof and hexagon PV panels.
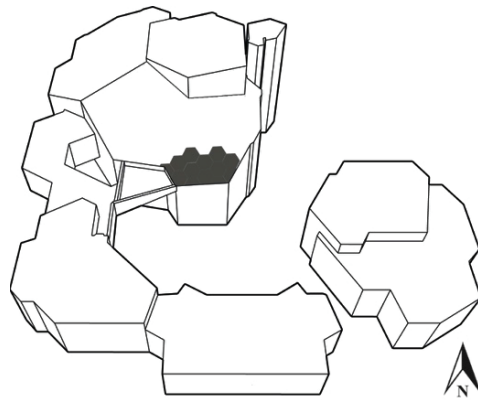
Figure 5.3-3: The location of BIPV in design PVPolygon.

5.3.3 Design 3 - PVTerrace

In comparison to design PVUp and PVPolygon, this design takes a relatively radical approach. The flat line from the higher roof of the pastor's office is extended to the north. The extension covers the terrace and creates extra space for outdoor activities (Figure 5.3-4). Standard PV panels are to be applied above the extended roof. The original rhythm of the architecture is not interrupted, and the extended roof is rather an imitation and prolongation of the existing architectural components. The advantage of this design is that for visitors standing in the courtyard, the PV above the extended roof would not be visible. Thus avoiding the trouble to deal with the reflection issues from the PV modules. The downside is that this approach is quite controversial. Some may consider the design to be successfully mingling into the existing context, others may consider the visual impact of the extended roof to be very high because the original silhouette of the building complex is altered.
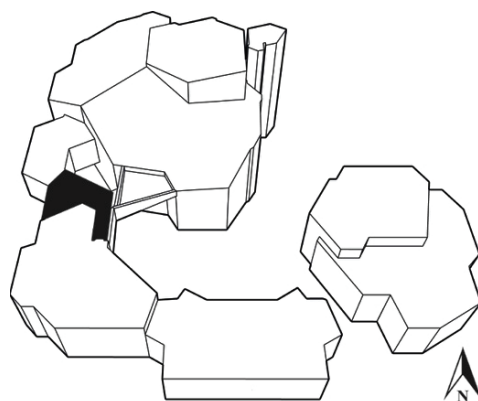

Figure 5.3-4. The location of BIPV in design PVTerrace.

5.3.4 Design 4 - PVBig

In this design, large standard BIPV modules cover the existing sloped roof of the church entirely (Figure 5.3-5). Dummy panels are to be used in places where a complete standard PV module could not fit in. The standard PV modules are of size 75cm x 100cm (Figure 5.3-6), each is covered by the modules above it by 35 cm. This is an imitation of the new tiles on the church roof, an architectural rendering with a perspective to the light tower can be seen in Figure 5.3-7. The visibility of the BIPV modules is high, but the tiled and homogenous pattern would make them less visually dominant. A mockup of the PV panels was also built so as to get better visual perception before the actual implementation. The cost for a 4m^2 mockup with these PV modules without miscellaneous parts, montage and transport is estimated to be approximately 750 CHF (Table 5.3-2). This design holistically preserves the original appearance of the existing church by arranging the BIPV in the similar patterned characteristics as before. No new silhouette will intrude the existing silhouettes and all the existing lines in the architectural context are respected.
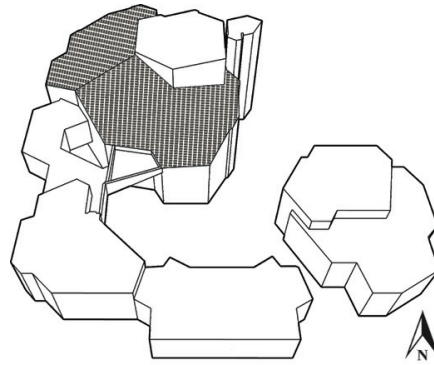

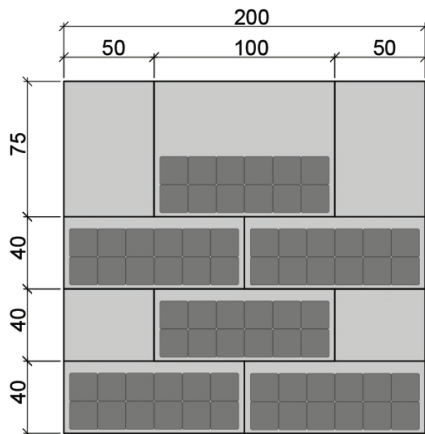Figure 5.3-5. The location of BIPV in design PVBig.

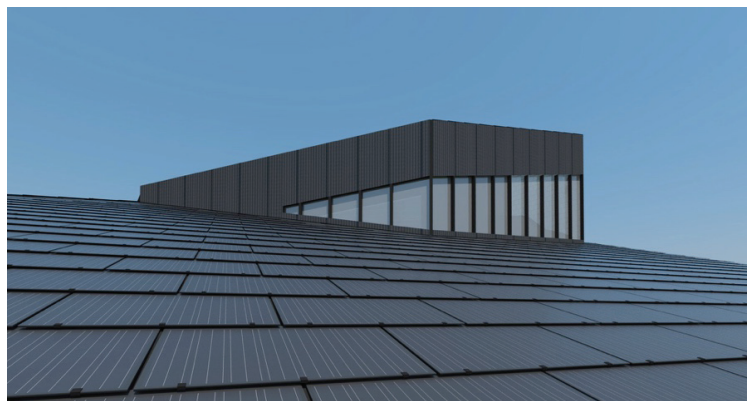Figure 5.3-6: Mockup of the large standard BIPV modules in design PVBig.

Figure 5.3-7: Architectural rendering of tiled roof surface with large standard BIPV modules in design PVBig.

PV Big	Unit	Number	Single price (CHF)	Sum (CHF)
PV module standard	Piece	6.00	100.00	600
Dummy module AURA	m^2	1.50	100.00	150
			Total sum	**750**

Table 5.3-2: Cost estimation for a 4m^2 mockup with large standard BIPV modules in design PVBig. (Credit: Christian Röske, CC EASE, HSLU)

5.3.5 Design 5 - PVSmall

This design is an upgrade on the basis of the design PVBig (see Figure 5.3-8). Custom-made BIPV modules of size 54 cm x 54 cm are used in this version (see Figure 5.3-9). This is architecturally speaking a very delicate approach because smaller BIPV modules should be closer in resembling the new Eternit tiles and their patterns than the large standard modules. Utmost respect is paid to the architectural appearance of the existing church complex. No strange lines are introduced to disturb the present silhouettes. Same as the design PVBig, in this design the BIPV modules are also very visually accessible for the visitors from almost all viewpoints, but still manage to keep them subtle by imitating the existing look of the Eternit roof tiles. Similarly, a mockup of approximately 4m^2 was also built using these custom-made BIPV modules. Since the prices for such custom-made BIPV modules range from 50 to 187 CHF per piece, the total sum of this mockup without miscellaneous parts, montage and transport is estimated to be 650 - 2157 CHF (Table 5.3-3). The drawback of such cautious and careful design approach is that it is achieved in exchange of heavy planning work, high costs and complicated technical requirements e.g. abundance of electric cables and extensive caring.
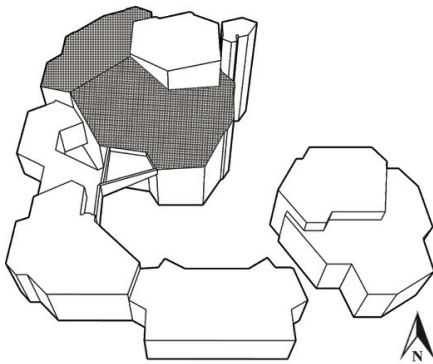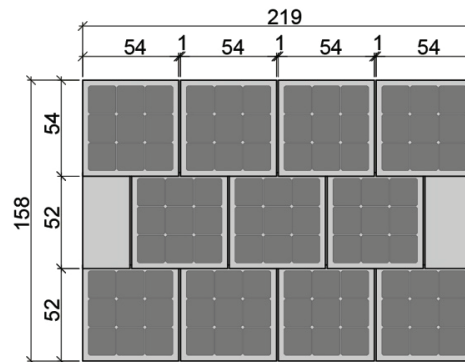

Figure 5.3-8: The location of BIPV in design PVSmall.

Figure 5.3-9: Mock Up of custom-made PV modules for design PVSmall.

PV Small	Unit	Number	Single price (CHF)	Sum (CHF)
PV module	Piece	11.00	50.00 – 187.00	550 - 2057
Dummy modules AURA	m^2	1	100.00	100
			Total sum	650 – 2157

Table 5.3-3: Cost estimation for a 4m^2 mockup with custom made BIPV modules in design PVSmall. (Credit: Christian Röske, CC EASE, HSLU)

5.4 Retrieving material properties of the PV samples

To study the BIPV visual impact, the material properties of two typical mono-crystalline BIPV modules were measured. 3D digital models of the designs were then coupled with these materials so as to generate plausible rendering images 'new' with RADIANCE.

5.4.1 PV samples

The PV sample 1 (Figure 5.4-1) is a custom-made, single mono-crystalline cell module with a regular glass as front glazing. The PV sample 2 (Figure 5.4-4) is a module with 4 mono-crystalline cells. On the first look, the main difference between these two PV samples can be found in their backsheet colours. The PV sample 1 has a more grey-ish backsheet, while the backsheet of the PV sample 2 tends to be black that resembles the colour of the mono-crystalline wafers. Therefore the overall appearance of the PV sample 2 is more homogenous than that of PV sample 1 (Figure 5.4-2 and Figure 5.4-5). Another observed difference between these two modules is the reflectivity of the front glazing due to different glass products (Figure 5.4-3 and Figure 5.4-6). The front glazing of the PV sample 2 is less reflective than the one of sample 1 due to application of an anti-reflection coating.
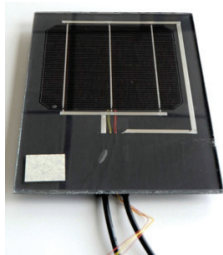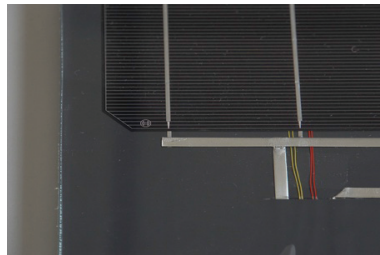

Figure 5.4-1: PV sample 1.

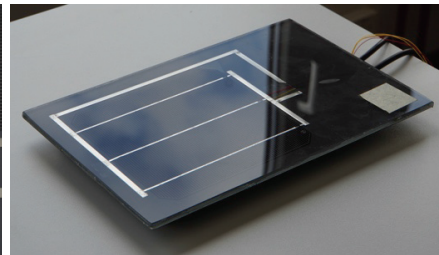Figure 5.4-2: Comparison between the wafer and backsheet colour of PV sample 1.

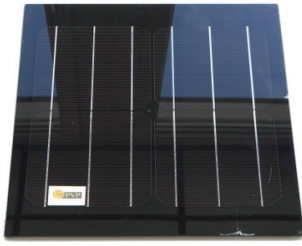Figure 5.4-3: Reflection from the PV sample 1.

Figure 5.4-4: PV sample 2.

Figure 5.4-5: Comparison between the wafer and backsheet colour of PV sample 2.
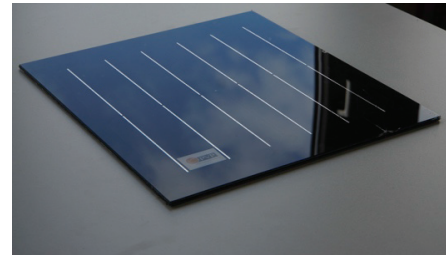
Figure 5.4-6: Reflection from the PV sample 2.

5.4.2 Measurements

The measurements were made with the scanning Goniophotometer in CC EASE, HSLU. The PV samples were attached to the round sample post, and the incident light beam was projected on the area on the module that was intended to be measured. For both PV samples, two typical testing points were chosen: one in backsheet and one in wafer area, resulting in 4 testing points in total. The radius of the incident light beam was set approximately to 10mm. For each testing point, the incident light beam came from directions of $\theta\epsilon[10°, 30°, 50°, 70°]$ combined with $\phi\epsilon[0°, 30°, 60°, 90°]$. An exception was made for the testing point on the backsheet area of PV sample 2 due to limited measuring area. Incident light beam coming from a high ϕ angle would result in a very large light spot on the PV sample that would inevitably include parts of wafers cell. Therefore all the θ angles were measured with only one ϕ angle ($\phi = 0°$). A detector then rotated around the PV sample and collected information about lights that were reflected off from the testing points. The BSDF data was interpolated into a tensor format with 16000 incident and 16000 outgoing directions. Applying an adaptive data reduction technique, the tensor size was then reduced by approximately 99% [183]. The mechanical accuracy and precision, the quality of the measured data and its numerical processing of this Goniphotometer can be found in [184]. Figure 5.4-7 shows that the coefficient of reflection of PV sample 1 is higher than that of PV sample 2. More detailed measurement data can be seen in Appendix 3.

Figure 5.4-7: The coefficient of reflection of the measured PV materials.

5.5 Radiance renderings

With the 3D digital model and material descriptions ready, they were fed into the RADIANCE software along with sky descriptions 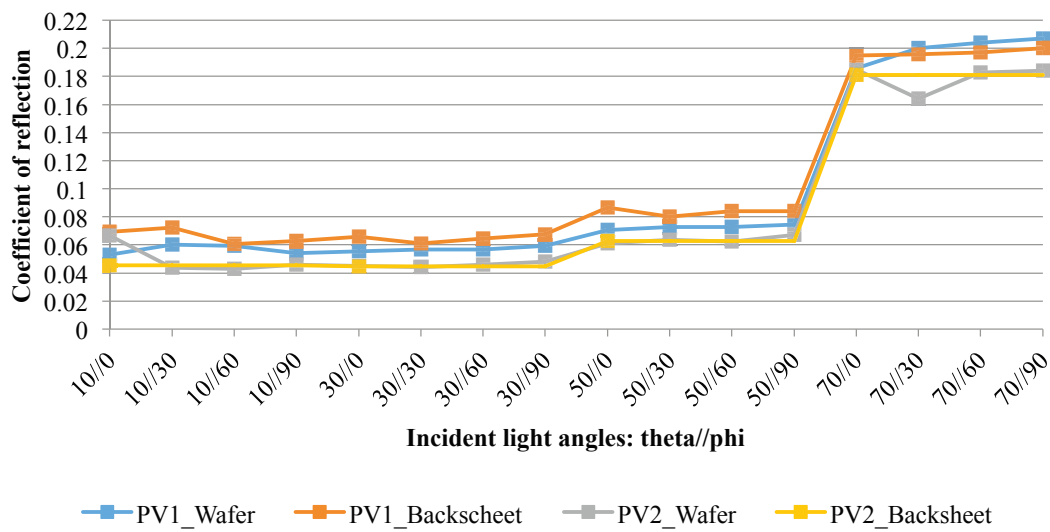and view angle information so as to get rendering images that were as realistic as possible. HDR images were originally generated from RADIANCE, but since the saliency models didn't accept HDR images therefore the command *ra_tiff* was used to transform them into images in TIFF format. TIFF format would allow much less information loss than images in JPG format and thus more credible input images could be applied for visual saliency analysis. Rendering software/plugins that are popular among architects were not preferred here, because they often put more emphasis on the outcome of the renderings instead of the techniques to derive them, e.g. the sky is coloured manually so as to make the outcome "appear" more realistic.

Trees were left out in the 3D models. The 2D rendering 'as is' should present the state of the church complex as the architect intended it to be. One exception was the new Eternit plates on the sloped roof of the church – the material description of tile texture was set in a more homogeneous black colour instead of the old, worn out ones. It would be unrealistic to produce the rendering 'as is' on the basis of the church with the now damaged roof tiles, because the tiles are going to be torn out and replaced with new tiles anyway. All the newly installed Eternit roof tiles were melded into one single, large geometry and applied with a patterned radiance material. Modelling every single Eternit tile in the 3D model was not rewarding due to the reason that their thickness was quite small compared to the BIPV modules so that it can be omitted. The second reason is that the thus generated 3D model would be very large in file size and hard to manipulate with the abundance of geometries.
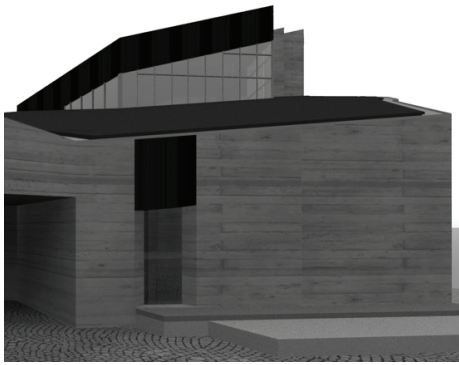
Figure 5.5-1: Viewpoint 1.
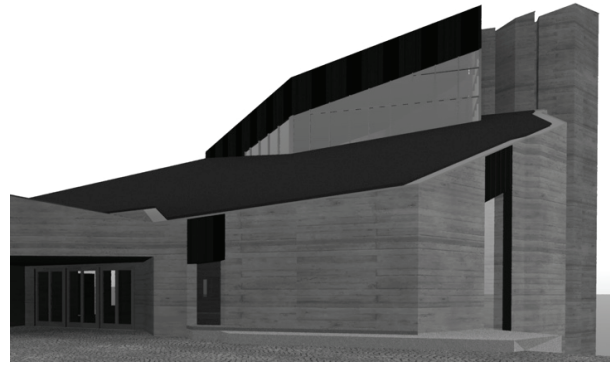
Figure 5.5-2: Viewpoint 2.
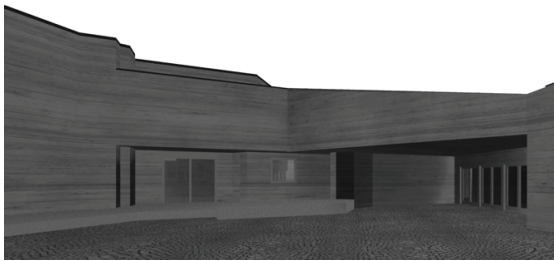
Figure 5.5-3: Viewpoint 3.
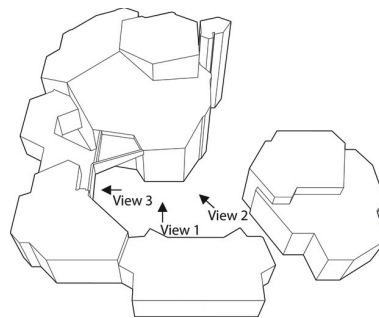
Figure 5.5-4: The view directions of the viewpoints.

Two viewpoints 1 and 2 are chosen in order to investigate the BIPV visual impact in different designs with BIPV placed on the sloped roof (Figure 5.5-1 and Figure 5.5-2). The viewpoint 1 is a stop that most visitors would take on the way to enter the church by the main entrance. Around half of the sloped roof would be visible. The lower the BIPV are located on the roof, the more they are visually accessible by the visitors. The viewpoint 2 is a stop most visitors might to make when approaching the courtyard from the secondary entrance in the east and halfway reaching the main church entrance. More than half of the sloped roof can be seen and height is not a decisive parameter for the visibility of BIPV installations for the visitors. The use of two different viewpoints also helps to check whether certain visual impact results are biased because that particular viewpoint is special. Design PVTerrace is special because the BIPV are only visible from viewpoint 3 (Figure 5.5-3). The renderings "new" (church with the BIPV) are then compared to the rendering "as is" (church without BIPV) to investigate the visual attention difference with the help of saliency models. Then the visual attention differences are transformed into visual impacts, which are presented using S values. The higher the S value, the higher is the BIPV's visual impact. Explanations of view 1-3 are presented in Figure 5.5-4.

Figure 5.5-5 shows the RADIANCE renderings 'new' of the BIPV designs generated from above mentioned viewpoints (larger renderings can be found in Appendix 5). Measured BSDF material properties were applied to all the BIPV designs except for the PVTerrace because its BIPV isn't visible at all, thus resulting in 17 renderings 'new' in total. Other materials such as concrete, metal

and glasses were defined with customary RADIANCE material properties. More detailed information can be found in Appendix 4.

	Viewpoint 1	Viewpoint 2
PVUp_S1		
PVUp_S2		
PVPolygon_S1		
PVPolygon_S2		
PVTerrace		
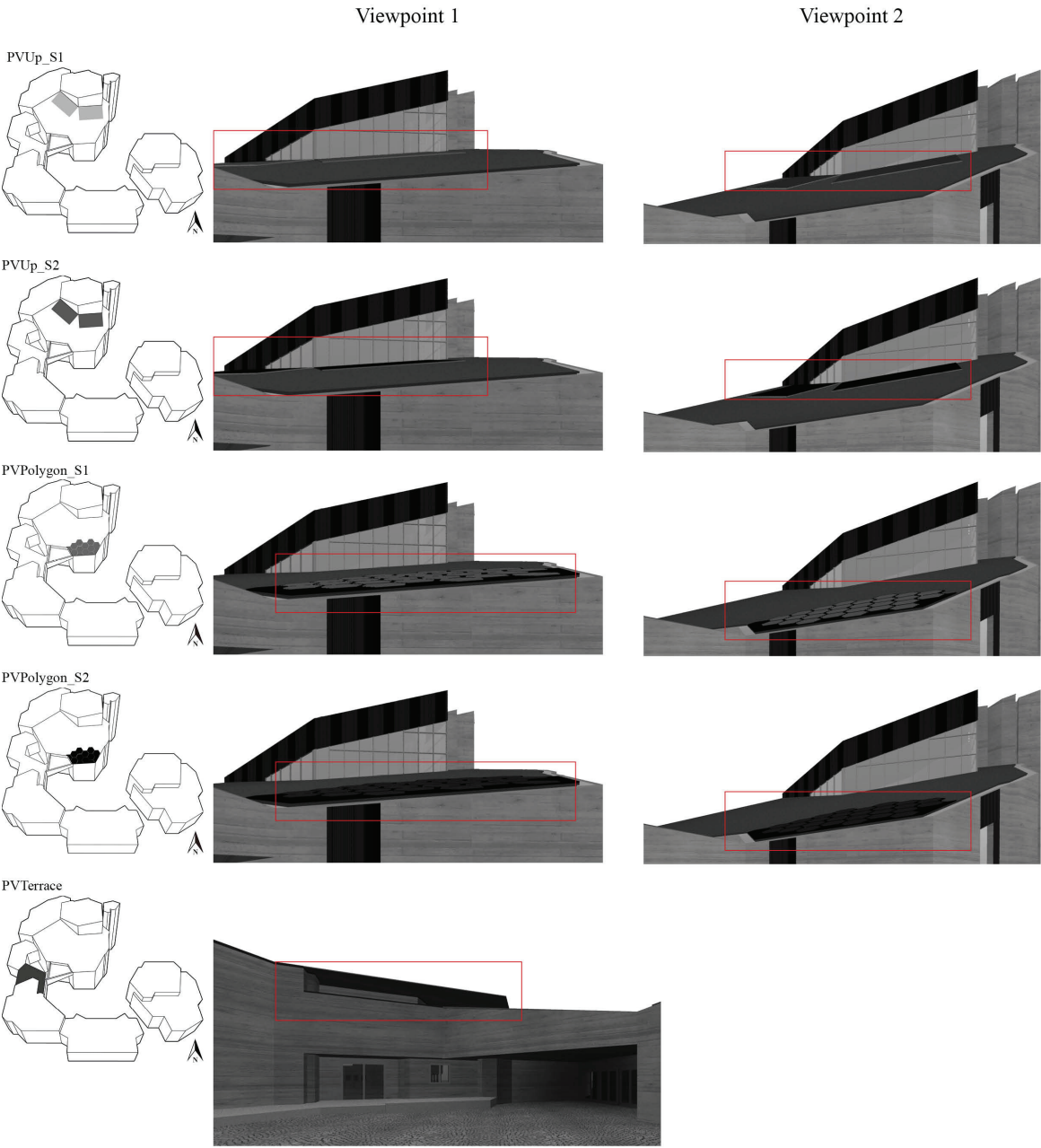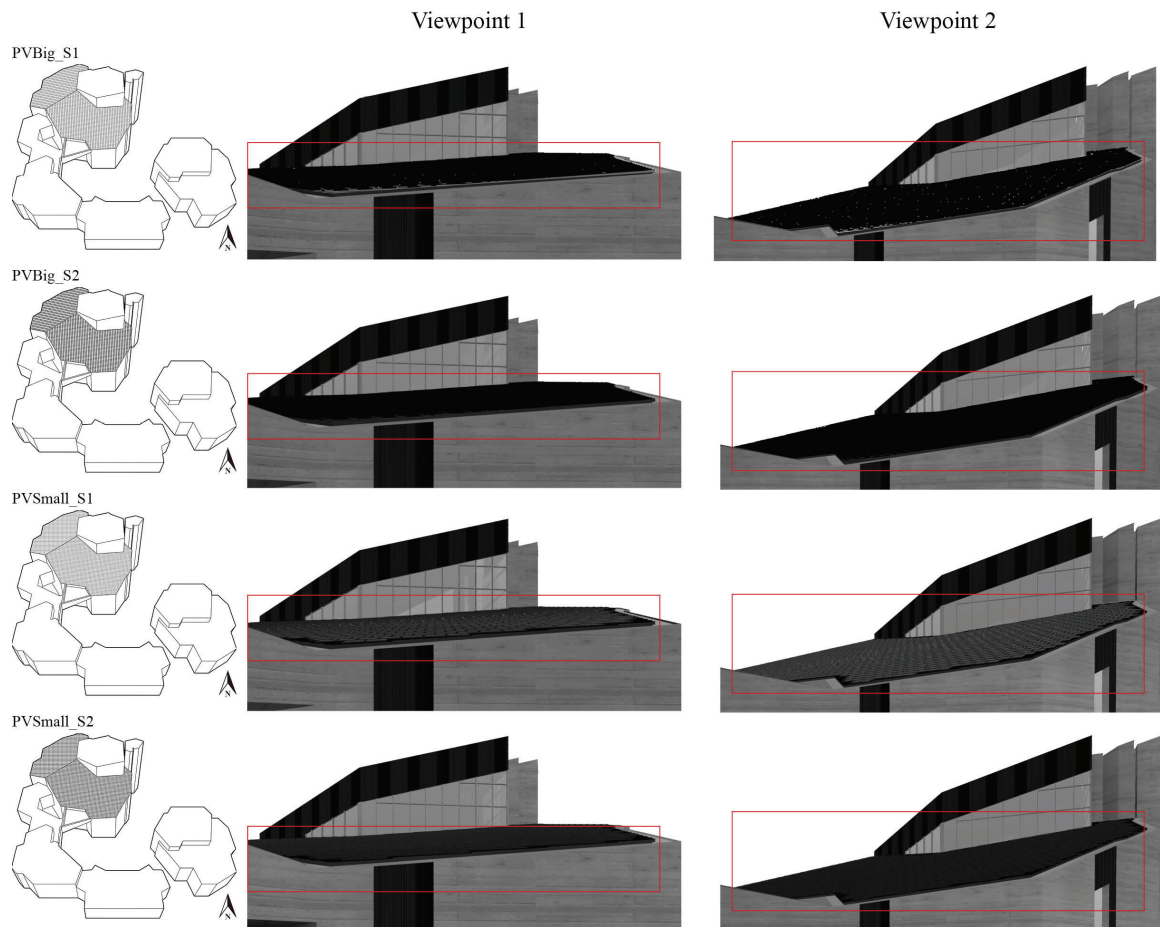
Figure 5.5-5. Radiance renderings of the respective BIPV designs. The red rectangles mark the locations of BIPV. The left colum presents the respective locations of the BIPV design and the applied PV material. The name above indicate which design and PV sample was used in the rendering, for instance "PVSmall_S2" means that this is the design PVSmall using BSDF materials of PV sample 2. The middle column shows the renderings made from viewpoint 1, and the right column shows the renderings made from viewpoint 2. The design PVTerrace is the exception with a rendering only made from viewpoint 3.

5.6 Results

Table 5.6-1-Table 5.6-2 and Figure 5.6-1-Figure 5.6-2 conclude the BIPV visual impacts of different designs and the ranking of their S values categorized by saliency model and viewpoint. More detailed information about the design analysis with saliency maps "new", "delta" map and binary maps 'result' can be found in Appendix 6.

View 1_Designs	GBVS (S value (ranking))	IKN (Harel) (S value (ranking))	SWD (S value (ranking))
PVUp_S1	0.158 (2)	0.152 (2)	2.287 (8)
PVUp_S2	0.163 (3)	0.129 (1)	1.732 (4)
PVPolygon_S1	0.361(7)	0.429 (5)	2.115 (7)
PVPolygon_S2	0.188 (4)	0.968 (8)	0.802 (2)
PV Terrace (viewpoint 3)	7.023 (9)	12.705 (9)	8.084 (9)
PVBig_S1	0.255 (6)	0.535 (6)	1.751 (5)
PVBig_S2	0.232 (5)	0.611 (7)	1.389 (3)
PVSmall_S1	0.478 (8)	0.261 (4)	1.867 (6)
PVSmall_S2	0.027 (1)	0.169 (3)	0.697 (1)

Table 5.6-1. The BIPV visual impact of different designs from viewpoint 1 (categorized by saliency models). The S1 and S2 in the design names respectively indicate the application of PV sample 1 and PV sample 2 BSDF materials in the design. The ranking starts from the design with the lowest visual impact.
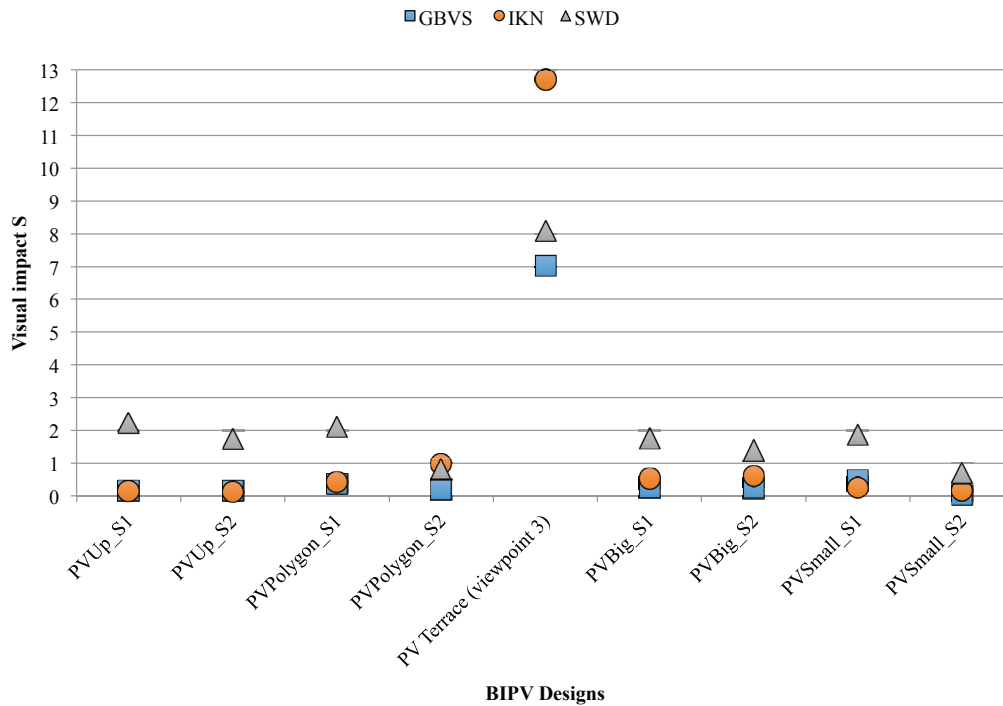
Figure 5.6-1: Visual impact values of different BIPV designs from view 1 according to different saliency models.

View 2_Designs	GBVS (S value (ranking))	IKN (Harel) (S value (ranking))	SWD (S value (ranking))
PVUp_S1	0.100 (4)	1.822 (6)	1.272 (3)
PVUp_S2	0.099 (3)	1.413 (3)	1.104 (2)
PVPolygon_S1	0.244 (8)	1.610 (5)	4.615 (8)
PVPolygon_S2	0.200 (5)	1.503 (4)	1.274 (4)
PV Terrace (viewpoint 3)	7.023 (9)	12.705 (9)	8.084 (9)
PVBig_S1	0.208 (6)	1.920 (7)	1.858 (5)
PVBig_S2	0.223 (7)	2.103 (8)	1.904 (6)
PVSmall_S1	0.065 (2)	0.628 (1)	1.904 (6)
PVSmall_S2	0.052 (1)	0.912 (2)	0.560 (1)

Table 5.6-2: The BIPV visual impact of different designs from viewpoint 2 (categorized by saliency models). The S1 and S2 in the design names respectively indicate the application of PV sample 1 and PV sample 2 BSDF materials in the design. The ranking starts from the design with the lowest visual impact.
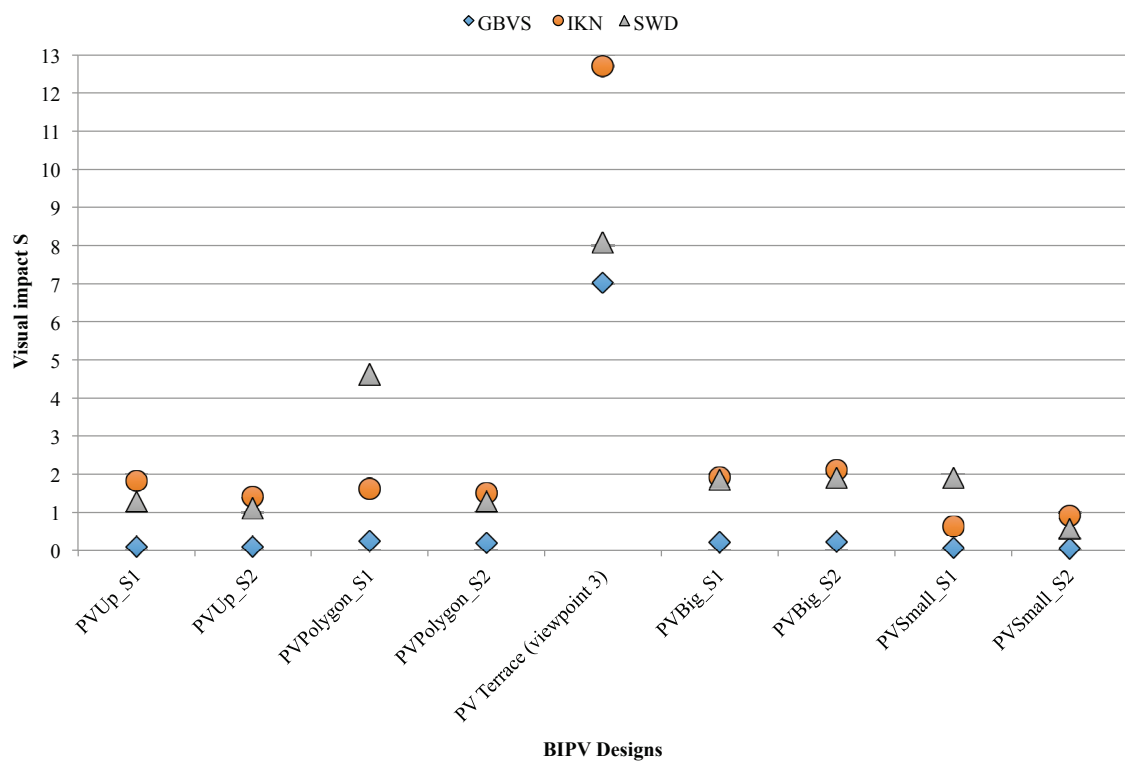
Figure 5.6-2: Visual impact values of different BIPV designs from view 2 according to different saliency models.

The design PVTerrace has by far the highest S values in all three saliency models and thus the highest visual impact on the existing church complex. Respective 'delta' maps not only mark the regions where the new terrace roof is located with values that simply cannot be overlooked, but also mark them with the highest values. Other regions such as façade openings also have some change in saliency values before and after the BIPV installation, but their values are relative insignificant.

PVPolygon design with PV sample 1 achieves, generally speaking, the second highest S scores in both viewpoints across all saliency models. The hexagon modules with the irregular upper edge of BIPV group change the visual perception of the roof by a large amount, because the existing roof silhouette is combined mostly of long, straight lines. The edge below causes less change in saliency value because the blank spaces between the PV group and the roof border are filled up with dummy panels. When applied with material properties of PV sample 1 to the BIPV in the 3D model, the upsides of the modules appear brighter due to more reflections. The vertical edges of the modules are less reflective and darker, therefore resulting in incoherent colour appearances on the same module. This incoherency becomes much weaker in the rendering when BIPV modules are applied with the materials of PV sample 2. The more homogenous colour combination of wafers and backsheets are also similar with the colour appearance of the new roof tiles. The border difference between the BIPV installation and the roof is blurred, so that the irregular shape of BIPV appears to be visually obscure. Therefore the S values of PVPolygon design with PV sample 1 materials are higher than that with PV sample 2 materials.

PVBig designs come next in line on the general ranking of S values. The BIPV appears to be quite homogeneous. No remarkable improvement can be observed when switching to PV sample 2. The possible reason for the relatively high S value is that the resulting appearance of BIPV actually makes more attention be drawn to window of the light tower and therefore takes away the visual attention that used to belong the window and door of the building in its original state. Meaning that a strong visual attention shift takes place from the entrance doors in the left of the image to the roof's upper edge (see the respective saliency map "delta"). The visual impact is therefore caused by the decreased visual attention in the right window and left entrance door area, and increased visual attention on the roof edges and light tower windows after the BIPV is installed, thus forcing a strong shift of visual attention within the entire visual scene.

The S values of PVUp designs range from the second highest (PVUp_S1-SWD) to the second lowest in several other categories. Corresponding renderings from viewpoint 1 show that, when installed very high up on the roof, quite a little of the BIPV can be seen from an observer from this viewpoint. The low S values in GBVS and IKN (Harel) categories are possibly due to the reason that these two saliency models are not likely to emphasize on small details, especially when the colour of BIPV is already quite similar to the colour of the new roof. The edges of the BIPV groups are outstanding, but very narrow. SWD saliency model, in comparison to the other two, is skilled in inspecting the narrow edges of the visible BIPV near the top of the roof and therefore relative high values were detected in 'delta' maps from view 1. In general, the PVUp with materials of PV sample 2 lowers the S values in comparison to materials of PV sample 1.

Overall, the PVSmall designs prove to be getting the lowest S values in both viewpoints and across all saliency models, and therefore causing the least visual impact. The tilting angle of the BIPV in addition to the reflectivity make the upper module side appears not entirely black, but slightly grey-ish as the new Eternit roof tiles. The pattern formation from small custom-made BIPV panels also makes the entire roof appear more monotonous. Especially when the BIPV installations are applied with material of PV sample 2, which have lower reflections and less contrasts between the wafer and back sheet of the PV modules compared to that of PV sample 1.

5.7 Discussion

Concerning the designs, PVTerrace has the highest S value and is predicted to be causing the largest visual impact on the existing church context. Therefore it can be quite risky when proposing this design to the heritage department. The PVPolygon and PVUp have less visual impact compared to the PVTerrace but probably aesthetically less pleasing, because the forms and silhouettes of the BIPV groupings have less relevance to the existing architectural context. However, in case of a limited budget, PVUp design would be an ideal choice with the small predicted visual impact in addition to the low monetary and manpower investment. The PVBig and PVSmall designs are definitely architecturally more acceptable than any other designs. PVSmall design is getting the lowest S values overall, but this low S value is achieved with much higher costs in monetary input and more complicated installation procedures, technical equipment and maintenance work than any other design. PVBig designs is a compromise on the basis of PVSmall design and can have excellent potentials to come down with a low S value as long as careful considerations are made in terms of material choice and tilting angle of the BIPV panels (as imitation of the existing Eternit roof tiles).

An interesting observation is that the manipulation of visual impact value is easy when only geometries and pattern changes are involved. However, when parameters such as colours, material reflectivity and tilting angle come into the play together, the manual predictions of visual impact become difficult and the results are often unexpected. Simple overlapping of the well-known empirical design principles does not always generate visual impact results that were expected. The parameter change doesn't only affect the visual perceptions in renderings regions concerning the BIPV installation, but also other remote regions and triggers a chain reaction in the visual attention shift. For instance the design PVBig, a slightly mis-targeted tilting angle results in visual attention shifts throughout the visual image. The visual attention from other areas are "absorbed" to the roof area and result in a decrease in other visual image regions. So from this perspective, the evaluation tool can provide some new insights to the qualitative design principles.

5.8 Conclusion

Overall, the evaluation method can successfully identify the designs with delicate architectural integration approach and right material choice to have lower visual impacts by giving them lower S values. BIPV designs with bolder approaches usually got higher S values, meaning that their predicted visual impacts are higher. So in general, the outcomes of S values roughly comply with what expected before the analysis. By using empirical design measures, such as using BIPV with lower coefficient of reflection, decreasing the visible BIPV area, using similar BIPV colour as the context, and giving the BIPV similar profile lines as the existing context, proved to be effective in reducing the visual impact value in most cases. However, the application also revealed some novel insights by showing how sometimes the traditional design measures can affect the BIPV visual aspect in unexpected ways.

Chapter 6   Discussion

6.1 Open questions

Format of input image

HDR images contain richer information than images in other formats. However, two bugs were observed when trying to process them with saliency models. The first one is the constant crashes in MATLAB whenever saliency analyses are made for two HDR images in a row. The cause of crash can not be identified yet. The second bug is that the HDR images produced unreasonable GBVS and IKN (Harel) saliency maps that were not at all reasonable compared to the maps generated with images in TIFF format (see Figure 6.1-1 and Figure 6.1-2). More intermediate image format transformation procedures are required for the SWD saliency models. The reason is that the command that imports the HDR images would transform the image data into m-by-n-by-3 RGB arrays of type *single* in the range [0, infinite], and the saliency models only accept m-by-n-by-3 RGB arrays of type *uint8* in the range of [0, 255]. Reasonable transformations from the HDR data type need to be developed in order to generate reasonable saliency maps. Therefore the advantages of HDR image over the TIF image can not be concluded yet in this phase of the research.
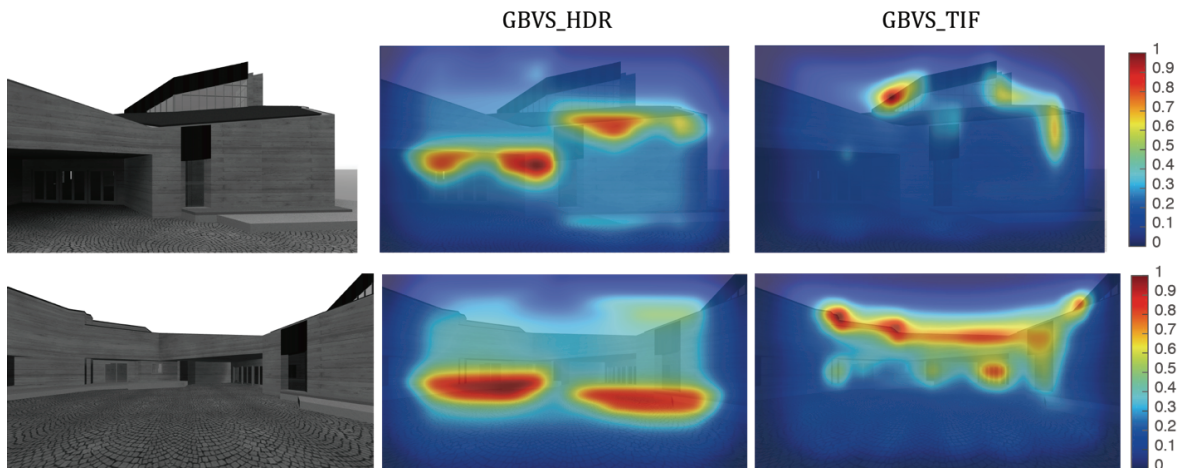

Figure 6.1-1: An example comparison of GBVS saliency maps generated with HDR and TIFF format input images.
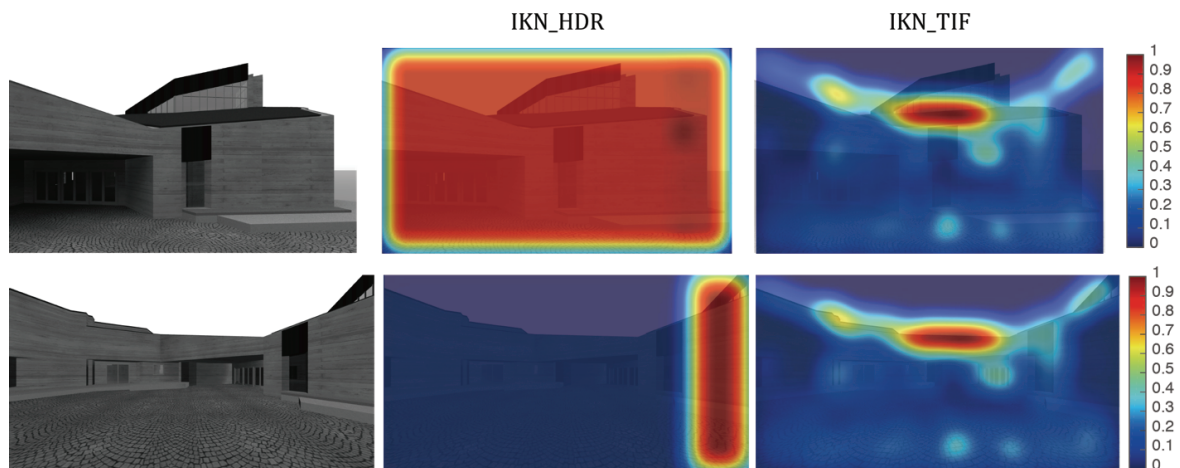
Figure 6.1-2: An example comparison of IKN (Harel) saliency maps generated with HDR and TIFF format input images.

Proportion of input image

Humans retrieve visual information from the surrounding environment by moving both of their eyes rapidly and simultaneously, and fixate on certain spots that they consider as salient or interesting. According to *Feature Integration Theory*, the salient regions will be "glued" together for object recognition. Therefore an ideal image proportion that corresponds to the human's perception of visual scene doesn't exist. However, for the sake of a consistent visual attention analysis in architectural scenes, the object of interest should probably take up certain percentage of the input image's area. As it was observed in the case study that if too many details exist throughout the image, or if the object of interest (BIPV) was too small, then high saliency values would be distributed in regions other than the object of interest (BIPV), and hence making the analysis less meaningful because the saliency model didn't consider the target object (BIPV) to be important. A possible solution is that before the actual visual saliency analysis, preliminary saliency evaluations of the input images (renderings) should be made so as to identify the salient values of the target objects. If saliency values of the target object (BIPV) were below certain thresholds, and higher values were on regions that were irrelevant for the purpose of the investigation, then the image should be cropped accordingly to eliminate this effect. The image will be cropped until the saliency values on the target object are beyond a certain threshold, which needs to be set in the future. This image proportion should then be used for further steps of the visual saliency analysis.

Creation of the input image

Even though in this doctoral thesis, renderings generated with RADIANCE software were used as input images for visual saliency analysis, such long preparation time for 3D digital model and measuring of the material properties with a Goniophotometer are not always possible in practice. Sometimes, in order to save time, photo montage of BIPV on existing building envelopes are already

sufficient for most of stakeholders. Architectural renderings with material assignments according to empirical knowledge of architects also require significantly less time. The feasibility of making visual saliency analysis with input images from sources other than RADIANCE needs to be verified in the future.

Resolution of the input image

As was verified in section 4.3.3, the input images should have resolutions beyond 800 x 800 pixels so as to generate reasonable saliency maps. For future development, the image quality should also be set to fixed values so as to develop standardized analysis procedures.

Viewpoints of input images

In this thesis, limited viewpoints were selected to investigate the visual impact of BIPV. For further development, videos made of continuous series of rendering images can be used to make holistic judgments of the BIPV visual impact on the existing building from all possible view angles. It is also important to apply more weights to views that have more observers than others.

Selection of saliency models and parameter settings

Different saliency models are developed based on different principles and each of them has its own strengths. How to decide which model to use in which situation, whether multiple models can be used for the visual saliency analysis of the same project, and how to combine their results will be the questions that need answers in the future. Due to simultaneous application of three saliency models in this thesis, it is also difficult to decide which amount of S value is considered as high, medium or low visual impact. Moreover, during the application on the case study, saliency models were not always possible to identify the regions that were crucial for the analysis. Possible solutions are the modifications of relevant parameters.

Case study number

Due to the novelty of the proposed evaluation method, the completed application project number is rather low at the moment. Despite the high feasibility of the method, it is without doubt that more case studies will provide more insights, reveal more open questions and require corresponding revisions.

Knowledge limitations of human vision

Limited by the present neuroscientific knowledge in human vision, the saliency models are imitations of mechanism of human visual attention, but most of them merely mimic the centre-surround contrast comparisons of the visual system and not much more than that. It can be

said with confidence that the accuracies of saliency models can be increased if more profound discoveries were made concerning human vision.

6.2 Advantages of the proposed evaluation method

Compared to the existing evaluation methods that assess the visual impact of BIPV, following advantages can be observed during the application of the proposed method:

o The visual analysis isn't based on abstract empirical, qualitative and formal design criteria, but rather on the contrast analysis between the pixels/patches within a visual image.

o The strength of the visual impact is quantified, so that the quantity of how much a BIPV design is visually more impacting than another design can be acknowledged.

o Saliency map can be used as a tool to ease the communications between different stakeholders during the design processes. Rosenholtz et al [204] presented the application of saliency map to several graphic designers and found out that most designers considered the visual attention analysis of their design works to be helpful during the communication with other stakeholders. The reason is that engineers usually use objective, quantitative descriptions in their working environment, therefore they are often puzzled by the subjective, qualitative descriptions used by designers.

o The resulting saliency maps and S values are repeatable; they are immune to personal preferences and independent of the person who is running the analysis process.

o Compared to the methods where visual impacts are investigated with questionnaires, the proposed evaluation method outperforms them in the aspects of cost and time.

6.3 Possible future applications

6.3.1 Complement the existing qualitative visual impact assessments

As was already stated in Chapter 2, the qualitative assessment of BIPV visual impact shows certain insufficiencies in practical applications. It is, of course, unbeneficial to eliminate subjective aspects from architecture design entirely. They are and must be very essential components of design activities. It is important to realize that subjective and objective assessments of BIPV visual impacts have different focuses and each of them can discover the bias of the other. Combining them together makes a well-rounded evaluation of the BIPV design possible.

6.3.2 Integration into the building labels

Existing building labels, as was already stated in Chapter 1, generally lack specific assessment of BIPV visual impact on retrofitted buildings. A possible integration of the proposed method into the existing building label is to employ BIPV visual impact as a criterion, along with other technical criteria, to holistically evaluate the quality of green architecture. The quantitative, objective nature of the proposed evaluation method and numeric expression of its result allow a seamless merging with other evaluation aspects such as energy production, energy cost, self consumption and similar. For instance in LEED building label, different credits are given depending on how much of the building's total energy consumption can be covered with renewable energy. The BIPV visual impact can be integrated in a similar way: BIPV design with low visual impact will be given more credit points, which will contribute positively to the final LEED certification; higher BIPV visual impact will be given less or negative credit points, which will affect negatively on the final LEED certification. The integration of proposed evaluation method in this doctoral thesis will on the one hand provide a more comprehensive quality evaluation of retrofitted green architectures, on the other hand also discourage BIPV designs that will affect the city image in negative ways.

6.3.3 Integration with urban planning

Swiss Federal Office of Energy published the tool sonnendach.ch, where the solar energy potential of building envelopes throughout Switzerland are analysed (solar cadastres) [10], [205]. An example of it is shown in Figure 6.3-1. The study was made in corporation with 3D models from Swisstopo [206] and satellite-based solar radiation data from MeteoSchweiz [207]. The objective of the findings is to act as a service for people who were interested in solar energy and helping them in finding out whether their building envelopes are suitable for PV or solar thermal collectors. These findings can also be helpful for the responsible authorities when developing strategies for future energy and urban planning.
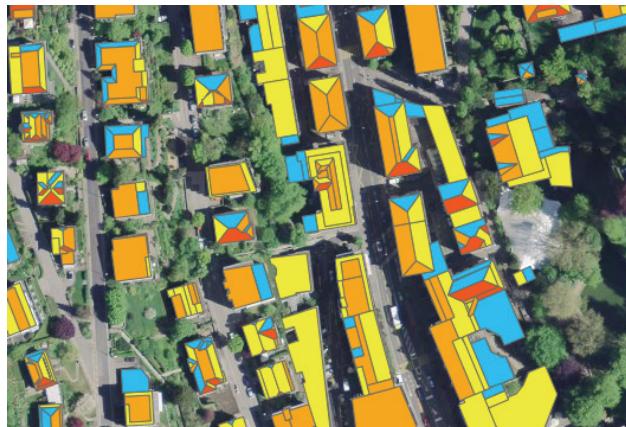

Figure 6.3-1: Analysis of solar radiation potential on roofs. A screenshot from website sonnendach.ch [208] with permission from Bundesamt für Energie (BFE).

However, it is not sufficient to plan such visionary strategies with only information concerning maximum energy gain, especially when heritage protection is involved. In order to make a considerate planning for future electricity mix and urban development, it is recommendable to combine the solar cadastres with the visual impact thresholds for different urban spaces.

In order to better demonstrate how the visual impact threshold can be developed for different urban zones, the Lucerne Watertower, which is a heritage architecture, was taken as a demonstration object. The Lucerne Watertower is composed of a stone tower with a wooden bridge. In combination with the surrounding environment, the whole complex comprised to one of the most valuable sceneries in Lucerne. The delicacy of the scene also makes the visual scene more sensitive and therefore easier to observe what visual impact is tolerable or recommendable for which urban zone.

A rectangle BIPV installation was hypothetically installed on the facade of the Watertower. Through manipulation with the RGB values within the dotted red frame in Figure 6.3-2, the hypothetical BIPV was applied with different glazing colours. Each value in the red, green and blue channels was set with changing values from 0-255 in step of 15. Thus resulting in 5832 different colours, and the same number of front glazing colours for the hypothetical BIPV on the Lucerne Watertower. Visual attention changes before and after the BIPV installation were presented by the visual impact values S using the proposed methodology in this doctoral thesis. By putting the results next to the respective renderings, a link can be established of how human perceive these visual changes sensually with the quantitative S values. In this investigation, the classic IKN (Harel) saliency model was used.

Figure 6.3-2: The Lucerne Watertower. The red area marks the location where BIPV are hypothetically placed.

The different glazing colours and their resulting visual impact value S are concluded in Figure 6.3-3. The dot colours represent the resulting BIPV glazing colours. The visual impact value S lie within the range of 0 to 8.3. The more similar the BIPV's glazing colour is to the facade colour of the Watertower, the lower the resulting visual impact. Those are the colours concentrated at the bottom of the graph. The middle part of the graph is mostly comprised of colours that are darker or brighter than the facade in a medium amount, causing medium level of visual impacts. The brighter the colour gets, the higher the responding visual impact. Those colours are located in the upper part of the graph.
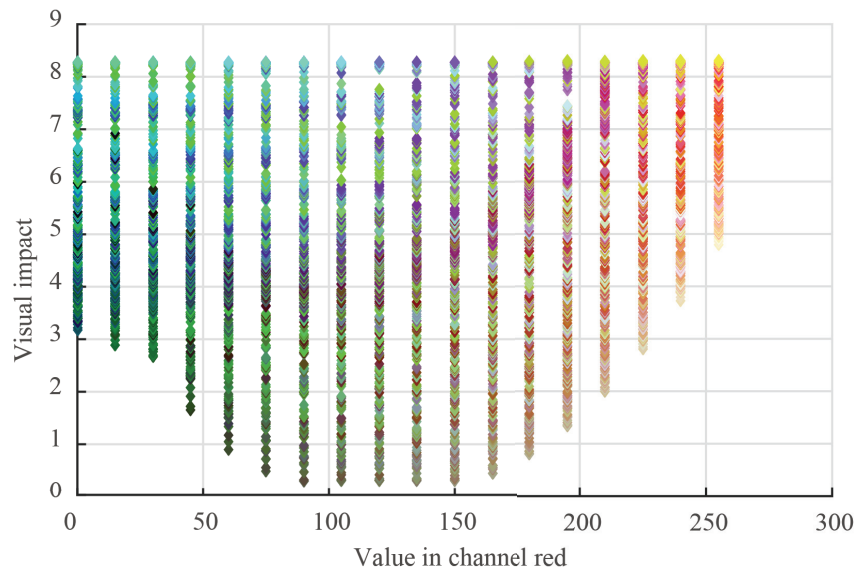
Figure 6.3-3: The colour of the glazing (organized along the horizontal axis that represents the red channel of the colour) and corresponding visual impact S caused by it.

Figure 6.3-4 and Figure 6.3-5 show some examples of the visual impact from different ranges with the hypothetical BIPV covered with the respective RGB colour. Thus it is possible to connect the sensual perception with quantified visual impact S values. It can be seen that when the S values are smaller than 0.5, the perception of the change is quite subtle. Within the range of [1,4], the glazing colours are either slightly darker or brighter than the Watertower's facade colour, and the visual perception of the BIPV is obvious but still acceptable in this context. When the S values exceed 4, then the colours appear to be almost neon and very eye-catching. Table 6.3-1 summarizes the suitable visual impact range for different urban zones. When the urban zone has a high preservation level, then the BIPV installation must be very subtly integrated onto the building envelope and the strength of its visual impact mustn't exceed 0.5 (0 < S < 0.5), because the visual scene must be maintained as original as possible visually speaking. When the urban zone is of medium sensibility, then the S value must be within the range of 0 to 4. Higher S values aren't permitted because the BIPV are too obvious for this area and negative for the city image. In urban zones with no preservation requirements, such as industrial zones, no restrictions are set for visual impacts caused by BIPV installations.

Range of visual impact (S)	Suitable urban zone
0 < S < 0.5	Sensitive heritage zone (old town centres, sensible landscapes)
0 < S < 4	Medium sensitive urban zones (residential zones, business zones, school zones, farmlands etc.)
No limitation	Low sensitive urban zones (Industrial zones)

Table 6.3-1: Ranges of suitable visual impact for different urban zones.

< 0.5

0.5 - 1

1.5 - 2

2.5 - 3

3.5 - 4
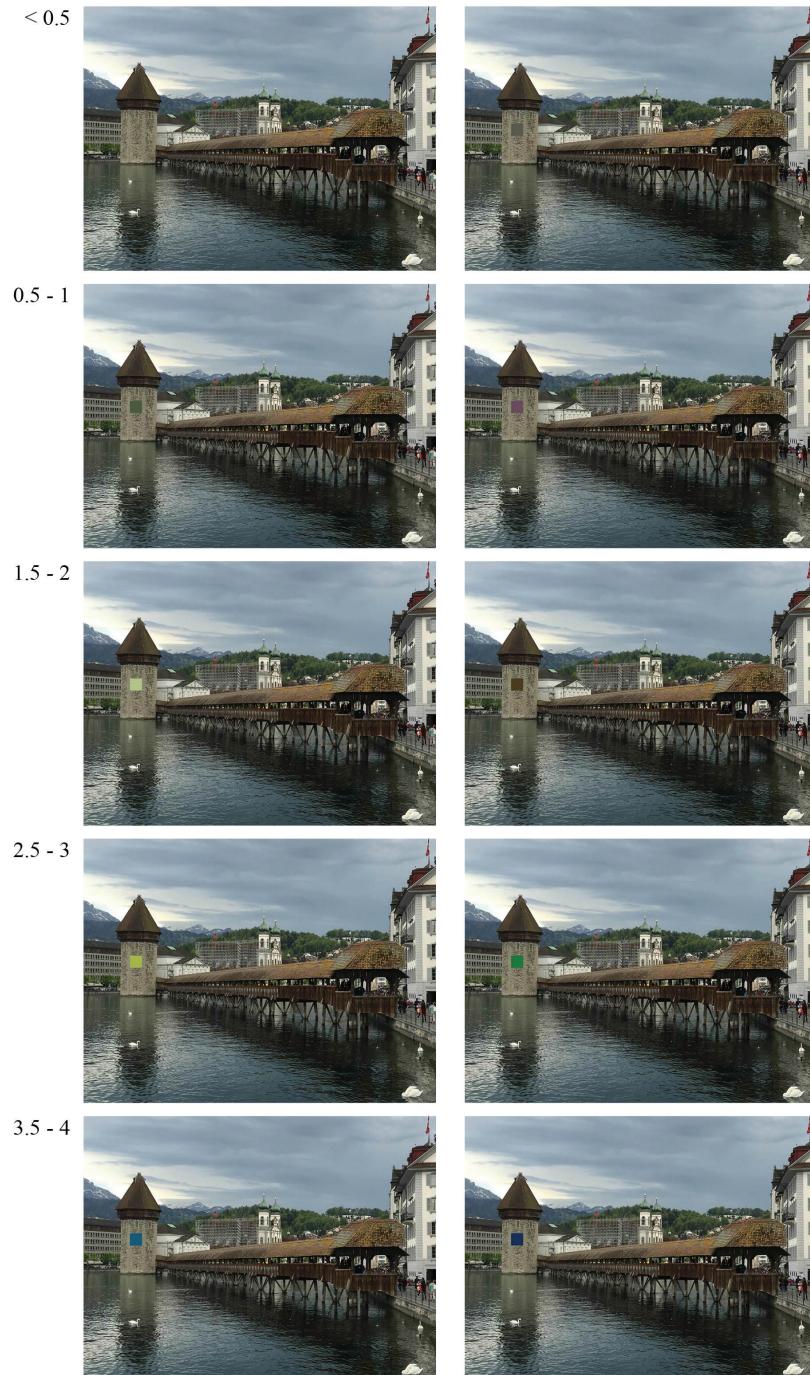
Figure 6.3-4: The ranges of visual impact S and example photomontage pictures. The hypothetical BIPV installation is covered with the respective RGB colour.

the range of S value
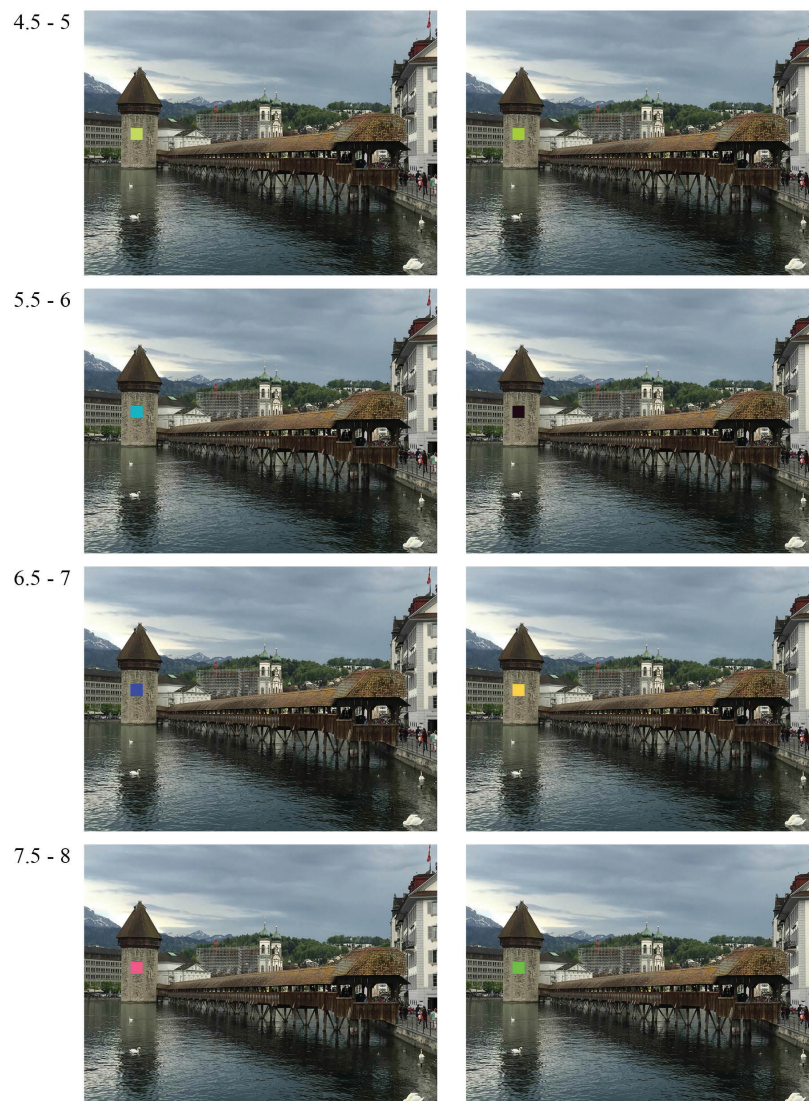
Figure 6.3-5: The ranges of visual impact S and example photomontage pictures. The hypothetical BIPV installation is covered with the respective RGB colour.

This section is a revised version of the conference paper [209]. It proposes the integration of BIPV visual impact thresholds with solar cadastre to holistically estimate potential for BIPV in urban spaces, so that the relevant authorities can be sufficiently informed when developing strategies for future energy mix and urban planning. The proposal is, of course, only a preliminary sketch, the main goal of it is to demonstrate how the evaluation method proposed in this doctoral thesis can be adapted in a potential application area.

Chapter 7　Conclusion

This doctoral thesis proposes a method that can quantitatively and objectively evaluate the visual impact of BIPV in facade retrofits. The method has neuroscientific base and the strengths of the BIPV visual impacts are presented with single values.

Facing the dilemma between PV expansion and heritage protections in urban spaces, it was realized that in the first place, the BIPV visual impact is the most apparent factor (Chapter 1). In order to minimize the possible negative visual impact, a method is needed that can appropriately measure it. However, following inadequacies were observed in the existing evaluation methods (Chapter 2):

1. Existing qualitative criteria have difficulties in maintaining objectivity and continuity of evaluation standards due to their vulnerability to subjective preferences.

2. Existing quantitative criteria lack neuroscientific base and generality of results, because they focus rather on formal design parameters than on actual working principle of human eyes.

3. Existing evaluation results come in all possible forms, making them difficult to be combined with other types of technical results (annual energy yield, payback time etc.).

The integration of saliency model, which is an imitation of the human visual attention mechanism, into the evaluation method tackles the first two problems mentioned above (Chapter 3). Images as snapshots of the visual scenes will be transformed into digital data and input to the saliency model. It then generates saliency maps, which are colour-maps that predict visual saliency of corresponding visual scenes. The predictions are made entirely in quantified manner without subjective factors, therefore the continuity of evaluation standards can be guaranteed. Beside modelling the mechanism of human visual attention by imitating the contrast comparison principles, the accuracy of the saliency models can be measured with several metrics. All accuracy metrics compare the saliency map results with actual human eye fixations using standard input images. Therefore the neuroscientific base and generality of the analysis results can be assured. So the saliency models can provide preliminary saliency information that need further processing to assess the BIPV visual impact in facade retrofits from a quantitative, objective and neuroscientific based approach.

Another achievement in this doctoral research is the development of a method that can generate the BIPV visual impact strength with a single value through weighted "extraction" of representative visual saliency information from saliency maps, whose format are matrices originally (Chapter 4). This is also the answer to the third research question. This kind of result provides a straightforward comparison between different BIPV designs. Being in the same format as other technical evaluation results also enables an easier integration with them, so as to generate a holistic evaluation for the BIPV system in the future.

Since the evaluation method predicts the potential BIPV visual impact, renderings with and without

BIPV act as input images for saliency model. In order to make reasonable predictions, the renderings must look as close to reality as possible. Therefore the generation of renderings requires certain realistic physical descriptions of the regarding the visual scenes. By following the physical behaviour of light as closely as possible, the lighting simulation software RADIANCE ensures that the imitation image of the visual scene is rendered as realistic as possible. Moreover, measured BSDF materials are applied to BIPV modules during rendering, so as to make reasonable estimations of their appearances in reality. The effect of input image resolutions on saliency maps was also investigated. The conclusion is that if the input image has resolutions above 800x800 pixels, then the quality of the resulting saliency maps is sufficient for further analysis.

In the proposed method, three representative saliency models IKN (Harel), GBVS and SWD are used simultaneously. Due to their different approaches in modelling the contrast comparison mechanism of human visual attention, each of them has its own advantages and disadvantages and they can complement each other. Therefore, it is important to apply them together in the analysis.

As a first application, the proposed methodology is used on a real project: BIPV need to be applied on the roof of a church, which is a protected heritage architecture (Chapter 5). In total, 5 different BIPV designs were developed. The designs present variations in BIPV installation location, roof coverage percentage, module size and design approach. Each of the designs exists in two versions: one uses PV materials with higher coefficient of reflection, and the other one with lower coefficient of reflection.

Overall, the ranking of the S value from the corresponding BIPV design proved the proposed evaluation method to be feasible to a large extend. All 'delta' maps could correctly detect visual attention differences in image regions where BIPV installations were applied. The largest S value was found on a BIPV design that has a very radical integration approach and was already assumed to have the largest visual impact before the analysis. The smallest S value was found on the most considerate design approach of all, where custom-made small-scale, low reflectance BIPV modules were used to imitate the morphology of Eternit-tiles on the existing church roof. Well known empirical design measures, such as using BIPV with lower coefficient of reflection, decreasing the visible BIPV area, using similar BIPV colour as the context, and giving the BIPV similar profile lines as the existing context, proved to be effective in reducing the visual impact value in most cases. However, it was observed that simply overlapping these measures does not guarantee that the BIPV visual impact will definitely decrease. For instance, when the custom-made BIPV modules from the design that had the lowest S value were replaced by larger standard BIPV modules using same identical materials, no obvious differences could be detected with human eyes on the renderings, but the proposed evaluation method generated significantly higher S values for the latter than for the former. The possible reason is that the larger, standard-sized BIPV modules with the particular given tilting angle, viewpoint and lower reflective materials tend to make the BIPV modules absorb more visual attention from other image regions, and hence resulting in stronger visual attention shift than other designs. So it can be concluded that the proposed evaluation system does not only investigate whether the BIPV installation stands out in the existing context, but also whether the visual attention towards a certain region has grown larger or smaller compared to before.

To conclude, the evaluation method proved to be feasible to a large extent. Besides measuring the BIPV visual impact, it indirectly verified the effect of conventional design disciplines when using

them separately to lower the BIPV visual impact. Moreover, it can also provide some novel insights for architects when the effects of several formal design parameters are correlated with each other in an unpredictable and complex way.

On a larger horizon, the benefits of neuroscience for architecture designs have been realized and promoted by professionals from both sides in the recent years [102], [210]-[213]. It is believed that neuroscience discoveries can contribute to a growing understanding of human responses to the built environment, and can provide scientific proof to qualitative parameters of design. In response to this trend, the proposed evaluation method applied saliency models as medium to investigate the visual impact of BIPV in facade retrofits. The effort to model the mechanism of human visual attention is connected with visual aspect of architecture design and solar energy technology. The application of this method is not limited to BIPV, but can be extended to any aspects in architecture design that wishes to investigate the visual saliency. Since architects have always strived to fully understand and engage all possible forces to create comfortable built environments, this evaluation tool has the potential to help them with the "visual forces" of designs.

References

[1]   RTS Coorporation (Japan), G. Masson, S. Nowak, International Energy Agency Photovoltaic Power Systems Programme (IEA PVPS), M. Brunisholz, NET Ltd, S. Orlandi, Becquerel Institute, "Trends 2015 in Photovoltaic applications," 2015.

[2]   The European Parliament and the Council of the European Union, "Directive 2009/28/EC of the European Parliament and of the Council of 23 April 2009 on the promotion of the use of energy from renewable sources and amending and subsequently repealing Directives 2001/77/EC and 2003/30/EC," *Office Journal of the European Union*, pp. 1–47, 2009.

[3]   cR Kommunikation AG (Bern), "Neue Energie. Neue Chancen.," in *Neue Energie für die Schweiz*, Verein KlartextEnergie, 2010, pp. 1–21.

[4]   Bundesamt für Energie (BFE), *Energiestrategie 2050*, 2016.

[5]   Der Schweizerische Bundesrat, *Botschaft zum ersten Massnahmenpaket der Energiestrategie 2050 und zur Volksinitiative "Für den geordneten Ausstieg aus der Atomenergie (Atomausstiegsinitiative),"* 2013.

[6]   Eidgenössisches Departement für Umwelt, Verkehr, Energie und Kommunikation (UVEK), Bundesamt für Energie (BFE), *Energieperspektiven 2050 - Zusammenfassung*, 2013.

[7]   Eidgenössisches Departement für Umwelt, Verkehr, Energie und Kommunikation (UVEK), Bundesamt für Energie (BFE), *Energieperspektiven 2050 - Anhänge*, 2013.

[8]   S. N. Grösser, *Co-Evolution of Standards in Innovation Systems*. Heidelberg: Physica-Verlag HD, 2013.

[9]   Der Schweizerische Bundesrat, *Energiegesetz (EnG) 730.0*. 2014.

[10]   D. Klauser, "Solarpotentialanalyse für Sonnendach.ch - Schlussbericht," Eidgenössisches Department für Umwelt, Verkehr, Energie und Kommunikation (UVEK), Bundesamt für Energie (BFE), 2016.

[11]   Der Schweizerische Bundesrat, *Bundesgesetz über die Raumplannung (Raumplannungsgesetz, RPG)*. 2016.

[12]   Kanton Luzern, Umwelt- und Wirtschaftsdepartement, *Richtlinien Solaranlagen*. 2015.

[13]   Regierungsrat des Kantons Bern, *Richtlinien - Baubewilligungsfreie Anlagen zur Gewinnung erneuerbarer Energien*. 2015.

[14]   Kanton Thurgau, Department für Bau und Umwelt, Departement für Inneres und Volkswirtschaft, *Solaranlagen richtig gut*. 2015.

[15]   Bau- und Verkehrsdepartement des Kantons Basel-Stadt, Department für Wirtschaft Soziales und Umwelt des Kantons Basel Stadt, *Richtlinie für Solaranlagen im Kanton Basel-Stadt*. 2013.

[16]   Denkmalpflege des Kantons Bern und des Kantons Zürich, "Energie und Baudenkmal - Gebäudehülle," 2014.

[17]   Denkmalpflege des Kantons Bern und des Kantons Zürich, "Energie und Baudenkmal - Solarenergie," 2014.

[18]   Eidgenössische Kommission für Denkmalpflege, Bundesamt für Energie (BFE), "Energie und Baudenkmal," 2009.

[19]   Bundesamt für Landestopografie,   Bundesamt für Energie (BFE), "Denkmal und Energie - Historische Bausubstanz und zeitgemässer Energieverbrauch im Einklang," 2015.

[20]   A. Zubriggen, "«Die Stadt Bern ist schizophren»," *Sacred Architecture Journal*, 21-Aug-2009. [Online]. Available: http://bo.bernerzeitung.ch/region/bern/Die-Stadt-Bern-ist-schizophren/story/12556875. [Accessed: 02-Dec-2014].

[21]   S. von Arx, "Solaranlage auf Kirchendach: «Das Bauvorhaben kann nicht bewilligt werden»,"
         www.grenchnertagblatt.ch, 02-Oct-2013. [Online]. Available:
         http://www.grenchnertagblatt.ch/solothurn/thal-gaeu-niederamt/solaranlage-auf-kirchendach-das-bauvo
         rhaben-kann-nicht-bewilligt-werden-127238528. [Accessed: 02-Dec-2014].

[22]   A. Mustedanagic, "«Die Genossenschaft wurde offensichtlich unprofessionell beraten»," *Tages Woche*,
         07-Aug-2013. [Online]. Available: http://www.tageswoche.ch/de/2013_31/basel/567131/. [Accessed:
         02-Dec-2014].

[23]   J. Vitelli, "Interpellation Nr. 60: betreffend fragwürdige Richtlinien für Solaranlagen," *Grosser Rat des
         Kantons Basel-Stadt*, 01-Sep-2013. [Online]. Available:
         http://www.grosserrat.bs.ch/dokumente/100376/000000376090.pdf. [Accessed: 02-Dec-2014].

[24]   S. Häne, "Heimatschutz warnt vor «Solarwelle» in Altstadt," *www.tagesanzeiger.ch*, 08-Feb-2012.
         [Online]. Available:
         http://www.tagesanzeiger.ch/zuerich/stadt/Heimatschutz-warnt-vor-Solarwelle-in-Altstadt/story/148948
         03. [Accessed: 02-Dec-2014].

[25]   C. Horisberger, "Solardach scheitert an Form und Denkmalschutz," *Basler Zeitung*, 30-Jun-2015.
         [Online]. Available:
         http://bazonline.ch/basel/gemeinden/Solardach-scheitert-an-Form-und-Denkmalschutz-/story/21696107.
         [Accessed: 25-Mar-2016].

[26]   K. Arni-Howald, "Er sorgt für die Erhaltung der Dachlandschaft in der Altstadt," *Solothurner Zeitung*,
         30-Jul-2015. [Online]. Available:
         http://www.solothurnerzeitung.ch/solothurn/stadt-solothurn/er-sorgt-fuer-die-erhaltung-der-dachlandsc
         haft-in-der-altstadt-129380387. [Accessed: 25-Mar-2016].

[27]   D. Scruzzi, "Unschöne Energiepolitik," *Neue Zürcher Zeitung*, 04-Jan-2016. [Online]. Available:
         http://www.nzz.ch/schweiz/unschoene-energiepolitik-1.18671945. [Accessed: 25-Mar-2016].

[28]   Schweizer Heimatschutz, "Solaranlagen, Baudenkmäler und Ortsbildschutz - Positionspapier," 2009.

[29]   T. C. Daniel, "Whither scenic beauty? Visual landscape quality assessment in the 21st century,"
         Landscape and Urban Planning, vol. 54, no. 1, pp. 267–281, 2001.

[30]   M. Rodrigues, C. Montañés, and N. Fueyo, "A method for the assessment of the visual impact caused
         by the large-scale deployment of renewable-energy facilities," *Environmental Impact Assessment
         Review*, vol. 30, no. 4, pp. 240–246, 2010.

[31]   M. Tolli, F. Recanatesi, M. Piccinno, and A. Leone, "The assessment of aesthetic and perceptual
         aspects within environmental impact assessment of renewable energy projects in Italy," *Environmental
         Impact Assessment Review*, vol. 57, no. C, pp. 10–17, 2016.

[32]   B. Möller, "Changing wind-power landscapes: regional assessment of visual impact on land use and
         population in Northern Jutland, Denmark," *Applied Energy*, vol. 83, no. 5, pp. 477–494, 2006.

[33]   A. M. Maehr, G. R. Watts, J. Hanratty, and D. Talmi, "Emotional response to images of wind turbines:
         A psychophysiological study of their visual impact on the landscape," *Landscape and Urban Planning*,
         vol. 142, pp. 71–79, 2015.

[34]   A. Z. Hamedani and F. Huber, "A comparative study of DGNB, LEED and BREEAM certificate
         systems in urban sustainability," in *Sustainable City VII: Urban Regeneration and Sustainability*, vol. 2,
         WIT Press, 2012.

[35]   C. Luft, "Das DGNB System im internationalen Vergleich: ein Überblick.," presented at the DGNB
         Impuls Session, 2013.

[36]   P. Klaunig, "Schön und Gut - Gestalterische Qualität im DGNB System," presented at the DGNB Impuls Session, 2015.

[37]   S. N. Grösser, "Swiss Residential Built Environment," in *Co-Evolution of Standards in Innovation Systems*, no. 4, Heidelberg: Physica-Verlag HD, 2013, pp. 73–109.

[38]   MINERGIE Switzerland, "Was ist MINERGIE?," *MINERGIE.ch*. [Online]. Available: http://www.minergie.ch/was-ist-minergie.html. [Accessed: 11-May-2016].

[39]   MINERGIE Switzerland, "MINERGIE - Objekte unter Denkmalschutz," 2009. [Online]. Available: http://www.minergie.ch/tl_files/download/Publikationen/Praxisbeispiel/Broschuere_Denkmalschutz.pdf. [Accessed: 20-Jun-2016].

[40]   Bundesamt für Energie (BFE), *Standard Nachhaltiges Bauen Schweiz - Hochbau*. Standard Nachhaltiges Bauen Schweiz (SNBS), 2013.

[41]   Eidgenössisches Departement für Umwelt, Verkehr, Energie und Kommunikation (UVEK), Bundesamt für Energie (BFE), "Marktbefragung Zertifizierung SNBS," pp. 1–28, 2014.

[42]   F. Sick and T. Erge, *Photovoltaics in buildings: a design handbook for architects and engineers*. Routledge, 1996.

[43]   T. Schoen, D. Prasad, D. Ruoss, and P. Eiffert, "Task 7 of the IEA PV power systems program– achievements and outlook," presented at the 17th European Photovoltaic Solar Conference, 2001.

[44]   H. Kaan and T. Reijenga, "Photovoltaics in an architectural context," *Progress in Photovoltaics: Research and Applications*, 2004.

[45]   T. Reijenga and H. F. Kaan, *PV in Architecture*. Chichester, UK: Handbook of Photovoltaics Science and Engineering, 2002.

[46]   I. Hermannsdörfer and C. Rüb, *Solar design: photovoltaics for old buildings, urban space, landscapes*. Jovis, 2005.

[47]   D. Ehrbar, A. Held, M. Hohl, E. Roesler, U. Sturm, P. Schwehr, S. Moosberger, and U.-P. Menti, "Methodik zur Umsetzung von solaren Strategien in der Architektur (project report)," *International Energy Agency Solar Heating and Cooling Programme Task 41*, 2012.

[48]   B. Weller, C. Hemmerle, S. Jakubetz, and S. Unnewehr, *Photovoltaik - Technik, Gestaltung, Konstruktion*. Institut für internationale Architektur-Dokumentation GmbH & Co. KG, 2009.

[49]   M. C. Munari Probst and C. Roecker, *Architectural Integration and Design of Solar Thermal Systems*. EPFL Press, 2011.

[50]   F. Frontini, M. C. Munari Probst, C. Roecker, A. Scognamiglio, K. Farkas, L. Maturi, and I. Zanetti, "Solar Energy Systems in Architecture (project report) ," *International Energy Agency Solar Heating and Cooling Programme Task 41*, pp. 1–228, 2012.

[51]   C. Vassiliades, A. Savvides, and A. Michael, "Architectural Implications in the Building Integration of Photovoltaic and Solar Thermal systems – Introduction of a taxonomy and evaluation methodology," presented at the World Sustainable Building 2014, 2014.

[52]   I. Zanetti, K. Nagel, and D. Chianese, "Concepts for solar integration development of technical and architectural guidelines for solar system integration in historical buildings," presented at the 25th European Photovoltaic Solar Energy Conference and Exhibition, Valencia, 2010.

[53]   C. S. P. López and F. Frontini, "Energy efficiency and renewable solar energy integration in heritage historic buildings," *Energy Procedia*, vol. 48, pp. 1493–1502, 2014.

[54]   F. Frontini, M. Manfren, and L. C. Tagliabue, "A Case Study of Solar Technologies Adoption: Criteria for BIPV Integration in Sensitive Built Environment," *Energy Procedia*, vol. 30, pp. 1006–1015, 2012.

[55]   C. P. Lopez, F. Frontini, and P. Bonomo, "PV and Façade Systems for the Building Skin. Analysis of Design Effectiveness and Technological Features," presented at the 17th European Photovoltaic Solar Conference, 2014.

[56]   J. Cronemberger, M. A. Corpas, I. Cerón, E. Caamaño-Martín, and S. V. Sánchez, "BIPV technology application: Highlighting advances, tendencies and solutions through Solar Decathlon Europe houses," *Energy & Buildings*, vol. 83, pp. 44–56, 2014.

[57]   T. Schuetze, W. Willkomm, and M. Roos, "Development of a Holistic Evaluation System for BIPV Façades," *Energies*, vol. 8, no. 6, pp. 6135–6152, 2015.

[58]   M. C. Munari Probst and C. Roecker, "Solar energy promotion and Urban context protection: LESO-QSV Tool (Quality-Site-Visibility)," presented at the Passive and Low Energy Architecture (PLEA), 2015.

[59]   P. Florio, C. Roecker, and M. C. Munari Probst, "Urban acceptability of solar installations: LESO-QSV GRID, a software tool to support municipalities," presented at the CISBAT, 2015.

[60]   G. Di Giovanni and P. Bonomo, "Analysis of the levels of PV integrability and definition of a performance scheme to control a BIPV project," presented at the World Sustainable Building Conference, 2011.

[61]   P. Bonomo, "Integrazione di sistemi fotovoltaici nell'involucro edilizio. Sviluppo di un metodo di valutazione per applicazioni di BiPV (doctoral thesis)," University of Pavia, 2012.

[62]   P. Bonomo and P. De Berardinis, "PV Integration in Minor Historical Centers: Proposal of Guide-criteria in Post-earthquake Reconstruction Planning," *Energy Procedia*, vol. 48, pp. 1549–1558, 2014.

[63]   A. D. C. Torres-Sibille, V.-A. Cloquell-Ballester, V.-A. Cloquell-Ballester, and M. Á. Artacho Ramírez, "Aesthetic impact assessment of solar power plants: An objective and a subjective approach," *Renewable and Sustainable Energy Reviews*, vol. 13, no. 5, pp. 986–999, 2009.

[64]   A. D. C. Torres-Sibille, "Visual impact assessment of human interventions of the landscape: The case of wind farms and solar power plants (doctoral thesis)," Universidad Politécnica de Valencia, 2010.

[65]   R. Chiabrando, E. Fabrizio, and G. Garnero, "On the applicability of the visual impact assessment OAI$_{SPP}$ tool to photovoltaic plants," *Renewable and Sustainable Energy Reviews*, vol. 15, no. 1, pp. 845–850, 2011.

[66]   M. Pellegrino, G. Flaminio, G. Leanza, and C. Privato, "Aesthetical appeal of BIPV or electrical performance," presented at the PV in Europe - From PV Technology to Energy Solutions, Rome, Italy, 2002.

[67]   V. Dessi, "Methods and tools to evaluate visual impact of solar technologies in urban environment," presented at the Conference of International Building Performance Simulation Association, 2013.

[68]   L. A. Fernandez-Jimenez and M. Mendoza-Villena, "Site selection for new PV power plants based on their observability," *Renewable Energy*, vol. 78, pp. 7–15, 2015.

[69]   R. Xu and S. Wittkopf, "Visuelle Beurteilung der Solaren Architektur," presented at the Swissbau, Basel, 2014.

[70]   M. S. Bittermann, *Intelligent Design Objects (IDO): A cognitive approach for performance-based design (doctoral thesis)*. Delft University of Technology, 2009.

[71]   A. Minelli, I. Marchesini, F. E. Taylor, P. De Rosa, L. Casagrande, and M. Cenci, "An open source GIS tool to quantify the visual impact of wind turbines and photovoltaic panels," *Environmental Impact Assessment Review*, vol. 49, no. C, pp. 70–78, Nov. 2014.

[72] X. Yang, L. Grobe, and W. Stephen, "Simulation of reflected daylight from building envelopes," presented at the Conference of International Building Performance Simulation Association, 2013.

[73] S. Wittkopf, Y. Xiaoming, and R. Xu, "Reflection from PV facades and roofs – New assessment methods based on annual weather data," presented at the European PV Solar Energy Conference and Exhibition, Amsterdam, 2014.

[74] R. Chiabrando, E. Fabrizio, and G. Garnero, "The territorial and landscape impacts of photovoltaic systems: Definition of impacts and assessment of the glare risk," *Renewable and Sustainable Energy Reviews*, vol. 13, no. 9, pp. 2441–2451, 2009.

[75] Power Engineers, "Pancho Valley Solar Farm Project (project report)," Power Engineers, 2010.

[76] E. Riley and S. Olson, "A Study of the Hazardous Glare Potential to Aviators from Utility-Scale Flat-Plate Photovoltaic Systems," *International Scholarly Research Network Renewable Energy*, vol. 2011, 2011.

[77] Spaven Consulting, "Solar photovoltaic energy facilities: Assessment of potential for impact on aviation (project report)," Spaven Consulting, 2011.

[78] C. Ballif, L.-E. Perret-Aebi, and P. Heinstein, "Neue Lösungen für Photovoltaik und Architektur," *Haustech*, 2014.

[79] "Turnhalle Burgweinting," 11-May-2016. [Online]. Available: https://www.dbu.de/index.php?menuecms=123&objektid=25487&menuecms_optik=1025. [Accessed: 11-May-2016].

[80] C. Lüling and T. Berlin, *Energizing architecture: design and photovoltaics*. Jovis, 2009.

[81] Y. Zhao, G. A. Meek, B. G. Levine, and R. R. Lunt, "Near-Infrared Harvesting Transparent Luminescent Solar Concentrators," *Advanced Optical Materials*, vol. 2, no. 7, pp. 606–611, 2014.

[82] S. Nigg, "Schön viel Strom produzieren," *Hoschule Luzern - Das Magazin*, vol. 2, pp. 44–45, 2015.

[83] J. Escarré, H. Y. Li, L. Sansonnens, F. Galliano, G. Cattaneo, P. Heinstein, S. Nicolay, J. Bailat, S. Eberhard, C. Ballif, and L. E. Perret-Aebi, "When PV modules are becoming real building elements: White solar module, a revolution for BIPV," presented at the Photovoltaic Specialist Conference (PVSC), 2015.

[84] L.-E. Perret-Aebi, P. Heinstein, V. Chapuis, S. Pelisset, C. Roecker, L. Friedli, K. Susan, Y. Leterrier, J.-L. Scartezzini, J.-A. Månson, C. Ballif, and A. Schueler, "New challenges in solar architectural innovation," presented at the CISBAT, 2011.

[85] Romande Energie, Mediacom, "EPFL's campus has the world's first solar window." [Online]. Available: https://actu.epfl.ch/news/epfl-s-campus-has-the-world-s-first-solar-window/. [Accessed: 23-Jun-2016].

[86] G. Nisato and J. Hauch, "Current and Future Directions in Organic Photovoltaics," in *Organic Photovoltaics Materials, Device Physics, and Manufacturing Technologies*, 2014.

[87] S. Choulis, "Printing highly efficient organic solar cells," *SPIE Newsroom*, pp. 1–2, 2007.

[88] T. Aernouts, T. Aleksandrov, C. Girotto, J. Genoe, and J. Poortmans, "Polymer based organic solar cells using ink-jet printed active layers," *Applied Physics Letters*, vol. 92, no. 3, pp. 033306–4, 2008.

[89] Technical Research Centre of Finland (VTT), "Decorative and flexible solar panels become part of interior design and the appearance of objects," *Technical Research Centre of Finland*, 2015. [Online]. Available: http://www.vttresearch.com/media/news/decorative-and-flexible-solar-panels-become-part-of-interior-design-and-the-appearance-of-objects. [Accessed: 2016].

[90]   R. Po, A. Bernardi, A. Calabrese, C. Carbonera, G. Corso, and A. Pellegrino, "From lab to fab: how must the polymer solar cell materials design change? – an industrial perspective," *Energy & Environmental Science*, vol. 7, no. 3, pp. 925–19, 2014.

[91]   M. Pagliaro, R. Ciriminna, and G. Palmisano, "Flexible Solar Cells," *ChemSusChem*, vol. 1, no. 11, pp. 880–891, 2008.

[92]   Z. Lakatos, "Untersuchung einer Membrandach-Konstruktion mit integrierten flexiblen Photovoltaikzellen (master thesis)," Hamburg University of Applied Sciences, 2011.

[93]   N. Zamora, "Alvin Huang – Interview | Technergeia," *Technergeia*, 22-May-2015. [Online]. Available: https://technergeia.org/2015/05/22/interview-with-alvin-huang/. [Accessed: 03-Jun-2016].

[94]   Eidgenössisches Departement für Umwelt, Verkehr, Energie und Kommunikation (UVEK),, Eidgenössische Energieforschungskommission (CORE), Bundesamt für Energie (BFE), *Konzept der Energieforschung des Bundes 2017–2020*, 2016.

[95]   Der Schweizerische Bundesrat, *Raumplannungsverordnung (RPV)*. 2016.

[96]   M. Duffy, S. Bailey, and B. Beck, "Preferences in Nursing Home Design: A Comparison of Residents, Administrators, and Designers," *Environment and Behavior*, vol. 18, no. 2, pp. 246–257, 1986.

[97]   W. Fawcett, I. Ellingham, and S. Platt, "Reconciling the architectural preferences of architects and the public: the ordered preference model," *Environment & Behavior*, vol. 40, no. 5, pp. 599–618, 2008.

[98]   C. Llinares, A. Montañana, and E. Navarro, "Differences in Architects and Nonarchitects' Perception of Urban Design: An Application of Kansei Engineering Techniques," *Urban Studies Research*, 2011.

[99]   K. H. Craik and N. R. Feimer, *Setting technical standards for visual assessment procedures*. United States Forest Service, 1979.

[100]   J. F. Palmer and R. E. Hoffman, "Rating reliability and representation validity in scenic landscape assessments," *Landscape and Urban Planning*, vol. 54, no. 1, pp. 149–161, 2001.

[101]   N. R. Feimer, K. H. Craik, R. C. Smardon, and S. R. J. Sheppard, "Appraising the reliability of visual impact assessment methods," presented at the Proceedings of Our National Landscape, Pacific Southwest Forest and Range Experiment Station, Berkeley, 1979.

[102]   S. Robinson and J. Pallasmaa, *Mind in Architecture*. MIT Press, 2015.

[103]   D. B. Vivek, *Ergonomics in the automotive design process*. Taylor & Francis Group, 2012.

[104]   R. Blake, "The visual system of the cat," *Perception & Psychophysics*, vol. 26, no. 6, pp. 423–448, 1979.

[105]   D. J. Felleman and D. C. van Essen, "Distributed Hierarchical Processing in the Primate Cerebral Cortex," *Cerebral cortex*, vol. 1, no. 1, pp. 1–47, 1991.

[106]   D. C. van Essen, D. J. Felleman, E. A. DeYoe, and J. J. Knierim, "Probing the Primate Visual Cortex: Pathways and Perspectives," in *From Pigments to Perception*, no. 28, Boston, MA: Springer US, 1991, pp. 227–237.

[107]   P.-Y. Burgi, "Understanding the Early Human Visual System Through Modeling and Temporal Analysis of Neuronal Structures (doctoral thesis)," University of Geneva, 1992.

[108]   M. Carandini, "Do We Know What the Early Visual System Does?," *Journal of Neuroscience*, vol. 25, no. 46, pp. 10577–10597, 2005.

[109]   D. H. Hubel, *Eye, brain, and vision*, 2nd ed. W. H. Freeman, 1995.

[110]   S. W. Kuffler, "Discharge patterns and functional organization of mammalian retina," *Journal of neurophysiology*, 1953.

[111]   J. L. Hemmen, J. D. Cowan, and E. Domany, *Models of neural networks IV: early vision and attention*. Springer, 2012.

[112]   D. H. Hubel and T. N. Wiesel, "Receptive fields of single neurones in the cat's striate cortex," *The Journal of physiology*, 1959.

[113]   M. Corbetta and G. L. Shulman, "Control of goal-directed and stimulus-driven attention in the brain," *Nature reviews neuroscience*, 2002.

[114]   D. Parkhurst, K. Law, and E. Niebur, "Modeling the role of salience in the allocation of overt visual attention," *Vision Research*, 2002.

[115]   S. Frintrop, E. Rome, and H. I. Christensen, "Computational visual attention systems and their cognitive foundations: A survey," *ACM Transactions on Applied Perception (TAP)*, vol. 7, no. 1, pp. 6–39, 2010.

[116]   J. M. Wolfe and T. S. Horowitz, "What attributes guide the deployment of visual attention and how do they do it?," *Nature reviews neuroscience*, 2004.

[117]   A. Borji and L. Itti, "State-of-the-Art in Visual Attention Modeling," *Sacred Architecture Journal*, vol. 35, no. 1, pp. 185–207, 2013.

[118]   J. M. Wolfe, S. R. Friedman-Hill, M. I. Stewart, and K. M. O'Connell, "The role of categorization in visual search for orientation.," *Journal of Experimental Psychology: Human Perception and Performance*, vol. 18, no. 1, pp. 34–49, 1992.

[119]   A. M. Treisman and G. Gelade, "A feature-integration theory of attention," *Cognitive psychology*, 1980.

[120]   C. Koch and S. Ullman, "Shifts in selective visual attention: towards the underlying neural circuitry," *Human Neurobiology*, no. 4, pp. 219–227, 1985.

[121]   L. Itti, C. Koch, and E. Niebur, "A model of saliency-based visual attention for rapid scene analysis," *IEEE Transactions on Pattern Analysis and Machine Intelligence (TPAMI)*, vol. 20, no. 11, pp. 1254–1259, 1998.

[122]   J. Movellan, "Tutorial on gabor filters, 2005." [Online]. Available: http://scholar.google.com/scholar?q=related:eTMrj4EalYkJ:scholar.google.com/&hl=en&num=20&as_sdt=0,5. [Accessed: 12-Jan-2016].

[123]   V. S. N. Prasad and J. Domke, "Gabor Filter Visualization," 11-May-2005. [Online]. Available: https://www.cs.umd.edu/class/spring2005/cmsc838s/assignment-projects/gabor-filter-visualization/report.pdf. [Accessed: 12-Jan-2016].

[124]   D. Walther, *Interactions of Visual Attention and Object Recognition: Computational Modeling, Algorithms, and Psychophysics*. ProQuest, 2006.

[125]   J. Harel, "Saliency Map Algorithm: MATLAB Source Code." [Online]. Available: http://www.vision.caltech.edu/~harel/share/gbvs.php. [Accessed: 12-Mar-2016].

[126]   J. Harel, C. Koch, and P. Perona, "Graph-based visual saliency," *Annual Conference on Neural Information Processing Systems (NIPS)*, 2006.

[127]   N. Privault, *Understanding Markov chains: examples and applications*. Springer, 2013.

[128]   J. Bang, *Digraphs: Theory, Algorithms and Applications*. Springer, 2007.

[129]   M. Biskupska, "Bottom-up saliency maps: a review," *Elektronika: konstrukcje*, 2013.

[130]   L. Duan, C. Wu, J. Miao, L. Qing, and Y. Fu, "Visual saliency detection by spatially weighted dissimilarity," *2011 IEEE Conference on Computer Vision and Pattern Recognition (CVPR)*, pp. 473–480, 2011.

[131]   N. Riche, M. Duvinage, M. Mancas, B. Gosselin, and T. Dutoit, "Saliency and Human Fixations: State-of-the-Art and Study of Comparison Metrics," presented at the 2013 IEEE International Conference on Computer Vision (ICCV), 2013.

[132] A. Borji, D. N. Sihite, and L. Itti, "Quantitative Analysis of Human-Model Agreement in Visual Saliency Modeling: A Comparative Study," *IEEE Transactions on Image Processing*, vol. 22, no. 1, 2013.

[133] T. Judd, F. Durand, and A. Torralba, "A benchmark of computational models of saliency to predict human fixations," *MIT Computer Science and Artificial Intelligence Laboratory Technical Report*, 2012.

[134] T. Judd, K. Ehinger, and F. Durand, "Learning to predict where humans look," *Computer vision*, 2009.

[135] O. Le Meur and T. Baccino, "Methods for comparing scanpaths and saliency maps: strengths and weaknesses," *Behavior Research Methods*, vol. 45, no. 1, pp. 251–266, 2012.

[136] D. H. Ballard and M. J. Swain, *Color indexing*. International Journal of Computer Vision, 1991.

[137] O. Pele and M. Werman, "Fast and robust earth mover's distances," *Computer vision*, 2009.

[138] R. J. Peters, A. Iyer, L. Itti, and C. Koch, "Components of bottom-up gaze allocation in natural images," *Vision Research*, vol. 45, no. 18, pp. 2397–2416, 2005.

[139] Y. H. Yee, S. N. Pattanaik, and D. P. Greenberg, "Spatiotemporal sensitivity and visual attention for efficient rendering of dynamic environments," *ACM Transactions on Graphics (TOG)*, vol. 20, no. 1, pp. 39–65, 2001.

[140] K. Cater, A. Chalmers, and G. Ward, "Detail to Attention: Exploiting Visual Tasks for Selective Rendering," *Rendering Techniques*, pp. 270–280, 2003.

[141] K. Debattista, V. Sundstedt, L. P. Santos, and A. Chalmers, "Selective component-based rendering," *GRAPHITE*, pp. 13–22, 2005.

[142] C. H. Lee, A. Varshney, and D. Jacobs, "Mesh Saliency," *ACM SIGGRAPH '05*, vol. 24, no. 3, pp. 659–666, 2005.

[143] Y.-S. Wang, C.-L. Tai, O. Sorkine, and T.-Y. Lee, "Optimized scale-and-stretch for image resizing," *ACM Transactions on Graphics (TOG)*, vol. 27, no. 5, p. 118, 2008.

[144] R. Achanta and S. Süsstrunk, "Saliency detection for content-aware image resizing," *International Conference on Image Processing (ICIP)*, pp. 1005–1008, 2009.

[145] Chenlei Guo and Liming Zhang, "A Novel Multiresolution Spatiotemporal Saliency Detection Model and Its Applications in Image and Video Compression," *IEEE Transactions on Image Processing*, vol. 19, no. 1, pp. 185–198, 2010.

[146] B. Suh, H. Ling, B. B. Bederson, and D. W. Jacobs, "Automatic thumbnail cropping and its effectiveness," *Proceedings of the 16th annual ACM symposium on User interface software and technology (UIST)*, pp. 95–104, 2003.

[147] J. Han, K. N. Ngan, Mingjing Li, and Hong-Jiang Zhang, "Unsupervised extraction of visual attention objects in color images," *IEEE Transactions on Circuits and Systems for Video Technology*, vol. 16, no. 1, pp. 141–145, 2006.

[148] R. Achanta, F. Estrada, P. Wils, and S. Süsstrunk, "Salient Region Detection and Segmentation," in *Computer Vision Systems*, vol. 5008, no. 7, Springer Berlin Heidelberg, 2008, pp. 66–75.

[149] Y. Hu, X. Xie, W.-Y. Ma, L.-T. Chia, and D. Rajan, "Salient Region Detection Using Weighted Feature Maps Based on the Human Visual Attention Model," in *Advances in Multimedia Information Processing - PCM 2004*, vol. 3332, no. 122, K. Aizawa, Y. Nakamura, and S. Satoh, Eds. Springer Berlin Heidelberg, 2005, pp. 993–1000.

[150] T. Kadir and M. Brady, "Saliency, Scale and Image Description," *International Journal of Computer Vision (IJCV)*, vol. 45, no. 2, pp. 83–105, 2001.

[151] S. Frintrop, A. Königs, F. Hoeller, and D. Schulz, "A Component-Based Approach to Visual Person Tracking from a Mobile Platform," *International Journal of Social Robotics (IJSR)*, vol. 2, no. 1, pp. 53–62, 2010.

[152] C. Davies, W. Tompkinson, N. Donnelly, L. Gordon, and K. Cave, "Visual saliency as an aid to updating digital maps," *Computers in Human Behavior*, vol. 22, no. 4, pp. 672–684, 2006.

[153] C. Breazeal and B. Scassellati, "A Context-Dependent Attention System for a Social Robot," *International Joint Conference on Artificial Intelligence (IJCAI)*, pp. 1146–1153, 1999.

[154] J. M. Wolfe, "Guided search 2.0 a revised model of visual search," *Psychonomic bulletin & review*, 1994.

[155] D. Meger, P.-E. Forssén, K. Lai, S. Helmer, S. McCann, T. Southey, M. A. Baumann, J. J. Little, and D. G. Lowe, "Curious George: An attentive semantic robot," *Robotics and Autonomous Systems (RAS)*, vol. 56, no. 6, pp. 503–511, 2008.

[156] X. Hou and L. Zhang, "Saliency Detection: A Spectral Residual Approach," *Computer Vision and Pattern Recognition*, 2007.

[157] C. Siagian and L. Itti, "Biologically Inspired Mobile Robot Vision Localization," *IEEE Transactions on Robotics (TROB)*, vol. 25, no. 4, pp. 861–873, 2009.

[158] S. Vijayakumar, J. Conradt, T. Shibata, and S. Schaal, "Overt visual attention for a humanoid robot," *International Conference on Intelligent Robots and Systems (IROS)*, pp. 2332–2337, 2001.

[159] F. Orabona, G. Metta, and G. Sandini, "Object-based visual attention: a model for a behaving robot," *Computer Vision and Pattern Recognition (CVPR)*, 2005.

[160] E. Todt and C. Torras, "Detection of Natural Landmarks through Multiscale Opponent Features," *International Conference on Pattern Recognition (ICPR)*, pp. 3988–3991, 2000.

[161] N. Ouerhani, A. Bur, and H. Hügli, "Visual attention-based robot self-localization," *Proceeding of European Conference on Mobile Robotics*, 2005.

[162] N. Ouerhani, H. Hügli, G. Gruener, and A. Codourey, "A Visual Attention-Based Approach for Automatic Landmark Selection and Recognition," in *Attention and Performance in Computational Vision*, vol. 3368, no. 14, L. Paletta, J. K. Tsotsos, E. Rome, and G. Humphreys, Eds. Springer Berlin Heidelberg, 2005, pp. 183–195.

[163] P. Green, "Driver distraction, telematics design, and workload managers: Safety issues and solutions," *Society of Automotive Engineers (SAE)*, 2004.

[164] W. J. Won, M. Lee, and J. W. Son, "Implementation of road traffic signs detection based on saliency map model," *Intelligent Vehicles Symposium*, 2008.

[165] S. Wang and Y. Tian, "Indoor signage detection based on saliency map and bipartite graph matching," *International Conference on Bioinformatics and Biomedicine (BIBM) Workshops*, pp. 518–525, 2011.

[166] S. Wang, X. Yang, and Y. Tian, "Detecting signage and doors for blind navigation and wayfinding," *Network Modeling Analysis in Health Informatics and Bioinformatics*, vol. 2, no. 2, pp. 81–93, 2013.

[167] N. Parikh, L. Itti, and J. Weiland, "Saliency-based image processing for retinal prostheses," *Journal of Neural Engineering*, vol. 7, no. 1, 2010.

[168] A. A. Salah, E. Alpaydin, and L. Akarun, "A Selective Attention-Based Method for Visual Pattern Recognition with Application to Handwritten Digit Recognition and Face Recognition," *Sacred Architecture Journal*, vol. 24, no. 3, pp. 420–425, 2002.

[169] L. Greco and M. La Cascia, "Saliency Based Aesthetic Cut of Digital Images," *Image Analysis and Processing (ICIAP)*, 2013.

[170]   R. T. Wilson, D. W. Baack, and B. D. Till, "Creativity, attention and the memory for brands: an outdoor advertising field study," *International Journal of Advertising*, 2015.

[171]   S. Berger, U. Wagner, and C. Schwand, "Assessing Advertising Effectiveness: The Potential of Goal-Directed Behavior," *Psychology and Marketing*, vol. 29, no. 6, pp. 411–421, 2012.

[172]   N. Holmberg, K. Holmqvist, and H. Sandberg, "Children's attention to online adverts is related to low-level saliency factors and individual level of gaze control," *Journal of Eye Movement Research*, 2015.

[173]   N. Koide, T. Kubo, S. Nishida, T. Shibata, and K. Ikeda, "Art Expertise Reduces Influence of Visual Salience on Fixation in Viewing Abstract-Paintings," *PLoS One*, vol. 10, no. 2, 2015.

[174]   Z. Bylinskii, T. Judd, F. D. Durand, A. Oliva, and A. Torralba, "MIT Saliency Benchmark," *saliency.mit.edu*. [Online]. Available: http://saliency.mit.edu. [Accessed: 07-Dec-2014].

[175]   M. Kümmerer, L. Theis, and M. Bethge, "Deep Gaze I: Boosting Saliency Prediction with Feature Maps Trained on ImageNet," presented at the Conference of International Building Performance Simulation Association, San Diego, USA, 2015.

[176]   M. Jiang, S. Huang, J. Duan, and Q. Zhao, "SALICON: Saliency in Context," *2015 IEEE Conference on Computer Vision and Pattern Recognition (CVPR)*, pp. 1072–1080, 2015.

[177]   J. Zhang and S. Sclaroff, "Saliency Detection: A Boolean Map Approach," *2013 IEEE International Conference on Computer Vision (ICCV)*, pp. 153–160, 2013.

[178]   E. Erdem and A. Erdem, "Visual saliency estimation by nonlinearly integrating features using region covariances," *Journal of Vision*, vol. 13, no. 4, 2013.

[179]   N. Riche, M. Mancas, M. Duvinage, M. Mibulumukini, B. Gosselin, and T. Dutoit, "RARE2012_ A multi-scale rarity-based saliency detection with its comparative statistical analysis," *Signal Processing : Image Communication*, vol. 28, no. 6, pp. 642–658, 2013.

[180]   H. R. Tavakoli, E. Rahtu, and J. Heikkilä, "Fast and Efficient Saliency Detection Using Sparse Sampling and Kernel Density Estimation," in *Image Analysis*, vol. 6688, no. 62, A. Heyden and F. Kahl, Eds. Springer Berlin Heidelberg, 2011, pp. 666–675.

[181]   G. Ward and R. Shakespeare, *Rendering with Radiance: the art and science of lighting visualization*. Morgan Kaufmann Publishers, 1998.

[182]   G. Ward, R. Mistrick, E. S. Lee, A. McNeil, and J. Jonsson, "Simulating the daylight performance of complex fenestration systems using bidirectional scattering distribution functions within Radiance," *LEUKOS*, vol. 7, no. 4, pp. 241–261, 2011.

[183]   G. Ward, M. Kurt, and N. Bonneel, "A Practical Framework for Sharing and Rendering Real-World Bidirectional Scattering Distribution Functions (Report Number: LBNL-5954E) ," *Technical Report Deliverable of Windows and Envelope Materials Group, Building Technology and Urban Systems Department, Environmental Energy Technologies Division*, 2012.

[184]   P. Apian-Bennewitz, "New scanning gonio-photometer for extended BRTF measurements," presented at the Proceedings of SPIE - The International Society for Optical Engineering, 2010.

[185]   M. Krehel, J. Kämpf, and S. Wittkopf, "Characterisation and Modelling of Advanced Daylight Redirection Systems with Different Goniophotometers," presented at the CISBAT, 2015.

[186]   International Commission on Illumination, "Spatial distribution of daylight. CIE standard general sky (ISO 15469:2004 (E)/CIE S 011/E:2003)," 2003.

[187]   R. Xu and S. Wittkopf, "Visual assessment of BIPV retrofit design proposals for selected historical buildings using the saliency map method," *Journal of Facade Design and Engineering*, 2015.

[188] R. Xu, "Visuelle Bewertung solarer Architektur," presented at the 12. Workshop Photovoltaik-Modultechnik, Cologne, Germany, 2015.

[189] Deutsche Bischofskonferenz, *Zukunft der Schöpfung-Zukunft der Menschheit: Erklärung der Deutschen Bischofskonferenz zu Fragen der Umwelt und der Energieversorgung*. Sekretariat der Deutschen Bischofskonferenz, 1980.

[190] Deutsche Bischofskonferenz, *Der Schöpfung verpflichtet - Anregungen für einen nachhaltigen Umgang mit Energie*. Sekretariat der Deutschen Bischofskonferenz, 2011.

[191] M.-C. A. Schürch, "Bewahrung der Schöpfung als christlicher Auftrag," *www.tagesanzeiger.ch*, 10-Sep-2015. [Online]. Available: http://www.horizonte-aargau.ch/5338-2/. [Accessed: 09-Apr-2016].

[192] World Council of Churches Central Commitee, "Statement towards a Nuclear-free World," *World Council of Churches*, 07-Jul-2014. [Online]. Available: https://www.oikoumene.org/en/resources/documents/central-committee/geneva-2014/statement-towards-a-nuclear-free-world. [Accessed: 09-Apr-2016].

[193] Pope Franciscus, "LETTER OF HIS HOLINESS POPE FRANCIS FOR THE ESTABLISHMENT OF THE 'WORLD DAY OF PRAYER FOR THE CARE OF CREATION'," *The holy see*, 10-Aug-2015. [Online]. Available: http://w2.vatican.va/content/francesco/en/letters/2015/documents/papa-francesco_20150806_lettera-giornata-cura-creato.pdf. [Accessed: 09-Apr-2016].

[194] B. Bowald, "Klimawandel – Den Worten Taten folgen lassen," *Schweizerische Nationalkommission Justitia et Pax*, 2009.

[195] R. Presse, "Solaranlagen sind ein starkes Symbol (Interview mit Kurt Aufdereggen)," *Reformierte Presse*, 18-May-2011. [Online]. Available: http://www.oeku.ch/de/documents/Solaranlagen-Ref-Presse-Mai-2011.pdf. [Accessed: 16-Apr-2016].

[196] H. Dietz, "The Eschatological Dimension of Church Architecture - Biblical Roots of Church Orientation," *Sacred Architecture Journal*, 2005. [Online]. Available: http://fathermarkspruill.com/wp-content/uploads/2015/09/12.9-The-Eschatological-Dimension-of-Church-Architecture.doc. [Accessed: 14-Apr-2016].

[197] Schweizerische Evangelische Kirchenbund SEK, *Energieethik*. 2007.

[198] Brot für alle / Fastenopfer-Aktion, "Medienmitteilung von Brot für alle und Fastenopfer," *Brot für alle*, 17-Sep-2009. [Online]. Available: http://www.brotfueralle.ch/index.php?id=16&tx_ttnews%5Btt_news%5D=109&cHash=cab2341e81a26ff258142db2ccc98cd9. [Accessed: 09-Apr-2016].

[199] K. Aufdereggenoeku Kirche und Umwelt, "Schöpfung bewahren – und dabei sparen," *oeku Kirche und Umwelt*, 30-Oct-2007. [Online]. Available: http://www.oeku.ch/de/documents/energietipps-allgemein.pdf. [Accessed: 09-Apr-2016].

[200] Reformierte Kirchen Bern-Jura-Solothurn, oeku Kirche und Umwelt, "Leitfaden Solaranlagen," 2013.

[201] oeku Kirche und Umwelt, *Energie sparen und Klima schützen - Ein Leitfaden für Kirchgemeinden und Pfarreien*. 2013.

[202] energie schweizBundesamt für Energie (BFE), *Solar-Architektur: Entwurfsprozess und Umsetzung*. 2006.

[203] "Hanns A. Brütsch, Architekt BSA/SIA." [Online]. Available: http://www.bruetscharchitekt.ch/. [Accessed: 17-Apr-2016].

[204] R. Rosenholtz, A. Dorai, and R. Freeman, "Do predictions of visual perception aid design?," *ACM Transactions on Applied Perception (TAP)*, vol. 8, no. 2, p. 12, 2011.

[205]   "sonnendach.ch zeigt Solarenergiepotenzial von Hausdächern," *Bundesamt fur Energie BFE*. [Online]. Available: http://www.bfe.admin.ch/energie/00588/00589/00644/index.html?lang=de&msg-id=60709. [Accessed: 22-May-2016].

[206]   Bundesamt für Landestopografie, "Swisstopo." [Online]. Available: http://www.swisstopo.admin.ch/internet/swisstopo/de/home/current.html. [Accessed: 22-May-2016].

[207]   Bundesamt für Meteorologie und Klimatologie MeteoSchweiz, "MeteoSchweiz." [Online]. Available: http://www.meteoschweiz.admin.ch/. [Accessed: 22-May-2016].

[208]   Bundesamt für Energie (BFE), "sonnendach." [Online]. Available: http://www.bfe-gis.admin.ch/sonnendach. [Accessed: 22-May-2016].

[209]   R. Xu and S. Wittkopf, "Visual impact thresholds of photovoltaics on retrofitted building façades in different building zones using the Saliency Map method," *CISBAT 2015*, 2015.

[210]   N. A. Salingaros, "Towards A Biological Understanding Of Architecture And Urbanism: Lessons From Steven Pinker," *Katarxis Nº*, 2004.

[211]   E. M. Sternberg and M. A. Wilson, "Neuroscience and architecture: seeking common ground.," *Cell*, vol. 127, no. 2, pp. 239–242, 2006.

[212]   J. P. Eberhard, "Applying Neuroscience to Architecture," *Neuron*, vol. 62, no. 6, pp. 753–756, 2009.

[213]   J. Eberhard, *Brain Landscape: The Coexistence of Neuroscience and Architecture*. Oxford University Press, 2009.

Appendix 1   MATLAB code example for post-processing stage

```
%GBVS saliency model
clear
clc
imagesize=(867*1450);

%setting the insignificance value
pvalue=0.90;
step=0.0001;

%GBVS saliency map 'original'
map_gbvs=gbvs('MainCourtyard.tif');
%

%GBVS saliency map 'new' of design PVBig_S1
figure
gbvs_result=gbvs('PVBig_S1.tif');
imshow(gbvs_result.master_map_resized)
colorbar
colormap jet

%GBVS delta map
gbvs_delta=abs(map_gbvs.master_map_resized-gbvs_result.master_map_resized);

figure
imshow(gbvs_delta)
colorbar
colormap jet

%----------------Percentage graph---------------------------
gbvs_pc=zeros(867,1450);
x=0:step:1;

%finding the threshold value (alpha)
b=gbvs_delta;
vector=reshape(b,[],1);
v=histc(vector,0:step:1);
flache=cumsum(v);
[row,col] = find(flache>pvalue*max(flache));
alpha=min(row)*step;

%calculating the visual impact S value
```

```matlab
y=flache(min(row));
gbvs_pcs=gbvs_delta>alpha;
weight=max(max(gbvs_delta));
pc1=100*(max(max(gbvs_delta)));
pc2=round(100*alpha*weight,2);

%plot binary map
figure
imshow(gbvs_pcs)
title({['percentage=',num2str(pc1),'   S=',num2str(pc2)]})

%plot percentage graph
figure
plot(x,flache)
hold
grid
line([alpha alpha], [0 y]);
plot(alpha,y,'r*')
title({[num2str(pvalue*100) '% of saliency values <',num2str(round(alpha,2))]})
```

Appendix 2   Image resolution and its effect on saliency map
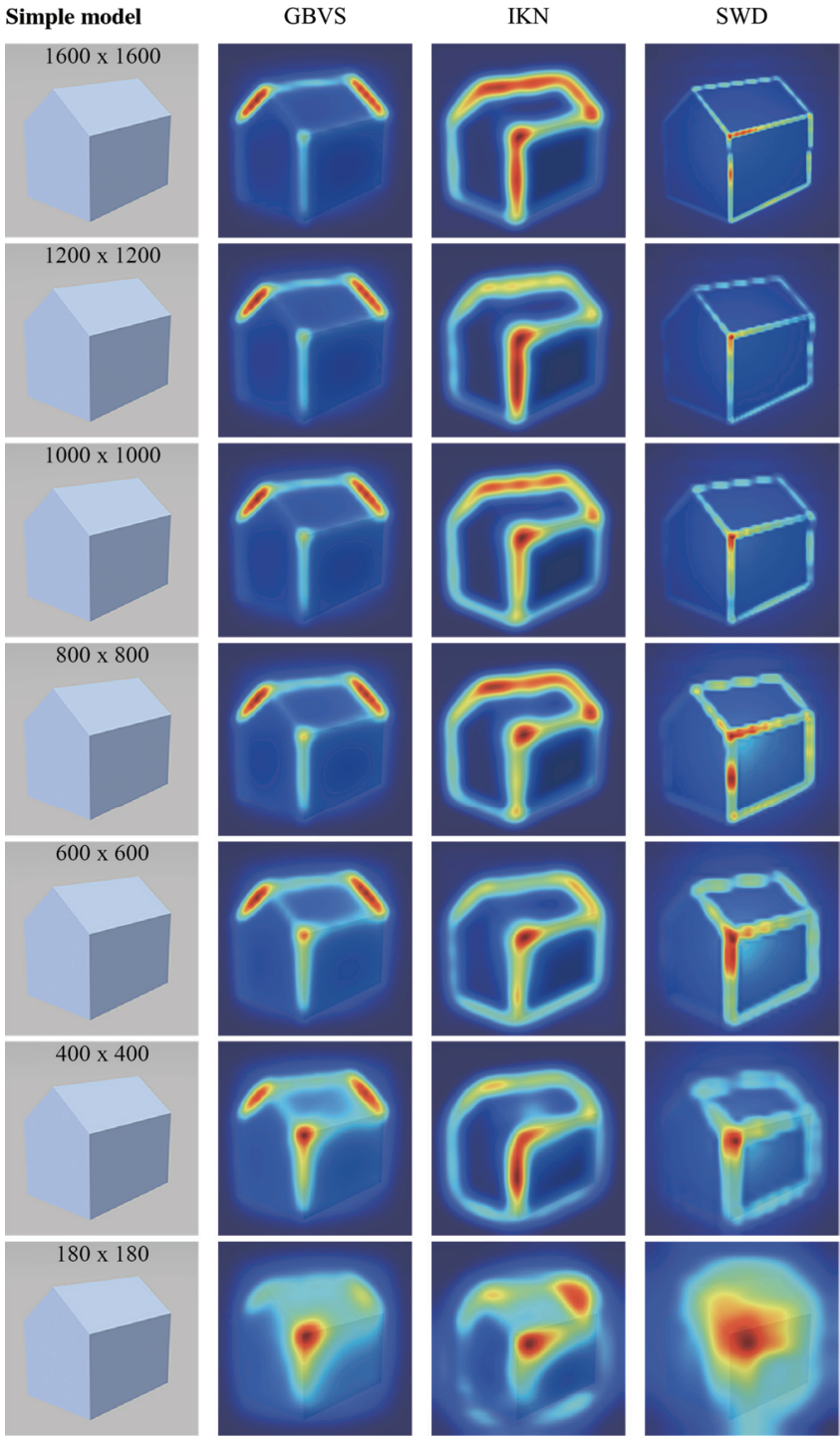
Left column: a hut of simple complexity in renderings with different resolutions. Second column from left: the resulting saliency map generated with GBVS saliency model. Third column from left: the resulting saliency map generated with IKN (Harel) saliency model. First column from right: the resulting saliency map generated with SWD saliency model.

	Medium model	GBVS	IKN	SWD
1600 x 1600				
1200 x 1200				
1000 x 1000				
800 x 800				
600 x 600				
400 x 400				
180 x 180				
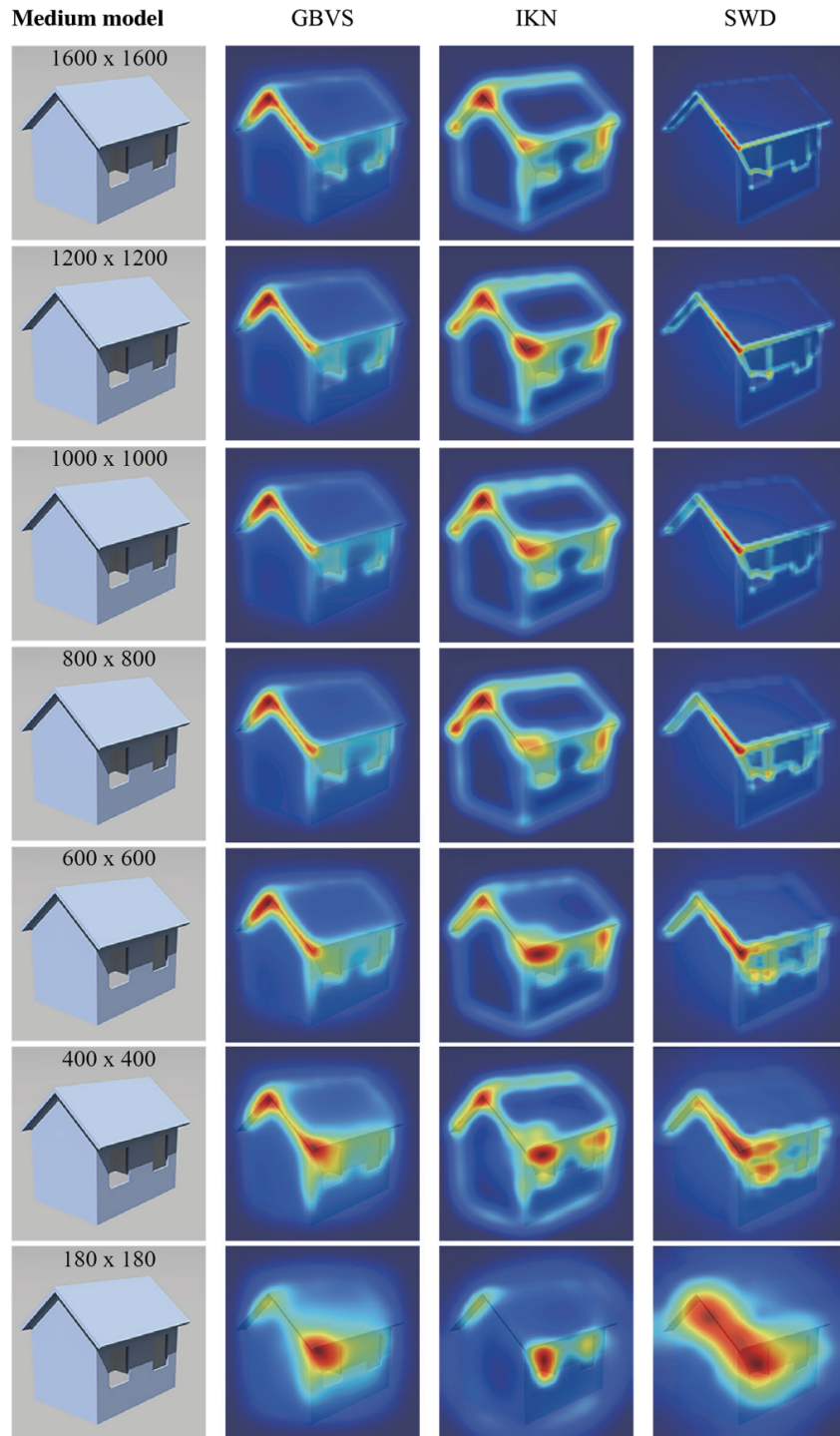
Left column: a hut of medium complexity in renderings with different resolutions. Second column from left: the resulting saliency map generated with GBVS saliency model. Third column from left: the resulting saliency map generated with IKN (Harel) saliency model. First column from right: the resulting saliency map generated with SWD saliency model.

Complex model	GBVS	IKN	SWD
1600 x 1600			
1200 x 1200			
1000 x 1000			
800 x 800			
600 x 600			
400 x 400			
180 x 180			
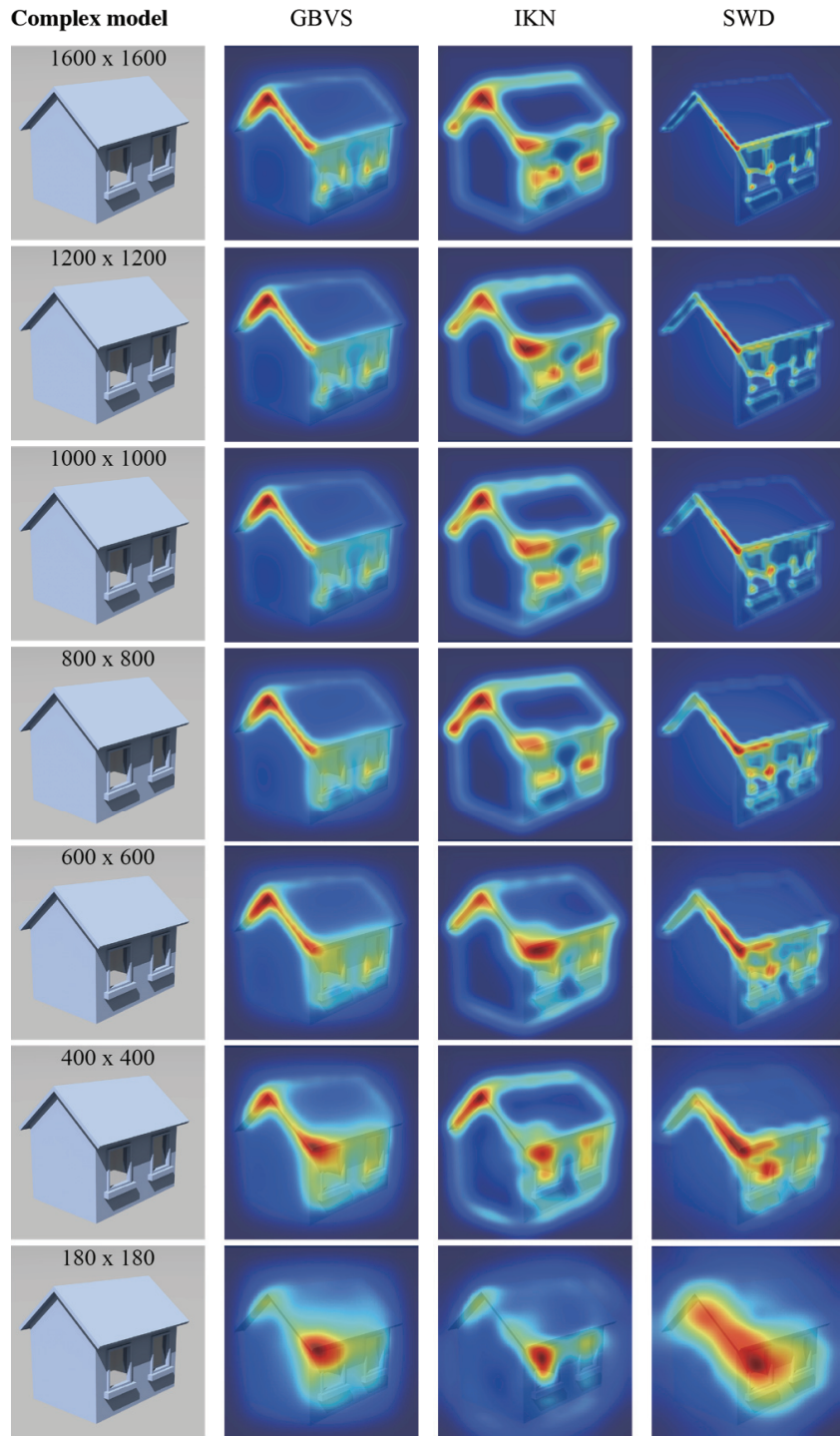
Left column: a hut of high complexity in renderings with different resolutions. Second column from left: the resulting saliency map generated with GBVS saliency model. Third column from left: the resulting saliency map generated with IKN (Harel) saliency model. First column from right: the resulting saliency map generated with SWD saliency model.

Appendix 3   Detailed BSDF properties of the PV samples

PV sample 1 (Backsheet)
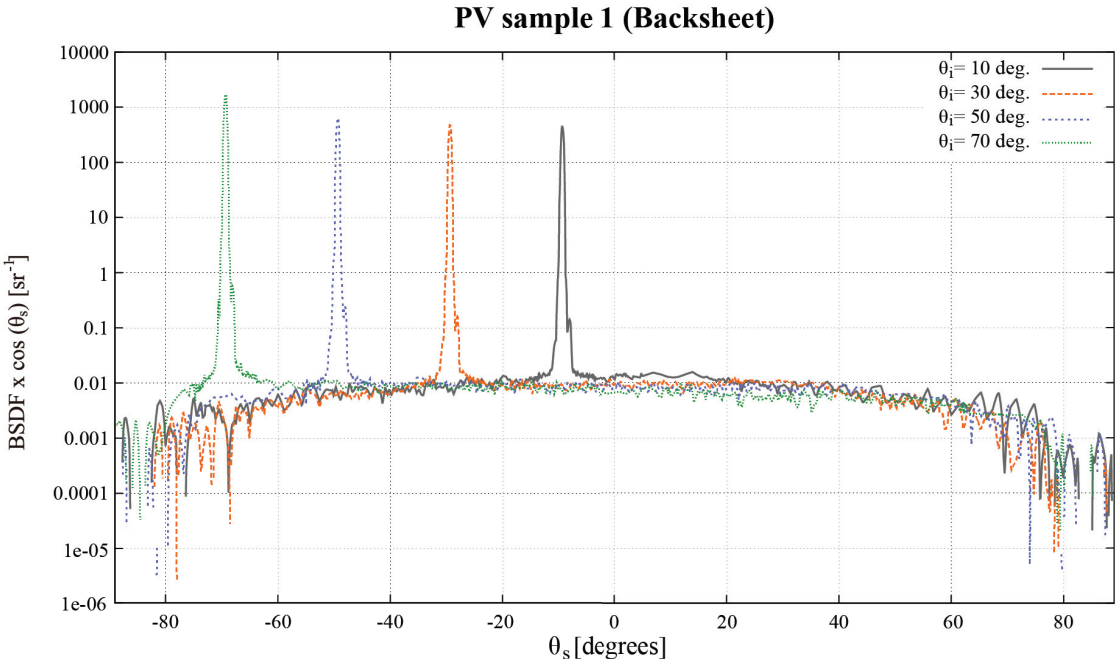
The BSDF properties of PV sample 1, backsheet area. The horizontal axis is the theta angle of the reflected light. The θ_i stands for the theta angle of the incident light. The ϕ angle of the incident light is 0 degree.
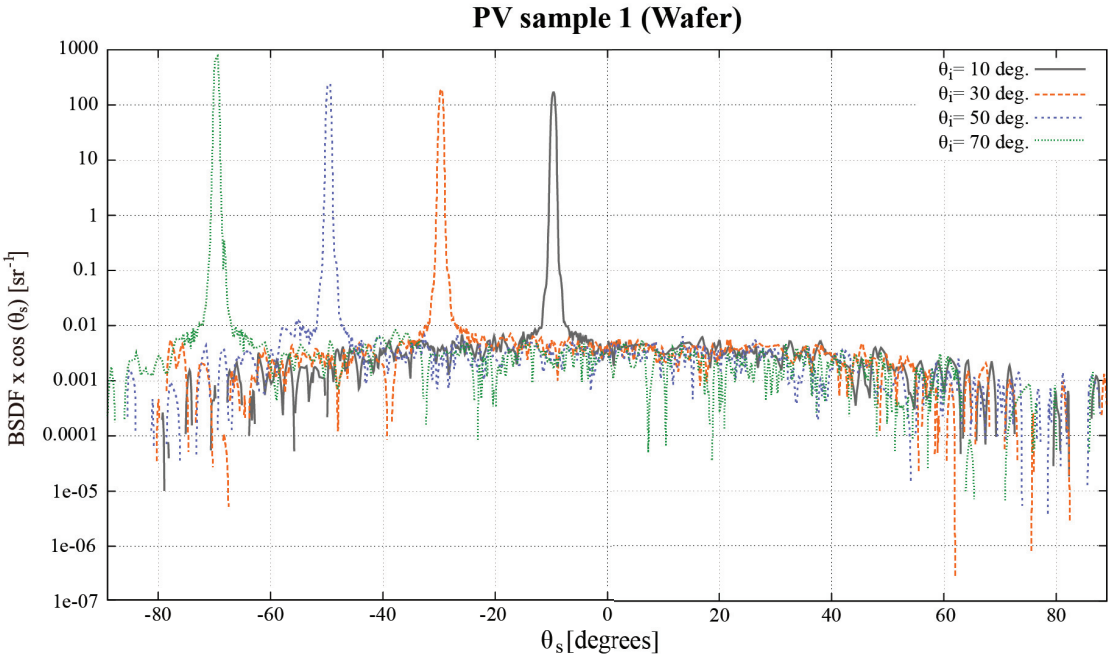
PV sample 1 (Wafer)

The BSDF properties of PV sample 1, wafer area. The horizontal axis is the outgoing theta angle. The θ_i stands for the theta angle of the incident light. The ϕ angle of the incident light is 0 degree.

PV sample 2 (Backsheet)
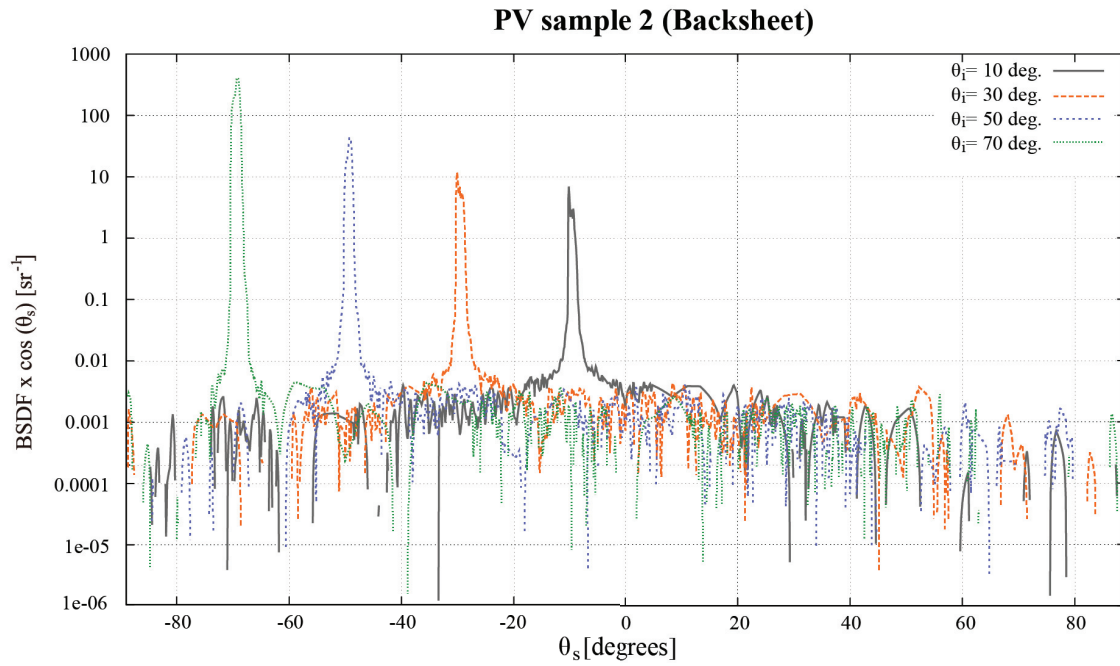
The BSDF properties of PV sample 2, backsheet area. The horizontal axis is the outgoing theta angle. The θ_i stands for the theta angle of the incident light. The ϕ angle of the incident light is 0 degree.
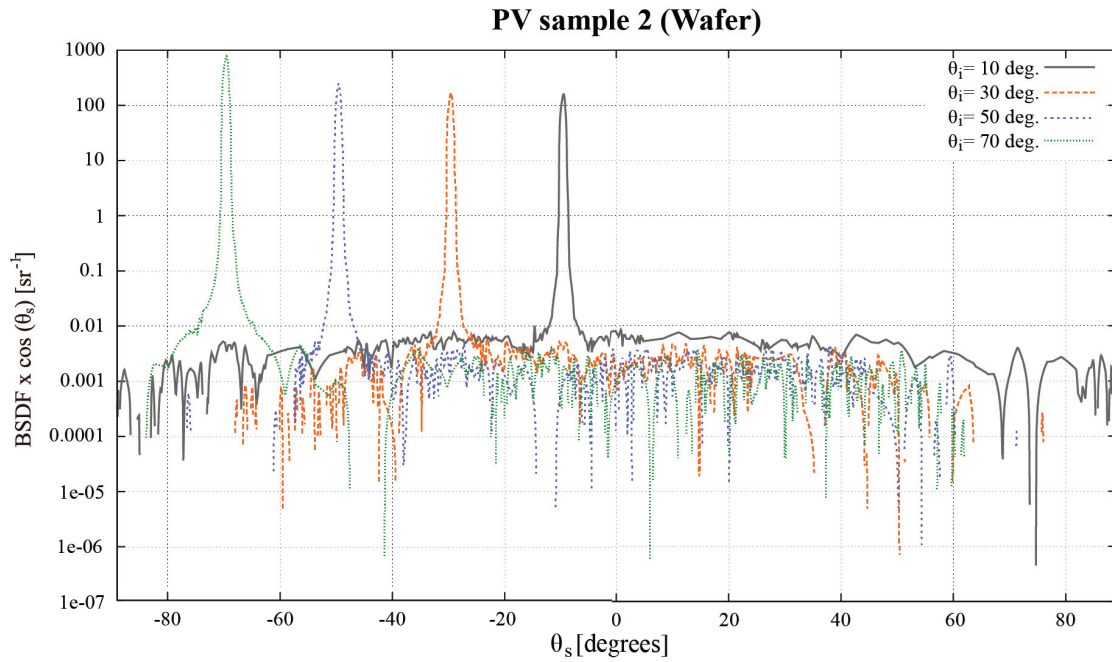
PV sample 2 (Wafer)

The BSDF properties of PV sample 2, wafer area. The horizontal axis is the outgoing theta angle. The θ_i stands for the theta angle of the incident light. The ϕ angle of the incident light is 0 degree.

Appendix 4   Radiance material settings for church St. Michael

No.	Building part	Material type	Material description in Radiance
1	New church roof with Eternit tiles	Black screed	dusty_tight_deep plastic Black_Roof 0 0 5 0.01 0.01 0.01 0 0
2	Window and door glasses	Glazing single pane	void glass Glazing_SinglePane_88 0 0 3 0.96 0.96 0.96
3	Window and door frames	Diffuse metal	void metal metal_diffuse 0 0 5 0.1 0.1 0.1 0.50 0.175
4	Window part (striped)	Diffuse metal	void colourpict metalstripe 9 red green blue StBlinds.hdr picture.cal tile_u tile_v -s 1 0 1 .578313253 metalstripe plastic MetalAboveWindows 0 0 5 0 0 0 0 0
5	Church facade	Bare concrete (striped)	dusty_med colourpict con1 13 red green blue StConcrete.hdr picture.cal tile_u tile_v -s 10 -rx 90 -rz 90 0 1 .578313253 con1 plastic Concrete1 0 0 5 0.2 0.2 0.2 0.0001 0.0001
6	PV sample 1	Wafer	PV sample 1, wafer part
		Back sheet	PV sample 1, backsheet part
		Dummy	Measured BSDF data
7	PV sample 2	Wafer	PV sample 2, wafer part
		Back sheet	PV sample 2, backsheet part
		Dummy	Measured BSDF data

Appendix 5   Radiance Renderings

Viewpoint 1
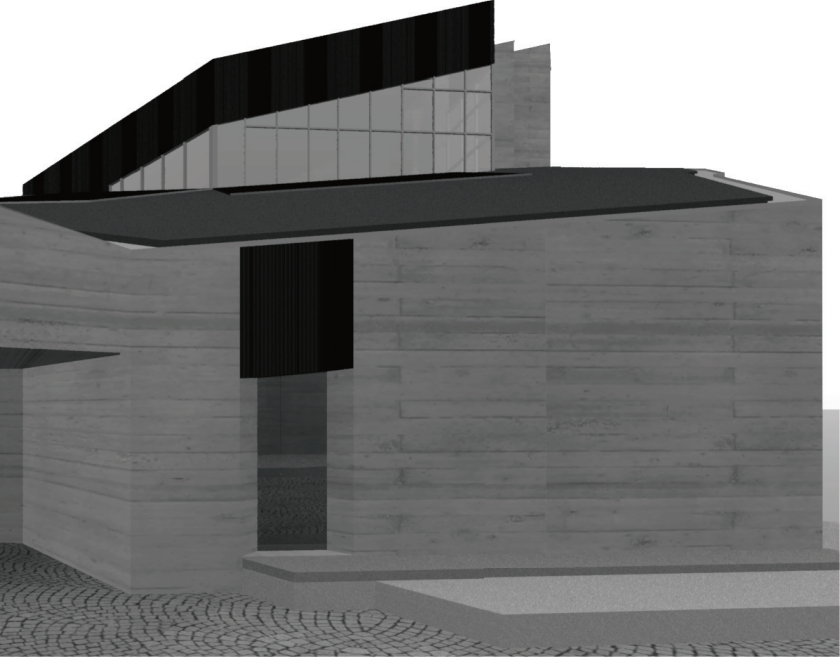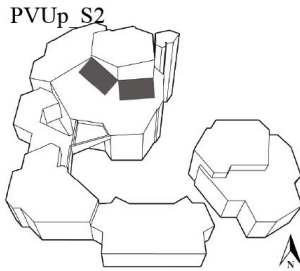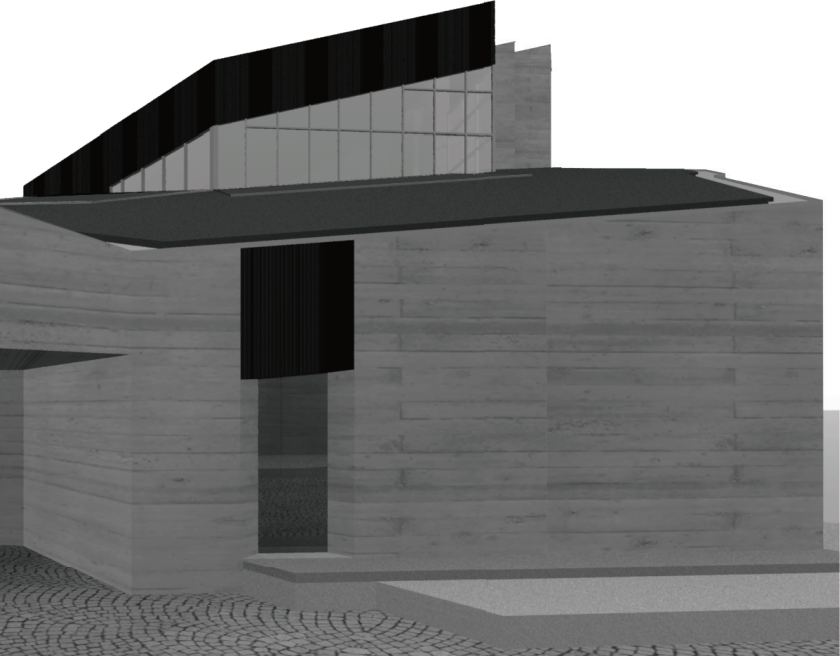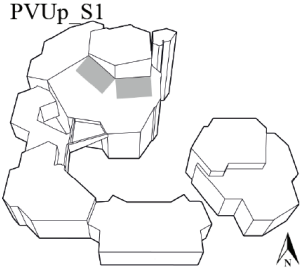
PVUp_S1

PVUp_S2

Viewpoint 1

PVPolygon_S1
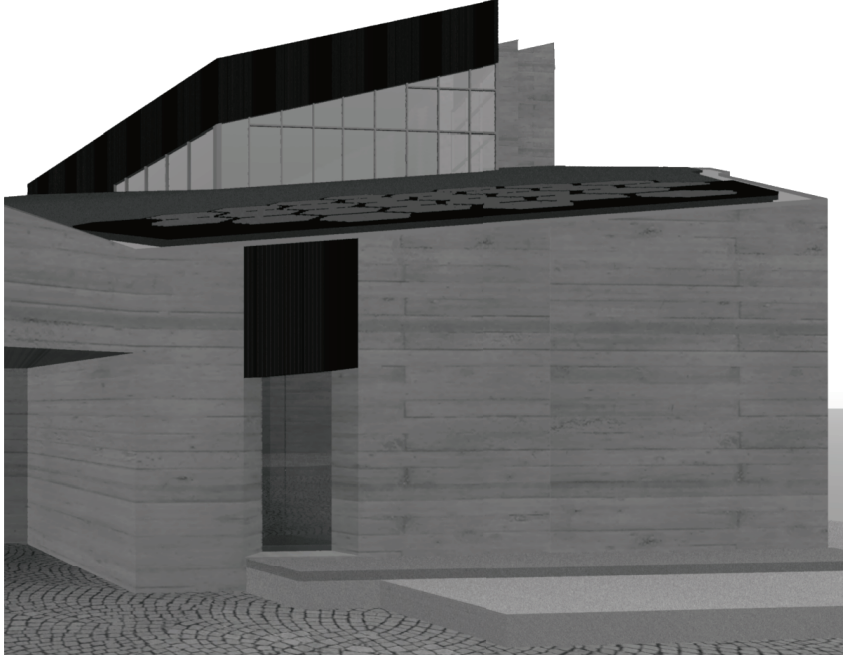
PVPolygon_S2
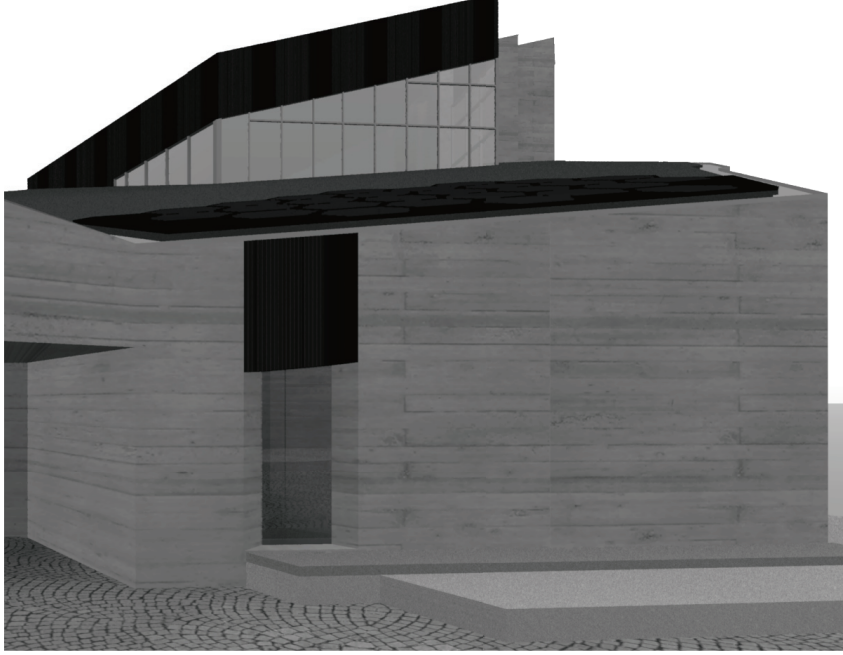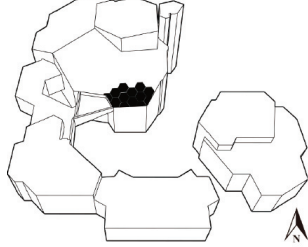
PVBig_S1

Viewpoint 1
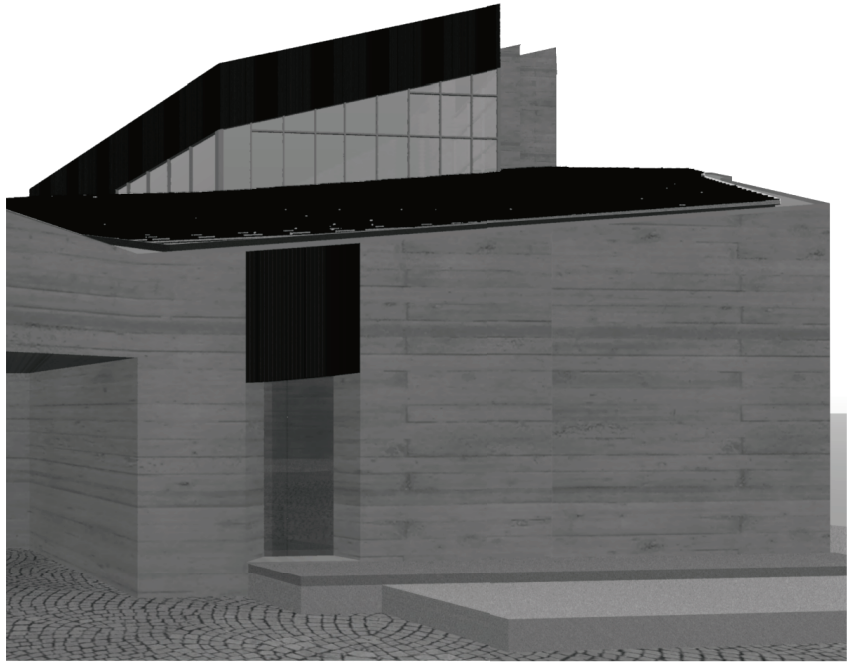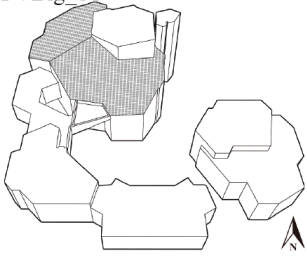
PVBig_S2
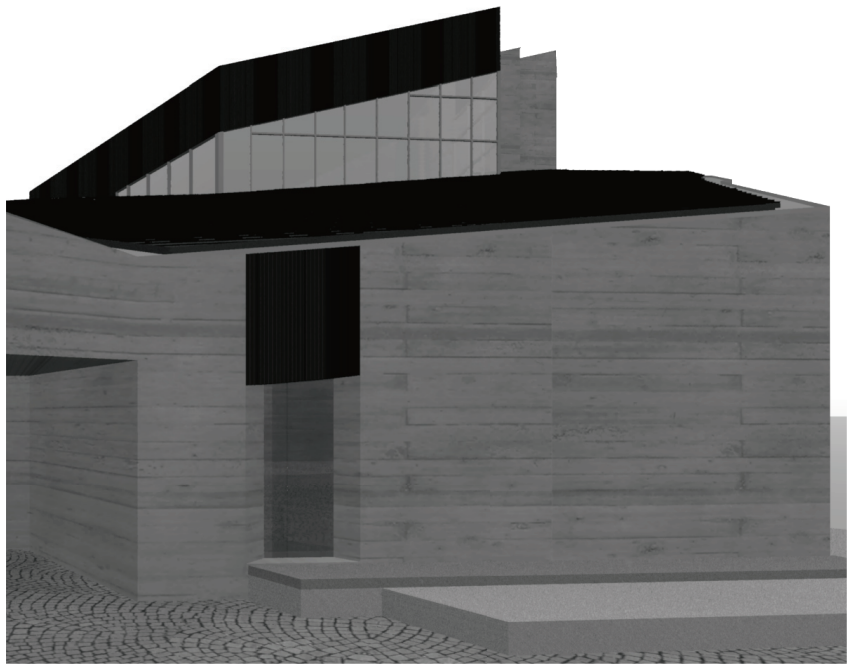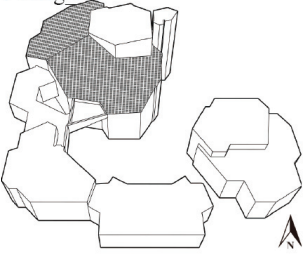
Viewpoint 1

PVSmall_S1
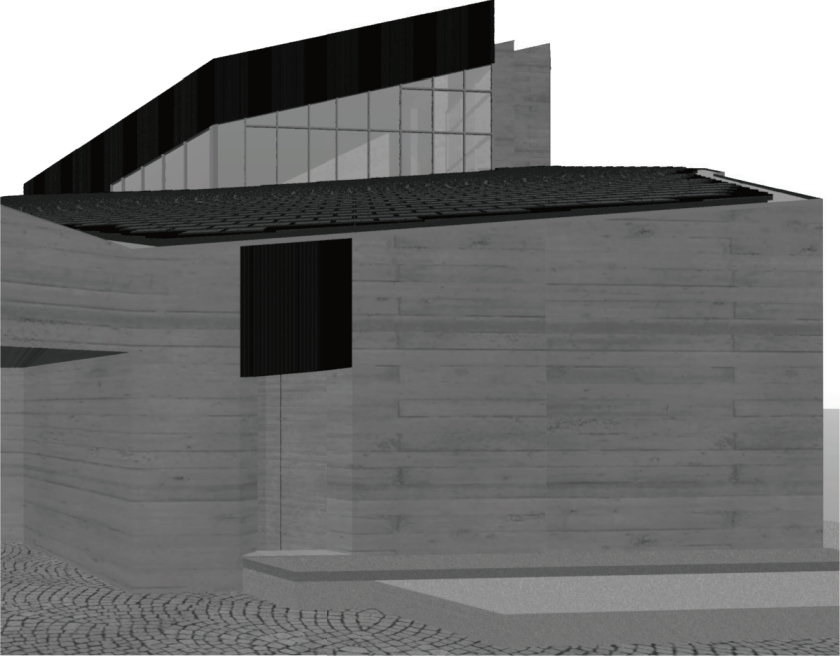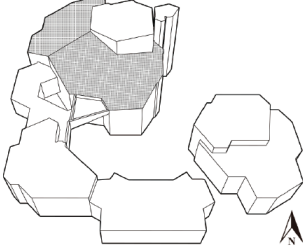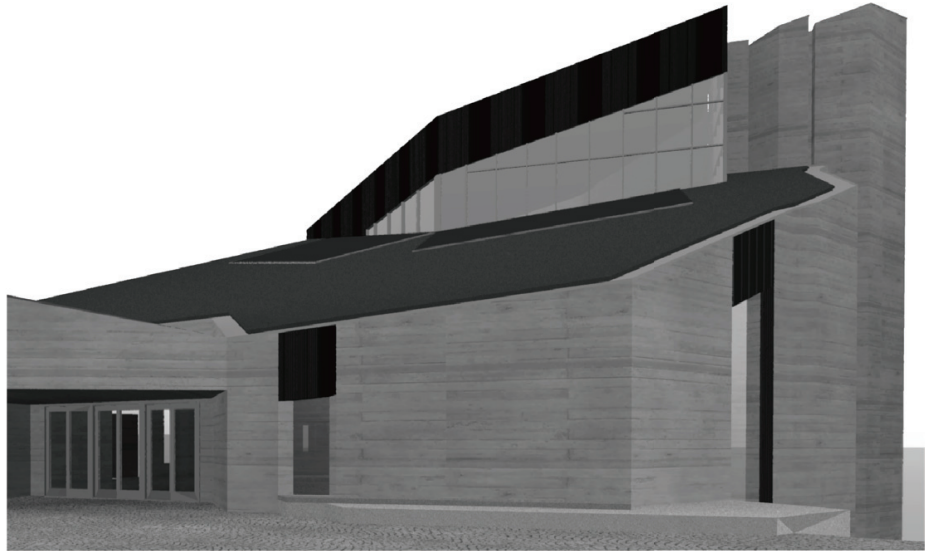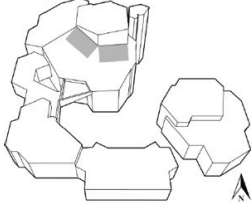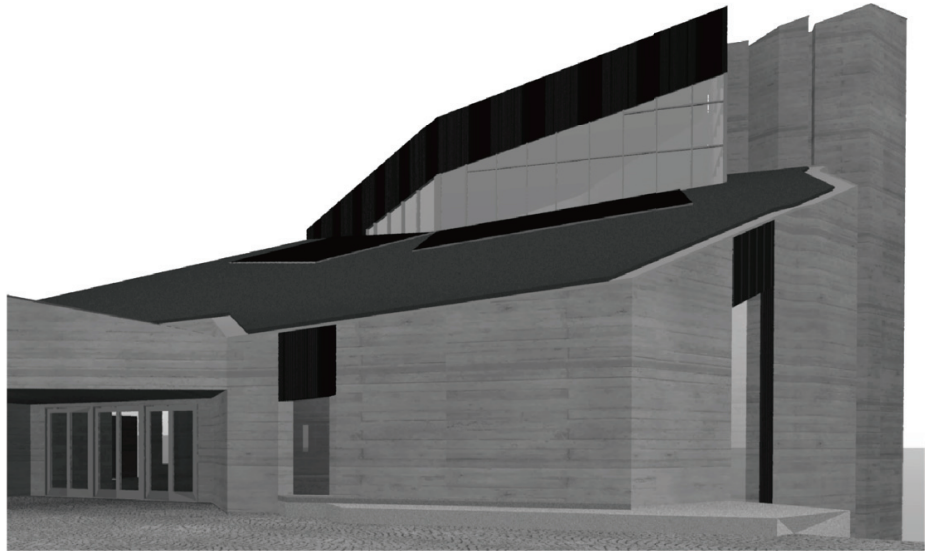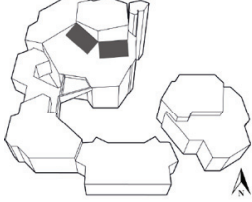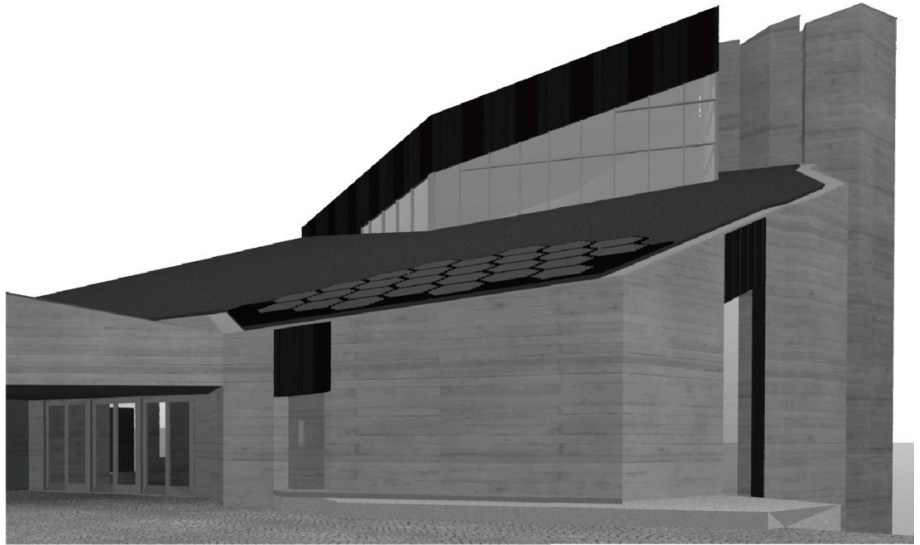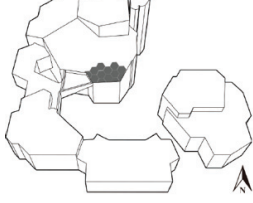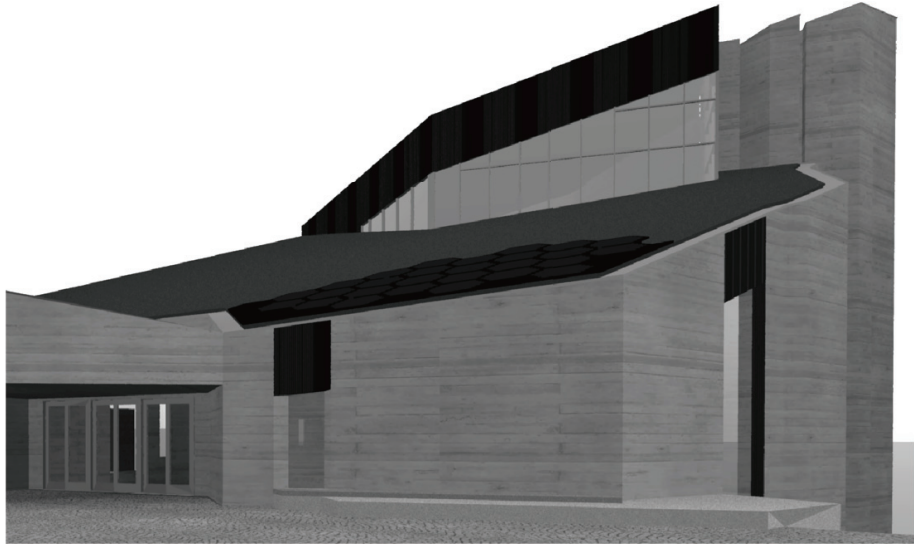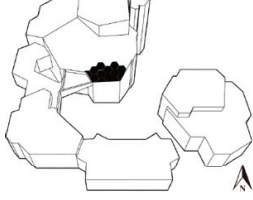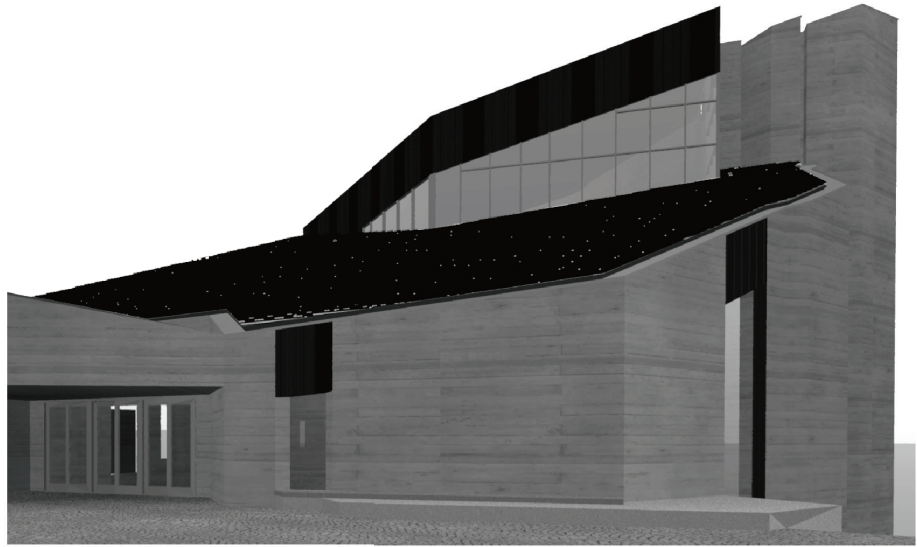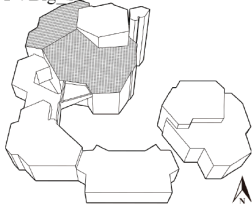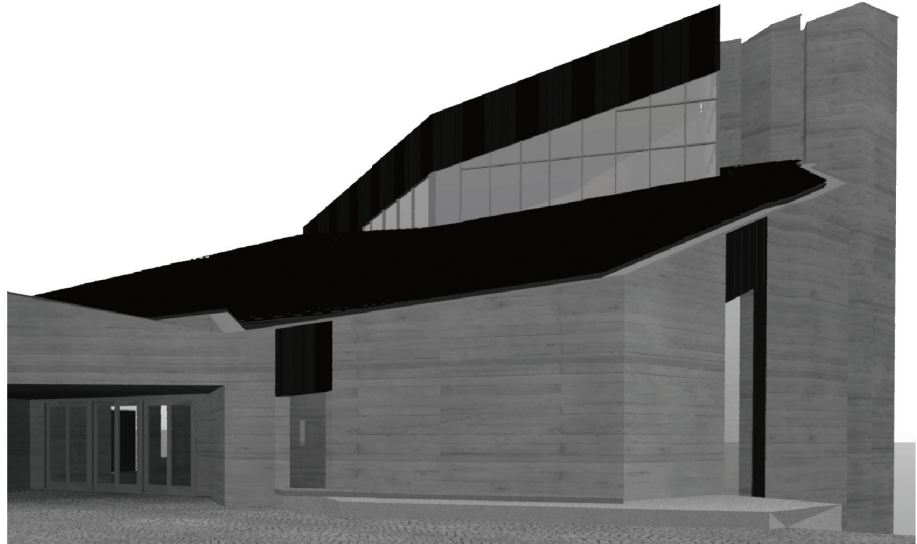

PVSmall_S2

Viewpoint 2

149

Viewpoint 2

PVPolygon_S1

PVPolygon_S2

Viewpoint 2

PVBig_S1

PVBig_S2
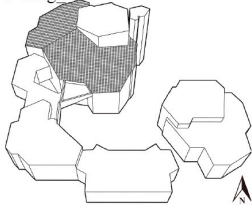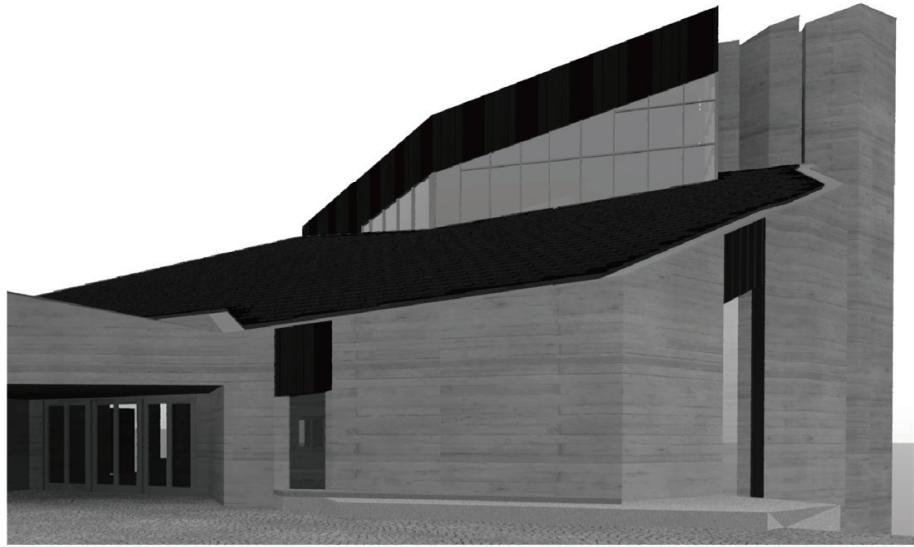
PVSmall_S1

Viewpoint 2

PVSmall_S2
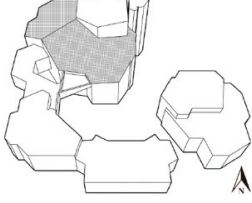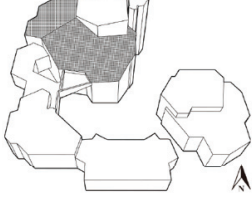
PVTerrace
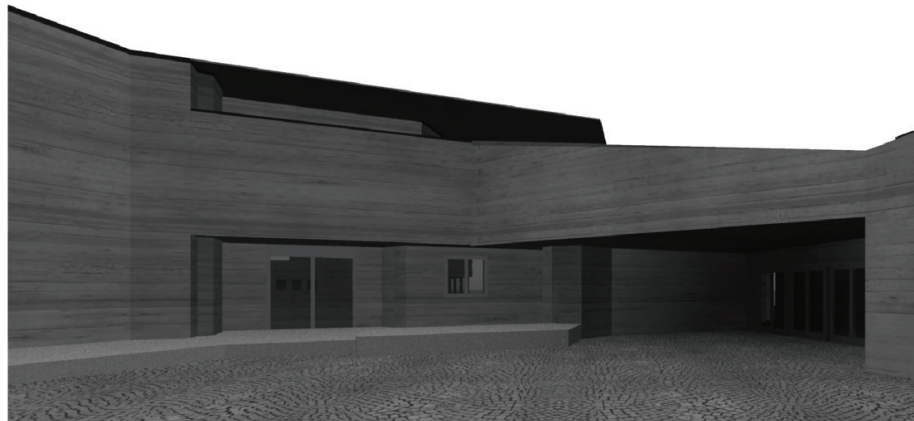
Viewpoint 3

Appendix 6   Analysis maps of St. Michael design variations
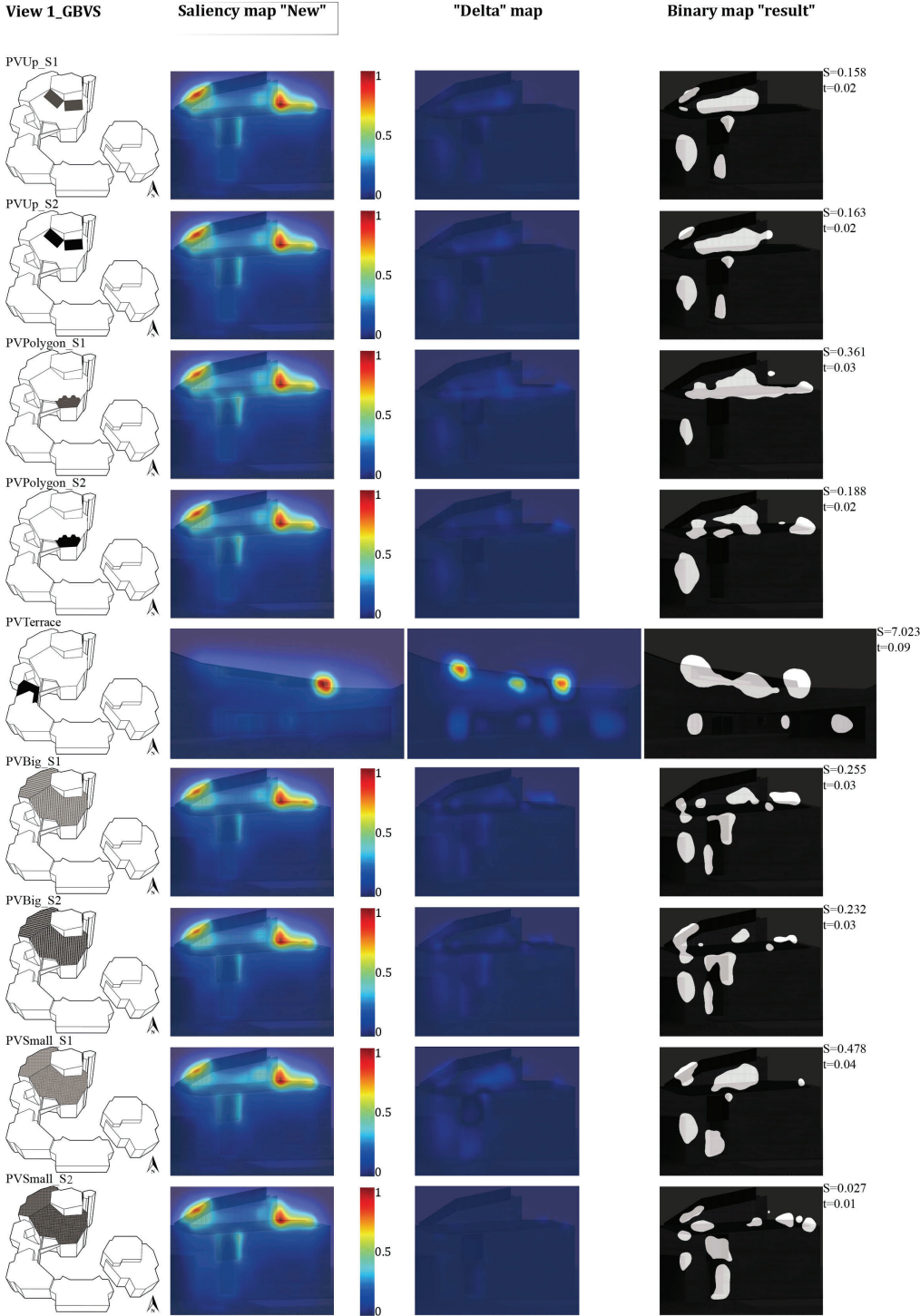
Different BIPV design variations for church St. Michael and the corresponding analysis made from viewpoint 1 and with GBVS saliency model. Exception in fifth row: analysis made from viewpoint 3.
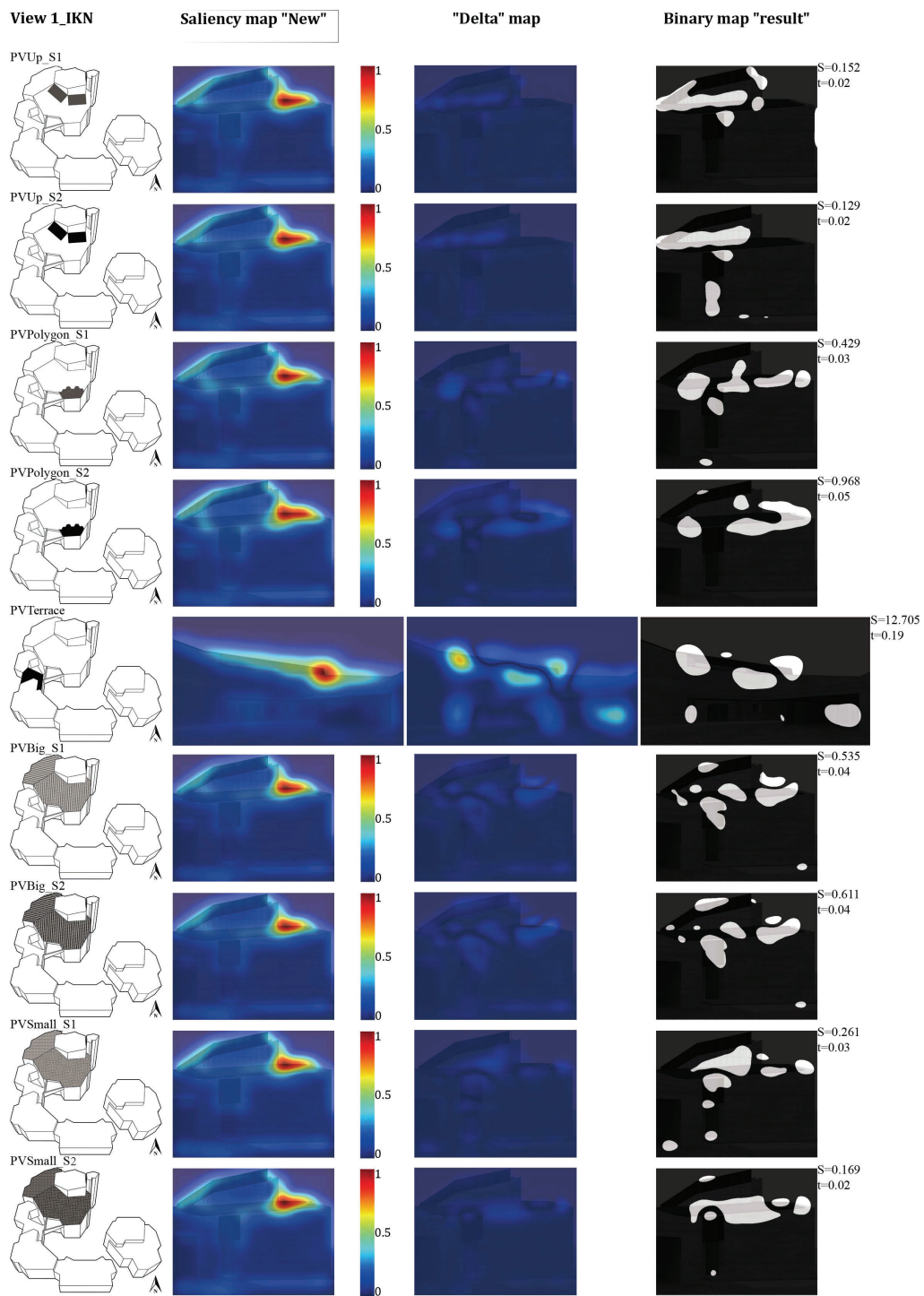
View 1_IKN	Saliency map "New"	"Delta" map	Binary map "result"

PVUp_S1 — S=0.152, t=0.02

PVUp_S2 — S=0.129, t=0.02

PVPolygon_S1 — S=0.429, t=0.03

PVPolygon_S2 — S=0.968, t=0.05

PVTerrace — S=12.705, t=0.19

PVBig_S1 — S=0.535, t=0.04

PVBig_S2 — S=0.611, t=0.04

PVSmall_S1 — S=0.261, t=0.03

PVSmall_S2 — S=0.169, t=0.02

Different BIPV design variations for church St. Michael and the corresponding analysis made from viewpoint 1 and with IKN (Harel) saliency model. Exception in fifth row: analysis made from viewpoint 3.
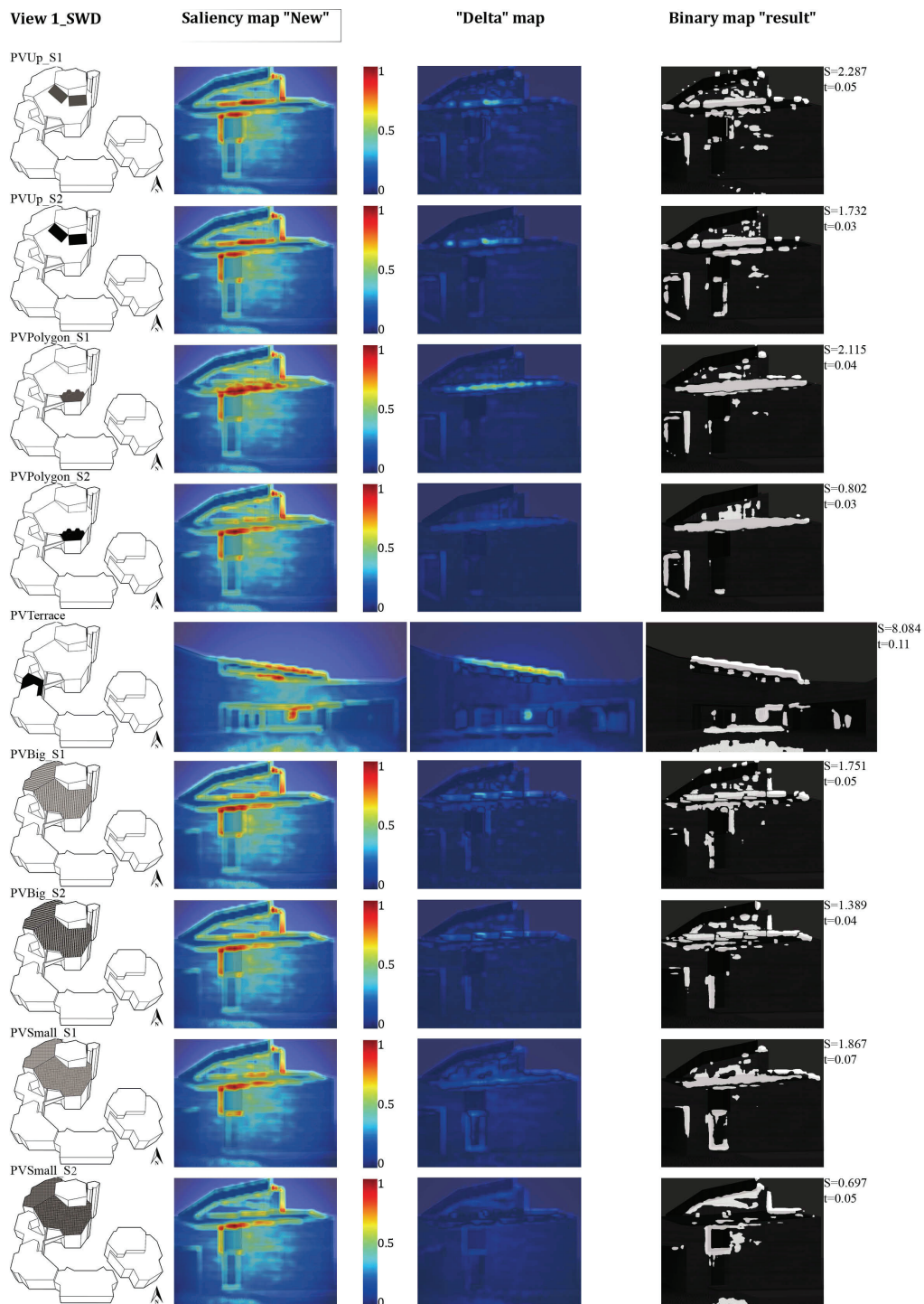
View 1_SWD	Saliency map "New"	"Delta" map	Binary map "result"

PVUp_S1

PVUp_S2

PVPolygon_S1

PVPolygon_S2

PVTerrace

PVBig_S1

PVBig_S2

PVSmall_S1

PVSmall_S2

S=2.287 t=0.05

S=1.732 t=0.03

S=2.115 t=0.04

S=0.802 t=0.03

S=8.084 t=0.11

S=1.751 t=0.05

S=1.389 t=0.04

S=1.867 t=0.07

S=0.697 t=0.05

Different BIPV design variations for church St. Michael and the corresponding analysis made from viewpoint 1 and with SWD saliency model. Exception in fifth row: analysis made from viewpoint 3.

| View 2_GBVS | Saliency map "New" | "Delta" map | Binary map "result" |

PVUp_S1 — S=0.100 t=0.02

PVUp_S2 — S=0.099 t=0.02

PVPolygon_S1 — S=0.244 t=0.02

PVPolygon_S2 — S=0.200 t=0.02

PVBig_S1 — S=0.208 t=0.03

PVBig_S2 — S=0.223 t=0.02

PVSmall_S1 — S=0.065 t=0.01
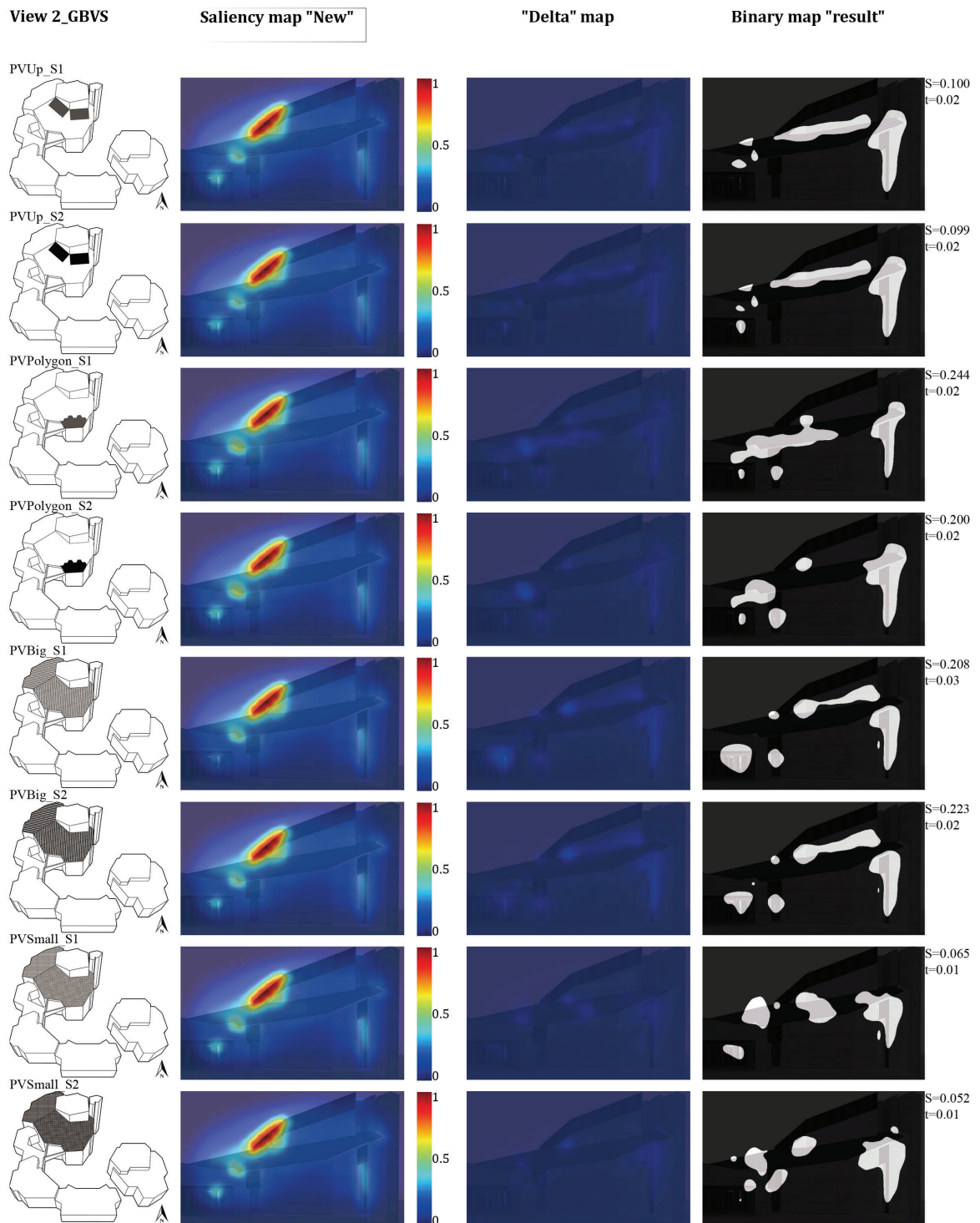
PVSmall_S2 — S=0.052 t=0.01

Different BIPV design variations for church St. Michael and the corresponding analysis made from viewpoint 2 and with GBVS saliency model.

| View 2_IKN | Saliency map "New" | "Delta" map | Binary map "result" |

PVUp_S1 — S=1.822 t=0.08

PVUp_S2 — S=1.413 t=0.08

PVPolygon_S1 — S=1.610 t=0.07

PVPolygon_S2 — S=1.503 t=0.07

PVBig_S1 — S=1.920 t=0.10

PVBig_S2 — S=2.103 t=0.09
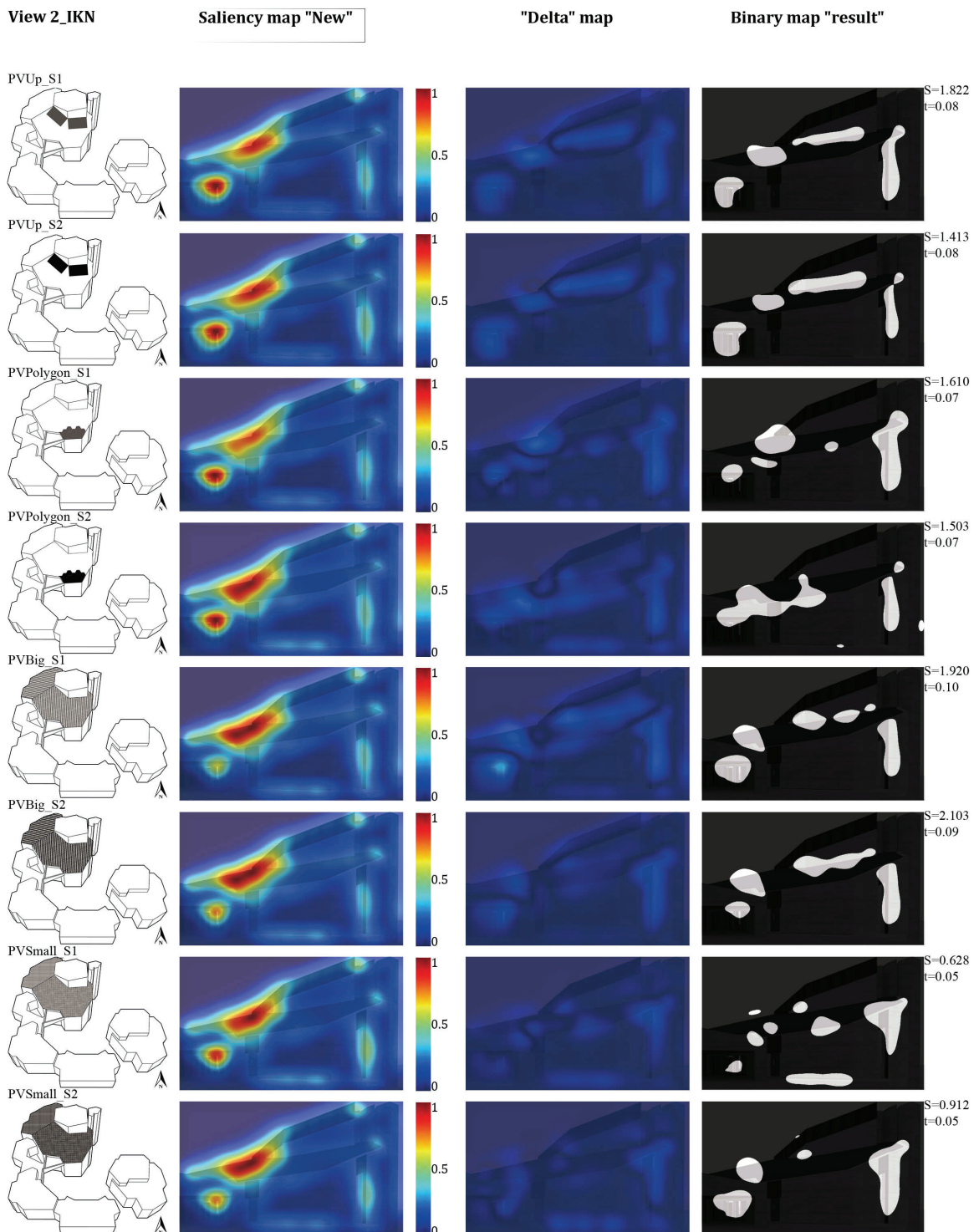
PVSmall_S1 — S=0.628 t=0.05

PVSmall_S2 — S=0.912 t=0.05

Different BIPV design variations for church St. Michael and the corresponding analysis made from viewpoint 2 and with IKN (Harel) saliency model.

View 2_SWD	Saliency map "New"	"Delta" map	Binary map "result"

PVUp_S1

S=1.272
t=0.03

PVUp_S2

S=1.104
t=0.03

PVPolygon_S1

S=4.615
t=0.07

PVPolygon_S2

S=1.274
t=0.06

PVBig_S1

S=1.858
t=0.06

PVBig_S2

S=1.904
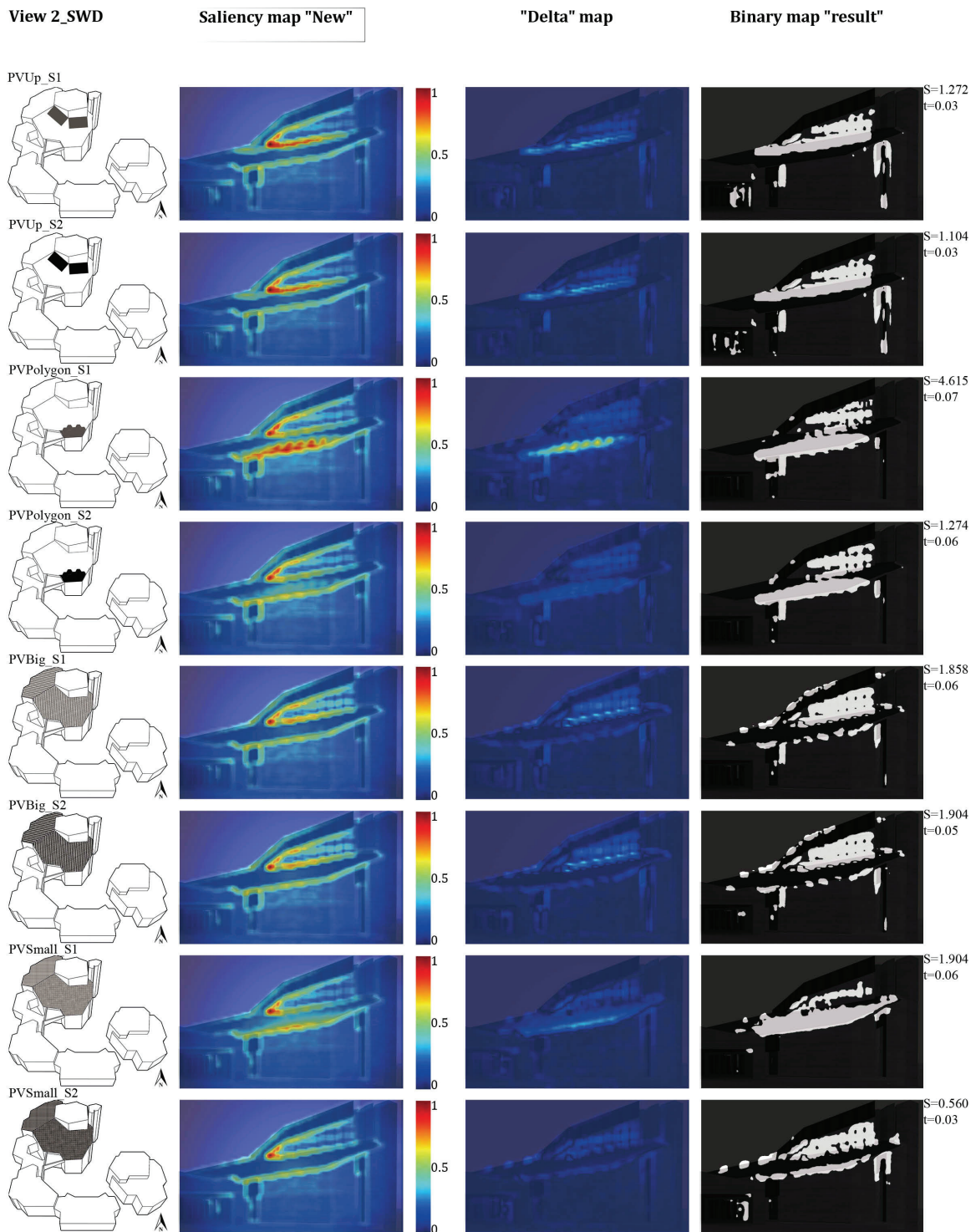t=0.05

PVSmall_S1

S=1.904
t=0.06

PVSmall_S2

S=0.560
t=0.03

Different BIPV design variations for church St. Michael and the corresponding analysis made from viewpoint 2 and with SWD saliency model.

Curriculum Vitae

Name: Ran XU

Nationality: Chinese

Academic preparation

–	Swiss Federal Institute of Technology Lausanne (EPFL), Switzerland	2012 - 2016
	PhD Student in Doctoral Program of Energy (EDEY), LESO-PB Laboratory	
	Topic: Visual impact assessment of BIPV in facade retrofits using saliency models	
–	National University of Singapore, Singapore	2012
	PhD Candidate in Architecture	
	Topic: Solar Energy Building Envelope	
–	Technical University Munich (TUM), Germany	2011
	Master of Architecture (Dipl.-Ing.)	
	Focus: Architecture Design and Building Technology	
–	Beijing Jiaotong University, China	2008
	Bachelor of Science (Architecture)	

Employments

–	Lucerne University of Applied Sciences and Arts (HSLU), Switzerland	- 2012
	Research Assistant in CC Envelopes and Solar Energy	
	With special focus on coloured BIPV and holistic BIPV assessments	
–	Solar Energy Research Institute of Singapore, Singapore	2012
	Research Assistant	
–	Architecture Studio Kühnl + Schmidt, Munich, Germany	2010
	Intern	
–	China Urban Construction Design and Research Institute	2007
	Intern	
–	The Beijing Organizing Committee for the Games of the XXIX Olympiad	2007
	Intern	

Selected grants

–	Full Research Scholarship from Solar Energy Research Institute of Singapore, Singapore	2012

Selected publications

– Herzog & de Meuron: 1989 - 1991, Volume 2: The Complete Works. Translation from the German and English Edition into Chinese. Published by China Architecture and Building Press (2010)

– Xu, Ran & Wittkopf, Stephen. *AIPV Visual Assessment for Architecture Retrofitting*. CISBAT 2013, Lausanne, Switzerland.

– Xu, Ran (22.01.2014). *Solare Fassaden – Technik und Architektur (Visuelle Beurteilung der Solaren Architektur)*. Swissbau 2014, Basel, Schweiz.

– Xu, Ran & Wittkopf, Stephen. *Visual assessment of BIPV retrofit design proposals for selected historical buildings using the saliency map method*. IOS Press: Journal of Facade Design and Engineering, 2014(2),

235-254. doi: 10.3233/FDE-150022

– Xu, Ran & Wittkopf, Stephen. *Visual Impact thresholds of photovoltaics on retrofitted building facades in different building facades in different building zones using the saliency map method*. CISBAT 2015, Lausanne, Switzerland.

– Xu, Ran (12.11.2015). *Visuelle Beurteilung solarer Architektur*. Programm 12. Workshop "Photovoltaik - Modultechnik", Cologne, Germany.

Software
– AutoCAD, Sketch Up, Rhinoceros
– Vray, Ecotect, DIVA and Honeybee for Rhino
– Adobe Photoshop, InDesign, Illustrator
– Grasshopper, Matlab

Languages
– Chinese (mother tongue), German and English (full professional proficiency)
– Russian (elementary proficiency)